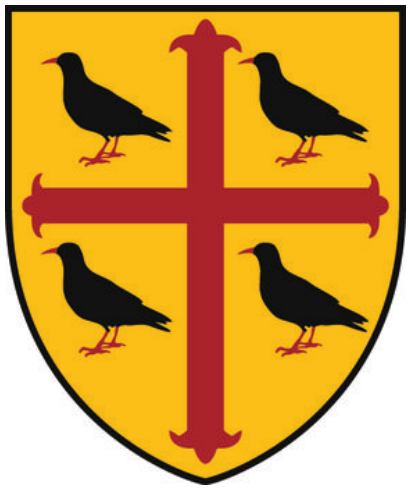
NMDAR-antibody encephalitis: psychopathology and immunobiology

Adam Al-Diwani MA BMBCh (Oxon)

A thesis submitted for the degree of Doctor of Philosophy



St Edmund Hall

University of Oxford

Trinity Term 2020

"A 15-year-old girl was admitted to hospital in August 1994, with an acute confusional state. She had been well until July 1994, when she developed impairment of recent memory. The memory impairment became severe, and she gradually lost contact with reality. On the morning of August 22, she became acutely confused and was transferred to a psychiatric unit. On admission, she had a stiff facial expression, incoherent thoughts, and was dismissive; we could not communicate with her at all. On physical examination, a mass was palpated in the lower abdomen. Neurological examination was unremarkable…Magnetic resonance imaging of the brain was normal…However, electroencephalographic tracings showed diffuse slow waves. We gave her chlorpromazine (maximum dose 150 mg daily), haloperidol (maximum dose 10 mg daily), and carbamazepine (maximum dose 600 mg daily); but she did not get better."

Okamura H, Oomori N, and Uchitumi Y.
An acutely confused 15-year-old girl.
Lancet 1997; 350: 488.

Text excerpt reprinted from above reference with permission from Elsevier.

Abstract

NMDAR-ANTIBODY ENCEPHALITIS: PSYCHOPATHOLOGY AND IMMUNOBIOLOGY by ADAM AL-DIWANI, ST EDMUND HALL, A THESIS SUBMITTED FOR THE DEGREE OF DOCTOR OF PHILOSOPHY, TRINITY TERM 2020.

Autoimmune encephalopathies are immunotherapy-responsive brain diseases mediated by autoantibodies against cell surface antigens. NMDAR-antibody encephalitis (NMDAR-Ab-E) is an autoimmune encephalopathy mediated by IgG against the NR1 NMDA receptor subunit. The illness has a psychiatric onset in most and an association with ovarian teratoma (OT) in a third. This thesis explores the psychopathology and immunobiology of NMDAR-Ab-E; it focuses on the pattern and evolution of mental state abnormalities and serological and cellular measures of autoimmunising mechanisms.

A systematic review identified 464 individually reported patients with more detail than 'psychiatric' and/or 'behavioural'. Granular lower-level phenomena were grouped into higher-level categories: behaviour (68%), psychosis (67%), mood (47%), catatonia (30%), and sleep (21%). These had a propensity to overlap within individual patients, most clearly in psychiatric-described reports (221/329, 67% vs 96/118, 81%). Network analysis suggested a complex pattern of disorganisation, disinhibition, and affective instability rather than sub-groups of patients with simple syndromes (network density and median closeness centrality of 1 in the psychiatric-described group). Further detailed interviews (n=5) revealed temporal progression: complete insomnia and depressive mood develop early, possession-like/drugged-dissociative appearance during the psychosis, and developmental regression and episodic amnesia as late features. Reductive framing as atypical/organic psychosis or delirium could help focus clinical recognition. Lumbar puncture in acute psychiatric services needs to expand and comparison with primary psychoses would help focus how far.

Using a live cell-based assay (CBA) with a 1:40 end-point dilution cut-off, 13/286 samples (5%) from bipolar depression, 12/101 (12%) from acute mania, 5/57 (9%) from traumatic brain injury (TBI) and 3/55 (5%) from healthy volunteer cohorts were NR1-IgG positive. 31 cerebrospinal fluid (CSF) samples from the TBI cohort were negative including two whose serum pair was positive. In contrast, 34/39 (87%) of NMDAR-Ab-E sera paired with CSF NR1-IgG positive samples were detectable at 1:40 and 39/39 at 1:20. Overlapping NR1-IgG levels meant that level could not fully discriminate between groups and a N368Q NR1 mutation abrogated binding in 18/20 (90%) comparator group positive samples suggesting that these were not false positives. However, no positive samples from the comparator group bound neurons, unlike 70% of the selected NMDAR-Ab-E positive sera. Therefore, the NMDAR-Ab-E NR1-IgG were probably of greater affinity and/or polyclonality compared to the comparators, consistent with a more fully realised autoimmunisation process.

Live CBAs for IgM and IgA NR1 autoantibodies were developed. NR1-IgM was common in NMDAR-Ab-E (121/285, 42% samples) and persistent (up to 2555 days post-onset). There was a time-dependent positive serum NR1-IgA association with OT (OR 6.32 P=0.005 <40 days post-onset). NR1-IgG and NR1-IgA but not NR1-IgM were common in tumour fluid, cultured explants produced NR1-IgG with and without activation cytokines, flow cytometry detected B cells from naïve through to class-switched memory and antibody-secreting phenotypes, and GC-like structures with BCL6+AID+ B cells and CD21+ sustentacular meshwork were found histologically. Ultrasound-guided fine needle aspiration (FNA) of cervical lymph nodes (LN) in patients with and without OT successfully detected distinct population frequencies in transitional B cells, T follicular helper cells (TfH), and CD83+ B cells. Cultured LN cells from three patients with fully resected OTs did not produce NR1-IgG whereas those from a patient with a partially treated OT and a relapsing patient without an OT did produce NR1-IgG. LN cells from this relapsing patient also produced NR1-IgG during remission. These data consolidate the status of NMDAR-Ab-E-associated OTs as tertiary lymphoid organs and provide direct evidence of secondary lymphoid organ involvement in pathogenesis.

The two areas converge: the immunological findings suggest early autoimmunising events that can propagate if left unchecked and a refined psychopathologic description could help better identify cases during this window of opportunity.

Acknowledgements

Firstly, I am very grateful to the patients and their friends and families who gave so much of their time to support this research, often whilst in the midst of very trying circumstances. Their donations were, often literally, the lifeblood of this study. I am hopeful that the findings will contribute to improving the diagnosis and treatment of this illness.

Secondly, I wish to thank my supervisors, Professor Belinda Lennox and A/Professor Sarosh Irani for both opening doors for me and helping me to walk through them. While the work presented here took place over three years, I first encountered the field over a decade ago when Sarosh approached us medical students to see if anyone was interested in 'helping go through some notes'. I think we can now say that the notes have been gone through. At a similar time whilst grappling with what sort of doctor I would be, I read Belinda's study of NMDAR antibodies in first episode psychosis and found this fascinating. Since then it's been a pleasure to learn about and eventually join a field that, all hyperbole aside, is an exciting frontier between human experience, the brain, and adaptive immunity. Thank you for supporting this project and I look forward to more studies in the years to come.

Thirdly, I am thankful to the staff of the University of Oxford Department of Psychiatry and Nuffield Department of Clinical Neuroscience who hosted me. Alongside this, a generous grant from the Wellcome doctoral training programme for clinicians allowed me the time and resources to develop my ideas and myself. Additionally, the NIHR Oxford and Oxford Health BRCs have also been generous with funding and opportunities, and I was delighted to be awarded the BMA foundation 2017 Margaret Temple prize for schizophrenia research, which has greatly supported the lymph node study.

Fourthly, there is a host of other scientific and clinical personalities I have met along the way whose mentorship I have treasured. One of the great pleasures in the fellowship was being able to be part of the autoimmune neurology clinical service. Here I encountered Dr Isabel Leite and Dr David Okai who taught me a great deal about the immunology, neurology, and psychiatry of these patients. Beyond this, they did all they could to facilitate patient involvement in research. As Isabel would say, "we must learn".

In the Oxford Autoimmune Neurology Group laboratory I was lucky to work with Andrew Fower (laboratory technician) who calmly kept the place running, Selina Thomsen (research assistant) a giant of efficient technique, and Alba Perez-Pons (research assistant) who provided great support. The diagnostic laboratory team were generous colleagues, particularly Dr Mark Woodhall who took great pride in giving extensive advice on how to best perform CBAs as well as extensive M40 traffic updates – a narrow escape from 'the beast from the east' was but one of many catastrophes averted. The head of the diagnostic lab, Dr Patrick Waters, also contributed to my CBAs and much more, particularly modelling tenacity and scrupulous technique that underpins obtaining reliable data. Venerable post-docs Dr Mateusz Makuch and Dr Anne-Katrin Kienzler tolerated my laboratory naivety and patiently showed me the way to experience and memory. Similarly, Dr Antonio Berretta gave vast hours of his time to teach me about the intricacies of neurons and astrocytes. Additionally, I enjoyed getting to know and collaborate with the other medics in the lab (James, Sophia, Sophie, Bettina, Valentina, Ronan, and Bo) – all neurologists I was certainly outnumbered, but the clinical barriers soon dissolved as we pursued our immunological travails. I have really valued working with

clinician-scientist colleagues Dr Jakob Theorell and Dr Adam Handel who have been generous with their time and knowledge.

Collaborations within and outside the University were an exciting part of the work. The WIMM flow cytometry team, particularly Craig Waugh and Sally-Ann Clarke provided outstanding support. The OCHRe and oncology histopathology teams, particularly Tasneem Hassan-Ali and Leticia Campo alongside Dr Darren Fowler and Dr Alistair Easton really helped bring the teratoma workstream to life. Ms Ruby Harrison joined me for her FHS project and I am very proud that she has now gone on to start her own DPhil in the group. Likewise, AFP medic Dr Leigh Townsend, ably assisted during the systematic review and has gone on to further research.

A/Professor Sanjay Manohar made me think carefully during several inspirational and productive conversations about modelling the psychopathology data. Professor Paul Harrison remained an important mentor and provided key tips at key times as well as linking me in with the CEQUEL team to facilitate the generous donation of samples. Dr Digby Quested generously donated MIAMI-UK samples and I enjoyed our discussions. While there is no neuroimaging presented here, I spent time in FMRIB/WIN and am hugely grateful to Professor Charlotte (Charlie) Stagg for involving me in her group and supporting fMRI scanning of these patients. At UCL, Dr Alex Tsui and Dr Daniel Davis have been engaging collaborators helping build bridges with delirium, Dr Neil Graham and Professor David Sharp similarly with traumatic brain injury, and Dr Marian Galovic and Professor Matthias Koepp with PET-MRI studies. I greatly enjoyed working with Dr Tom Pollak (IoPPN/KCL), and further afield Dr David Nauen (Johns Hopkins, USA), Professor Keiko Tanaka (Kanazawa, Japan), Professor Russell Dale (Sydney, Australia), Professor Raffaele Iorio (Rome, Italy) and Professor Soon-Tae Lee (Seoul, South Korea) have been highly generous and enthusiastic collaborators.

Last, but not least, thank you to my parents for making me always seek to learn and contribute to knowledge – hopefully we can now conclude that I have completed higher education! And Hanine for agreeing to join me on this and future journeys. Thank you.



Sgt. Wilcox's Pathogenic Antibodies Club Band
(2017-2020)

Table of Contents

Abstract ***3***

Acknowledgements ***4***

List of figures ***8***

List of tables ***10***

Abbreviations ***11***

1 Introduction ***14***

1.1 Innate versus adaptive immunity 14

1.2 Antibodies and autoantibodies 16

1.3 Autoantibody-mediated encephalopathies 28

1.4 N-methyl-d-aspartate receptor-antibody encephalitis 35

1.5 NMDAR-autoantibodies in non-encephalitic psychiatric and neurological disorders 56

1.6 Summary and aims 61

2 Materials and methods ***62***

2.1 Clinical material 62

2.2 Laboratory methods 64

3 The psychiatric phenotype of definite NMDAR-Ab-E in adults ***79***

3.1 Introduction 79

3.2 Systematic review and phenotypic analysis of individual patient data 82

3.3 Oxford autoimmune neurology cohort sub-group: retrospective and prospective psychiatric phenotyping 103

3.4 Discussion and limitations 116

4 The prevalence and clinical associations of NR1-IgG in non-encephalitic neuropsychiatric cohorts compared with NMDAR-Ab-E: bipolar disorder and traumatic brain injury ***123***

4.1 Introduction 123

4.2 Cohort description 124

4.3 NR1-IgG in non-encephalitic cohorts: seroprevalence and clinical associations 126

4.4 Binding properties in NR1-IgG positive samples from non-encephalitic cohorts compared to NMDAR-Ab-E 134

4.5 Discussion and limitations 146

5 The prevalence and clinical associations of IgM and IgA NR1-antibody isotypes in encephalitic and non-encephalitic cohorts ***151***

5.1 Development of a live CBA for IgM antibodies against NR1 151

5.2 Development of a live CBA for IgA antibodies against NR1 162
5.3 The prevalence and longitudinal evolution of NR1-IgA and NR1-IgM antibodies in serum and CSF NMDAR-Ab-E patients with and without ovarian teratoma 168
5.4 NR1-IgM and NR1-IgA in non-encephalitic neuropsychiatric comparator and healthy volunteer cohorts 183
5.5 Discussion and limitations 184

6 NR1-specific germinal centre reactions in ovarian teratoma associated with NMDAR-Ab-E: a tertiary lymphoid organ? 187

6.1 Introduction 187
6.2 Patient cohort 187
6.3 Cell culture and measurement of NR1-specific and total antibody in resulting supernatant 190
6.4 Flow cytometric characterisation of B cell infiltrates 195
6.5 Immunohistochemistry 200
6.6 Discussion and limitations 213

7 Ultrasound-guided fine needle aspiration to investigate cervical lymph nodes as a source of NR1-specific B cells 218

7.1 Inception of project 218
7.2 Technical development 221
7.3 Flow cytometric characterisation of CLN versus PBMCs 228
7.4 Lymphocyte cell culture 238
7.5 Discussion and limitations 257

8 Conclusion 261

9 Appendix 265

References 267

List of figures

Figure	Title	Page
1.1	Generic antibody structure	17
1.2	Secondary lymphoid organs are structured to facilitate the development of germinal centres	23
1.3	Summary of B cell development including changes in key surface phenotypic markers	25
1.4	Examples of assays used in the detection of neuronal surface antibodies against conformational epitopes	34
1.5	Structural and functional properties of NMDA receptors	35
1.6	Diagnostic criteria for NMDAR-Ab-E as per consensus guidelines of Graus *et al.* 2016	42
1.7	Demographic and tumour associations of NMDAR-Ab-E and therapeutic associations	49
1.8	The relationship between cytokine condition, serum NR1-IgG level and production of total and NR1-specific IgG *in vitro*	53
1.9	Post-mortem examination of lymphatic sinusoid with CD138 staining from a case of rituximab-resistant NMDAR-Ab-E	54
1.10	Possible immunising sites in NMDAR-Ab-E	55
1.11	NR1-specific immunobiology as a unifying approach to underlying NR1 serological data in varying clinical contexts	60
3.1	Study selection strategy – PRISMA diagram	84
3.2	Demographic features of the individual patient data cohort	86
3.3	Pregnancy-associated onset of illness in relation to ante- and post-partum timing and age of patient	87
3.4	Frequency of higher- and lower-level features in the cohort	91
3.5	Plot of residual differences in lower-level features in six dichotomous comparisons of clinical factors associated with NMDAR-Ab-E	92
3.6	Psychiatric symptom clusters identified by bespoke classification and by recorded categorical diagnoses	94
3.7	Reporting of lower-level features according to specialty	97
3.8	Venn diagrams of higher-level feature overlap in individual patients according to specialty of report	98
3.9	Visualisation of lower-level feature networks in non-psychiatric- and psychiatric-described sub-groups	101
3.10	Lower level frequency in a series of patients seen in the Oxford autoimmune neurology service with those from the systematic review of world literature	106
3.11	Visualisation of network properties in the Oxford autoimmune neurology mini-series	108
3.12	Childhood soft toys seen consistent with regressed personality secondary to NMDAR-Ab-E	112
3.13	Psychopathology time course in two consecutive patients with ovarian teratoma-associated NMDAR-Ab-E	115
4.1	Relationship between serum and CSF NR1-IgG end-point dilutions	131
4.2	Distribution of NR1-IgG serum assays in definite NMDAR-Ab-E compared to healthy volunteers and non-encephalitic neuropsychiatric cohorts	133
4.3	Patient IgG from non-encephalitic neuropsychiatric comparator groups co-localises with cell-surface expressed NR1	135
4.4	Binding properties of NR1-IgG on N368Q mutant NR1	137
4.5	Live NBA positive and negative binding patterns	139
4.6	The effect of adding an additional reporter antibody on signal detection from live neuron based assay (NBA) – paired values	140
4.7	The effect of adding an additional reporter antibody on signal detection from live neuron based assay (NBA) – images	141
4.8	Relationship between NBA score at sample dilution of 1:100 and NBA end-point dilution of these samples	141
4.9	Distribution of live NBA scores from NR1-IgG live CBA negative healthy volunteers and positive autoimmune encephalitis and non-encephalitic neuropsychiatric comparator groups	143
4.10	Correlation between CBA and NBA end-point dilutions analysed by OT status	145
5.1	Representative images from initial NR1-IgM live CBA	153
5.2	CBA scores in serially diluted high and low positive NR1-IgM positive samples using a serially diluted range of IgM secondary antibody	155
5.3	CBA scores in a control cohort of 20 healthy volunteers and 24 cases of neuropsychiatric systemic lupus erythematosus (NPSLE)	156
5.4	Co-localisation of patient IgM antibodies with NR1 expressed on transfected HEK293T cells using a commercial antibody against NR1	158
5.5	Depletion of serum samples of IgG and IgM and NR1-IgG and -IgM CBA on depleted samples	159
5.6	Individual and summated time-courses of serum NR1-IgG and -IgM	161
5.7	Co-localisation of patient IgA antibodies with NR1 expressed on transfected HEK293T cells	165
5.8	Depletion of antibody isotypes in a serum sample triple positive for NR1-IgG/IgA/IgM antibodies	167
5.9	Evolution of serum NR1-IgA:NR1-IgM end-point dilution ratios in patients with and without OT	171

5.10	Time course of NR1-IgA:NR1-IgM serum ratios in individuals with OT and relationship with oophorectomy	172
5.11	Distribution of CSF NR1-IgA and NR1-IgM end-point dilutions and ratio between them in OT and non-OT sub-groups	177
5.12	Evolution of CSF NR1-IgA:NR1-IgM end-point dilution ratios and patients with and without OT	177
5.13	Longitudinal CSF NR1-IgA:NR1-IgM in individual patients	178
5.14	Relationships between NR1-IgA and NR1-IgM in serum and CSF in patients with and without an OT	183
6.1	Culture of ovarian teratoma material under activation and maintenance cytokine conditions	193
6.2	NR1-autoantibody isotype levels in four OT lesions and paired serum	194
6.3	Flow cytometric analysis of dissociated material from ovarian teratoma and paired PBMCs from two patients	197
6.4	Flow cytometric analysis of dissociated material from OT JR819b	199
6.5	Panel 1 immunohistochemistry on serial sections from OT JR748	202
6.6	Panel 2 immunohistochemistry on serial sections from JR817 ovarian teratoma	205
6.7	Multiplex immunofluorescence staining with B, T and FDC panels of post-mortem lymph node from a patient with NMDAR-Ab-E	209
6.8	Multiplex immunofluorescence staining with B, T and FDC panels of colorectal carcinoma from patient with NMDAR-Ab-E.	210
6.9	Multiplex immunofluorescence staining with B, T and FDC panels of an OT from a patient with NMDAR-Ab-E	211
7.1	Ultrasonographic identification of cervical lymph node and fine needle aspiration	224
7.2	Fine needle aspiration sample preparation	227
7.3	Comparison of peripheral blood and lymph node flow cytometry	228
7.4	Gating strategy for B cell lineages in peripheral blood and lymph node material	229
7.5	Frequency of B cell lineage sub-sets in paired peripheral blood and lymph node samples in 10 participants with NMDAR-Ab-E	230
7.6	Gating strategy for B cell accessory panel in peripheral blood and lymph node material	231
7.7	Frequency of CD83+ B cell sub-set in paired peripheral blood and lymph node aspirate	232
7.8	Gating strategy for T cell lineages in peripheral blood and lymph node material	233
7.9	Frequency of T cell lineage sub-sets in paired peripheral blood and lymph node	234
7.10	Correlation of T follicular helper cells (CD3+CD4+CXCR5+PD1+) as a percentage of T helper cells (CD3+CD4+ cells) from lymph node and peripheral blood versus B cell subsets	236
7.11	Correlation between NR1-IgG level and frequency of antibody-secreting cells and T follicular helper cells in peripheral blood and lymph node	237
7.12	Cell culture plate set-up used in unfractionated culture experiments	239
7.13	IgG production from peripheral blood and lymph node cultured under activation and maintenance conditions	240
7.14	Total IgG in culture supernatants from unfractionated paired PBMC and lymph node aspirate cell cultures	243
7.15	Relationship between NR1-IgG and total IgG production *in vitro* from peripheral blood and lymph node cell culture	245
7.16	Time course of serum NR1 antibody levels relative to clinical phases, treatments and aspiration visits in lymph node cell culture NR1-IgG positive patients	246
7.17	Relationship between germinal centre-related flow cytometry parameters and lymph node cell culture NR1-IgG positivity	248
7.18	Comparison of CXCL13 levels in different compartments	251
7.19	Total IgG and IgM produced from sorted PBMC and lymph node memory and naïve B cell cultures	254

List of tables

Table	Title	Page
2.1	Samples from patients with definite NMDAR-Ab-E and healthy volunteers from the Oxford study	62
2.2	Samples from patients with definite NMDAR-Ab-E and healthy volunteers from collaborators	63
2.3	Total cohort of serum and CSF samples from patients with definite NMDAR-Ab-E	64
2.4	Cytokines used in lymphocyte culture	74
2.5	Total Ig ELISA detection antibody set-up	76
3.1	Demographic, teratoma, and neurological profile of group vs. individually-reported cases	84
3.2	Classification of cases based on the source of their description	94
3.3	Demographic, teratoma, and neurological features stratified by specialty of reporting journal	95
3.4	Network properties of non-psychiatric-described versus psychiatric-described lower-level feature sub-groups	99
3.5	Coalescent patterns identified within lower-level features from literature review	102
3.6	Baseline demographic variables of participants interviewed	103
3.7	Journey to presumptive diagnosis and treatment for autoimmune encephalitis	104
3.8	Network properties in the Oxford autoimmune neurology mini-series	106
3.9	Ten characteristic mental state features noted during interview with patients, relatives, partners and healthcare staff in this series	111
4.1	Summary of cohorts used for NR1-IgG serum studies	124
4.2	Mean, median and derivatives of end-point dilutions of NR1-IgG in a healthy volunteer cohort	126
4.3	NR1-IgG seropositivity rates in bipolar depression and acute mania cohorts	127
4.4	Demographic and clinical associations with seropositive cases in CEQUEL and MIAMI-UK cohorts compared to healthy volunteers	128
4.5	NR1-IgG seropositivity rates in a traumatic brain injury cohort	129
4.6	Cohort of samples used for the live CBA versus live NBA study	138
5.1	Initial samples screened for NR1-IgM from a discovery cohort of ten patients with NMDAR-Ab-E	153
5.2	CBA score for NR1-IgA in initial samples from four cases of OT-associated NMDAR-Ab-E	163
5.3	Mean, median and derivatives of end-point dilutions of NR1-IgM and NR1-IgA sera in a healthy volunteer cohort	168
5.4	Rate of positivity for NR1-IgM and NR1-IgA in 284 serum samples from patients with definite NMDAR-Ab-E	169
5.5	Prevalence of NR1-IgM and NR1-IgA positivity in serum samples from OT and non-OT sub-groups	169
5.6	Per-patient prevalence of NR1-IgM and NR1-IgA positivity in time-restricted serum samples from OT and non-OT sub-groups	172
5.7	Positivity rate of NR1-IgA, NR1-IgM and both in CSF samples tested for both	174
5.8	Association between OT and CSF NR1-IgA in the published study of Desestret *et al.* compared to the current study	174
5.9	Association between OT and CSF NR1-IgM	175
5.10	Contingency table analysis of OT status and CSF NR1-IgA NR1-IgM double positives	175
5.11	Time-restricted prevalence and OT associations of CSF NR1-IgA, NR1-IgM, and double positive patients	178
5.12	Clinical and demographic properties of serum-CSF pairs	179
5.13	Prevalence and OT associations of CSF NR1-IgA, NR1-IgM, in paired serum-CSF samples with and without time-restriction	181
5.14	Prevalence and level of NR1-IgA and NR1-IgM in healthy volunteers and non-encephalitic neuropsychiatric comparator cohorts	183
6.1	Participants participating in chapter 6 and 7 studies	188
6.2	B cell-focused staining panel used to study OT samples	194
6.3	B cell flow cytometry staining panel to investigate surface immunoglobulin expression	197
6.4	Immunohistochemistry panels for chromogenic OT staining	200
6.5	Multiplex immunofluorescence histology B and T/FDC cell staining panels	206
7.1	Antibody staining panels used in fine needle aspiration experiments	221
7.2	Anticipated populations using B cell, B cell accessory and T cell panels developed for fine needle aspiration study	221
7.3	Participant demographic and clinical factors at fine needle aspiration visits in the unfractionated culture method series	240
7.4	Frequency of NR1-IgG positivity from paired PBMC-lymph node aspirate cell cultures	243
7.5	Frequency of antigen-specific IgG and IgM positivity from paired PBMC-lymph node aspirate bulk B cell-sorted cell cultures	254

Abbreviations

AChR	acetylcholine receptor
AF	Alexa-Fluor
AID	activation-induced cytidine deaminase
AMPAR	α-amino-3-hydroxy-5-methyl-4-isoxazolepropionic receptor
ANOVA	analysis of variance
APC (cell)	antigen presenting cell
APC (stain)	allophycocyanin
APE-1	apurinic/apyrimidinic endonuclease 1
ASC	antibody secreting cell
ATD	amino terminal domain
Aza	azathioprine
BAFF	B cell activating factor
BBB	blood brain barrier
BCL6	B cell lymphoma 6
BCM	B cell medium
BCR	B cell Receptor
BOLD	blood oxygen level dependent
BPAD	bipolar affective disorder
BSA	bovine serum albumin
BV	brilliant violet
CASPR2	contactin-associated protein-like 2
CBA	cell based assay
CD	cluster of differentiation
CD40L	cluster of differentiation 40 ligand
CDR	complementarity determining region
CEQUEL	Comparative Evaluation of Quetiapine plus Lamotrigine combination versus quetiapine monotherapy (and folic acid versus placebo) in bipolar depression trial
CLN	cervical lymph node
CMV	cytomegalovirus
CNS	central nervous system
CSF	cerebrospinal fluid
CSR	class-switch recombination
CTD	carboxyl terminal domain
CXCL	C-X-C Motif Chemokine Ligand
CXCR	C-X-C Motif Chemokine Receptor
CyP	cyclophosphamide
DAPI	4',6'-diamidino-2-phenylindole
DIV	day *in vitro*
DMEM	Dulbecco's Modified Eagle medium
DMSO	dimethyl sulfoxide
DNA	deoxyribonucleic acid
DZ	dark zone
EEG	electroencephalogram
EGFP	enhanced green fluorescent protein
ELISA	enzyme-linked immunosorbent assay
EphB2	ephrin type-B receptor 2
Fab	fragment antigen binding

Fc	fragment crystallisable
FBDS	faciobrachial dystonic seizures
FCB	flow cytometry buffer
FCS	foetal calf serum
FDC	follicular dendritic cell
FEP	first episode psychosis
FITC	fluorescein isothiocyanate
FM	freezing medium
FMO	fluorescence minus one
FNA	fine needle aspiration
FOXP3	forkhead box protein P3
GABAR	gamma-aminobutyric acid receptor
GC	germinal centre
GCBC	germinal centre B cell
GFAP	glial fibrillary acidic protein
GFP	green fluorescent protein
GRIN	glutamate ionotropic receptor NMDA type gene
HBSS	Hank's balanced salt solution
HEPES	4-(2-hydroxyethyl)-1-piperazine ethane sulfonic acid
HEV	high endothelial venule
HIV	human immunodeficiency virus
HLA	human leukocyte antigen
HRP	horseradish peroxidase
HSVE	herpes simplex virus encephalitis
HEK293	human embryonic kidney 293 cells
ICOS	inducible T-cell co-stimulator
ICU	intensive care unit
IFN	interferon
IgA	immunoglobulin A
IgG	immunoglobulin G
IgM	immunoglobulin M
IL	interleukin
IVIG	intravenous immunoglobulin
IVMP	intravenous methylprednisolone
IQR	inter-quartile range
LAMP3	lysosome-associated membrane glycoprotein 3
LCA	leucocyte common antigen
LEMS	Lambert-Eaton myaesthenic syndrome
LGI1	leucine-rich glioma inactivated-1
LN	lymph node
LBD	ligand binding domain
LZ	light zone
MAP2	microtubule-associated protein 2
MG	myaesthenia gravis
MHC	major histocompatibility complex
MIAMI-UK	Melatonin In Acute Mania Investigation – United Kingdom trial
MMF	mycophenolate mofetil
NBA	neuron-based assay
NMDAR	N-methyl-D-Aspartate Receptor
NMDAR-Ab-E	N-methyl-D-Aspartate Receptor-antibody encephalitis

NIHR	National Institute for Health Research
NPI-NH	neuropsychiatric inventory – nursing home edition
NSAbs	neuronal surface antibodies
NTD	N-terminal domain
MRI	magnetic resonance imaging
NOS	not otherwise specified
O&G	obstetrics and gynaecology
OCHRe	Oxford Centre for Histopathology Research
OD	optical density
OR	odds ratio
OT	ovarian teratoma
PB	pacific blue
PBMC	peripheral blood mononuclear cell
PBS	phosphate buffered saline
PC	plasma cell
PCP	phencyclidine
PCR	polymerase chain reaction
PD1	programmed cell death protein 1
PE	phycoerythrin
PEI	polyethyleneimine
PET	positron emission tomography
PLEX	plasma exchange
PLL	poly-L-lysine
PNAd	peripheral node addressin
PPiP	prevalence of pathogenic antibodies in psychosis study
PPP	post-partum psychosis
PRISMA	preferred reporting items for systematic reviews and meta-analyses
PROSPERO	international prospective register of systematic reviews
PSA	penicillin/streptomycin/amphotericin
QIDS-SR	quick inventory of depressive symptomatology – self report
R848	resiquimod
RNA	ribonucleic acid
RPMI	Roswell Park Memorial Institute
SHM	somatic hypermutation
SLE	systemic lupus erythematosus
SLO	secondary lymphoid organ
STDEV	standard deviation
TCR	T cell receptor
TBA	tissue-based assay
TBI	traumatic brain injury
TfH	T follicular helper
TfR	T follicular regulatory
TLR	toll-like receptor
TMB	3,3′,5,5′-tetramethylbenzidine
TNF	tumor necrosis factor
VGKC	voltage-gated potassium channel
YMRS	Young mania rating scale

1 Introduction

1.1 Innate versus adaptive immunity

The main function of the immune system is to protect the host organism from infection. Innate immunity is phylogenetically ancient and exists across multiple biological kingdoms. An innate response will occur in the same way to broad groups of insults irrespective of prior exposure whereas adaptive immunity 'adapts' to specific exposures and re-exposures forming immunological memory (1).

Adaptive immunity is phylogenetically newer, having evolved in vertebrates. It depends on lymphoid lineage T and B lymphocytes, which respond to specific molecular patterns called antigens which are recognised by surface T and B-cell receptors (TCRs and BCRs) (2). Each T or B cell has a unique TCR or BCR generated by somatic gene recombination and with additional mechanisms each individual has a unique diversity of TCR and BCR-expressing lymphocytes known as the immune repertoire. Both cell types differentiate from haematopoietic stem cells via haematopoietic progenitor cells and then common lymphoid progenitors in the bone marrow (3). While B cells remain in the bone marrow to begin to mature, T cells migrate to colonise the thymus from where they are released into the peripheral pool. B cell lymphopoiesis continues throughout life whereas T cell differentiation slows following early postnatal development later proceeding to thymic involution (4,5).

The BCR contains a unique surface-expressed immunoglobulin which binds protein epitopes whereas the TCR reacts with peptide fragments presented to it in the groove of major histocompatibility complex (MHC) surface molecules. Hence, unlike BCRs, TCRs are 'MHC-restricted' giving the MHC an important role in defining the

extent of T cell reactivity. The MHC is encoded by human leucocyte antigen (HLA) genes which are highly polymorphic due to a selective pressure to retain population-level diversity to protect against emerging infections. Class I MHCs are expressed on all nucleated cells and present intracellular antigens defining 'self', whereas class II MHCs present extracellular antigens (6). T cells expressing CD4 on their surface bind to class II MHCs whereas those expressing CD8 allow binding to class I MHCs. CD4+ T cells are helper T cells and co-ordinate adaptive immunity including B cell activation via surface molecules and secreted cytokines, whereas CD8+ T cells are cytotoxic, providing defence against cells infected with intracellular pathogens such as viruses, and dysplastic host cells. There are multiple sub-sets beyond this principal distinction (2). They are largely beyond the scope of this thesis but are discussed further where relevant.

Whereas T cells provide cell-mediated immunity, B cells provide humoral immunity. Upon activation, B cells can differentiate into antibody-secreting cells (ASCs), which secrete a soluble form of the membrane-bound immunoglobulin in the BCR, known as an antibody (7). Antibodies circulate in plasma and provide passive immunity via mechanisms including neutralisation, opsonisation, and complement fixation (2). They are a central focus of this thesis and discussed further in 1.2.

In addition to antigen specificity derived from their receptors, the cardinal feature of adaptive immunity is antigenic memory; antigen-inexperienced naïve lymphocytes differentiate into antigen-experienced memory lymphocytes upon encountering their cognate antigen in the presence of co-stimulation. Memory cells can be activated and readily proliferate upon antigen re-encounter (8,9). This forms the cellular basis

of secondary and tertiary immune responses being faster and more robust than the primary encounter. Memory B cells are usually affinity matured in germinal centres via somatic hypermutation (SHM) and selection (10). Upon differentiation into ASCs, their secreted antibodies have a higher affinity (11).

1.2 Antibodies and autoantibodies

1.2.1 Structure and function

Immunoglobulins (Ig) are Y-shaped proteins made up of a pair of heavy (H) chains bound together in a hinge region by disulphide bridges, and a pair of light (L) chains, each bound to a heavy chain independent of the hinge region. The polypeptide light chains can be either kappa (κ) or lambda (λ) types. Both chains have variable domains at their N-terminal end (V_H and V_L) and constant domains at their C-terminal end (C_H and C_L) (2,12). The light chains each have a single constant domain C_L whereas the heavy chains each have three: C_H1-3 (figure 1.1). These domains derive from their respective IG genes, discussed further in 1.2.2.

Papain proteolysis reveals three fragments per Ig protein: one fragment crystallisable (Fc) and two fragment antigen-binding (Fab) (2,12). The N-terminal region of the Fab fragment contains the antigen binding site (paratope) formed from the variable regions of a light and a heavy chain. The paratope is a unique structure creating a steric lock accessible to specific antigenic regions called epitopes akin to its key. Epitopes are usually thought of as either linear such that the primary polypeptide sequence binds, or conformational where tertiary protein structures bind; some are thought to be a combination of both (13).

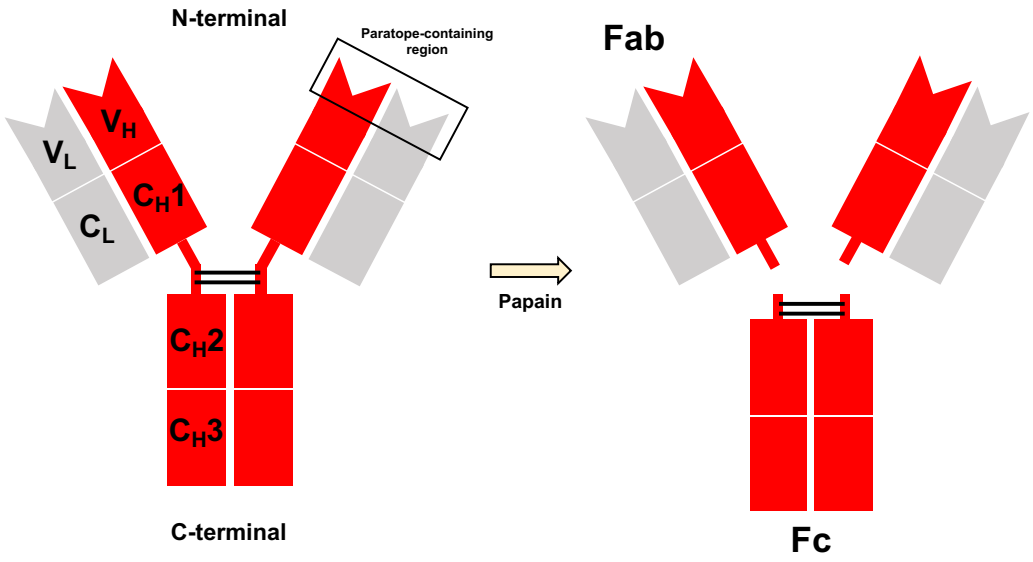


Figure 1.1 – **Generic antibody structure.** A pair of immunoglobulin heavy chains are joined at a hinge region and at the N-terminal end of the protein, each heavy chain is joined to a light chain. The N-terminal variable regions contain complementarity-determining regions which form the epitope-binding paratope region. The constant heavy chains determine the antibody isotype. Papain digestion gives two paratope-containing Fab fragments and one Fc fragment.

Abbreviations used: V=variable, C=constant, H=heavy, L=light; Fab=fragment antigen-binding, Fc=fragment crystallisable; Red = immunoglobulin heavy chain, Grey = immunoglobulin light chain [Redrawn image inspired by diagrams from Janeway's Immunobiology, 9th edition 2017]

The paratope is formed by the variable domain of a heavy and a light chain which each contains framework and hypervariable regions. The hypervariable regions form complementarity determining regions of which there are three in each chain's variable domain (CDR-H1-3 and CDR-L1-3). CDRs are thought to determine the majority of binding specificity but the framework regions contribute in the overall structural orientation. Since each Ig molecule has two paratopes it is described as divalent. The residues contributing to hinge region angle also confer differing binding overall binding dynamics (12).

Unlike Fab, the Fc region is a constant structure that interacts with Fc receptors and provides the effector function of the molecule. Each protein will contain one of five different constant structures that gives the Ig its overall class/isotype (δ, μ, γ, α, ε),

corresponding with IgD, IgM, IgG, IgA, and IgE isotypes. All except IgD are secreted as antibodies by substituting hydrophobic C-terminal residues for hydrophilic (2). Membrane-bound Ig forms the core component of the B cell receptor. Mature naïve B cells express surface IgD and IgM. During antigen recognition IgD expression declines and the Ig isotype of the BCR can switch by looping out initial IGHC gene elements to bring in alternative classes (14). Class switch recombination (CSR) is discussed further in 1.2.2.

IgM and IgA can multimerise whereas IgG and IgE are monomers. IgM forms pentamers with high avidity but usually low affinity giving it a role in early phase immune responses, IgA dimerises in mucosal secretions, whilst IgG is the dominant isotype in affinity matured responses against most pathogens (2). IgE binds Fcε receptors; it is thought to have a role with mediating a co-ordinated response against parasites, but also mediates allergic responses. Some isotypes have further sub-classes: IgA has two (IgA_1 and IgA_2) and IgG has four (IgG_{1-4}). These are numbered by their frequency in serum but not by the order in which they are arranged in IGHC genes.

1.2.2 Genetic basis of antibody diversity

A remarkable feature of adaptive immunity is the huge diversity of potential BCR specificities. Rather than encode each specificity in the germline, instead a smaller number of genes are recombined in each B cell during development, generating combinatorial diversity. Immunoglobulin genes contain variable (V), diversity (D), and joining (J) segments. IG heavy chain genes contain all three, whilst IG κ and λ light chain genes contain V and J. In humans, there are thought to be for heavy chains 65

IGHV, 27 IGHD and 6 IGHD segments, for κ light chains 40 IGKV and 5 IGKJ segments, and for λ 30 IGLV and 5 IGLJ segments (2). During B cell development these are recombined in each cell via recombination-activating gene proteins (RAG-1 and RAG-2)-dependent V(D)J recombinase complex (15). This process adds further diversity by the addition and deletion of nucleotides during the recombination process giving rise to a final V-domain exon for the heavy and light chain genes. The CDR3 region contains J±D segments giving it the most diverse of the CDRs. Finally, the pairing of the resultant heavy and light chain pairs gives rise to an overall estimated 10^{11} of possible BCRs (2,16).

Beyond this, B cells entering germinal centre reactions undergo somatic hypermutation whereby hypervariable regions become deliberately unstable during DNA replication leading to point mutations and structurally altered BCRs, discussed further in 1.2.4 (15).

1.2.3 B cell self-tolerance mechanisms

The price for such a large potential diversity is the inevitable generation of BCRs that could react with self-proteins – autoantigens. Indeed, the mature naïve B cell repertoire contains far fewer reactivities than the mathematical potential, consistent with mechanisms to reduce this diversity and limit self-reactivity. This occurs at checkpoints during B cell lymphopoiesis in the bone marrow. Following differentiation events from progenitor to pro- then pre-B cells, an immature B cell is formed which is tested against self-antigens in the bone marrow. If the membrane-bound IgM BCR strongly cross-links self-antigens then the cell is clonally deleted via apoptosis. Importantly, this does not remove weakly self-reactive cells as this would over-

restrict the repertoire. Hence a degree of potential autoreactivity is inevitable (17). An alternative fate for a smaller proportion of strongly self-reactive cells is receptor editing where RAG proteins are reactivated, and a new receptor is produced which may render it below the threshold of permitted self-reactivity. A further mechanism is clonal anergy whereby the cell is not deleted but survives in a state such that the BCR is desensitised and co-stimulation fails to activate the cell (18). The retention of many autoreactive cells had previously been hard to explain but recent work suggests that the peripheral anergic pool is an important source of reactivities against pathogens whereby very strong antigen stimulation can allow it to enter a germinal centre reaction to undergo SHM and its BCR be 'redeemed' making it useful in the immune response (19). A final mechanism is clonal ignorance where antigen is insufficiently available to activate the BCR e.g. sequestered antigens. Such cells are another source of potential autoreactive B cells in states where the antigen later becomes sufficiently concentrated e.g. anti-nuclear antibodies during cell breakdown in systemic lupus erythematosus (SLE).

1.2.4 Affinity maturation via germinal centre reactions

Affinity maturation is the process by which B cells activated by cognate antigen and T cell help increase BCR affinity. This occurs in specialised transient foci called germinal centres (GC) within B cell follicles of secondary lymphoid organs (SLO) such as lymph nodes and the spleen. Lymph nodes contain afferent and efferent lymphatic vessels and blood vessels (figure 1.2a). They have an inner T cell zone, an outer B cell zone containing B cell follicles, and a marginal zone where they meet. The main participants in a GC reaction are antigen complexes, B cells and T helper cells (20). Immune complexes drain into the SLO from lymphatic fluid and are held

on follicular dendritic cells (FDC) within B cell follicles. These express high levels of Fc receptors and complement receptors to retain complexed antigen often for protracted periods of time up to months (21). Naïve B cells from the periphery enter via high endothelial venules (HEV). If a BCR encounters cognate antigen then this is processed and presented on peptide-MHCII. The cell migrates to the marginal zone and processed antigen is presented to T cells. If this activates the T helper cell then in turn it provides co-stimulation via CD40 ligand (CD40L) to the B cell and secreted cytokines such as IL-2, IL-4, and IL-21. In a classical GC reaction both cell types express the transcription factor B-cell lymphoma 6 protein (BCL6), associated with naïve B cells differentiating into germinal centre B cells (GCBC) and T helper cells becoming T follicular helper cells (TfH) (22). Both upregulate surface expression of the chemokine receptor CXCR5 to retain them via C-X-C motif chemokine ligand 13 (CXCL13). The activated GCBC clonally proliferates forming the germinal centre. The GCBCs take on two phenotypes which are spatially distributed into two zones visible under light microscopy: the dark zone (DZ) where GCBCs enter the cell cycle to proliferate, becoming larger and are called centroblasts, and the light zone (LZ) where GCBCs leave the cell cycle, become smaller and are called centrocytes. In the dark zone centroblasts express activation-induced cytidine deaminase (AID) triggering a cascade leading to SHM: point mutations within largely hypervariable regions of the variable exons in heavy and light genes change CDRs and hence the paratope structure. To leave the CXCL12-rich DZ, centroblasts reduce the expression of CXCR4 and under the influence of unopposed CXCR5 enter the CXCL13-rich CXCL12-poor LZ. Here the newly mutated BCRs on the centrocytes bind again to antigen and present it to TfH TCRs. Centrocytes are highly prone to apoptosis without anti-apoptotic T cell-derived signals, hence a process of natural

selection takes place whereby well-tuned BCRs survive and undesirable clones die. Following several rounds of this cyclic re-entry, the B cells exit the GCBC phenotype whereupon they are antigen-experienced post-GC B cells with affinity matured BCRs (figure 1.2b). These cells either leave the SLO either as a memory B cell or differentiate further to become an ASC including the shortest-lived plasmablasts (PBs) or short- and long-lived plasma cells (PCs). Long-lived PCs are thought to return via efferent lymphatics to bone marrow and other trophic niches where they receive survival signals allowing tonic antibody secretion, the traditional basis of long-term humoral immunity (23,24). Memory B cells are primed to expand upon re-encounter of antigen and are a key cellular substrate of immunological memory.

A CD4+ T cell population expressing the FOXP3 transcription factor known as T regulatory cells (Treg) are important in the peripheral maintenance of self-tolerance. They either differentiate in the thymus or can be induced in the periphery. They exert a broad influence on T cells, antigen presenting cells and also B cells. A subpopulation of FOXP3+ TfH cells known as T follicular regulatory (TfR) are increasingly studied (25). Their full discussion, however, is beyond the scope of this project.

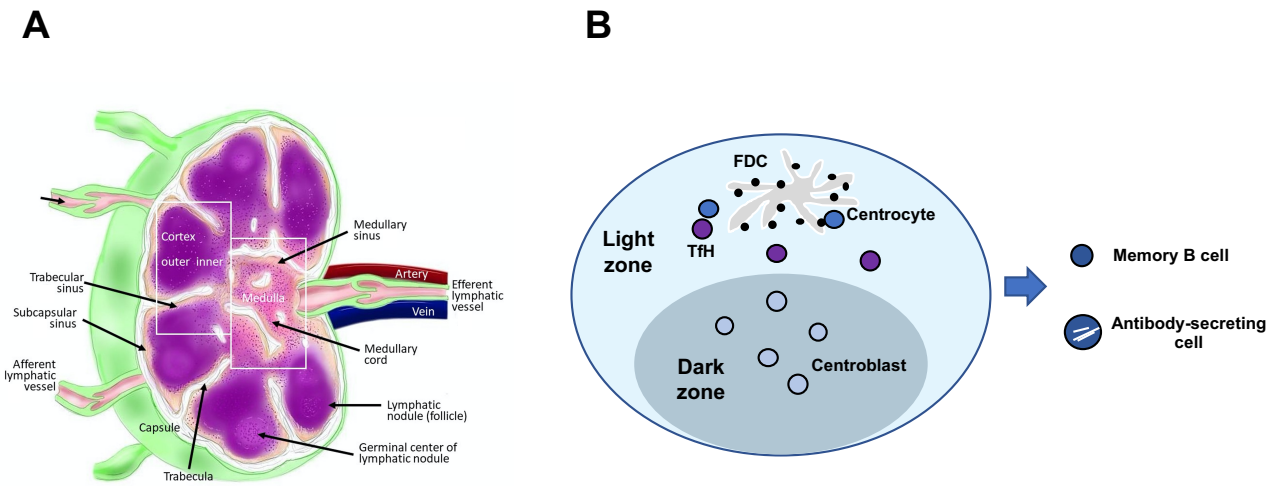


Figure 1.2 – **Secondary lymphoid organs are structured to facilitate the development of germinal centres.**

A – Antigen enters the lymph node in complexes and/or on dendritic cells where it may encounter cognate B cells in the B cell zone which in turn may activate and migrate towards the T cell zone. This can develop into a B cell follicle then germinal centre.

B – An active germinal centre is polarised into a light and dark zone. Germinal centre B cell divide and mutate in the dark zone as centroblasts encounter antigen presented on FDCs and compete for T-cell help. Those selected re-enter the dark zone, without which the centrocytes apoptose. Cells exciting this cyclical process include memory B cells and antibody-secreting cells of which long-lived plasma cells can migrate to survival niches in bone marrow underlying the maintenance of long-term antigen-specific antibody.

Abbreviations used: HEV = high endothelial venule, TfH = T follicular helper cell, FDC = follicular dendritic cell. [A – Image reproduced from Wikimedia commons, Sullivan C., 11.10.19 open access CC 4.0 license, modified minimally to remove lymph flow direction numbers; B – Redrawn image inspired by illustration in Brink *et al.* 2018 (26)]

Beyond improved affinity of the BCR, SHM is usually thought to be accompanied by CSR in GC reactions. CSR ideally shifts antibody isotype specificity from IgM to the most appropriate isotype for the antigenic challenge, as in a classical immunisation paradigm where the antigen-specific response is initially IgM with some IgG, which become IgG-dominant upon re-exposure boosters. New evidence suggests that the mechanism of this, although associated with the onset of GC reactions and hence affinity maturation, is not dependent on the GC reaction itself. Using an immunisation model Roco *et al.* recently suggested that CSR is largely complete prior to the

majority of SHM. They provide evidence that it occurs at the onset of B cell activation with ongoing BCL6 expression in the GCBC phenotype maintaining AID but suppressing downstream enzymes such as apurinic/apyrimidinic endonuclease 1 (APE1) involved in CSR (27). They suggest that uncoupling CSR from SHM can yield a sub-population of affinity matured IgM+ memory B cells that can provide flexibility in future antigenic re-challenge. Hence recurrent antigen-specific IgM production could be suggestive of both early recurrent new GC reactions but also recurrent antigenic challenge without new GC reactions. The overall process of generating antigen-specific affinity-matured antibody-secreting cells is outlined in figure 1.3.

Finally, while most physiological GC reactions are confined to SLOs, they can also occur ectopically in unconventional sites whereupon such tissues are known as tertiary lymphoid organs (TLOs) (28,29). Classical features include development of HEVs leading to lymphocytic infiltration and organisation into B cell follicles, T cell zones and FDCs. Examples include sites of chronic inflammation such as joint synovium in rheumatoid arthritis (30), the meninges in multiple sclerosis (31), or tumours (32). In inflammatory/autoimmune disease they can contribute to pathogenic antibody formation whilst in cancer they are often a positive prognostic factor likely by contributing to anti-tumour immunity (33,34). Whilst this has recently been extended to multiple tumour types, one of the best studied lymphocytic infiltrates has been germ cell tumours. These have been shown to often develop B cell-rich germinal centre-like structures. BCR sequencing has shown the B cells to be clonally expanded, somatically hypermutated, and class-switched – suggestive of local antigen-dependent affinity maturation (35).

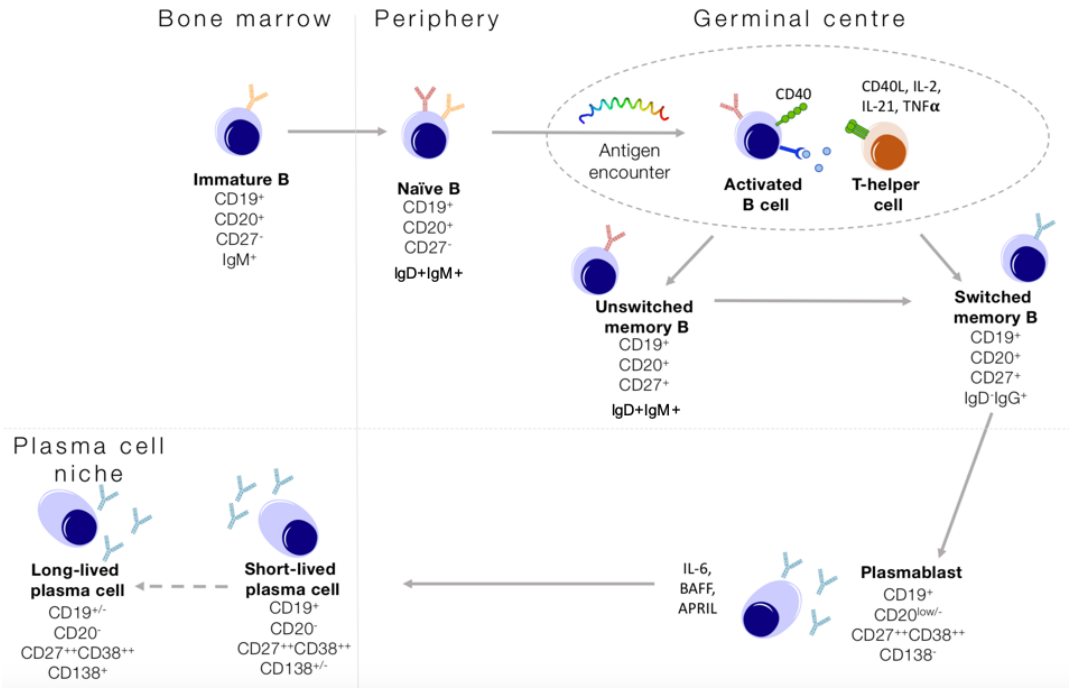


Figure 1.3 – **Summary of B cell development including changes in key surface phenotypic markers.**

Following development from stem cell to an immature B cell in the bone marrow, the cell migrates to the periphery becoming a naïve B cell expressing IgM and IgD. Antigen encounter and a germinal centre reaction produces memory B cells identified by CD27 expression. Many cells undergo class-switching: IgD is lost and IgM switches to an alternative isotype, often IgG. Having gained antigenic memory some of these cells will further differentiate into antibody-secreting cells during which CD20 reduces, CD27 increases and CD38 is newly expressed. In the presence of survival and differentiation factors these cells become further committed to becoming long-lived plasma cells and become CD20 negative and express CD138. They are thought to migrate to plasma cell niches such as in bone marrow where they can also lose CD19.

[Image reproduced from Wilson *et al.* 2018 (36) – open access CC4.0 license]

1.2.5 Autoantibody-mediated autoimmune disease

While autoreactive B cells are to some extent inevitable in the mature naïve B cell repertoire, the relative infrequency of autoantibody-mediated clinical pathology suggests that a strategy to limit this is largely effective. Conversely, it suggests that to activate clones with reactivity against functionally important autoantigens and drive autoantibody responses sufficient to cause clinical levels of pathology there must be failures at some of the junctures.

Autoantibodies can be classified into those that are physiological and those that are associated with pathology within which there is a sub-group of pathogenic autoantibodies (37,38). Natural autoantibodies are usually polyreactive unmutated IgMs and are thought to assist in the clearance of autoantigens released during tissue damage thereby reducing the risk of pathological autoimmunity. In contrast, autoantibodies (39) can also be a characteristic feature of autoimmune diseases. They can be purely epiphenomenal caused by exposure of autoantigens by processes such as T-cell mediated cytotoxicity e.g. glutamic acid decarboxylase (GAD-65) autoantibodies in type 1 diabetes mellitus, generated secondary to the releasing of intracellular enzymes during pancreatic cell death; these are useful biomarkers. Conversely, autoantibodies can be absolutely pathogenic e.g. acetylcholine receptor (AChR) autoantibodies in myasthenia gravis (MG) – both defining and mediating the disease. Sometimes they can be a mixture of both such as Ro or La autoantibodies which can be innocuous, but mediate congenital heart block in neonates following maternofoetal transfer from mothers with SLE (40).

Criteria have been developed to better standardise the conception of antibody-mediated autoimmune diseases. The main criteria of interest are for autoimmune diseases in general so also apply to pathogenic T cells. Witebsky's initial criteria were along similar lines of Koch's postulates to define the relationship between microorganisms and infectious disease, tending towards an absolute distinction between absence and presence of the entity and the pathology (41). In the same way that understanding of the relationship between potentially pathogenic microorganisms became more nuanced, so too was the relationship between autoreactive T cells or antibodies. Hence in 1993, the criteria were updated by Rose

and Bona to account for the realisation that the healthy immune repertoire contained plenty of potential autoreactivity (42). These continue to form the yardstick by which contemporary antibody-mediated autoimmune diseases are judged and were elegantly summarised in their abstract as:

1. Direct evidence from transfer of pathogenic antibody or T cells
2. Indirect evidence based on reproduction of disease in experimental animals.
3. Circumstantial evidence from clinical clues.

Examples of point 1 include maternofoetal transfer leading to congenital disease in the neonate or induction of disease in an animal model by infusion of purified antibody while point 2 is exemplified by immunization with the autoantigen of interest. The clues in point 3 may include: other autoimmune diseases in the same individual or family, lymphocytic infiltration of target organ, human-leucocyte-antigen (HLA) haplotype association, and favourable response to immunotherapy.

In terms of autoantibody-mediated autoimmune disease myasthenia gravis is probably the best example where such experiments and observations have been performed (43). Other examples with a similar level of evidence include Lambert-Eaton Myasthenic Syndrome (LEMS) and voltage-gated calcium channel autoantibodies, and pemphigus vulgaris and desmoglein autoantibodies. Whilst these show that autoantibodies can be the proximate mediator of pathology, the overall response usually requires T cell help. However, unlike the autoantibodies, the autoreactive T cells would only be necessary but not sufficient for the autoimmune disease.

Neurological disease is well represented in the list of autoantibody-mediated autoimmune diseases. This may be due to the relative sequestration of neural antigens, which with sufficient stimulation via over-expression or altered expression of autoantigen such as tumour neoantigens is sufficient to activate clonally ignorant B cells. Others have even speculated that this propensity is a consequence of the co-evolution of nervous and immune systems and is a risk inherent in normal co-development of both systems (44).

1.3 Autoantibody-mediated encephalopathies

1.3.1 Peripheral nervous system

Autoantibody-mediated diseases of the neuromuscular junction were paradigmatic not only of an autoantibody-mediated neurological disease but as discussed above for the whole disease concept per se. The key lessons learned from MG and LEMS included: antigen targets were surface proteins, their function was signalling, the syndromes were immunotherapy-responsive and there could be distinctive HLA haplotypes (e.g. AH8.1 haplotype in MG) and/or tumour associations (e.g. small cell lung carcinoma in LEMS and thymoma in MG). However, the path to the discovery of similar mechanisms operating in the central nervous system (CNS) and consequently being of psychiatric relevance has been more circuitous.

1.3.2 Central nervous system: from paraneoplastic limbic encephalitis to autoimmune encephalopathies

The classical limbic encephalitis syndrome of subacute onset confusion, amnesia, seizures, and psychiatric disturbance affecting older adults was described by Brierley *et al.* in 1960 (45) with an association with lung carcinoma and possible paraneoplastic mechanisms elaborated further by Corsellis *et al.* in 1968 (46). Over

the next few decades the syndrome was established with characteristic tumour and circulating ‘onconeural’ autoantibody associations e.g. anti-Hu with small-cell lung cancer or anti-Ma2 with testicular cancer. Although useful biomarkers readily identifiable by immunoblot assay, their therapeutic modification did not ameliorate the syndrome, and the neuropathology was most consistent with T-cell mediated cytotoxicity with any improvement coming from tumour treatment (47). Unlike in MG and LEMS, these autoantibodies were not pathogenic and portended a negative prognosis.

The application of the voltage-gated potassium channel (VGKC) radioimmunoassay (RIA) firstly in the peripheral syndrome, acquired neuromyotonia (48), but then in the dual peripheral-central disorder, Morvan’s syndrome (49), and then CNS-only limbic encephalitis (50) (51) was a crucial sequence of discoveries suggesting that autoantibodies can directly cause encephalopathy. Further investigation found that rather than VGKCs per se, the autoantibodies were binding to proteins complexed with the VGKC that were present in the brain homogenate upon which the VGKC-RIA was based (52) (53). The two surface targets that associated with these immunotherapy-responsive syndromes were leucine-rich glioma inactivated 1 (LGI1) and contactin associated protein 2 (CASPR2). They were shown to be detected best using a live cell-based assay (CBA) in which human embryonic kidney (HEK) 293T cells were transiently transfected with vectors encoding the protein antigen, expressing them on their cell surface in the native conformation and incubated with patient serum whilst alive, only fixing the cells once any binding had been given time to occur. Therefore, the target epitopes were highly likely to be conformational rather

than linear and intuitively be within an extracellular region such that the target is accessible by the autoantibody *in vivo*.

Alongside this series of discoveries in the 2000s, Dalmau and colleagues identified autoantibodies against the N-methyl-D-aspartate (NMDA) receptor in cases of young women with a progressive encephalopathy leading to autonomic and ventilatory failure associated with ovarian teratoma (OT) (54) (55). Once again similar principles were present: starting with a well demarcated clinical syndrome and using assays that preserved native antigen conformation. While the initial description was in young adults all with OT, later children and non-tumour-associated cases were described alongside the application of a live CBA transfected with NR1 and NR2b NMDAR sub-units to detect the antibodies in serum and CSF (56). The target was later shown to be the NR1 subunit only (57) (58).

This illness and NR1 autoantibodies are the subject of this thesis and discussed in further detail in 1.4. However, as for the concept of autoantibody-mediated encephalopathies per se, the discovery of NMDAR, LGI1 and CASPR2-antibody encephalopathies marked the start of an era of profound expansion of basic and clinical knowledge. Autoimmune encephalitis began to be increasingly recognised on clinical grounds (59) and was recently found to be at least as common as infectious encephalitis (0.8 and 1.0/100,000 person-years, respectively) (60). Alongside this, novel neuronal surface antigenic targets were identified. The antigens were often involved in synaptic signalling e.g. receptors for gamma-aminobutyric acid (GABA), α-amino-3-hydroxy-5-methyl-4-isoxazolepropionic acid (AMPA), and glycine. The majority of these were not tumour-associated but some had classic associations e.g.

small cell lung carcinoma in ~50% with $GABA_BR$-antibody encephalitis (61) (62). This condition also exemplifies that some autoimmune encephalopathies were found to be very similar to classical 'limbic encephalitis' with prominent seizures and temporal lobe inflammation seen on brain imaging, whereas some such as LGI1-antibody encephalitis could progress to look like this, but in their earliest stages often presented solely with dystonic face and/or arm seizures marking a point for potential immunotherapeutic prevention of prevention to cognitive impairment (63) (64). Meanwhile others, such as NMDAR- and $GABA_AR$-antibody encephalitis, could be dominated by psychiatric disturbances for much of the illness course, if not entirely (65,66). Furthermore, unlike classical LE, many autoimmune encephalopathies yield functional disturbances such as EEG abnormalities without frank evidence of structural abnormalities or classical signs of inflammation.

1.3.3 Immunopathology

Bien *et al.* investigated the immunopathology of onconeural versus NSAb-associated disorders (67). They found that the onconeural antibody-associated limbic encephalitis cases consistently showed evidence of T-cell mediated cytotoxicity such as a raised CD8/CD3 ratio and granzyme-B+ cytotoxic T cells apposed to neurons with associated neuronal loss which was absent in the NSAb-associated VGKC-complex and NMDAR- antibody cases. The VGKC-complex-antibody cases showed evidence of complement deposition while the NMDAR-antibody cases were conspicuous for the absence of antibody and complement-mediated damage with normal neuronal appearance and few inflammatory cells. Another study looking at NMDAR-Ab-E found inflammatory infiltrates, predominantly B and T cells perivascularly and ASCs in perivascular, interstitial, and Virchow-Robin spaces (68).

Whilst the weight of evidence now suggests that these are *bona fide* autoantibody-mediated autoimmune diseases, blood-brain barrier (BBB) antibody permeability has been an influential concept throughout the development of the field. This has sometimes lead to on the one hand incredulity of CNS-directed pathogenicity but on the other assertions that it is the key determinant of disease expression (69) (70).

While largely beyond the scope of this discussion these views are worth briefly summarising. For the most common disorders, LGI1- and NMDAR-Ab-E, the criteria of Rose and Bona are fulfilled with direct passive transfer animal models being achieved (71) (72), as well as cellular and molecular demonstrations of pathogenic effects likely to account for the clinical observations (73), distinctive clinical patterns including HLA association for LGI1 (74), OT association for NMDAR, and demography for both. Moreover, the autoantibodies are often directly detectable in CSF as are antigen-specific memory B cells and ASCs (75). However, CSF is sometimes negative in clear-cut clinical cases, particularly LGI1-antibody encephalitis (76). There is an animal model which suggests that the relative abundance of autoantigen compared to autoantibody may mop up the autoantibodies rendering free antibody in the intrathecal compartment below the limit of detection (77). Overall, some of these diseases and/or individual instances of them probably tend to depend more on peripheral antibody and others more on intrathecal synthesis. Unlike LGI1-antibody encephalitis, NMDAR-Ab-E has a prerequisite of detectable CSF NR1 autoantibodies but in both conditions identical clinical presentations may or may not have CSF lymphocytosis, unmatched oligoclonal bands, whilst both may be highly responsive to peripherally directed

treatments such as plasma exchange. There is no positive evidence of BBB dysfunction in AE, but it has not been studied extensively.

A lymphocyte-centred approach to investigate how autoantigen-specific cells are primed to cross into the CNS in these diseases would probably yield the most answers. Neuropathological samples from these patients were rare when first discovered, with better treatments and no need to biopsy to make the diagnosis, they are now even rarer. Therefore, such studies will need to make use of animal models and novel imaging methods to address this sort of questions.

1.3.4 Neuronal surface antibody assays

Delineation of the typical clinical syndromes and optimisation of neuronal surface antibody (NSAb) detection methods has developed reciprocally (78). As outlined above, the fundamental paradigm has been that target antigens for autoimmune encephalopathies are conformational epitopes on surface targets which almost universally require assay systems that can replicate this (figure 1.6). During the discovery phase when the target antigen is unknown, methods that display multiple antigens are useful e.g. immunohistochemistry of fixed rodent brain slices ('Tissue-based assay'; TBA) or immunofluorescence using live primary rodent neurons ('Neuron-based assay'; NBA). CBAs that expose a single transfected antigen are useful during both the discovery to test candidate antigenic targets, and also post-discovery for diagnostic testing. TBAs and NBAs can be used in the post-discovery phase for validation of CBA results (figure 1.4). This is usually the case when fixed CBAs are used where exposure of intracellular irrelevant antigens risks non-specific binding. Using a live version of the CBA avoids this by only exposing surface

epitopes to the sample, and has been shown to have the best performance for some CNS antigens (79) (80). These considerations are discussed with reference to the detection of NMDAR NR1 subunit autoantibodies in 1.4 and throughout the data chapters.

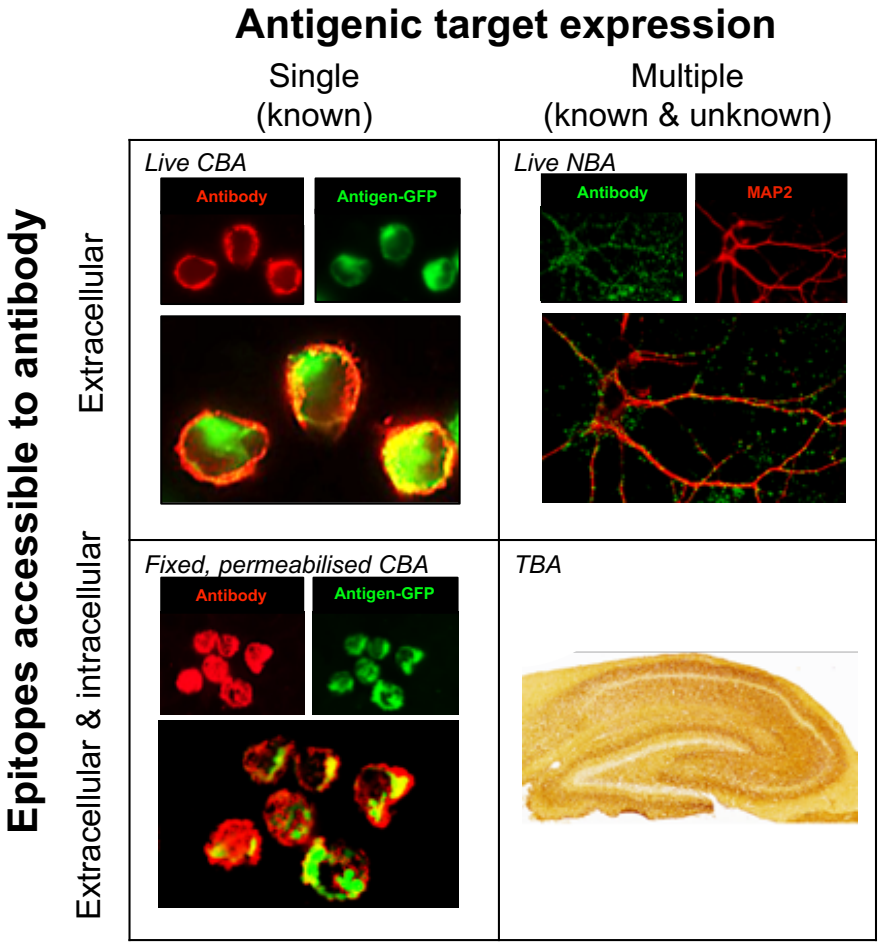


Figure 1.4 – **Examples of assays used in the detection of neuronal surface antibodies against conformational epitopes.**

Methods cluster into broadly two categories: single or multiple target antigens and intracellular antigen exposure or not. A single antigen is by definition a known antigen. These assay properties render different roles during the discovery and diagnostic testing of neuronal surface antibodies.

Abbreviations used: CBA = cell based assay, NBA = neuron based assay, TBA = tissue based assay.

[Figure reproduced from Ramanathan, Al-Diwani *et al.* 2019 – open access CC4.0 license]

1.4 N-methyl-d-aspartate receptor-antibody encephalitis

1.4.1 N-methyl-d aspartate receptors (NMDARs)

1.4.1.1 Structure and function

NMDARs are ionotropic glutamate receptors permitting the influx of sodium and calcium ions when stimulated by the agonist glutamate and co-agonist glycine or D-serine. They are tetramers composed of two dimeric pairs, i.e. heterodimers. The obligate subunit, NR1, makes up one pair and one of NR2A-D or NR3A-B makes up the other pair (figure 1.5a). Subunit structure includes an amino terminal domain (ATD) which is the most extracellular component, linked to an agonist binding domain (ABD; also called ligand binding domain, LBD), and then a transmembrane domain (TMD) and intracellular carboxy terminal domain (CTD) (figure 1.5b). Subunit combinations vary by brain region and also during development according to functional demands. The subunits are now called GluN1, GluN2, and GluN3, however in the context of autoimmune encephalitis NR1 continues to be used commonly and continued in this thesis.

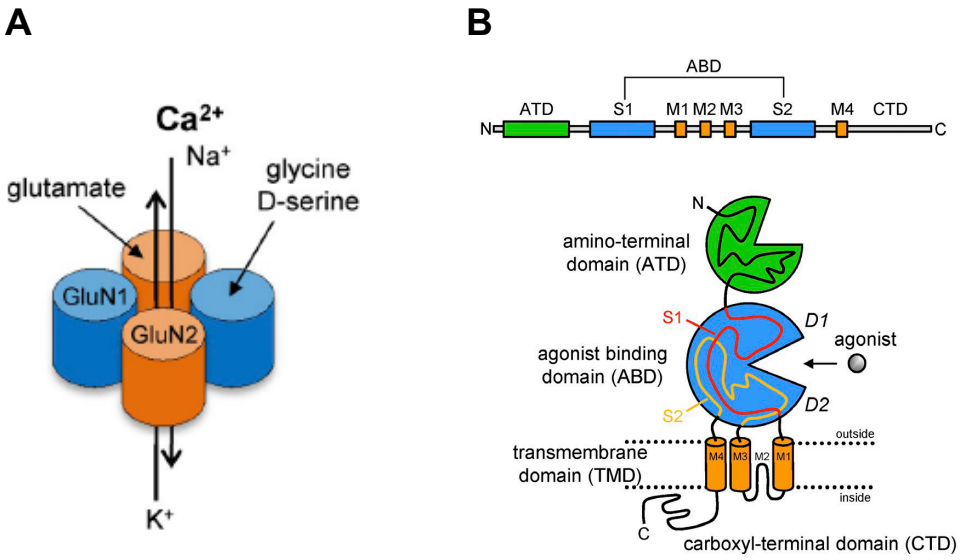


Figure 1.5 – **Structural and functional properties of NMDA receptors.**

A – Generic tetrameric structure, channel pore, and agonist binding sites.
B – Subunit structural domains.
[Figures reproduced from Hansen *et al.* 2018 (81) – open access CC4.0 license]

The most studied function of NMDARs is in the regulation of synaptic plasticity. The channel contains a magnesium ion that is removed in a voltage-dependent manner prior to cationic influx. By opening in the context of temporally-summated fast excitatory post-synaptic currents they are regarded as a coincidence detector. This regulates downstream signalling and is fundamental to the neurophysiology of learning and memory.

1.4.1.2 The clinical phenomenology of NMDAR pore-blocking drugs

There are a variety of substances that interact with NMDARs. The agents most relevant in the context of antibody-mediate NMDAR disruption are drugs that block the channel pore such as Phencyclidine (PCP), ketamine, and dextromethorphan. These have been of particular interest to model core domains of schizophrenia psychopathology under experimental conditions (82).

PCP was originally developed as a dissociative anaesthetic. However, often drastic mental state changes detracted from its popularity in the operating theatre but boosted its value on the illicit market (83). This reached epidemic levels in the 1970s-1980s, providing opportunities to profile its psychopathologic sequelae (84). Characteristic findings included: time distortion, emotional instability, imperviousness to pain, alternating stupor-excitement, aggression with violence and self-mutilation, possession-like ‘superhuman strength’ and bizarre posturing (85,86). Indeed, contemporary phenomenology studies noted a lower rate of Schneider’s first rank symptoms compared to both acute schizophrenia and cocaine-induced psychosis (87). Rosse *et al.* found that PCP was more closely associated with: “delusions of physical power, altered sensations, and unusual experiences [e.g., out of body

experiences, experiencing religious figures or events directly (e.g., being with Noah at the time of the Arc)]" than paranoia and suspiciousness. The presentation of PCP use was noted to be highly dose-dependent with a psychiatric syndrome expected between 5-10mg orally escalating to coma at doses >10mg with autonomic and dystonic-choreoathetoid movements often noted. A further relevant clinical experience was that PCP-induced syndromes were usually benzodiazepine-responsive whereas anti-psychotics could worsen hyperthermia and movement disorder (88).

The PCP-derivative ketamine, while currently of interest as a rapidly-acting anti-depressant, has through most of its history largely been conceptualised as a dissociative anaesthetic. It has similar properties to PCP including analgesia and a vasopressor effect, making it of use in battlefield trauma. It is also used recreationally with some overlaps with PCP such as prominent time distortion and loss of body ownership (the so-called 'K hole') (89). Ketamine has also been shown to cause the most phenomenologically-robust near-death experience in a large catalogue of reports (90).

Dextromethorphan is common in cough syrups and is sometimes known as 'the poor man's PCP', i.e. it can induce a syndrome similar to PCP if taken at a high enough dose. Such 'robotripping' can cause insomnia, vivid and terrifying dreams, dissociation, and violence (91). Indeed, an informative case report from Stanciu *et al.* described a 20 year-old woman who had taken large amounts of cough syrup leading to uncontrollable screaming, disorganised behaviour, labile mood, and

incoherent, pressured speech containing both grandiose, hyper-religious and paranoid ideas (92).

1.4.1.3 The clinical phenomenology of NMDAR gene mutations

The NR1 autoantigen in NMDAR-Ab-E is encoded by the gene GRIN1, of which mutations can cause a rare disorder called 'Neurodevelopmental disorder with or without hyperkinetic movements and seizures'. Despite affecting neurodevelopment and leading to severe intellectual disability, there are several aspects of the phenotype that may anticipate patterns from acquired NR1 antibody-mediated NMDAR dysregulation. In addition, in a large series reported by Lemke *et al.*: 8/23 had a sleep disorder, 4/23 had a behavioural syndrome involving aggression and self-injury, and 1/23 had inappropriate alternating laughter and crying (93). Genetic disorders of non-NR1 NMDAR subunits such as NR2a (GRIN2A) and NR2b (GRIN2B) whilst also associated with intellectual disability do not appear to cause such a characteristic pattern of movement and mental state abnormalities. This may be due to NR1 being present in all NMDARs whereas NR2a and NR2b show greater region- and time-dependent specificity (81).

1.4.2 Initial description and historical precedents

As noted in 1.3 the likely NSAb-mediated nature of the syndrome was first demonstrated by Vitaliani *et al*. who in 2005 reported four young adult female patients with a clinical syndrome of acute psychiatric features, amnesia, speech disturbance and seizures followed by a precipitous fall in consciousness and need for invasive ventilation whose serum or CSF avidly bound hippocampal neuropil on rat brain tissue slices and live cultured neurons. The pattern was not seen in control

samples and differed from VGKC-complex autoantibody samples. Their follow-up study in 2007 expanded the cohort to a total of 12 cases with the same clinical pattern and identified the target as the NMDAR by expressing subunits in a fixed CBA. In both series all the patients had a co-incident OT; resection was associated with recovery.

While these two papers have become the starting point of most accounts since, the clinical syndrome had been described previously, as noted by the authors. In 1997 two case reports from Japan reported an OT-associated encephalopathy with a prominent mental disturbance including psychotic, catatonic, and amnestic features, unresponsive to psychotropic medication but clinically and electrophysiologically responsive to OT resection (94) (95). Also in Japan, an established syndrome known as ‘acute juvenile non-herpetic encephalitis’ was later shown to largely be accounted for by NMDAR-Ab-E (96). Further expanding the foray into historical entities, Dale and colleagues found that stored sera from patients with dyskinetic encephalitis lethargica were seropositive for NMDAR autoantibodies and matched the clinical profile of NMDAR-Ab-E (97). There are many case reports prior to the conceptualisation of the syndrome as an autoimmune disease that providing useful natural history. For example, in 2000 Shill *et al.* reported a case of ‘malignant catatonia secondary to sporadic encephalitis lethargica’ where a 22 year old female presented with progressive catatonia, oculogyric crises, and dysautonomia with CSF lymphocytosis, bifrontal slowing on EEG and normal brain MRI that responded to electroconvulsive therapy (98). As well as malignant catatonia, cases were also reported in presentations initially suspected to be neuroleptic malignant syndrome but were actually anti-psychotic-mediated decompensation of NMDAR-Ab-E (99)

(100). Finally, several cases have been reported of atypical long-term disorders thought to be primary psychiatric syndromes such as schizophrenia or bipolar disorder, which upon review fit far better with NMDAR-Ab-E, proven by detection of NR1 autoantibodies in CSF (101) (102). This was famously demonstrated by a neurologist who developed a severe mental illness aged 48, eventually having his CSF tested which revealed CSF NR1 autoantibodies and a favourable response to immunotherapy (103). This neurologist, Dr. Escudero, has since gone on to be a vocal advocate for the need to consider the diagnosis in new-onset severe mental illness.

1.4.3 Consensus diagnostic criteria

In 2016 an international group of expert clinicians and scientists published a position paper containing consensus opinion on possible, probable and definite criteria for multiple autoimmune brain disorders, including a specific section on NMDAR-Ab-E (104). Like any such exercise, this aimed to standardise diagnostic strategies by being clear about the circumstances that definitively rule the disease in or out so as to avoid under-diagnosis by encouraging clinical recognition and empirical treatment as well as over-diagnosis and unnecessary treatment (105). The most important decision with respect to NMDAR-Ab-E was to prioritise CSF NR1-IgG positivity. For example, while the diagnosis of ‘probable’ disease requires all three of: 4/6 symptom groups, EEG and/or CSF abnormalities, and reasonable exclusion of other disorders, ‘definite’ disease only needs 1/6 symptom groups and CSF NR1-IgG on any assay platform. Serum NR1-IgG is only equivalent if a ‘confirmatory test’ is obtained in addition to a CBA result.

This approach reflected a combination of the extremely low likelihood of detectable NR1-IgG in CSF outside of this disease (although it is possible) (106) leading to almost complete specificity of the finding, as well as commercially available fixed CBA kits performing better on CSF than serum (107). It also reflected an increasing number of positive serum results from live CBAs in multiple clinical contexts, including psychiatric *prima facie* plausibly relevant presentations (108), but also conditions such as Creutzfeldt-Jakob disease, in which as an irreversible prion-mediated disease, seropositivity is highly unlikely to indicate a primary or even secondary NMDAR-Ab-E but instead arise epiphenomenally from neuronal destruction akin to the onconeural antibodies seen in classical paraneoplastic limbic encephalitis (109,110). These considerations are explored further in 1.6 and a key starting point for the investigations in subsequent data chapters. To briefly foreshadow this, it is useful to look at the strict application of this approach in the published record.

In a study published in 2015, serum samples previously collected from women with postpartum psychosis were screened in a discovery manner using a TBA and live NBA in the laboratory of the proponents of this approach (111). Samples from 4/96 PPP cases and 0/64 control healthy postpartum women were found to be TBA and NBA positive. 2/4 of these went on to be positive for NR1-IgG using a fixed CBA. Consequently, these were reported as NMDAR-Ab-E. However, beyond an acute psychiatric syndrome, the only differentiating factor was slight extra-pyramidal sensitivity to haloperidol. The authors note that this can be observed in NMDAR-Ab-E, but it is also observed in anyone given any drug with sufficient dopamine D2 receptor antagonism, particularly younger patients (112). The patients did not have

OTs, a movement disorder, seizures, dysautonomia, and all improved with usual management of PPP – i.e. they could not be differentiated prospectively. Hence, these highly robust assay protocols showed that there were undoubtedly NSAbs to NR1 and unknown neuronal surface targets present in the serum of these cases. However, even when acknowledging the caveat that clinically-limited spontaneously-remitting cases of NMDAR-Ab-E do occur, these are a rare exception, and therefore disease classification and the associated inference of definitive causality because an additional test was positive appears inconsistent with biological likelihood and the clinically-driven essence of the consensus criteria.

Panel 4: **Diagnostic criteria for anti-NMDA receptor encephalitis**

Probable anti-NMDA receptor encephalitis*

Diagnosis can be made when all three of the following criteria have been met:

1 Rapid onset (less than 3 months) of at least four of the six following major groups of symptoms:
- Abnormal (psychiatric) behaviour or cognitive dysfunction
- Speech dysfunction (pressured speech, verbal reduction, mutism)
- Seizures
- Movement disorder, dyskinesias, or rigidity/abnormal postures
- Decreased level of consciousness
- Autonomic dysfunction or central hypoventilation

2 At least one of the following laboratory study results:
- Abnormal EEG (focal or diffuse slow or disorganised activity, epileptic activity, or extreme delta brush)
- CSF with pleocytosis or oligoclonal bands

3 Reasonable exclusion of other disorders (appendix)

Diagnosis can also be made in the presence of three of the above groups of symptoms accompanied by a systemic teratoma

Definite anti-NMDA receptor encephalitis*

Diagnosis can be made in the presence of one or more of the six major groups of symptoms and IgG anti-GluN1 antibodies,† after reasonable exclusion of other disorders (appendix)

*Patients with a history of herpes simplex virus encephalitis in the previous weeks might have relapsing immune-mediated neurological symptoms (post-herpes simplex virus encephalitis). †Antibody testing should include testing of CSF. If only serum is available, confirmatory tests should be included (eg, live neurons or tissue immunohistochemistry, in addition to cell-based assay).

Figure 1.6 – **Diagnostic criteria for NMDAR-Ab-E as per consensus guidelines of Graus *et al.* 2016.**

[Table reproduced from Graus *et al.* 2016 (104) with permission from Elsevier.]

1.4.4 Neurobiological disease mechanisms

There have now been several studies that have investigated the effects of patient NR1-IgG on synaptic NMDARs. These have largely shown that antibodies cross-link receptors triggering their internalisation and/or displacement from their post-synaptic clusters. For example, Moscato *et al.* showed a selective reduction in NMDAR neuronal surface availability after application of purified patient IgG (113) which was also shown by Kreye *et al.* with patient-derived recombinant monoclonal antibodies (75). In both instances this was reversible upon removal of the IgG. This does not occur with patient IgG-derived Fab fragments alone but when these were cross-linked with Fab antibodies the effect was restored showing that divalent binding is necessary for pathogenicity (114). It was later shown that the antibodies disrupt interaction between NMDARs and EphB2 in the post-synaptic density leading to their extra-synaptic displacement which contributes to pathogenesis alongside internalisation (115) (116) (73). Despite the NR1-IgG antibodies being largely of the IgG1 sub-class and able to fix complement *in vitro* (56), post-mortem studies did not find evidence of complement deposition (68).

A passive transfer animal model using cerebral intra-ventricular osmotic pumps to infuse the brain with purified patient IgG showed that the antibodies could recapitulate aspects of the human syndrome including memory disruption and anhedonia but without seizures or a movement disorder. These were associated with reduction in NMDAR cluster availability, greatest in the hippocampus and both the pathology and the behavioural effects were reversible on withdrawal of the antibodies (71). This has been complemented by non-invasive studies of patients using electroencephalography (EEG) and structural/functional brain magnetic

resonance imaging (MRI). Dynamic causal modelling of EEG from patients has suggested specific NMDAR-mediated circuit dysfunction leading to distinct fronto-parietal network changes (117). MRI has shown generally absent or mild gross structural changes but white matter changes using diffusion tensor imaging (DTI) and blood oxygen level dependent (BOLD) fMRI has shown marked network disruption between multiple distributed large-scale networks (118,119).

1.4.5 Immunobiological disease mechanisms

1.4.5.1 – NR1 as the target antigen

Initial studies showed that the target antigen was within the NMDAR and also conformational because it could only be identified using structurally intact antigen, not on systems where the protein is denatured such as Western blot. The target was first thought to be in the NR2b subunit (55). However, a year later using differential combinations of NMDAR subunits in fixed CBAs this group found that NR1-NR1 dimers had the same positivity rate as NR1-NR2B meaning that NR1 was sufficient to explain the binding. Furthermore, a NR1 deletion construct that removed ATD residues 25-380, markedly abrogated binding. This was extended in 2012 by Gleichman *et al.* who found via site-directed mutagenesis of residues that could undergo N-linked glycosylation that changing residue 368 from asparagine (N) to glutamine (Q) abrogated binding to a similar extent as deletion of the whole region (120). They found these patterns consistently between IgG from the original young female and other childhood onset and older male onset patients suggesting that the autoantigen was the same across differing disease-associated demographic groups. Taken together this suggested that the conformational epitope or possibly several

epitopes lay within the an extracellular ATD regional structure influenced by post-translational modification by N-linked glycosylation.

1.4.5.2 – NMDAR-Ab-E with ovarian teratoma

OTs are the most common germ cell tumour, a class of neoplasm arising from gametes. They classically involve all three germinal layers and consequently can form a full array of differentiated tissue types including teeth, hair, epithelia and neuro-glial elements. They can be mature, containing largely differentiated tissue, well-encapsulated, and benign, or immature, with less differentiation and greater likelihood of malignant transformation.

As described in 1.3.2, NMDAR-Ab-E was discovered in the context of co-existent OT and initially thought to be a paraneoplastic disease entirely (55). The remarkable observation in these cases was the neuropsychiatric therapeutic efficacy of OT resection and conversely the negative prognostic implications in cases where this was not done (121). Within OTs, there have been no systematic differences in this pattern found between mature or immature, and/or unilateral or bilateral combinations (122). As non-OT-associated cases were increasingly described and indeed found to be the majority, in contrast to the OT-associated sub-group, these cases had a greater propensity to treatment resistance, often requiring multiple immunotherapies. These findings directly implicated the NMDAR-Ab-E-associated OTs with encephalitis pathogenesis. This could be as a source of antigen, antibody, and/or antibody-secreting cells.

Another clear and intriguing observation is that OTs are a common ovarian tumour type; they account for 10-20% of ovarian tumours, yet despite their clear aetiological association with NMDAR-Ab-E the vast majority do not have autoimmune complications. Indeed, NR1-IgG is not found in patients without the clinical syndrome of NMDAR-Ab-E implying that when an OT autoimmunises against NR1 this tends to produce a full-blown NMDAR-Ab-E rather than asymptomatic seroconversion (123-125). Cases where NMDAR-Ab-E has been triggered by the removal of OTs suggest that there can be considerable NR1 autoimmunisation without peripheral spillover (126,127). It may be that the often-marked encapsulation of OTs not only provides a cytokine-enriched microenvironment trophic for immune reactions, leading to a highly concentrated NR1-autoantigen/autoantibody/autoreactive cell environment that when this does rupture, an encephalopathy is inevitable. A prospective study of NR1-autoimmunisation in OTs has not yet been done and would be needed to test this concept.

Nonetheless, the relationship between OTs and autoantibody-mediated autoimmune disease is not unique to NMDAR-Ab-E. Non-neurological autoimmunity has been OT-associated in a minority of autoimmune haematological disorders such as autoimmune haemolytic anaemia (128) (129) and immune thrombocytopenic purpura (130). Similar to autoimmune encephalitis, such otherwise treatment-resistant cases were profoundly responsive to removal of the OT with ongoing remission after the withdrawal of disease-modifying drugs.

Furthermore, autoimmune encephalopathies have begun to be described that are OT-associated and resection-responsive against other neuroglial surface antigens such as glycine receptor (131) and CASPR2 (132). The novel glial fibrillary acidic protein (GFAP) autoantibody-associated meningoencephalitis is largely T cell-mediated and GFAP is intracellular, but some cases have an OT association and some of these have detectable NR1-IgG with a clinical flavour of the full NMDAR-antibody syndrome e.g. dyskinesia or bizarre behaviours (133). These rarer examples suggest that OTs can be a source of neural autoimmunity against a variety of targets but that NR1 appears to be the most common.

Taken together, these findings are best considered as an interaction between OT factors and 'host' factors. While it is possible that OTs are uniform and the major distinction is in the host e.g. HLA polymorphism, chance development of NR1-reactivity in the naïve repertoire, a recent study of OTs with and without NMDAR-Ab-E found that the encephalitis-associated cases were more likely to have pathological hallmarks such as Rokitansky nodules and for infiltrating lymphocytes to organise as germinal centres (134). Furthermore, it has been suggested that neuro-glial elements in disease-associated OTs are more likely to be dysplastic and reminiscent of glioma potentially invoking the presence of NR1 neoantigens, perhaps sufficiently different in epitope structure from native NR1 to drive a nonetheless cross-reactive NR1 immune response (126) (135) (136).

Meanwhile, the 'host-centred' view has found fewer clues. The main association is young females, which is the association of OTs per se so not useful. While robust HLA associations of very large effect sizes have been found for LGI1 and CASPR2-

autoimmunity (74), such irrefutable associations have not been found for NMDAR-Ab-E; neither overall nor for OT-associated cases specifically (137). Alternatively, a view centred around there being mature naïve B cells ignorant of NR1 due to largely CNS sequestration is possible. This is also needed because the sheer number of antigens expressed in OTs yet NR1 emerging as the dominant autoantigen is otherwise improbable.

Analysis of patient CSF-derived recombinant MAbs has surprisingly found a predominance of unmutated sequences which are able to easily bind NR1 (75) adding empirical weight to this option. This would also be a starting point in non-OT-associated cases as well. In stark contrast, the infrequency of reports of testicular teratoma-associated NMDAR-Ab-E (138) suggests that there is a probably a sex-related difference of which either circulating or local ovarian oestrogens is the main candidate perhaps lowering B cell activation threshold (139).

1.4.5.3 – NMDAR-Ab-E without ovarian teratoma

As outlined in 1.4.5.2, NMDAR-Ab-E without ovarian teratoma is now established as the most common presentation of the disease. It is still most common in young adult females, but unlike OT-associated cases also occurs in infants, children and older adults (figure 1.7a). It is also more prone to treatment-resistance and/or relapse without the use of 2nd line therapies (121) (figure 1.7b,c). These clinical factors provide important clues to guide investigation of the autoimmunising mechanisms in these patients. The dominant young female demographic is shared with many other autoantibody-mediated diseases but the lack of a significant peak in older adults unlike MG suggests that being female, post-pubertal and pre-menopausal is a

relevant factor and probably relates to oestrogenic effects on B cell activation, but this has not been formally investigated in this disease.

1st line treatments include steroids, intravenous immunoglobulin (IVIG), and plasma exchange (PLEX), and probably reduce complications and disease episode length. These therapies will not directly modify B, T or ASC populations, hence if autoimmunisation generates significant antigenic memory and/or niched ASC populations, particularly if these become resident within the CNS, then it makes sense that a discrete disease episode may perpetuate and the propensity for new disease episodes to initiate would have been unmodified. In contrast, 2nd line therapies such as rituximab, cyclophosphamide, or bortezomib will modify B, B+T, or plasma cells respectively, which is the likely explanation for their apparent efficacy. Therefore, the notion that these should be withheld as a 2nd line treatment in NMDAR-Ab-E without OT is increasingly questioned.

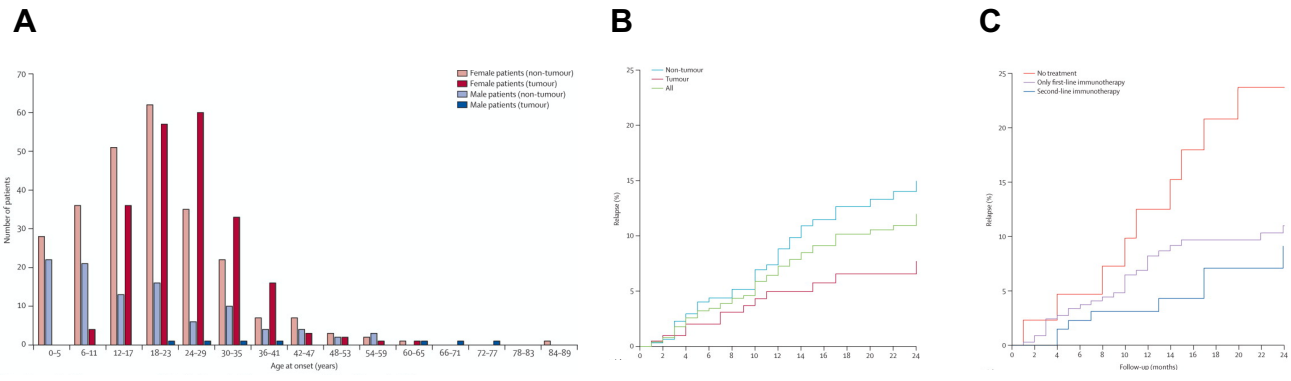


Figure 1.7 – **Demographic and tumour associations of NMDAR-Ab-E and therapeutic associations.**

A – Age, sex and tumour distribution.
B – Relapse risk according to tumour association.
C – Relapse risk according to use of 1st vs 2nd line immunotherapy. Tumour is almost entirely ovarian teratoma in this study.

[Figures reproduced from Titulaer *et al.* 2013 (121) with permission from Elsevier.]

Unlike in OT-associated cases, the trigger in these patients is largely unclear. However, a sub-group who develop the illness as a secondary encephalitis following an initial primary viral, largely herpes simplex, encephalitis (HSVE) provide a valuable model. These cases were first described in children who developed a choreo-athetoid movement disorder after having recovered from HSVE and CSF testing showed negative HSV PCR but positive NR1-IgG, and the syndrome showed immunotherapy-responsiveness (140-142). Of relevance to mechanism, TBA and NBA on CSF often showed clear neuronal staining patterns without NR1 positivity on CBA or with NR1 plus reactivity to additional antigens. This contrasts with primary NMDAR-Ab-E where reactivity to non-NR1 neuronal antigens with patient samples is rare. A larger follow-up prospective study of HSVE patients confirmed that secondary autoimmune encephalitis occurred at a highly appreciable rate (14/51, 27%) with NR1 the dominant antigen (9/14) but the other TBA/NBA positive patients were against other antigens. Moreover, of those that did not develop autoimmune encephalitis, seroconversion occurred at a similar rate (11/37, 30%) of which 3/11 were NR1 and the rest against other antigens (143). Given that HSV can be highly destructive to brain tissue this is most consistent with the desequestration of brain antigens into the periphery leading to autoimmunization rather than antibodies raised against HSV cross-reacting with NR1. The overall rate of 25/51 (49%) of neuronal autoimmunization implies that BCRs in the mature naïve repertoire with potential reactivity with neuronal epitopes are common.

The threshold determining conversion to the clinical syndrome is likely multifactorial. The overall dominance of NR1 (12/25, 48%) could be related to NR1 being highly expressed in the temporal lobes, the region for which HSV is most tropic, and/or

frequency of potentially NR1-cross-reactive BCRs. The other factor that probably renders HSVE so effective at provoking this response is the TLR-mediated danger signal provided by the virus itself potentially providing sufficient stimulation for the brain self-antigens to be treated as pathogenic. The main points of contrast with OT-associated disease are that the post-HSVE cases have a clinico-pathologic spectrum with asymptomatic seroconversion through to partial phenotypes occasionally spontaneously remitting through to severe AE, whereas OT-associated cases are either the full syndrome or nothing. Furthermore, post-HSVE serum/CSF is frequently reactive against multiple neuronal surface targets whereas OT-associated NMDAR-Ab-E cases tend to only react with NR1.

The overall message is consistent with classical immunisation mechanisms i.e. B cells encountering cognate antigen with some form of help to drive activation and differentiation. The common aspect of HSVE and OT as triggers is the desequestration of neural antigens; HSVE via frank necrosis of brain tissue and OT via ectopic over-expression. If the naïve BCR repertoire is as leaky as it appears for neural antigens and if danger signals associated with viraemia or a tumour microenvironment exceed potentially counter-acting peripheral tolerance mechanisms then neural autoimmunity may be triggered. If during their activation these NR1-specific lymphocytes express ligands that allow transmigration through the BBB then the antigen-rich environment of the CNS may be sufficient to perpetuate these populations possibly over time becoming independent from the periphery. Indeed, in a recently reported mouse model immunisation with NR1 successfully induced a fulminant encephalitis with detectable NR1-IgG and recapitulation of several clinical features including seizures. Conformational-

stabilisation of the antigen was necessary to achieve this, consistent with observations from assay methods in human samples (144) and the lack of such a response in other NR1 active immunization models that were less likely to achieve such a concentrated exposure of conformational epitopes (145).

These suggestions of a peripheral onset prior to a migration into the CNS have been complemented from a study of patient derived peripheral blood mononuclear cells (PBMCs) which found that TLR-stimulation and/or cytokine conditions resembling T-cell help were sufficient to differentiate ASC populations from NMDAR-Ab-E PBMCs that produced NR1-IgG *in vitro* proportionate to serum levels (146). The optimised cytokine conditions reported in this study established by these experiments were continued in the cell culture experiments conducted in this thesis (Figure 1.8).

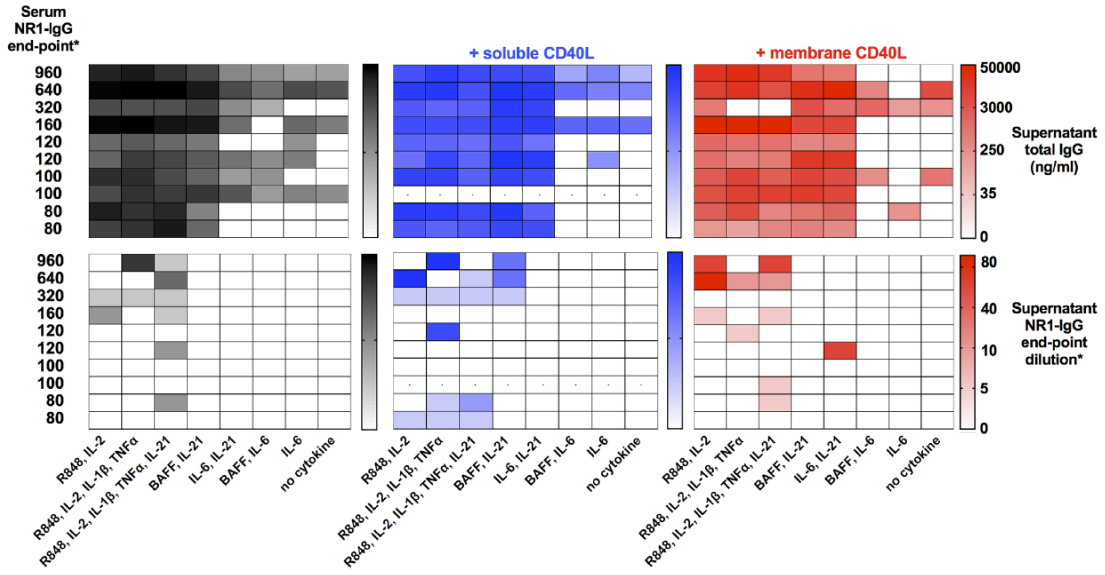


Figure 1.8 – **The relationship between cytokine condition, serum NR1-IgG level and production of total and NR1-specific IgG *in vitro*.**

PBMCs from 10 patients with NMDAR-Ab-E were cultured under differing cytokine conditions with or without CD40 ligand either soluble (blue) or expressed on co-cultured feeder cells surface membrane (red). Maintenance conditions (BAFF/IL-6) occasionally produced total IgG (upper heat map row) but never NR1- specific (lower heat map row) whereas combinations of IL-1β, IL-2, IL-21, IL-2, TNFα and R848, particularly in the presence of CD40 ligand consistently produce total IgG and often NR1-specific IgG. CD40 ligand, IL-2, and R848 was the most successful.

Abbreviations used: Ig=Immunoglobulin, CD40L=CD40 ligand, IL=interleukin, BAFF=B cell activating factor, TNF=tumour necrosis factor.

[Image reproduced from Makuch *et al.* 2018 (146) – open access CC 4.0 license.]

A further unresolved question is the location of the meeting of antigen and cognate B and T cells. The most obvious site would be in secondary lymphoid organs such as lymph nodes because this tissue is specialised for bringing antigen into contact with B and T cells and potentially triggering germinal centre reactions to generate affinity matured antibodies from ASCs and derive antigen-specific B memory cell populations. In recent years, meningeal lymphatics have been rediscovered, principally by the Kipnis laboratory, who have also explored experimental models that have suggested that these vessels provide a route by which CNS proteins can enter the periphery, draining into cervical lymph nodes (147,148). This could be highly relevant for post-HSVE neural autoimmunization and may be relevant to the

majority of NMDAR-Ab-E cases where the trigger is unclear. Indeed, in one rituximab-refractory case who died, post-mortem examination revealed clusters of CD138+ cells morphologically consistent with plasma cells distributed along cervical lymphatic sinusoids but not in the spleen (Figure 1.9) (149). The antigen-specificity of the plasma cells was not proven but the patient was NR1-IgG seropositive 4 days prior to death despite several cycles of PLEX and B cell depletion, consistent with these cells probably contributing significantly to circulating NR1-IgG, and given an absence of B cells and plasma cells within brain sections, possibly disease-mediating CSF NR1-IgG too. Given their location in efferent sinusoids, this was consistent with cervical lymph node germinal centre reactions occurring in proximal lymph nodes, most likely prior to rituximab administration.

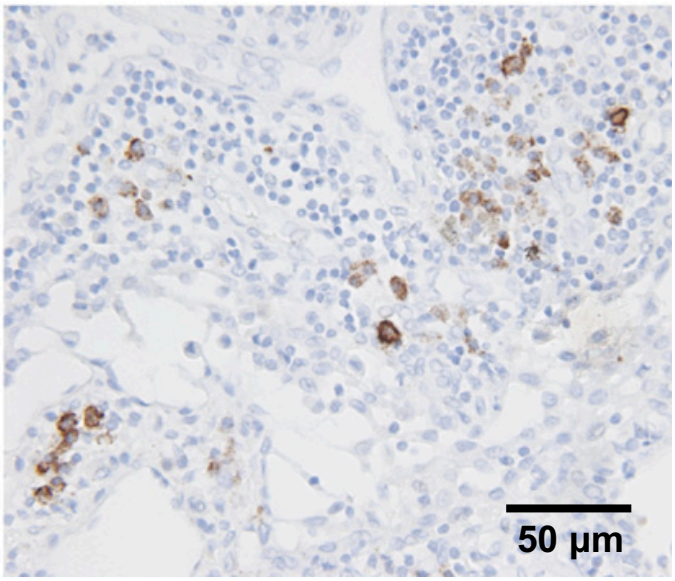


Figure 1.9 – **Post-mortem examination of lymphatic sinusoid with CD138 staining from a case of rituximab-resistant NMDAR-Ab-E.**

This revealed clusters of CD138+ cells with cellular features of plasma cells including eccentric nuclei and characteristic chromatin appearance.

[Image reproduced from Nauen 2017 (149) with permission from Elsevier.]

Taken together, lymphoid tissues are an intuitive and partially empirically demonstrated site of autoimmunization and ASC niche provision in NMDAR-Ab-E. A summary of potential mechanisms has been summarised by Dalmau (150) and is reproduced in figure 1.10. Direct testing of these possibilities is a key aim of this thesis.

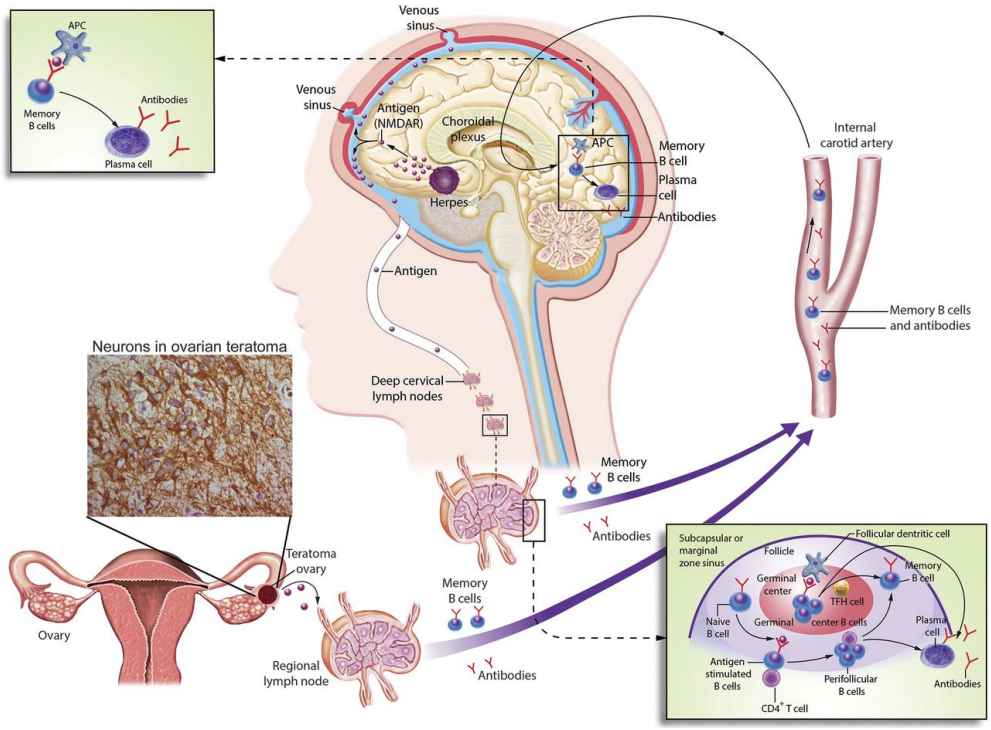


Figure 1.10 – **Possible immunising sites in NMDAR-Ab-E.**

It is predicted that autoimmunisation can happen distant from the brain via ectopic neural tissue in ovarian teratoma or proximal to the brain in cervical lymph nodes. Classical antigen-B-T interactions in germinal centres within these lymphoid sites are predicted to play a role and disease-mediating autoantibodies could be secreted by plasma cells in the periphery or those that have differentiated within the brain.

[Figure reproduced from Dalmau 2016 (150) with permission from Wolters Kluwer Health.]

1.5 NMDAR-autoantibodies in non-encephalitic psychiatric and neurological disorders

Following the discovery of NMDAR-Ab-E there followed a number of investigations to ascertain the relevance of the discovery to common broad syndromes such as first episode and chronic psychoses. The logic was clear: NMDAR antagonism can induce schizophreniform features, and NMDAR-Ab-E presents with a psychiatric syndrome with prominent psychotic features. Hence a number of studies sought to investigate whether there was a clinical sub-group of primary psychosis with serum NMDAR-antibodies that demarcated immunotherapy-responsiveness (151), which should be considered within a longer history of conceptualisations of schizophrenia as an immune-mediated disorder, eitehr in part in many or wholly in sub-groups (152-155).

An initial study by Zandi *et al.* found 3/46 patients with first episode psychosis recruited from an early intervention surface that tested positive for NR1-IgG using a live CBA. All three were men and were reported to have satisfied DSM-IV criteria for schizophrenia without any clinical suspicion of an encephalitic illness. This phenotype was markedly different from the clinical picture of NMDAR-Ab-E emerging worldwide as discussed in 1.4.2. Therefore, these findings were provocative and potentially heralded the coming of the long-prophesised immune sub-group of schizophrenia. Furthermore, given that first episode psychosis and subsequent schizophrenia are common, the findings could potentially have applied to millions worldwide, with manifold implications including understanding of aetiology and opening up a whole new wave of treatments centred around immune modulation rather than neurotransmitter blockade.

This field evolved alongside the evolution of criteria for definite NMDAR-Ab-E. In this context it became reasonably clear that the iceberg of unequivocal NMDAR-Ab-E masquerading as chronic primary psychiatric illness probably did not extend too deep. Analysis of these cases found that despite disease relapses often being less polysymptomatic than index episodes of encephalitis, there usually was an index episode with an organic presentation that had not been aetiologically linked to the later relapsing psychiatric disorder due to it preceding the discovery of autoimmune encephalitis (65,156,157).

In newer-onset cases the findings have been more variable. Using the same live CBA assay approach as the Zandi *et al.* 2011 report, Lennox *et al.* provided further evidence of NR1-IgG seropositivity in first episode psychosis that was absent in healthy volunteers (7/228, 3% vs. 0/105, 0%). However, another similarly-designed study using the same assay did detect positivity in healthy controls (1/98, 1%) (158). Neither study found clear clinical differences between seropositive and seronegative cases. Screening treatment-refractory psychosis also using the same live CBA did not find a vastly different rate to the acute cases (3/43, 7%) (159).

In all of these reports, the positive results in cases and controls were at the lower end of titre range. Furthermore, studies using both the live and commercial fixed versions of the NR1 CBA found positivity in multiple neurological phenotypes (110) and healthy controls (160). Studies using the more restrictive approach of TBA and/or NBA prior to CBA which was developed during the discovery of NMDAR-Ab-E rarely finds positivity outside of autoimmune encephalitis (161-164). It is likely that this approach is less sensitive to lower affinity and/or level of NR1-IgG because it

does not detect serum NR1-IgG in 15% of definite CSF-defined cases (107). As demonstrated by the broader phenotypic associations of serum NR1-IgG using a live CBA alone, the stricter approach gives comparatively improved disease-specificity, but whether this unfairly excludes positive results becomes a matter of definition.

Taken together, both types of study do not support a prevalence-based argument for attributing pathological weight to NMDAR seroreactivity irrespective of clinical context. Broadly, opinions have tended to say either the autoantibodies are present across health and disease fairly equally (165,166), or that they are completely absent outside of a well-circumscribed disease. In terms of clinical diagnosis of NMDAR-Ab-E, this allows for clear rules to be formed including clinical prior probability and interpret results in the context of the sample type (serum and/or CSF) and assay approach (fixed/live CBA, CBA only, or CBA combined with TBA/NBA).

Although categorising cases with low clinical probability and weak positivity on a single assay platform as not autoimmune encephalitis is an important clinical distinction, from a research perspective dismissing these findings is likely premature. Indeed, studies from the Groc laboratory have cut through this debate by showing that purified IgG from both definite NMDAR-Ab-E and live CBA positive samples from patients with first episode psychosis both bind NMDARs at single receptor molecular scale. However, whilst the IgG from the autoimmune encephalitis group cause widespread disorganisation at the synapse, the non-encephalitis live CBA positive IgG causes a variety of effects which are distinct from the encephalitis cases but still potentially relevant to a psychosis phenotype (167) (168).

Confirmation that NR1-IgG identified on live CBA are not false positives opens up an immune-centred perspective linking the dramatic clinico-pathologic picture of definite NMDAR-Ab-E with seropositivity in healthy and non-encephalitic control groups. The widespread seroconversion post-HSVE suggests that NR1 and other neuronal targets are well represented in the mature naïve BCR repertoire which makes it entirely plausible that NR1-IgGs are generated without a more realised autoimmunisation process that most likely underlies the florid picture in NMDAR-Ab-E. It may be that these are somehow secondary to processes central to the risk and/or propagation of primary severe mental illnesses and would therefore potentially have value as a biomarker, or alternatively they could be generated in a manner detached from the illness. Irrespectively, they may be able to modulate the brain under certain conditions (70,169). Such a putative effect would not need to be a NMDAR-Ab-E picture, it could be more subtle which would leave multiple phenotypes open to investigation (figure 1.11). On the other hand, this is challenged by both the slightly artificial conditions used in the single molecular tracking studies (large concentrations of IgG are used that are unlikely to be achieved *in vivo*), and the clinical observation that post-NMDAR-Ab-E the majority of patients given sufficient treatment recover close to baseline neuropsychiatric function despite persistent seropositivity.

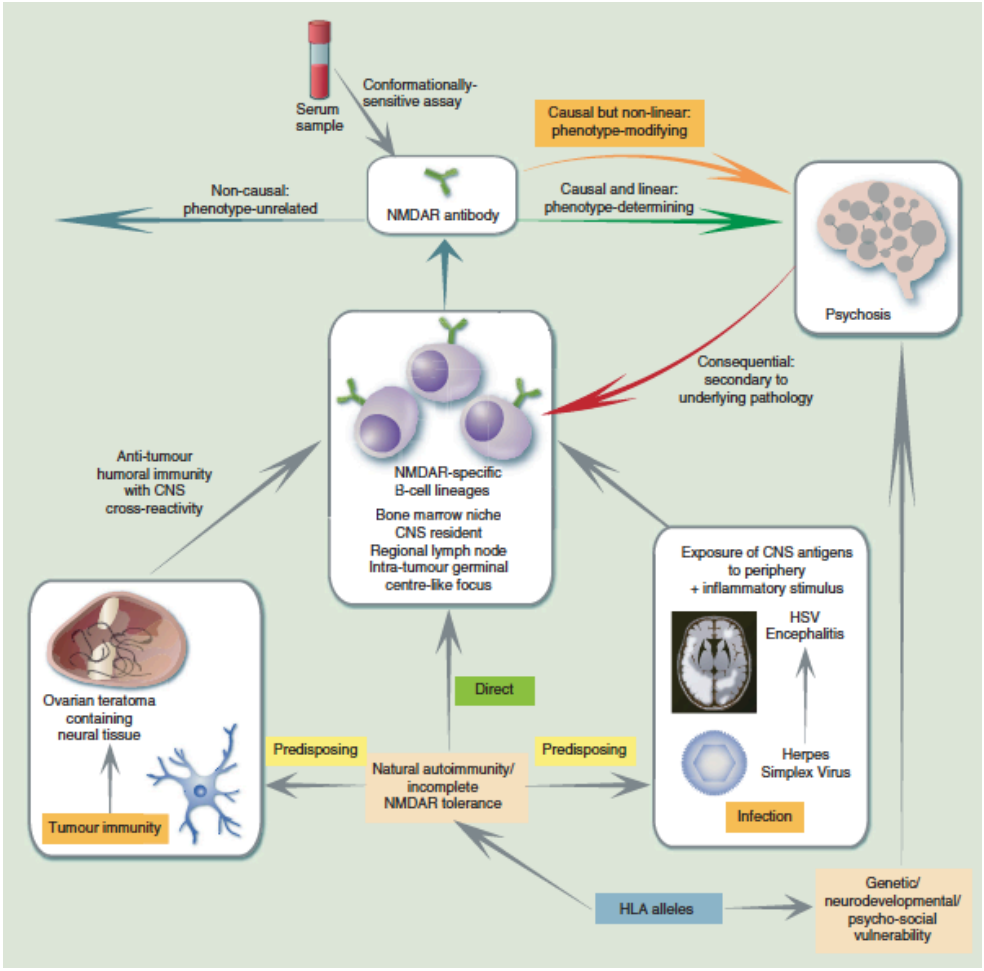


Figure 1.11 – **NR1-specific immunobiology as a unifying approach to underlying NR1 serological data in varying clinical contexts.**

Populations of NR1-specific naïve B cells may arise by genetic predisposition or chance, become expanded by ectopic NR1 in the context of other co-stimulating signals and secrete NR1-autoantibodies. This can lead to no phenotype, an encephalopathic phenotype, or potentially determine or modify intermediate phenotypes. The encephalopathic phenotype is strongly associated with NR1-autoantibodies detectable in the CSF likely predominantly driven by intrathecal expansion of NR1-antibody-specific cells, whereas an intermediate phenotype would not have detectable CSF NR1-autoantibody. The extreme ends of this phenotypic spectrum are widely-accepted to be possible but the latter is more uncertain. A better understanding of how autoimmunisation happens along this spectrum would set the scene for a more nuanced approach to interpreting NR1-seropositivity.

[Figure reproduced from Al-Diwani *et al.* 2017 (155) with permission from Wiley.]

1.6 Summary and aims

In summary, antibody-mediated autoimmune encephalitis is now an established entity, of which NMDAR-Ab-E is one of the most common and most likely to present to psychiatrists. In the spirit of the growing field of 'autoimmune neuropsychiatry' the project aims to embrace both autoimmunity and psychiatry. Indeed, despite the dramatic progress over the past 20 years there remain many clinically-relevant lacunae both in basic psychopathologic description and underlying immunobiologic mechanisms (170). Consequently, the project aims to be useful to practicing psychiatrists but also explore immunological mechanisms informative to disease biology of definite NMDAR-Ab-E and isolated NR1-seroreactivity in other neuropsychiatric clinical contexts.

Specifically, I revisit the initial psychiatric phase of definite NMDAR-Ab-E via a systematic review and phenotypic analysis of published cases and directly assessed patients (chapter 3). This is designed to be relevant to everyday psychiatric practice but also set the scene for thinking about immunobiologic findings both within the confines of this narrowly-defined category and in broader non-encephalitic neuropsychiatric syndromes. Samples from these syndromes (bipolar disorder and traumatic brain injury) are screened for NR1-IgG using a live CBA and then compared with NR1-IgG from the definite disease with and without an associated OT (chapter 4). This aims to assess whether the live CBA NR1-IgG are equivalent. To further explore differences in immunising mechanisms NR1-autoantibody isotypes are explored across these syndromes (chapter 5) and then germinal centre biology is probed in OT samples and fine needle aspiration of cervical lymph nodes in definite NMDAR-Ab-E with and without an associated OT (chapters 6 and 7, respectively).

2 Materials and methods

2.1 Clinical material

2.1.1 Oxford autoimmune neurology group patients and controls

Patients with definite NMDAR-Ab-E as per consensus criteria were recruited to the umbrella study 'Immune Factors in Neurological Diseases' (NHS Health Research Authority, Yorkshire and the Humber – Leeds East Research Ethics Committee REC16/YH/0013) from the Oxford autoimmune neurology clinical service and clinical collaborators elsewhere in the UK.

Samples were obtained during routine clinical care or research visits, and in accordance with the Declaration of Helsinki following written informed consent, or written consultee consent if decision-specific mental capacity to give informed consent was temporarily impaired. Samples or clinical data acquired via consultee consent were followed up and ongoing consent confirmed with the participant once capacity to consent returned.

These samples were supplemented by archived samples from a previous study (56) and samples shared from the local NHS immunology diagnostic service. Additional clinical data or samples from this study are documented in the relevant chapter.

Centre	Patients, n	Serum samples, n	CSF samples, n	Median age at onset (or sampling for controls), range (years)	Female, %	Ovarian teratoma-associated illness, %
Definite NMDAR-Ab-E						
Oxford modern	21	149	25	22, 16-74	95	43
Irani *et al.* 2010 study	25	25	1	23, 8-59	76	20
Oxford NHS immunology laboratory	14	14	14	24.5, 1-68	14	7
All Oxford	60	188	40	23, 1-74	68	25
Healthy volunteers						
	55	55	0	36	64	N/A

Table 2.1 – **Samples from patients with definite NMDAR-Ab-E and healthy volunteers from the Oxford study.**

2.1.2 Samples from collaborating groups

Additional serum and CSF samples from patients with definite NMDAR-Ab-E and non-encephalitic comparator neurological and psychiatric disorders were kindly shared from collaborating centres in Oxford and around the world. The samples were obtained with consent according to the Declaration of Helsinki in studies approved by the ethical committee overseeing the respective centre.

Centre	Patients, n	Serum samples, n	CSF samples, n	Median age at onset (or sampling for controls), range (years)	Female, %	Ovarian teratoma-associated illness, %
Definite NMDAR-Ab-E						
Seoul	26	26	26	23.5, 13-57	77	50
Sydney	11	28	11	7, 1-14	58	0
Rome	7	9	5	15, 3-27	86	14
Prague	5	45	10	13, 7-18	100	0
Non-encephalitic comparator neurological and psychiatric disorders						
Traumatic brain injury	57	57	31	31	23	N/A
Bipolar disorder – depression (CEQUEL)	183	293	0	45, *16- (>50)	53	N/A
Bipolar disorder – acute mania (MIAMI-UK)	39	101	0	43	56	N/A

Table 2.2 – **Samples from patients with definite NMDAR-Ab-E and healthy volunteers from collaborators.**

*precise upper age limit not available

2.1.3 Overall NMDAR-Ab-E cohort

Summating the Oxford and non-Oxford cases of definite NMDAR-Ab-E gives the following overall serum and CSF cohort.

Centre	Patients, n	Serum samples, n	CSF samples, n	Median age at onset, range (years)	Female, %	Ovarian teratoma-associated illness, %
All	109	296	92	20.5, 1-74	71	30

Table 2.3 – **Total cohort of serum and CSF samples from patients with definite NMDAR-Ab-E.**

2.2 Laboratory methods

All protocols were carried out by the author unless otherwise stated.

2.2.1 Solutions

2.2.1.1 Poly-L-lysine (PLL) solution

A stock solution of 1mg/mL PLL (P2636 Sigma) pre-dissolved in sterile milliQ water was thawed from -20°C to room temperature, dissolved in 500mL of sterile water, filtered and stored at 4°C and used within 4 months of preparation.

2.2.1.2 HEK cell medium

A 500 ml bottle of Dulbecco's Modified Eagle Medium (DMEM) was supplemented with 50ml fetal calf serum (FCS) (10%) and 5mL Antibacterial / Antimycotic solution (Penicillin / Streptomycin / Amphotericin (PSA) (1%), stored at 4°C and used within 1 month of preparation.

2.2.1.3 CBA sample buffer

A 500mL bottle of DMEM was supplemented with 5g of bovine serum albumin (BSA) (1%) and 2.3g of 4-(2-hydroxyethyl)-1-piperazineethanesulfonic acid (HEPES) (200mM).

2.2.1.3 CBA wash buffer

A 500mL bottle of DMEM was supplemented with 2.3g of 4-(2-hydroxyethyl)-1-piperazineethanesulfonic acid (HEPES) (200mM).

2.2.1.4 Neuron culture medium

A 500mL bottle of neurobasal medium (Thermo 21103-049) was supplemented with 5mL PSA (1%) and 5mL Glutamax (1%). 1mL of B27 (Thermo 17504-044) was added to 50mL aliquots of this solution prior to use.

2.2.1.5 B cell medium (BCM)

A 500mL bottle of Roswell Park Memorial Institute (RPMI) 1640 medium without phenol red was supplemented with 25mL FCS (5%), 5mL PSA (1%), 5mL Glutamax (1%), 50µL beta-mercaptoethanol (0.1%), and 50µL IgG-depleted transferrin (20 µg/mL) (0.1%), stored at 4°C and used within 1 month of preparation.

2.2.1.6 Freezing medium (FM)

A 25mL aliquot of BCM was supplemented with 20mL FCS (40%) and 5mL dimethyl sulfoxide (DMSO) (10%), stored at 4°C and used within 4 months of preparation.

2.2.1.7 Flow cytometry buffer (FCB)

A 500mL bottle of Dulbecco's PBS (D-PBS) was supplemented with 500µL of BSA solution to make a 0.1% solution.

2.2.2 Live cell-based assay (CBA)

2.2.2.1 Culture of human embryonic kidney 293T (HEK293T) cells

A HEK293 cell line previously stably transfected to express the SV40 virus large T-antigen (HEK293T) was grown in HEK cell medium in a Corning T175 flask within a sterile incubator at 37°C with 5% CO_2 and 90% humidity until approximately 80-90% confluent (usually 3-4 days).

To prepare a HEK293T cell mixture the following was done: HEK medium aspirated with a sterile glass pipette, 2mL of 10% trypsin solution added onto the adherent cells, the flask was agitated to detach the cells, resuspension of cell mixture in 8mL fresh HEK medium, and transfer to a universal container. This 10mL mixture was centrifuged for 3 minutes at 1200G. The supernatant was aspirated and cells resuspended in fresh HEK medium.

Cell concentration was determined using 0.04% Trypan Blue and a haemocytometer. A portion of this cell mixture was then diluted in HEK medium in order to make a concentration of 6 x 10^5 cells per mL. 2mL of this cell suspension was added to each well of a 6 well plate containing x4 13mm glass cover slips previously coated with PLL by overnight incubation in sterile PLL solution.

A proportion of the remaining cells were resuspended in a total of 35mL HEK medium in a fresh Corning T175 flask and returned to the incubator. A single batch of HEK293T cells were passaged up to 20 times before they were disposed and a previous stock of cells were thawed from long-term liquid nitrogen cryopreservation to initiate a new batch.

2.2.2.2 Transfection of human embryonic kidney 293T cells

Having been plated out on the morning of day 1 of the assay, HEK293T cells were grown on glass cover slips for ~30 hours (evening of day 2 of the assay), and then transfected with plasmid DNA. Per well, a total of 3µg DNA consisting of 2.8µg of NR1 DNA and 0.2µg of EGFP DNA was mixed with 1.5µg of PEI in 250µL of nuclease-free water. After 10 minutes at rest, HEK medium was added to make a

transfection mixture to a volume of 2mL/well. The HEK medium in which the cells had been incubating was aspirated and transfection medium was added. The cells were incubated in this medium overnight (~15 hours) and the following morning (day 3 of the assay) this medium was aspirated and replaced with fresh HEK medium containing 1.4 μL/ml of ketamine to minimise activation of functional surface NR1 tetramers.

2.2.2.3 Performing a live CBA

On day 4 of the assay, 24 hours following media change cells were viewed using a fluorescence microscope looking for evidence of EGFP expression indicating that transfection had occurred. If this was seen, then the assay was performed. The material of interest (e.g. serum/CSF/teratoma fluid/culture supernatant) was diluted in CBA sample buffer to a total volume of 250μL in a well of a 24 well plate. Each assay included a positive and negative control sample. At this stage 6 well plate(s) containing cover slips were moved to the bench at room temperature and a cover slip was added to each well of the 24 well plate containing diluted sample and was incubated for 1 hour. The diluted samples were then aspirated, and each well was washed 3 times with CBA wash buffer. Each cover slip was then fixed with 4% formaldehyde for 5 minutes and then washed 3 times with CBA wash buffer. Following this, 250μL of secondary antibody diluted in CBA sample buffer was added to each well and incubated in the dark for 45 minutes. If the assay used a tertiary antibody then the secondary antibody was aspirated, cover slips washed three times in CBA wash buffer and the diluted secondary antibody added for a further 45 minute incubation in the dark. This was then aspirated, and each well was washed twice in CBA wash buffer then twice in PBS. Each coverslip was individually removed and

inverted to mount the cell-coated surface in 4′,6-diamidino-2-phenylindole (DAPI)-supplemented mounting medium on a superfrost glass slide.

2.2.2.4 Reading and recording outcomes of live CBA

Following review of positive and negative control cover slips test samples were read at 40x zoom on a Leica DM2000 fluorescence microscope. Samples were trichotomized into clearly negative, positive or strong positive. Positivity was determined by the presence of a characteristic coronal cell surface deposition of fluorescent reporter antibody on multiple cells. All positive samples were repeated on an independent assay and serially diluted to establish an end-point dilution, the dilution at which the positive signal was still unambiguously present. Samples of particular interest were digitally imaged at 40x or 100x oil immersion using a Qimaging Rolera-XR Fast1394 camera and Qimaging QCapture Pro software version 6.0.0.605 for Windows.

2.2.3 Live neuron-based assay (NBA)

2.2.3.1 Isolation and culture of rat hippocampal neurons

This protocol was performed by Dr Antonio Berretta to ensure reproducibility of neurons. E15 pups were retrieved from a gravid Wistar Han time-mated female rat and then decapitated. Using sharp forceps, the skull was opened, the brain was isolated, and placed in a 35mm petri dish containing ice-cold Hank's balanced salt solution (HBSS) using a spatula. Then, using fine-tipped forceps the hemispheres were separated and brain stem was removed. The hippocampus was then isolated from each hemisphere with care to avoid including meningeal tissue. Following isolation of each hippocampus, it was transferred to a separate 35mm petri dish with

ice-cold HBSS. Then in a sterile class II tissue culture hood the hippocampi were added to a trypsin-HBSS solution (0.5mL trypsin added to 4.5mL HBSS in a 5mL bijou) and then incubated for 15 minutes (37°C, 5% CO_2). Following the incubation, the solution was aspirated, the tissue was washed 3 times with HBSS, and then suspended in 1mL of neuron culture medium. The hippocampi were gently dissociated by repeated pipetting with sterile P1000 then P200 tips. The cells were counted and resuspended in neuron culture medium to a target cell concentration of 2×10^5 cells/mL.

In a 96 well plate previously coated with PLL/0.1% gelatine and washed with sterile water, outer wells were filled with 60µL sterile PBS and not used for culture due to likelihood of evaporation, and inner wells were filled with 60µL of cell resuspension. Each plate was then incubated (37°C, 5% CO_2) with addition of 60µL of neuron culture medium on day 4.

2.2.3.3 Performing a live NBA

Live NBA was performed after 21 DIV unless otherwise specified. By this stage evaporation of culture medium would tend to leave ~100µL meaning that by adding 1µL of sample a 1:100 dilution could be achieved. The 96 well plate(s) were removed from the tissue culture incubator and brought to the tissue culture hood. 1.1µL of serum sample was added to conditioned media in which the neurons had been cultured. Positive and negative controls samples were included in each batch.

When performing an assay to find the end-point dilution the sample was serially diluted in neuron culture medium from 1:10 to 1:320 by 1:2 steps (starting with 3µL

serum in 27μL of neuron culture medium and moving 15μL into 15μL of neuron culture medium in subsequent wells. Allowing for pipetting error, 12μL of each dilution step was transferred into 100μL of conditioned neuron culture medium creating a dilution 10x more dilute. Hence 1:10 became 1:100 in the well and 1:20 became 1:200 through to 1:320 becoming 1:3200, the final dilution.

After each sample was added to the respective well, the plate was returned to the incubator for 30 minutes (37°C, 5% CO_2). The plate was then removed and returned to the hood where the conditioned media was aspirated. The wells were then washed twice with 120μL of PBS-Sucrose (4%), fixed with 120uL 4% FA (in PBS-Sucrose 4%) and washed twice with PBS. The wells were then sequentially incubated with secondary (goat anti-human IgG Fc-γ), tertiary (rabbit anti-goat IgG AF488) ± quaternary (goat anti-rabbit IgG AF488) antibodies for 45 minutes in the dark with two PBS washes between each incubation. All antibodies were diluted 1:750 in PBS.

The wells were then read as described below. For imaging purposes selected wells were stained for MAP2 to reveal neuronal structure. Here, PBS was aspirated, and the cells were incubated with PBS 0.3% Triton-X-100 for 15 minutes. This was aspirated, washed twice with PBS and then incubated with mouse anti-rat microtuble associated protein 2 (MAP2) antibody (diluted 1:1000 in PBS), washed twice with PBS and incubated with anti-mouse AF568 antibody (diluted 1:750 in PBS), and again washed twice with PBS.

2.2.3.4 Reading and recording outcomes of live NBA

The plate was read directly on an inverted fluorescence microscope. The samples were numbered and read blind to clinical association. A well was considered positive when cells of neuronal morphology had a clear punctate surface staining pattern that was greater than background staining. Such samples were given a score between 2-4. The samples were read independently by two assessors (Dr Berretta and myself), scores were compared afterwards, and any differences were re-evaluated. A final score was then assigned to the sample on that particular assay. Positive wells were repeated in an independent assay and diluted to find the dilution at which the sample clearly scored 2, the end-point dilution.

2.2.4 Multicolour flow cytometry

2.2.4.1 Staining cells and single stain controls

A cell suspension of the material of interest was prepared in flow cytometry buffer (FCB) and held at 4°C until use. Flow cytometry antibodies were diluted for the application in FCB as either a single stain in a single Eppendorf vial or as a staining mix together in a single vial and held at 4°C until use.

When optimising panels or staining cells for cell sorting, fluorescence minus one (FMO) panels were also prepared in which the entire staining panel was made minus a single antibody. These were made for each antibody on the main staining panel.

The cell suspension of interest was centrifuged at 300G and resuspended in 50µL of FCB. Each experiment would include a duplicate of the cell sample in a separate

well and not stained with antibody to act as an unstained control. If FMO panels were run, then further cell suspension replicates were prepared.

The cell samples were added to a 96 well round bottom plate and positive and negative compensation beads were added to 50µL of FCB. This plate was then centrifuged at 300G for 3 minutes. The supernatant buffers were aspirated and staining antibody mixes added to cell samples and compensation beads. These were resuspended 3 times to ensure adequate mixing. Unstained cells were resuspended in FCB only. The plate was then incubated in the dark at 4°C for 30 minutes.

Following incubation, the plate was centrifuged at 300G for 3 minutes and staining mixes aspirated. Cell samples were resuspended in FCB with DAPI (1:1000). Unstained cells and compensation beads were resuspended in FCB without DAPI. The plate was centrifuged again at 300G for 3 minutes, buffer was aspirated, and cells and beads resuspended in 200µL FCB. These were then transferred to cluster tubes and supplemented with further FCB: 200µL for cells and 600µL for beads.

2.2.4.2 Cytometric signal acquisition and analysis

Immunophenotypic data was acquired at the Weatherall Institute for Molecular Medicine (WIMM) flow cytometry facility on either an Attune NxT flow cytometer (Thermo Fisher) or for cell sorts, on a FACS Aria III (Beckton Dickinson), during which phenotypic data was acquired in parallel. Compensation matrices were optimised using single stain controls, unstained cells ± FMO panels prior to acquisition of the main sample(s). The FACS Aria III was operated by Mr Craig Waugh, flow cytometry technician. Data was saved in the Flow Cytometry Standard

format as .fcs files and exported for further analysis. Analysis was performed using FlowJo™ 10, for Mac OS X (FlowJo LLC, Becton Dickinson).

2.2.5 Lymphocyte isolation and culture

Isolation and culture of lymphocytes from peripheral blood samples is discussed here. The development of a modified protocol for fine needle aspiration samples is discussed in chapter 7. Furthermore, discussion of modification of culture system for bulk sorted samples is also discussed in chapter 7.

2.2.5.1 Peripheral blood mononuclear cell (PBMC) isolation by density gradient centrifugation and cryopreservation

Blood was drawn from the research participant with an aseptic non-touch technique using a butterfly needle and x6 9mL sodium heparin coated vacuette® sample tubes (Greiner Bio-One 455051). The tubes were centrifuged at 500G for 10 minutes (acc. 9, dec. 5). Plasma was removed and stored. The remaining sample was diluted with an equal volume of D-PBS-1% BSA. 15mL of this diluted sample was gently pipetted down the side of each SepMate™ 50 tube (Stemcell™ technologies) with 15mL Ficoll density gradient added to the lower chamber beforehand. The SepMate™ tubes were centrifuged at 1200G for 10minutes (acc. 9, dec. 9). The layer above the plastic separating line was poured off into a separate 50mL Corning® centrifuge tube and D-PBS-1%BSA added to make a total volume of 50mL total volume. These tube(s) were then centrifuged at 200G for 10 minutes (acc. 8, dec. 7), the supernatant was aspirated, replaced with D-PBS-1%BSA to a total of 35mL, centrifuged again on the same settings, supernatant aspirated and resuspended in 20mL of D-PBS-1%BSA. A cell count was then performed and a volume containing the number of cells

needed for the downstream application was removed. If the cells were not needed immediately they were stored. This involved centrifuging the final sample on the same settings and resuspending in 500µL of B cell media (BCM) for each 1.8mL cryovial, aiming for 5-10 x 10^6 cells per tube. 500µL of resuspended cells was added to each cryovial with 500µL of freezing media. The cryovials were immediately added to a CoolCell® container (BioCision) and placed in a -80°C freezer overnight. The next day they were transported on dry ice to liquid nitrogen storage.

2.2.5.2 Lymphocyte culture

Cells were either used fresh from isolation or thawed from cryopreservation. To thaw cells, the vial(s) were retrieved from liquid nitrogen on dry ice, immersed in a 37°C bead bath then transferred using a Pasteur pipette into a 50mL Corning® centrifuge tube containing 10mL of RPMI 1640-40% FCS. This was then centrifuged at 200G for 10 minutes (acc. 8, dec. 7), resuspended in 20mL of PBS-1% BSA and a cell count was performed.

Prior to cell culture cytokine solutions had been prepared according to manufacturer's instructions, made up to optimal concentration based upon previous experience in the laboratory, aliquoted into 20µL volumes, frozen to -20°C and thawed to room temperature prior to use.

Cytokine	Company	Reference	Concentration used *in vitro*
CD40 ligand (CD40L)	R&D Systems	6420-CL	50ng/mL
Interleukin 2 (IL-2)	PeproTech	200-02	50ng/mL
Interleukin 21 (IL-21)	PeproTech	200-21	50ng/mL
Interleukin 6 (IL-6)	PeproTech	200-06	10ng/mL
Interleukin 1β (IL-1β)	PeproTech	200-01B	1ng/mL
Tumor necrosis factor α (TNFα)	PeproTech	300-01A	1ng/mL
Resiquimoid (R848)	Enzo Life Sciences	ALX-420-038-M005	2.5µg/mL

Table 2.4 – **Cytokines used in lymphocyte culture.**

Unfractionated PBMCs were cultured in a total volume of 200 µL/well (50% unsupplemented BCM and 50% BCM-cytokine mix) in a clear plastic flat bottom 96 well plates for 13 DIV. Two cytokine mixes were used in culture experiments. The 'activation' mix included all cytokines in table 2.4 due to the previously demonstrated effect to cause B cells to divide and differentiate into antibody-secreting cells (36) and the 'maintenance' mix included only IL-6 due to its effect to maintain pre-existing plasmablasts/plasma cells. Due to propensity to evaporation, the outer wells were not used for cells and instead filled with 200 µL/well D-PBS supplemented with penicillin/streptomycin to reduce contamination risk.

2.2.5.3 Harvest of culture supernatants

After 13 DIV the culture plate(s) were retrieved from the incubator. They were centrifuged at 300G for 4 minutes. The supernatant fluid was transferred to a 2nd V-bottomed plate and centrifuged at 300G for 4 minutes to remove remaining cells. The remaining supernatant (160-170µL) was transferred to a round bottom plate for storage at -20°C and thawed for subsequent antibody assays.

2.2.6 Enzyme-linked immunosorbent assay (ELISA)

2.2.6.1 Immunoglobulin (Ig) ELISA

The following Ig ELISA kits from Bethyl Laboratories were used: IgG E80-104, IgA E80-102, and IgM E80-100. The assays followed the same approach with differences relating to coating and secondary antibodies. Therefore, the general approach will be described with differences described afterward in table 2.5.

A clear plastic 96 well plate supplied by the manufacturer was coated with affinity purified coating antibody at a dilution of 1:100. 100µL of coating antibody was added per well which was incubated for 1 hour at room temperature. The plate was washed 5 times with ELISA wash solution (50mM Tris, 0.14M NaCl, 0.05% Tween 20, pH 8.0) then 200µL of ELISA blocking solution (50 mM Tris, 0.14 M NaCl, 1% BSA, pH 8.0) was added per well. The plate was blocked for 30 minutes at room temperature then washed 5 times with ELISA wash solution. Standards 1-7 were made by serial dilution as per the manufacturer's instructions in ELISA sample buffer (50 mM Tris, 0.14 M NaCl, 1% BSA, 0.05% Tween 20) with the final standard being a blank (sample buffer only). Samples were diluted with ELISA sample buffer to be within the range of the standards. All standards and samples were run in duplicate. The standards and samples were incubated for 1 hour at room temperature then washed 5 times with ELISA wash buffer. Next, 100µL of diluted HRP detection antibody was added to each well and incubate for a further hour followed by a further 5 washes with ELISA wash buffer. Then, 100µL of TMB substrate solution was added to each well which was allowed to develop for 20 minutes in the dark. The reaction was then stopped using ELISA stop solution (82% distilled water, 12% sulphuric acid) resulting in a colour change from blue to yellow. A plastic adherent cover was placed on top of

the plate, which was then read on a plate reader (light absorbance at 450nm) and results exported into a Microsoft excel spreadsheet. The OD values were analysed using the four parameter logistic curve tool offered by myassays.com (MyAssays Ltd) including averaging duplicates and subtracting background.

	IgG	**IgA**	**IgM**
Coating antibody	Goat anti-Human IgG-Fc Fragment Antibody Affinity Purified (Bethyl - A80-104A)	Goat anti-Human IgA Antibody Affinity Purified (Bethyl - A80-102A)	Goat anti-Human IgM Antibody Affinity Purified (Bethyl - A80-100A)
Standard concentrations	500 – 7.8 ng/mL	500 – 7.8 ng/mL	1000 – 15.6 ng/mL
Serum dilution	1:100,000	1:10,000	1:10,000
Culture supernatant dilution **Unfractionated** **Memory B cell** **Naïve B cell**	 1:100 1:300 1:30	 1:100 1:300 -	 1:100 1:30 1:300
HRP detection antibody dilution	1:150,000	1:100,000	1:100,000

Table 2.5 – **Total Ig ELISA detection antibody set-up.**

2.2.6.2 C-X-C Motif Chemokine Ligand 13 (CXCL13) ELISA

The Human CXCL13 Quantikine® ELISA kit was used (R&D systems, DCX130). This is a sold phase sandwich ELISA which includes a pre-coated 96 well plate (892424). Human CXCL13 standard (892426) was reconstituted with distilled water. 50µL of the standard (5000pg/mL) was added to 450µL of calibrator diluent RD6-41 (895840) to make a starting dilution of 500pg/mL. This was then serially diluted to 7.81pg/mL. 100µL of each standard was added to 100µL of assay diluent RD1S (895137) to make a range of 250 – 3.4 pg/mL and a blank sample containing calibrator and assay diluent without CXCL13. Samples were either neat or diluted 1:2 in assay diluent. All standards and samples were run in duplicate and incubated for 2 hours at room temperature. The plate(s) were then washed 4 times with wash buffer previously dilute from concentrate (895003). Next, 200µL of human CXCL13

conjugate (892425), a monoclonal antibody against CXCL13 conjugated to HRP, was added to each well in incubated for 2 hours at room temperature followed by 4 washes. Next, a substrate solution was prepared by adding colour reagent A to colour reagent B, and 200µL was added to each well and incubated for 30 minutes in the dark. After this, 50µL of stop solution added to each well to stop the reaction leading from a colour change from blue to yellow. A plastic adherent cover was placed on top of the plate, which was then read on a plate reader (light absorbance at 450nm) and results exported into a Microsoft excel spreadsheet. The OD values were analysed using the four parameter logistic curve tool offered by myassays.com (MyAssays Ltd) including averaging duplicates and subtracting background.

3 The psychiatric phenotype of definite NMDAR-Ab-E in adults

3.1 Introduction

Since its initial description, the psychiatric onset of NMDAR-Ab-E has been central to interest from both clinicians and the public (54,55,171). Indeed, in the first large case series, 77/100 were originally assessed by mental health system in one guise or another (57). Consequently, awareness of the illness has gradually grown amongst the psychiatric community, in particular illness progression from mental state abnormalities to frank neurological features then potentially life-threatening cardio-respiratory decompensation (56,172). While 'red flag' features such as seizures, complex movement disorder, or falling conscious level should be sufficient to prompt a neurological referral (151,173), the timing of these is variable and they sometimes may not occur at all raising the diagnostic relevance of the mental state.

Early clinical suspicion has the capacity to avoid harm and do good: outcomes are strongly associated with early immunotherapy (121), psychiatric units are poorly suited to managing seizures and dysautonomia (174), and commonly used anti-psychotics that are usually tolerated in primary psychiatric disorders can frequently decompensate NMDAR-Ab-E. Indeed, the decompensation can extend a neuroleptic malignant syndrome-like picture (175). Despite this, the actual nature of the mental state disturbance has usually been described as 'psychosis', or even less specifically, 'psychiatric'.

If the clinical picture is indeed this amorphous, an argument can be made for screening for the causative NMDAR (NR1-IgG) antibodies. However, a blood screening approach uninformed by clinical parameters is vulnerable to under- or

over-diagnosis, no matter which assay combination is used (107,110). CSF testing is the gold standard and ultimately needed to make a definite diagnosis (104). It may be that in coming years lumbar punctures are increasingly rolled out in first episode psychosis services to permit CSF screening for this and other putative 'autoimmune psychoses' (176) (177). However, even if such a major shift in clinical culture occurred, NMDAR-Ab-E stands out for its potentially rapid progression and the need for urgent referral to regional neuroscience centres that can cope with the broad symptom array and potential need for neuro-intensive care. Therefore, approaches to refine clinical suspicion remain critical, not only to inform selection for lumbar puncture ± direct referral to neurology.

Unusually for descriptive psychopathology, in NMDAR-Ab-E the physical substrate underling the mental state abnormalities is understood a great deal. As discussed in 1.4.4, sophisticated single receptor tracking studies have shown that NR1-IgG antibodies from patients with NMDAR-Ab-E cause reversible internalisation of post-synaptic NMDARs (73,167). Furthermore, emerging evidence using the NMDAR-specific PET tracer [18F]GE-179 shows clear signal reduction in the acute phase that resolves in remission (Galovic *et al.*, International Epilepsy Congress, Bangkok 2019). Consequently, improving understanding of the nature of the mental state is not only clinically-relevant, but study of antibody-mediated NMDAR dysfunction could feed back into the nuances of NMDAR hypofunction in general psychiatry (178). Alongside the drug and genetic models described in 1.4.1 in mind, this study aimed to characterise the mental state of definite NMDAR-Ab-E in a fine-grained manner using published individual patient data and the direct study of patients. The ambition of this work was to better inform clinical detection of the illness in the mental health

system, add to knowledge about the phenomenological consequences of NMDAR disruption, and provide a framework for future validation studies. Additionally, refining the psychopathology in a clinical context where NR1-IgG is definitely driving mental state dysfunction provides a reference standard for other disorders where NR1-IgG is detected in serum such that if a causal role is suggested then aspects of the principal syndrome may be expected to be present.

3.2 Systematic review and phenotypic analysis of individual patient data

3.2.1 Search strategy and study selection

Firstly, the study was pre-registered with the NIHR PROSPERO database of systematic review protocols. It was approved and assigned the number CRD42017068981 on 7th June 2017. A search strategy was developed that aimed to include as many likely cases as possible. Although the disease is probably not new, it was only formally described to a degree that contemporary criteria can be applied from ~2005 onwards. Therefore, the data range used was 1st January 2005 until the date when the search was run, 7th October 2017. The following search string was used, aiming to account for variations in nomenclature: ((anti-N-methyl-d-aspartate OR NMDA receptor OR NMDAR OR NMDAR-antibody OR anti- NMDA OR anti-NMDAR OR NMDA OR NMDA-antibody) AND (encephalitis OR autoimmune encephalitis)). Results were restricted to English language reports and the search was run on the US national library of medicine PubMed search engine.

The two inclusion criteria (and reciprocally, exclusion criteria) were age (≥ 18 years) and satisfying criteria for definite disease as per Graus *et al.* ((104).) While infants and children are affected by NMDAR-Ab-E, the disease is known to have a more movement disorder-dominant onset. Additionally, the assessment of psychopathology in this age range is distinct enough from adults that to include them with adult patients could limit the ability to unambiguously identify phenomena. At face value cases of older teenagers appeared to follow similar patterns as adult patients, however given the division of adult services at 18 years, this age was chosen as a pragmatic and clinically relevant cut-off. Although, the category of probable NMDAR-Ab-E was initially considered, pilot searches revealed the bulk of

published cases provided evidence of CSF NR1-IgG with a compatible clinical picture. Therefore, given the simplicity to ascertain this more impactful group versus the relative difficulty of ascertaining a more problematic and less frequent group, only definite cases were included. Studies were also excluded if they did not provide clinical information, e.g. laboratory studies that used samples from definite patients but did not reported the history.

The studies were independently screened by the author and a 2nd member of the study team, Dr Leigh Townsend. The clear inclusion and exclusion criteria helped simplify the selection process. The initial search gave 1096 reports. Any cases of uncertainty were resolved by the study senior author, Professor Irani, of which there was one case of lupus with CSF NR1-IgG, which on review was not consistent with NMDAR-Ab-E. This yielded 333 reports containing 1100 cases (figure 3.1). These were then classified on whether data could be extracted from individual cases or if only group-level descriptions were possible. Next, each group was further classified on a psychopathological filter of whether the terms “psychiatric” and/or “behavioural” were used in the description of the patient and then whether any further attempt was made to further characterise. The first filter was attempting to gauge the frequency of psychiatric phenomena per se whilst the second was trying to generate a cohort where an inventory of individual phenomena would be possible, albeit potentially still rudimentary.

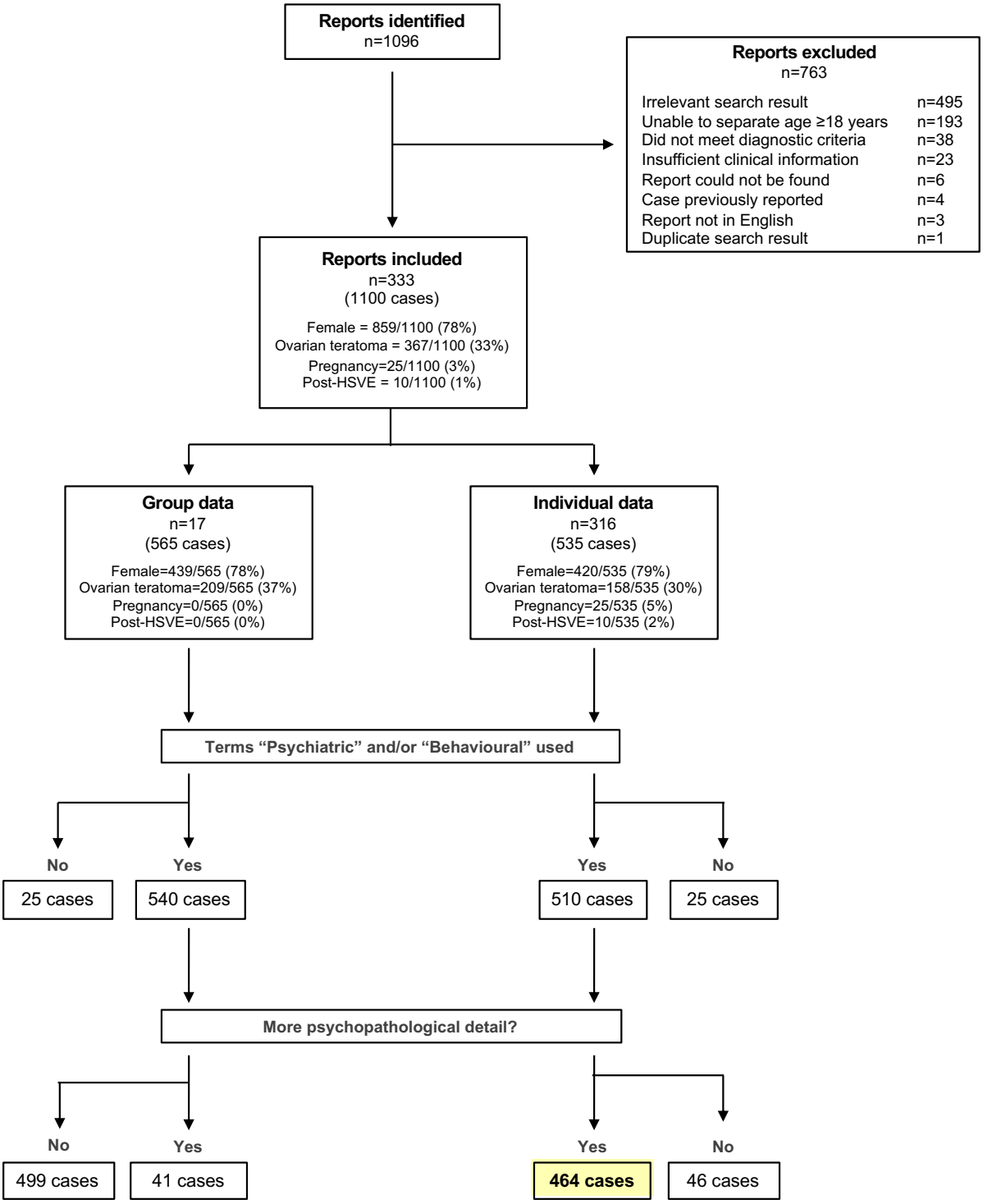


Figure 3.1 – **Study selection strategy – PRISMA diagram.** The eventual cohort of 464 individually reported cases are highlighted.

As expected, the majority of cases reported psychiatric and/or behavioural features 510/535 (95%) of individually-reported, and 540/565 (94%) of group-reported cases were included following the first filter. Consistent with the group studies usually being broad overviews of the condition, only 41/540 (8%) passed the second filter, whereas 464/510 (91%) did so in the individually reported group.

The following features were extracted: age, sex, ovarian teratoma status, prior herpes simplex virus encephalitis, cardinal neurological symptoms and psychopathological phenomena including initial psychiatric diagnosis if reported. The cardinal neurological features recorded were seizures, movement disorder, dysautonomia, and central hypoventilation. The approach to psychopathology is described below in 3.2.3. Given that many of the individually reported patients were single case reports there was a risk of including atypical patients, however, the demographic, teratoma, and neurological profile of the individually reported patients was not different from the group reports (one-way ANOVA, P=0.894; table 3.1). Therefore, the 464 individually reported patients satisfying consensus criteria for definite NMDAR-Ab-E, with psychiatric and/or behavioural features described further, and not inconsistent with the overall clinical pattern in the group-reported patients, were included as the main study population.

	Group reported	Individually reported		
		All	Case reports	Case series
Number of cases	565	464	237/464 (51%)	226/464 (49%)
Median age	26	27	28	26
Female n (%)	439/565 (78%)	368/464 (79%)	192/237 (81%)	176/226 (78%)
Psychiatric n (%)	540/565 (96%)	439/464 (94%)	229/237 (96%)	210/226 (93%)
Seizure n (%)	381/565 (67%)	270/464 (58%)	143/237 (60%)	127/226 (56%)
Movement disorder n (%)	364/565 (64%)	256/464 (55%)	133/237 (56%)	123/226 (54%)
Dysautonomia n (%)	241/565 (43%)	209/464 (45%)	112/237 (47%)	97/226 (43%)
Central hypoventilation n (%)	189/565 (33%)	130/464 (28%)	79/237 (33%)	51/226 (23%)
Post-HSVE n (%)	0/565 (0%)	7/464 (1·5%)	7/237 (3%)	0/226 (0%)
Ovarian teratoma n (%)	209/565 (37%)	147/464 (32%)	82/237 (35%)	65/226 (29%)

Table 3.1 – **Demographic, teratoma, and neurological profile of group vs. final individually-reported cases.**

3.2.2 Demographic trends

The cohort was consistent with prior knowledge of the disease. Firstly, while there were cases described as far as the 9th decade, the distribution was skewed towards younger adults with a median age of 27 (figure 3.2a, blue line). Secondly, the majority of patients were female (overall rate=368/464, 79%), however this appeared to be age-dependent, with the proportion female always >0.5 for patients ≤40 years but not so for patients >40 years old (median proportion female 0.86 vs. 0.50, P=0.001 Two-tailed Mann-Whitney test) (figure 3.2a red line, and 3.2b). Indeed, using >40 years as a cut-off, the odds ratio for female was 2.8 (P<0.0001 Two-tailed Fisher's exact test). Thirdly, ovarian teratoma was a common association (overall rate=147/464, 32%; figure 3.2a, green line), and although it mapped onto the overall younger female trend, with no cases >44 years, it did not account for all the female cases.

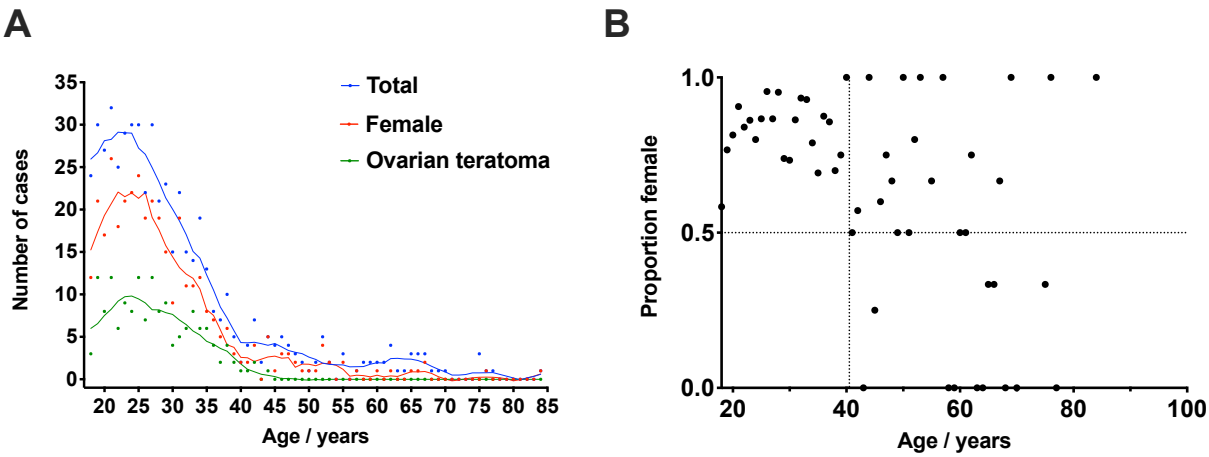


Figure 3.2 – **Demographic features of the individual patient data cohort.**

A – Age-specific rates of all cases (blue), female cases (red), ovarian teratoma-associated cases (green). Trend lines were drawn with a smoothing function (second-order with eight nearest neighbours).

B – Age-specific proportion female plotted against age (black dots). Horizontal line plotted at proportion 0.5. The vertical line represents the last point at which each age has a proportion >0.5.

There were reports of onset associated with pregnancy and post-partum. This was not unexpected given that the cohort was largely women of childbearing age. In total there were 24 cases (5%) with a pregnancy-associated onset, ranging from age 18-37 years. 13/24 cases were ante-partum, 11/24 were post-partum, and 7/24 cases were associated with ovarian teratoma (figure 3.3). Of the ante-partum cases, 7/13 were in the first trimester and all but 2/11 post-partum cases were <12 weeks post-partum.

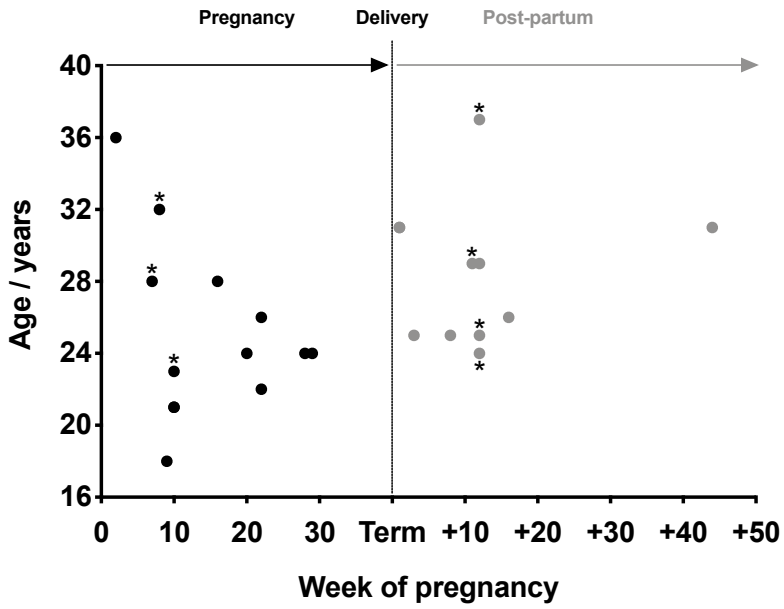


Figure 3.3 – **Pregnancy-associated onset of illness in relation to ante- and post-partum timing and age of patient.** To facilitate plotting both phases, a 40 week delivery time was assumed. *ovarian teratoma-associated

Although it is a reasonably small sub-group, these trends are consistent with disease activity of other autoimmune diseases in pregnancy with diminishing incidence as pregnancy progresses with a rebound post-partum (179). This means that the biology of pregnancy could potentially be a relevant factor in the threshold of disease with other factors present or it could be coincidental. Larger epidemiological studies and laboratory models would be needed to evaluate this further. Notwithstanding this pathophysiological relevance, from a clinical perspective this data provides an

important reminder to perinatal psychiatrists to consider this diagnosis in compatible symptom groups, most obviously postpartum psychosis. This particular overlap is discussed further in 3.2.4.

3.2.3 Inventory of psychopathology

The aim was to extract as much psychopathological information as possible whilst grounding the study in everyday mental state examination. Prior knowledge of the field informed the initial inventory, for example psychosis and catatonia were usually listed in authoritative reviews (180) so features from these syndromes were included. However, in terms of casting a wide enough net to not miss other features and avoid reifying a potentially inaccurate picture, additional symptom groups were also included: mood, eating, suicidality, obsessive-compulsive, and distinctive behavioural features which were harder to categorise.

A two-level approach was taken whereby more discrete features were considered lower level and their parent categories considered higher level. It was anticipated that reports would vary in their granularity such that some would only give higher level descriptions, along the lines of ‘the patient was psychotic and catatonic’, whereas others would be detailed, expanding to ‘the patient reported that they were being imprisoned by the devil and held strange postures for several hours’. It was also anticipated that there would be variability in the usage of technical terms such that, like the previous example, interpretation would be needed. Here the first component would be regarded as a lower-level feature, a likely delusion of a religious nature and additionally categorised as psychosis in the higher-level features. The second component would also be a lower-level feature, ‘posturing’, but

also categorised as the higher-level feature category, ‘catatonia’. The more problematic aspect anticipated, consistent with the report authors’ broad clinical backgrounds, was the use of technical terms without plain description to judge their accuracy. For example, ‘agitation’ stated in a table without a clinical vignette to confirm the intended meaning. These descriptions could either be prospectively excluded from the analysis or included and controlled for post-hoc. In the interests of not only sampling the illness phenomenology per se, but also sampling trends in the nature of the reporting, the inclusive approach with post-hoc quality control was chosen.

Given the variable completeness of the source material, an additional consideration was whether to regard lack of reporting of a feature as evidence of its absence. Again, aiming for a pragmatic rather than nihilistically strict position, it was decided to take absence of a feature at face value and regard it as if the feature were positively stated as absent. Caveats such as this are reflected upon and shape the approach to analysis in this study and the cohorts reported in 3.3 and 3.4.

The other aspect of reporting to consider was symptom progression over time, both within and between illness episodes i.e. in relapse. The initial aim was to capture time series data, but on pilot evaluation it was clear that the literature was far too variable to robustly ascertain timings for the majority of phenomena in the majority of cases. Instead, this was a focus for the local cohort reported in 3.3 and 3.4. Relapses were similarly reported too variably to make genuine inferences from analysing these separately to the initial episodes. Instead these were amalgamated together with first episodes within each case. Therefore, temporal resolution was

consciously collapsed in exchange for a greater total amount of individual information.

To test the inventory, lower and higher-level features from the first 100 cases were extracted. This found very few unanticipated features. ‘Wandering aimlessly’ and ‘incongruent laughter-crying’ were added and some eating features, ‘purging’ and ‘eating sweet foods,’ were not identified and removed. This resulted in a list of 50 lower-level features and 8 higher-level features which were applied to the remaining cases. This did not require further modification. To review the accuracy of extraction, the 2nd reviewer Dr Townsend, evaluated 67 cases finding largely similar findings (4121/4154 matrix boxes, 99%). The differences were not misclassifications but missing items that had required a degree of interpretation to detect.

Higher-level features could be derived from all cases directly and/or categorised from lower-level features. At least one lower-level feature was reported in all cases. The most common higher-level feature domains were behaviour (316, 68%), psychosis (310, 67%), mood (219, 47%), catatonia (137, 30%), and sleep (97, 21%) (figure 3.4). In the lower-level features, the most common were not restricted to one higher-level feature but spanned several, consistent with the most common higher-level features being at reasonably similar frequencies: agitation (203, 44%), hallucinations (198, 43%), delusions (133, 37%), aggression (93, 20%), anxiety/panic (92, 20%), mutism (85, 18%), irritability/mood instability (83, 18%), disorganised/bizarre (73, 16%), insomnia (66, 14%), depression (50, 11%), and mania (50, 11%). At this level of analysis, a picture could be derived that was undoubtedly psychotic in nature but with prominent catatonic, disorganised, disinhibited and mood-disordered aspects.

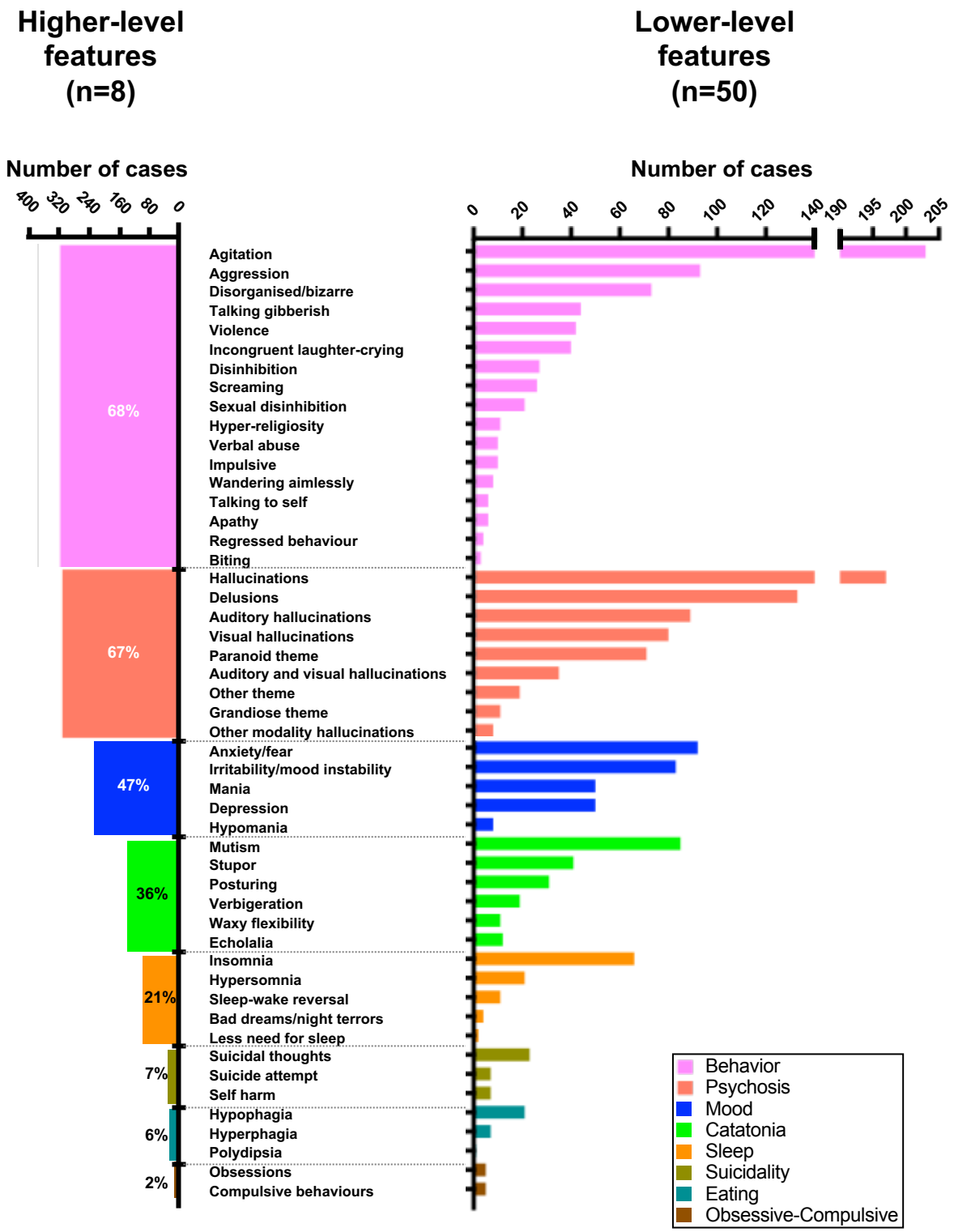


Figure 3.4 – **Frequency of higher- and lower-level features in the cohort.**

The 50 lower-level features are listed in the centre and listed by frequency within their respective higher-level features. The higher-level features are ordered by frequency and colour-coded (box).

Next, the following associations of the illness were compared to assess for differences in the symptom profile: age, sex, pregnancy, ovarian teratoma, post-herpes simplex virus encephalitis and isolated psychiatric presentation. The lower-level feature rates were normalised by sub-group percentage and subtracted from each other to give residuals. Each comparison was analysed by two-way ANOVA with Bonferroni correction for multiple comparisons. There was no significant difference either before (figure 3.5) or after correction (P=1), consistent with a convergent expression of neuropsychiatric disturbance. The caveat was that some of these groups were small and not necessarily well-described, therefore genuine differences may have been lost.

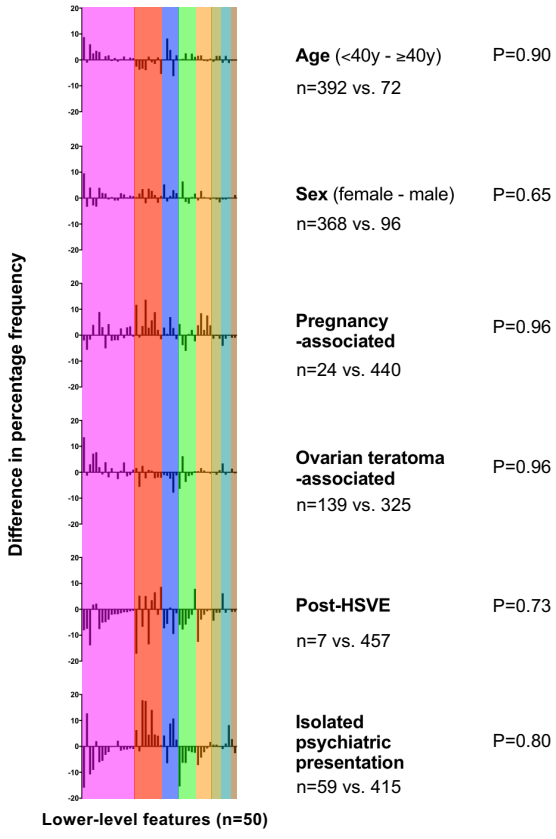


Figure 3.5 – **Plot of residual differences in lower-level features in six dichotomous comparisons of clinical factors associated with NMDAR-Ab-E.**

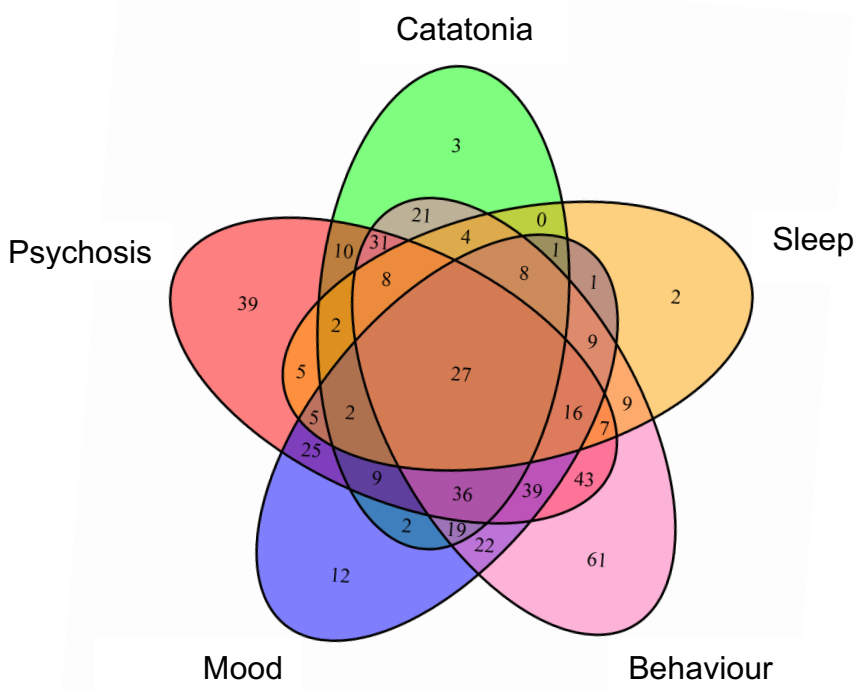
Frequency of each feature is normalised by percentage of sub-group. Each higher-level domain is colour coded by strips running between the plots as per figure 3.4 scheme. Uncorrected P values from two-way ANOVA of each comparison are given.

3.2.4 Relationships between psychopathologic features

To further explore the potentially overlapping nature of higher-level domains amongst individual patients a Venn diagram was made using the R package 'VennDiagram' with assistance from Dr Adam Handel. The five most common higher-level features were included: behaviour, psychosis, mood, catatonia, and sleep. This found at least one overlap in 334/451 (74%) of patients (figure 3.6a). The most common areas of non-overlap were in psychosis (39/451, 9%) and behaviour (61/451, 14%).

A similar mixed picture emerged from initial psychiatric diagnoses. Of the 44 cases in which this was available, 27 (61%) were psychoses (figure 3.6b, red), 10 (23%) were mood disorders (figure 3.6b, blue), and 5 were postpartum psychosis (figure 3.6b, purple). Although called a psychosis, research finds strong genetic and clinical associations of postpartum psychosis with bipolar disorder (181). One case was described as an acute stress reaction and in one case a co-morbid state with three diagnoses was recorded: Somatoform disorder NOS, Psychotic disorder NOS, and Dissociative disorder NOS. Of the psychosis diagnoses in the context of the discussion of NMDAR-antagonist drugs discussed in 3.1, it was relevant that the clinical picture was such that 2 were called drug-induced, despite no clear evidence of drug taking and 6/27 applied a catatonia specifier. Consistent with the overlapping nature of the higher-level features, the overall impression from this was that clinicians had found the syndrome difficult to classify and both psychosis and mood disorder features were sufficiently prominent that both concepts had been used. The need to apply multiple diagnoses simultaneously rather than a parsimonious single category also points to this.

A



B

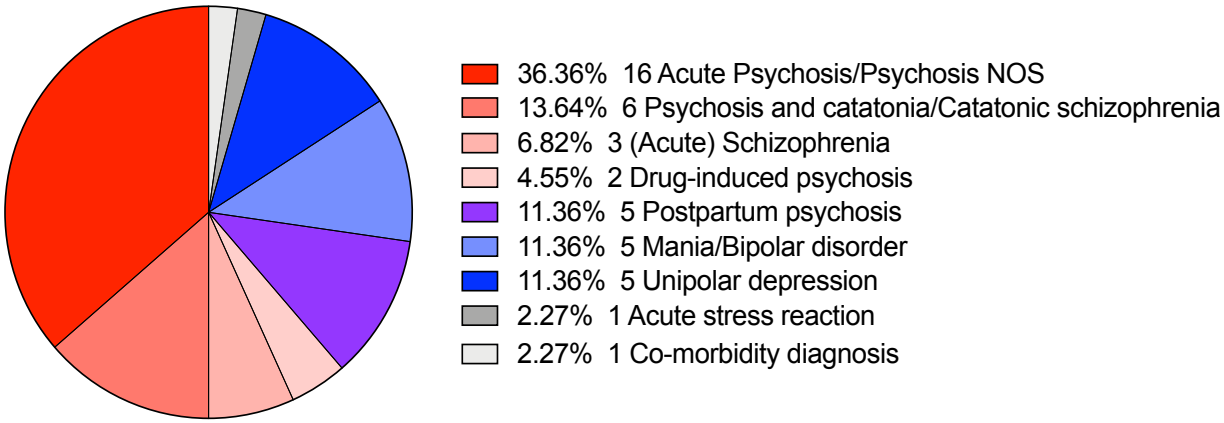


Figure 3.6 – **Psychiatric symptom clusters identified by bespoke classification and by recorded categorical diagnoses.**

A - Venn diagram demonstrating overlaps of higher-level features in individual patients. Each ellipse is a higher-level feature and each patient who had that feature is within it. The ellipses are arranged such that if a patient had an additional higher-level feature they are clustered into that overlapping segment. The total number of patients satisfying a particular overlap is given within that overlap.

B – Pie chart representing the initial diagnoses available from the reports. The legend for the colour-coded segments of the pie is given alongside it with number of cases. Psychoses are coloured red hues, mood disorder blue hues and postpartum psychosis purple; others are grey.

Given the frequency with which there were multiple overlaps and the diagnostic picture suggested, it was important to attempt to determine the extent to which the non-overlapping cases could be explained due to limited descriptions, i.e. minimal features noted and those that were, lead to higher-level classification as psychosis or behaviour. For example, of the 78 cases that reported only 1 lower-level feature the most common were delusions (23, 29%) and agitation (18, 23%).

As none of the reports followed formal psychiatric interviewing schemes, a proxy of descriptive psychopathologic expertise was sought that was common to the reports. The simple and easily classifiable variable of psychiatric authorship was chosen. Papers were classified as 'psychiatric-described' if any one of the authors was a psychiatrist or from a department of psychiatry and/or if the journal had a psychiatry theme. For these purposes, psychology and other definitively mental health professions and journal were equated with psychiatry, but this was rarely needed.

		Psychiatry specialty journal		
		-	+	*Row totals*
Psychiatrist and/or Department of Psychiatry authorship	+	**51**	**55**	106
	-	335	**23**	358
	Column totals	386	78	

Table 3.2 – **Classification of cases based on the source of their description**. Cases in black boxes were categorised constituted the 'psychiatric-described' sub-group.

This remained a reasonably permissive approach, for example reports from the Journal of Neurology, Neurosurgery and Psychiatry would enter this category despite some cases reported here potentially largely concerning a neurological aspect. Nonetheless, on applying this filter clear differences in reporting emerged. Prior to

sub-grouping the median number of features was 3 (IQR=2-5). In the non-psychiatric-described group this was effectively unchanged (median 3, IQR 2-4.5, upper limit 10) but in the psychiatric-described group the median increased to 5 with a broader IQR of 3-9 and upper limit of 20 (figure 3.7a). This indicated that although there were reports with very few features, there was a greater tendency towards more descriptive reports. This may have been reporting bias and simply a reflection of more psychiatrically complicated patients, however, there were no significant differences in demography, teratoma association or neurological profile (one-way ANOVA, P=0.429; table 3.3) This implied that fundamentally the patients were not pathologically distinct groups and favoured the explanation that they were overall describing the psychiatric phenotype in more detail.

	Individually reported				
	Psychiatry	**Neurology**	**Internal medicine**	**Obstetrics & Gynaecology**	**Other**
Number of cases	78	249	66	17	54
Median age	27	27	28	27	26
Female n (%)	62/78 (79%)	191/249 (77%)	53/66 (80%)	17/17 (100%)	45/54 (83%)
Psychiatric n (%)	78/78 (100%)	231/249 (86%)	62/66 (94%)	17/17 (100%)	51/54 (94%)
Seizure n (%)	43/78 (55%)	147/249 (59%)	39/66 (59%)	10/17 (58%)	31/54 (57%)
Movement disorder n (%)	40/78 (51%)	136/249 (55%)	47/66 (71%)	9/17 (53%)	24/54 (44%)
Dysautonomia n (%)	33/78 (42%)	103/249 (41%)	41/66 (62%)	10/17 (58%)	22/54 (41%)
Central hypoventilation n (%)	12/78 (15%)	72/249 (29%)	22/66 (33%)	6/17 (35%)	18/54 (33%)
Post-HSVE n (%)	0/78 (0%)	6/249 (2·4%)	1/66 (1·5%)	0/17 (0%)	0/54 (0%)
Ovarian teratoma n (%)	19/78 (24%)	65/249 (26%)	26/66 (39%)	12/17 (71%)	25/54 (46%)

Table 3.3 – **Demographic, teratoma, and neurological features stratified by specialty of reporting journal.**

This was explored further by looking at the reporting of the lower-level features within the higher-level domains (figure 3.7b). The black line (psychiatry journals) tends to be higher and uninterrupted implying a more consistent fine-grained reporting of features.

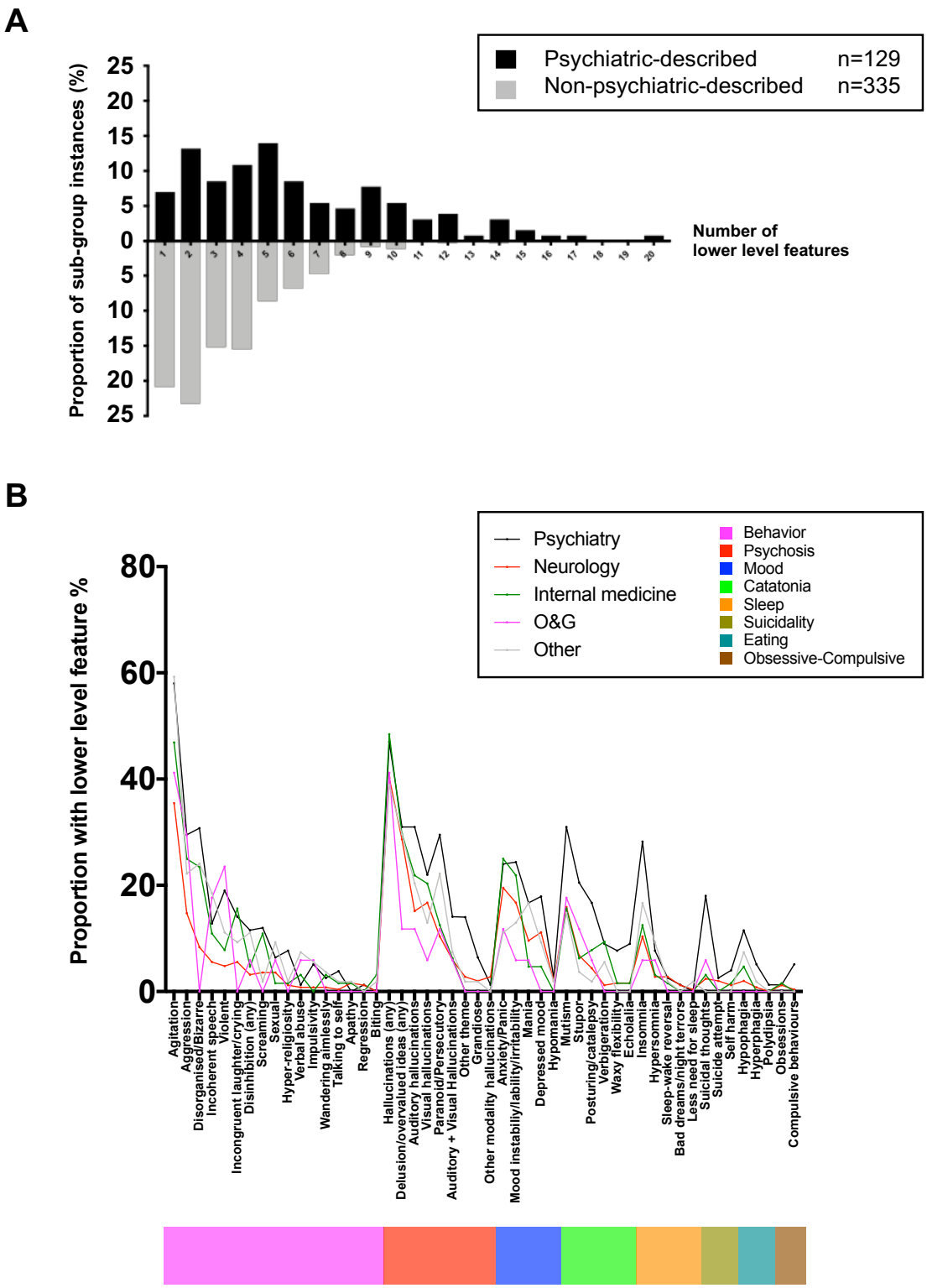


Figure 3.7 – **Reporting of lower-level features according to specialty.**

A – Histogram of lower-level features in psychiatric- and non-psychiatric-described sub-groups. Normalised to percentage of total sub-group size.

B – Frequency of lower-level features in specialty journals. Lower-level features arrange by overall frequency within higher-level groups as indicated by block colours.

The psychiatric- vs. non-psychiatric-described dichotomy was first applied to the higher-level feature Venn diagram clusters. This found a significant difference in overlap, consistent with reducing the proportion of single feature descriptions in the psychiatric-described sub-group (96/118, 81% vs. 221/329, 67%; P=0.0032; two-tailed Fisher's exact test). This demonstrates that when incorporating probable improved description, higher-level overlap is more likely than suggested from the whole cohort Venn diagram.

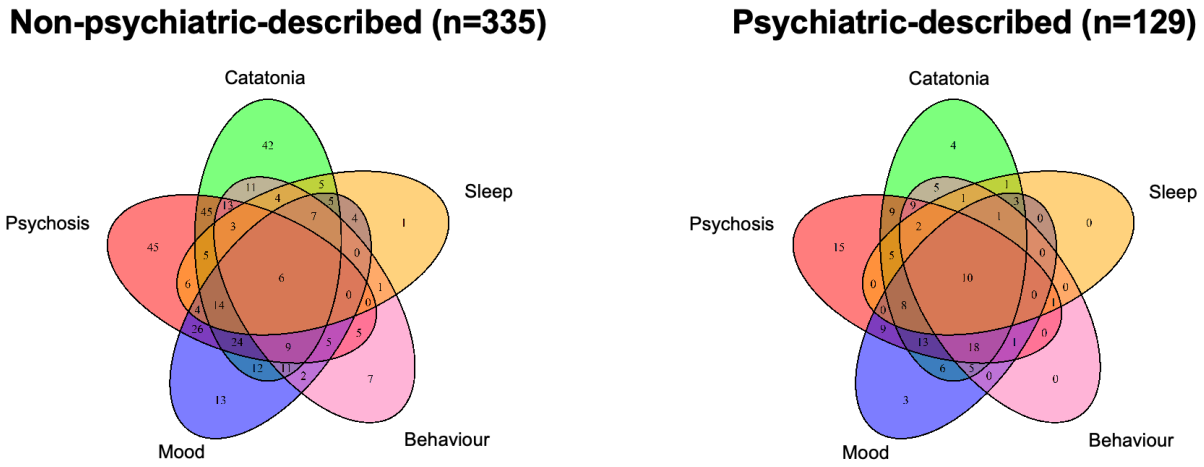


Figure 3.8 – **Venn diagrams of higher-level feature overlap in individual patients according to specialty of report.**

Cases were split on the basis of whether the report in which they were described involved a psychiatrist and/or was reported in a psychiatry journal.

Next, network analysis was used to further understand the relationships between the lower-level features and the structure of the syndrome across individuals. This approach has been increasingly used in psychopathology research to understand relationships between symptoms independent of categorical diagnosis (182,183). If multiple individual cases were to generate a highly connected network then this would be more consistent with a stereotyped complex syndrome whereas multiple

poorly-connected clusters would suggest that the illness could present as separate syndromes.

Firstly, given that many of the lower-level features were relatively rare compared to the most common, the set was simplified by excluding those that were <10% of the most common feature (agitation). This yielded a list of 27 lower-level features which remained sufficiently diverse to represent the varied phenomenology seen so far. Next, each lower-level feature was assigned node status and labelled with an abbreviation. The array of features and patients was transformed into a correlation matrix using the MMULT function in Microsoft Excel. This was used to derive edge weights, the strength of the connections between each node. These were exported as a .csv file and imported into the network analysis software package, Gephi (Version 0.9.2. for Mac OS X). The edges were deemed undirected, consistent with the correlational nature of the analysis.

The network properties are shown in table 3.4. Both networks showed high levels of interconnectedness between the features, but in each metric this was greater in the psychiatric-described sub-group. For example, density, a measure of completeness of actual compared to potential connections was 0.83 in the non-psychiatric-described but 1 indicating completeness in the psychiatric-described sub-group. In the psychiatric-described sub-group centrality indices pointed towards a highly interconnected network. For example, closeness centrality, a measure of how close each node is to every other node whereby a higher number indicates greater closeness was on average high in both groups (median closeness centrality=0.94 in non-psychiatric and =1 in psychiatric-described) but the range was narrower in the

psychiatric-described with no node falling below 0.84 whereas the non-psychiatric-described had nodes as low as 0.66 (figure 3.9). Consistent with the far greater completeness of the psychiatric-described network, betweenness centrality, a measure of the influence of a node on the network, was higher and distributed more broadly in the non-psychiatric-described compared to the psychiatric-described network (median=2.5, range=0.1-5 vs. median=0.48, range=0.05-0.48).

Parameter	**Non-psychiatric-described**	**Psychiatric-described**
Graph density	0.83	1
Average clustering coefficient	0.89	0.98
Average path length	1.17	1.03
Closeness centrality		
Mean	0.91	0.98
Median	0.94	1
Range	0.66-1	0.84-1
Betweenness centrality		
Mean	2.36	0.42
Median	2.5	0.48
Range	0.1-5	0.05-0.48

Table 3.4 – **Network properties of non-psychiatric-described versus psychiatric-described lower-level feature sub-groups.**

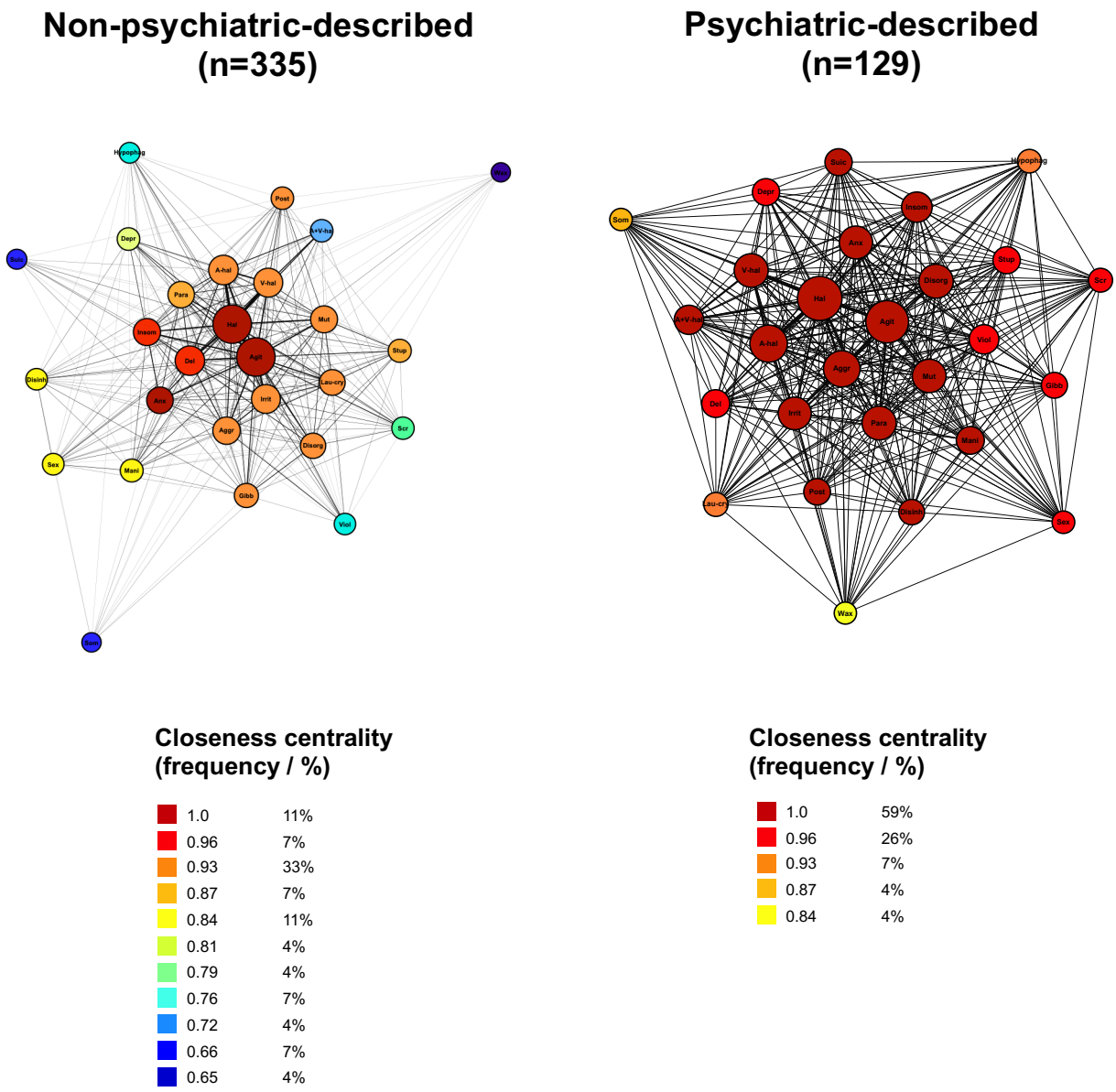


Figure 3.9 – **Visualisation of lower-level feature networks in non-psychiatric- and psychiatric-described sub-groups.**

Each network was plotted in Gephi with the Force atlas algorithm which places better connected nodes towards the centre and minimises edge crossover(184). The node size is scaled to the frequency of the lower-level feature and edge thickness is scaled to level of co-occurrence. The nodes are colour-coded according to closeness centrality which is summarised below each network alongside the percentage frequency of each centrality amongst the nodes.

Abbreviations used: Agit = agitation, Aggr = aggression, A-hal = auditory hallucinations, A-V hal = auditory and visual hallucinations, Anx = anxiety/fear, Del = delusion, Depr = depression, Disorg = disorganized/bizarre, Disinh = disinhibition, Gibb = talking gibberish, Hal = hallucinations, Insom = insomnia, Irrit = irritability/mood instability, Lau-cry = incongruent laughter-crying, Mani = mania, Mut = mutism, Para = paranoid theme, Phag = hypophagia, Post = posturing, Scr = screaming, Sex = sexual disinhibition, Som = hypersomnia, Stup = stupor, Suic = suicidal thoughts, V-hal = visual hallucinations, Viol = violence, Wax = waxy flexibility.

3.2.5 Discussion and limitations

This study firstly showed that there are many psychiatric features in reports of definite NMDAR-Ab-E and that these are from multiple domains of psychopathology including but not restricted to cardinal psychotic features. This mixing shares much with the unusual movement disorder caused by the disease (185). Secondly, it showed that even when pre-enriching for reports that could have been expected to give detail, reporting of mental state was often coarse, and that to extract a pattern that correlated with NMDAR models, prior experience, and internally consistent with the best-described cases, psychiatric involvement in the report was needed. Thirdly, it showed that this disease was confusing to clinicians with many reports of an initial psychiatric rather than neurologic diagnosis, and that these psychiatric diagnoses were not only psychoses but mood disorders about half of the time. Of particular interest were the patients with onset after delivery who were diagnosed with postpartum psychosis. This is a disorder that is labelled a ‘psychosis’ but has very little in common with an archetypal psychotic disorder like schizophrenia, instead having more in common with an organic mental state like delirium with rapid onset, fluctuating course, disorientation, prominent agitation, albeit with prominent delusional and hallucinatory components (186).

Taken together, this study set the scene for the direct study of patients. The most prominent consideration was the need for detailed clinical interview incorporating informant histories and ideally prospective description; there was likely under-reporting and mis-reporting present in the literature. Furthermore, it argued against the use of psychiatric scales validated for use in the diagnosis and monitoring of primary psychiatric disorders which are a poor fit for this syndrome.

3.3 Oxford autoimmune neurology cohort sub-group: retrospective and prospective psychiatric phenotyping

3.3.1 Introduction

Although the systematic review aimed to maximise granularity, there was a level of hierarchy within the lower-level features such that interesting but relatively rarely described phenomena were not directly reported. However, these were noted and inspired detailed assessment of local patients (table 3.5).

Category	Example
Auditory hallucinations	Music Music Musical Electronic dance music Sounds of drums Chill out music Rhythms Telephone ringing, bells playing, children Hearing echoes Background humming
Disorganised/bizarre	Hebephrenic charging behaviour Rocking back and forth striking her head with her fist repeating "I'm a good boy" Eating hand lotion Taking off clothing at inappropriate times Picking at her clothes and bedsheets He crouched on the floor, stood up, lay down, sat up, pointed to himself and to his examiner alternately, climbed several times on the scales when not requested. Orgasmic like behaviour
Suicide attempts / self harm	Defenestration and strangulation attempts Attempted defenestration Defenestration Defenestration Defenestration Defenestration Head banging Head banging against wall Banging head on concrete

Table 3.5 – **Coalescent patterns identified within lower-level features from literature review.** Each line is a direct quotation from a separate case.

3.3.2 Cohort description

Five patients and relatives recruited under the Immune factors in neurological diseases study from the Oxford autoimmune neurology service were assessed. Baseline demographic variables are listed in table 3.6. All were female with a definite diagnosis of NMDAR-Ab-E based on a typical clinical syndrome and CSF NR1-IgG confirmed by live CBA. All were assessed retrospectively including collateral history from relatives and two were also assessed prospectively during their inpatient admission.

Participant	Age at onset	Prior medical and psychiatric history	Occupation	Substance use
JR007	16	None	High school student	No
JR748	23	None	Shop manager	No
JR817	31	Acquired hypothyroidism	Healthcare professional	No
JR819	19	Premature birth with intraventricular haemorrhage	High school student	No
JR027	20	Eating disorder – remission	University student	No

Table 3.6 – **Baseline demographic variables of participants interviewed.**

The journey to eventual diagnosis and treatment for NMDAR-Ab-E is summarised in table 3.7. All were seen by a general practitioner or emergency department ± a mental health practitioner before a neurologist. 4/5 were given a primary psychiatric diagnosis which reflected those seen in the literature: psychosis, mood disorder, and acute stress reaction. For all, temporally-antecedent life events were invoked to reinforce the suspected diagnosis. Those who were initially referred to a mental health practitioner were detained under a mental health act section to psychiatric hospitals. In all cases relatives were clear that the patient was not under a level of stress inconsistent with their usual lives. The cases in which autoimmune encephalitis was suspected most quickly were all admitted to general hospitals rather than psychiatric hospitals. For the cases admitted to psychiatric hospitals, one

(JR027) was referred soon after admission on the grounds of the nature of the psychiatric presentation and a clear movement disorder while the other (JR748) was transferred due to a combination of family request combined with the realisation that a large abdominal mass could be a teratoma and therefore causally linked.

Participant	Presented to	Life event antecedent	Initial working diagnosis; treatment	Involuntary psychiatric admission?	Time to first suspicion of AE (days from onset); reason	Suspected by
JR007	GP	Preparing for exams	Stress-induced depression; advice	No	21 seizures	Medicine/ Neurology
JR748	ED + MH	Managing shop	Stress-induced first episode psychosis; olanzapine, lorazepam, admission	Yes	28 insistence from relatives and large abdominal mass	Psychiatry/ Neurology
JR817	ED	Driving lessons	Stress-induced adjustment reaction; advice	No	4 rapid progression and movement disorder	Medicine/ Neurology
JR819	GP	Preparing for exams	Stress-induced migraine; advice	No	12 seizures, exclusion of obstructive hydrocephalus	Neurosurgery / Neurology
JR027	ED + MH	University study	Stress-induced first episode psychosis; olanzapine, diazepam, community treatment then admission	Yes	21 psychiatric features and movement disorder	Psychiatry/ Neurology

Table 3.7 – **Journey to presumptive diagnosis and treatment for autoimmune encephalitis.**

Abbreviations used: AE = autoimmune encephalitis, ED = emergency department, GP = general practitioner, MH = mental health practitioner

3.3.3 Retrospective characterisation of psychopathology

Retrospective interviews were conducted with both patients and relatives/friends and were either video-taped with permission or discussed on the telephone and notes taken. Additionally, for JR027, the patient's initial inpatient Consultant Psychiatrist was also interviewed. Retrospective assessment consisted of a clinical history with a specific review of the patterns suggested by the systematic review.

Firstly, to permit direct comparison with the literature data the lower- and higher-level features identified in the systematic review were evaluated over the course of the whole illness. Consistent with the variable detail noted in the literature reports, here the majority of the features were far more common (figure 3.10). Accepting the clear caveat of a far smaller sample size, features that were uncommon in the literature were present in most patients probably implying under-reporting in the literature. Consequently, the higher-level features were more evenly covered with all 5 patients having features from behavioural, psychotic, mood, catatonic, and sleep domains.

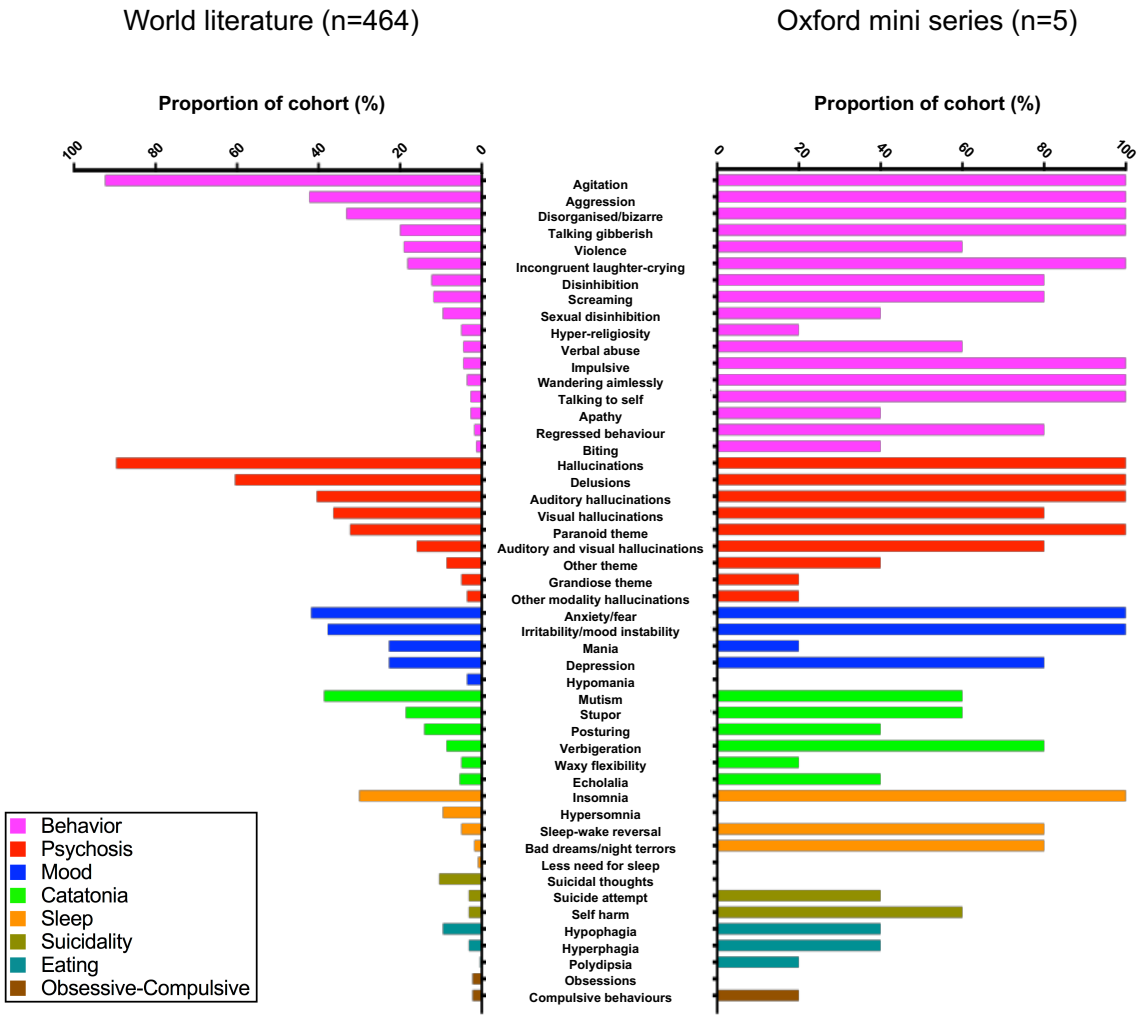


Figure 3.10 – **Lower level frequency in a series of patients seen in the Oxford autoimmune neurology service (n=5, right) with those from the systematic review of world literature included for comparison (n=464, left).** The previous order from the literature is retained as well as higher-level colour coding (box).

Next, network properties of the lower-level features in this series were derived (table 3.8 and figure 3.11). Except for five lower-level features that were not detectable, the other features were relatively common, so all were included. This makes the overall network properties slightly less directly comparable. However, even in this small sample, once again higher quality description revealed a tightly connected core group of features with complete levels of closeness centrality sampling mood, psychotic, catatonic and regressed/disorganised/disinhibited behaviours (figure 3.11, dark red). Indeed, the median closeness centrality was 1 with a range of 0.83-1, almost identical to the psychiatric-described literature group. The higher betweenness centrality in this network compared to the psychiatric-described literature group (median=2.24 vs. 0.48) reflects the more peripheral lower-level features which are more dependent on the central nodes for connections elsewhere, consistent with not thresholding the number of nodes included to the same extent as the literature data.

Parameter	**Oxford mini series n=5**
Graph density	0.979
Average clustering coefficient	0.952
Average path length	1.067
Closeness centrality	
Mean	0.94
Median	1
Range	0.83-1
Betweenness centrality	
Mean	1.46
Median	2.24
Range	0-2.24

Table 3.8 – **Network properties in the Oxford autoimmune neurology mini-series.**

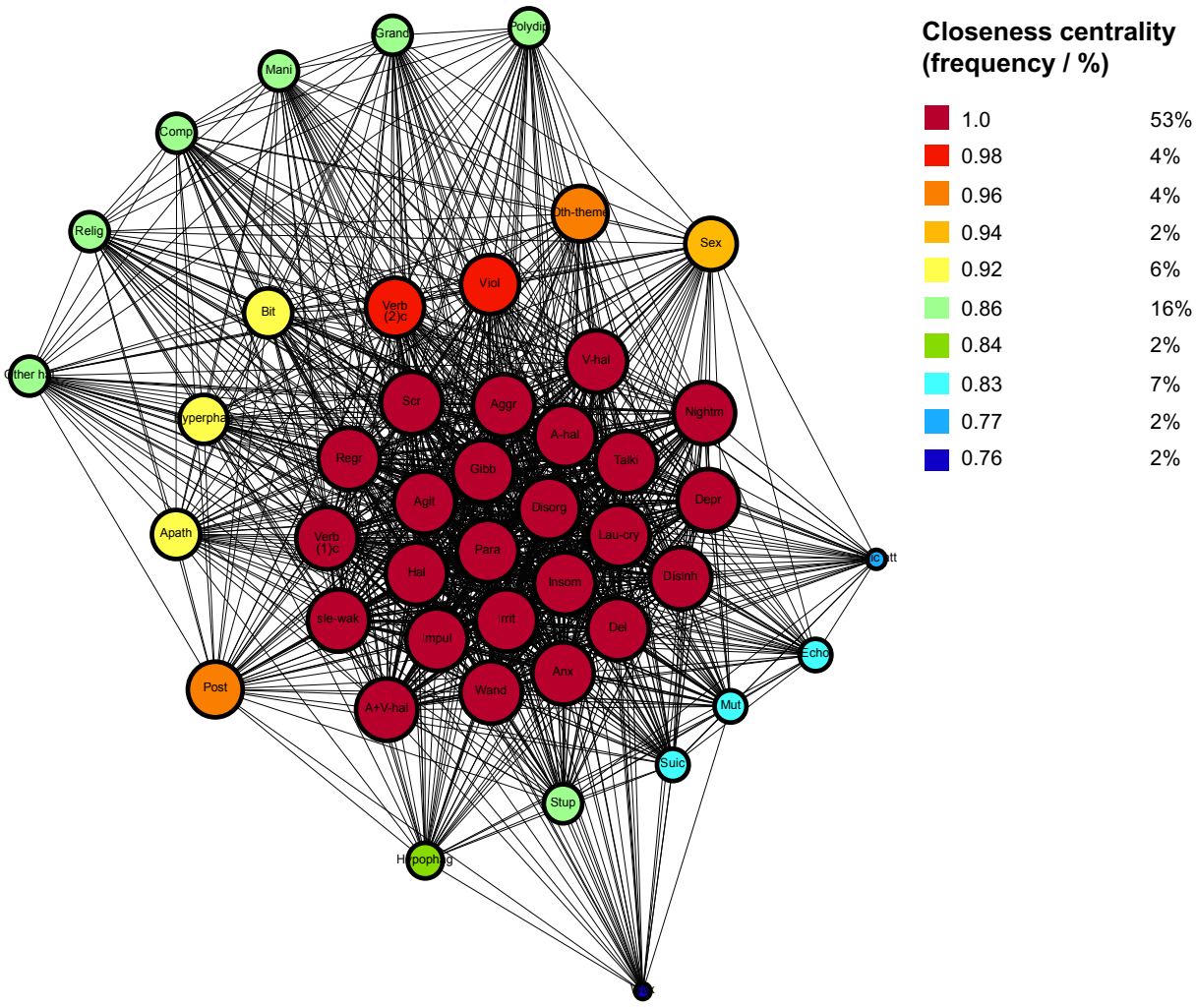


Figure 3.11 – **Visualisation of network properties in the Oxford autoimmune neurology mini-series.** Features with at least one instance were included (n=45) and plotted using the Force Atlas algorithm. Nodes were colour-coded according to closeness centrality with frequency of each given alongside. Nodes were scaled according to degree, a measure of the number of connections per node and edges scaled to frequency of connection. This shows a core highly interconnected group of lower-level features spanning multiple higher-level domains suggesting a shared complex syndrome.

Abbreviations used: A+V-hal = auditory and verbal hallucinations, Aggr = aggression, Agit = agitation, A-hal = auditory hallucinations, A-V hal = auditory and visual hallucinations, Anx = anxiety/fear, Apath = apathy, Bit = biting, Comp = compulsive behaviours, Del = delusions, Depr = depression, Disinh = disinhibition, Disorg = disorganized/bizarre, Echo = echolalia, Gibb = talking gibberish, Grand = grandiosity, Hal = hallucinations, Hyperphag = hyperphagia, Hypophag = hypophagia, Impul = impulsivity, Insom = insomnia, Irrit = irritability/mood instability, Lau-cry = incongruent laughter-crying, Mani = mania, Mut = mutism, Nightm = bad dreams/night terrrors, Other hal = other modality hallucinations, Oth-theme = other delusional theme, Para = paranoid delusional theme, Polydip = polydipsia, Post = posturing, Regr = regression, Relig = hyperreligiosity, Scr = screaming, Sex = sexual disinhibition, Sle-wak = sleep-wake reversal, Stup = stupor, Suic = suicidal thoughts, Suic att = suicide attempt, Talki = talking to self, Verb(1) = verbigeration Verb(2) = verbal abuse, V-hal = visual hallucinations, Viol = violence, Wand = wandering aimlessly, Wax = waxy flexibility.

Overall, this began to validate and provide nuance to the findings from the literature. The notable areas enriched in this cohort were hebephreniform behaviours such as: incongruent laughter-crying, disinhibition (including impulsivity), violence, verbal abuse, and regression, alongside associated behaviours such as biting and screaming. From a mood perspective, there was an absence of hypomania and lower rate of elevated mood. This was potentially consistent with misclassification in the literature of disorganised and disinhibited features as elevated mood. This interpretation is supported by sleep phenomena in which none of the patients had less need for sleep, a core feature of mania, whereas all patients had an inability to sleep and 4/5 had bad dreams and sleep-wake reversal. There was also a higher rate of depressed mood which could have been due to under-recognition of early downward deflection in mood.

Next, beyond classifying experiences into the lower- and higher-level features list, the interviews were examined aiming to extract key psychopathologic themes. These are listed in table 3.9. All reported that following a headache or flu-like symptom, the first notable change in mental state was related to sleep with an almost complete inability to fall asleep despite needing to sleep. Associated with this, two patients had vivid terrifying nightmares with themes such as being captured and killed or taken to hell.

Alongside this, or soon after a clear change in mood was noted, usually depressive with pervasive sadness, anhedonia, and sense of powerlessness, e.g. “She was saying she was depressed and kept saying 'I can't do this'.". This would give way to a mood state more consistent with perplexity and delusional mood as seen in

incipient psychosis. Multiple parents and partners reported patients saying things like: “help me, there’s something wrong…I think I’ve been drugged” or “I don’t feel myself…something’s happening”.

Soon after this, insight tended to diminish with mood becoming volatile, mixed and more bizarre e.g. “She was very emotional, happy then crying, telling everyone she loved them.”. Alongside this, patients became increasingly disorganised, with unpredictable patterns of behaviour. This could be associated with a degree of genuine anaesthesia or at least dissociative indifference to pain. For example, one patient suddenly charged into a wall fracturing her nose and another whilst under the care of a neurosurgical team pulled out a cerebral intraventricular drain. Several parents described a very flat expressionless facial expression almost as if the personality of their daughter had been removed and instead ‘possessed’ e.g. "She wasn't there at all, she wasn't the same person.”. As part of generally violent behaviour and need for restraint, several noted that their quite small daughters would need multiple professional security guards or mental health nurses to securely restrain them.

Alongside worsening short-term memory, speech would usually break down with catatonic phenomena such as echolalia and verbigeration which for some would manifest with repetitive text messages to relatives. Delusional ideas would begin to coalesce including paranoid or grandiose themes sometimes mapping onto personal history. For example, one patient whose parents had divorced many years ago believed she had special powers to bring them back together and another who was a regular Church-goer thought that she was in hell being subjected to experiments by

the devil. Hallucinations in both auditory and visual modalities were common and patients could be seen responding to them; none were ‘first rank’ in nature. All auditory hallucinations included music. In one there was an autobiographic element in that it was Bollywood music and she had been closely following a Bollywood ‘X factor’-style show prior to becoming unwell.

This hyper-agitated state in some gave way to a developmentally regressed and affectively flattened state. Mothers in particular noted how they were having to relate to a previously independent adult daughter as a child as if they had gone back a decade or more in development. This was accompanied by an ‘elephant in the room’ sign where patients were seen gripping and relating to soft toys in a child-like manner (figure 3.12). Although previously noted in children with NMDAR-Ab-E, this had rarely been noted in adult cases but from this series appears common. Some patients also developed a new interest in colouring.

Feature	Example
1. Marked sleep disturbance	*"She was not sleeping at all."*
2. Vivid nightmares	*"I had the worst nightmare ever…I dreamt I'd been taken to hell; it was so real."*
3. Mixed unstable affect	*"She was very emotional, happy then crying, telling everyone she loved them."*
4. Perplexity	*"She kept saying 'I don't feel myself; I don't know what's wrong.'"*
5. Incoherent repetitive speech	*"She was rambling repetitively...she sent the same text message 10 times"*
6. Catatonic facies	*"She had a very strange look on her face…like an emotionless staring."*
7. Possession-like / "drugged"	*"She wasn't there at all, she wasn't the same person." "It was like a different person, like she was on drugs." "…phenomenal strength - it took 6 people to hold her down."*
8. Musical / visual hallucinations	*"I heard Bollywood music coming through the pillow."*
9. Dissociative-disorganised	*"She went from being glazed over to suddenly getting up and charging into a wall, breaking her nose." Attempted to jump out of a window. Pulling out lines, catheter, intra-ventricular drain – without pain.*
10. Regression	*Teddy bear and/or colouring book*

Table 3.9 – **Ten characteristic mental state features noted during interview with patients, relatives, partners and healthcare staff in this series.**

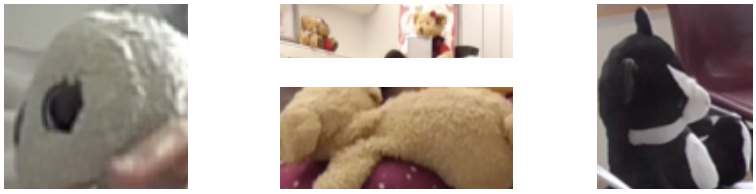


Figure 3.12 – **Childhood soft toys seen consistent with regressed personality secondary to NMDAR-Ab-E.**

3.3.4 Prospective characterisation of psychopathology

The rare opportunity arose to study these phenomena prospectively in 2/5 patients in this series (JR817, JR819). Both patients had ovarian teratoma-associated NMDAR-

Ab-E, which also gave an opportunity to observe improvement following definitive surgical management.

Relatives gave consultee consent in the initial phase and when patients regained capacity to consent, the study was discussed with them and they gave direct consent. Relatives gave detailed accounts in real time of the initial presentation prior to the diagnosis being confirmed potentially reducing recall bias. During the admission a time series was generated via regular multi-disciplinary assessment. This team consisted of: Consultant Neurologist (Dr M Isabel Leite), Consultant Neuropsychiatrist (Dr David Okai), and neurology ward sisters Ruth Linighan and Cheryl Perkins. Assessment was guided by covering the literature features identified as well as the neuropsychiatric inventory nursing home edition (NPI-NH), which bore a close similarity to the data-derived list. Due to clinical commitments, meetings took place opportunistically with a range of 10 – 22 days. This longer interval was associated with JR817 being admitted to intensive care post-oophorectomy and intubated. The final data point was the first outpatient follow-up.

The findings are summarised in figure 3.13. Consistent with the overall qualitative impression this shows that mood and sleep disturbance were the very earliest features (insomnia, depressed mood and anxiety/panic: mean onset = 0 days). Depressive aspects of mood gave way in the first week, but mood instability/irritability persisted (mean duration = 78 days). This was followed by agitated disinhibition with disorganised, catatonic, and psychotic features beginning within a week and ending within a month. This culminated in a large

psychopathologic burden which peaked within three weeks in both patients (figure 3.13b).

The peak burden was large and crossed multiple higher-level features. As shown in figure 3.12b, both patients improved following definitive treatment. Despite appearing dramatically, frank psychotic features did not endure (hallucinations: mean offset = 35 days, mean duration = 32.5 days; delusions: mean offset = 40 days, mean duration = 28 days). For JR817 these had resolved at the time of initial outpatient follow-up, three months after onset, with the only clinically detectable deficit being amnesia for the illness. In contrast, JR819 had a residual psychopathology more clearly consistent with acquired brain injury: abnormal eating patterns, compulsive behaviours, irritability, sleep dysregulation, and apathy. Interestingly, JR819 was initially treated with ovary-sparing cystectomy rather than oophorectomy and relapsed 3 months later with lesion recurrence detected on imaging. This ongoing antigenic stimulus is relevant to the greater residual symptom burden as well as a structurally abnormal brain at baseline (ventriculomegaly), which may have contributed to reduced functional reserve. Both time courses serve to demonstrate that the complex overall pattern demonstrated previously also has a complex time course that shifts from dominant mood to psychotic-catatonic to neurobehavioural phases.

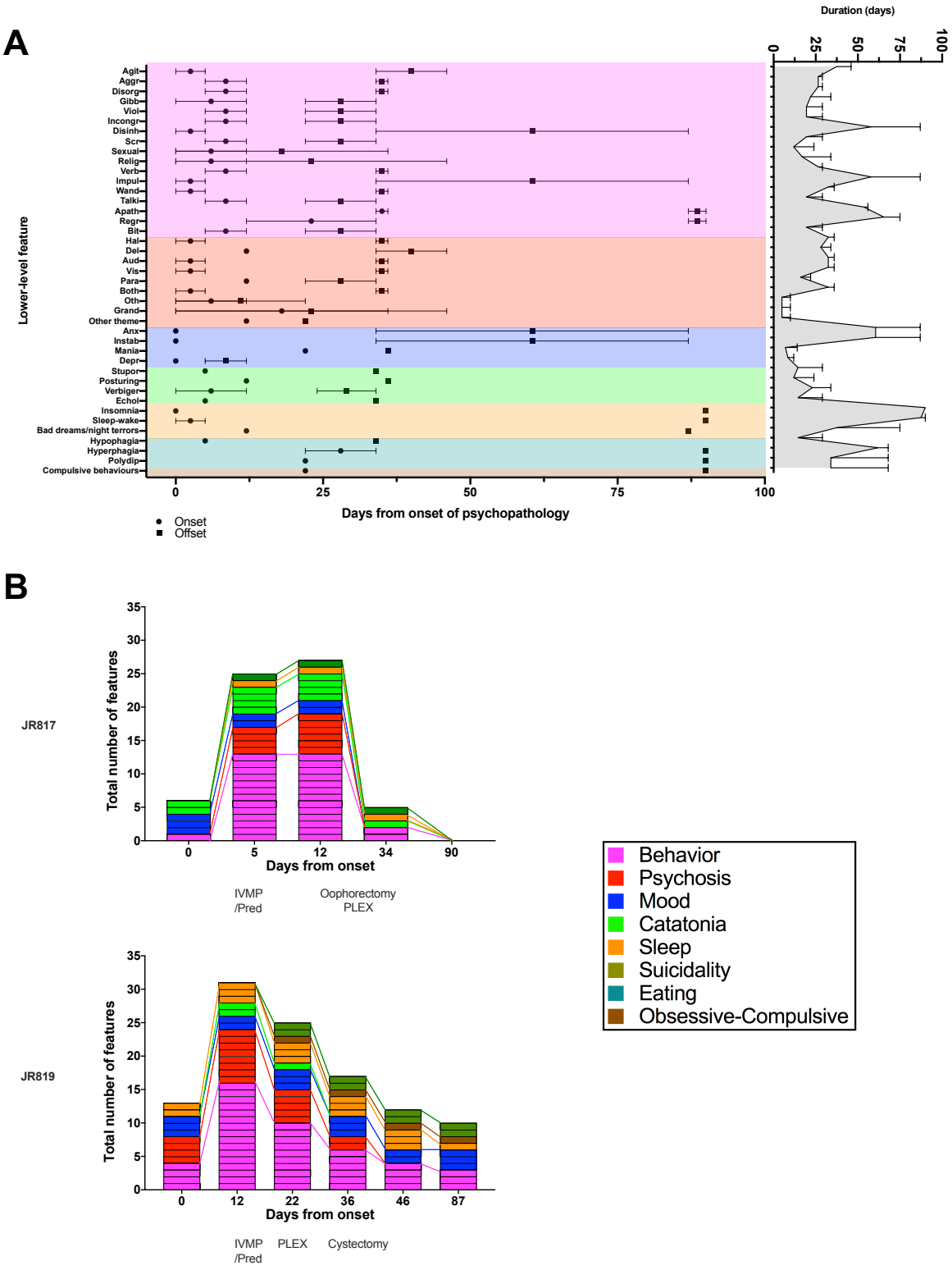


Figure 3.13 – **Psychopathology time course in two consecutive patients with ovarian teratoma-associated NMDAR-Ab-E.**

A – Mean symptom-onset and -offset times (circles and squares, respectively) for each lower-level feature present in at least one of the two patients. On the right, mean duration of each feature is plotted. Error bars indicate range.
B – Lower-level features at each assessment are plotted and colour-coded by higher-level category.

Abbreviations used: IVMP = intravenous methylprednisolone, Pred = oral prednisolone, PLEX = plasma exchange

3.4 Discussion and limitations

The aim of this study was to better define the clinical psychopathology of definite NMDAR-Ab-E using everyday mental state description. This work has attempted to organise and extract key themes from what transpired to be a considerable worldwide case literature. It then went on to apply this in a more standardised approach in a smaller group of directly assessed cases. The main findings were that changes in mental state are almost universal in definite NMDAR-Ab-E, that this psychopathology is usually severe and both qualitatively mixed and temporally oscillating within patients, but when described accurately shows consistency between patients.

As expected, psychotic features were a core component of the mental state deterioration, however initial onset as a more clearly mood-disordered presentation was more unexpected. Furthermore, despite persecutory aspects to many of the patients' experiences the overall nature of the psychotic components was not strongly in keeping with a Schneiderian-type psychosis. Indeed, first rank symptoms were rarely reported in the literature and were not found in the directly assessed patients on direct questioning. Moreover, the most psychotic phase of the illness appears to be relatively short-lived, giving way to a more regressed deficit state prior to illness resolution after treatment. In this transition between perplexity, and, in effect, positive then negative symptoms, the syndrome does resemble a classical account of schizophrenia, however the crucial distinction is the vastly accelerated and condensed time course such that in real time two exemplar patients would not appear similar.

One aim of the work was to inform discussion on early identification of these cases from within the mental health system. Patients and clinicians agree that this is desirable and almost always with the benefit of hindsight psychiatry tends to be singled out for not having considered the diagnosis earlier (187). The evidence presented here concerns NMDAR-Ab-E but not the nature of first episode psychosis and severe mental illness such that disease sensitivity but not specificity can be discussed. Studying non-encephalitis comparators with the same methods was beyond the scope of resources available in this study but is an important next step and possible approaches discussed further on. Nonetheless, much is already known about such comparators to enable a discussion.

The most obvious sensitive feature was that the NMDAR-Ab-E cases were very unwell and this evolved quickly. This permits a statement that this disease should be rarely, if at all, considered outside of this group. However, within this group which commonly presents to emergency departments and first episode psychosis services, are there truly unique ‘rule in’ features? The concept of first episode psychosis which has evolved alongside early intervention paradigms is necessarily broad, encompassing many patterns. One line of argument would be that no matter how consistent NMDAR-Ab-E is within itself, the syndromes with which it needs to be differentiated in the early acute phases are so potentially variable that the likelihood of prospectively differentiating them without something like either a ‘hard’ neurological feature that would never be expected in a primary psychiatric disorder or an objective laboratory test is impossible. That is to say, that while NMDAR-Ab-E does not look like a single categorical disorder like schizophrenia or bipolar disorder, these concepts largely only carry validity in the fullness of time (188), which is less

relevant in the first weeks of an illness, the time frame most relevant to this discussion.

Real world studies offer a chance to evaluate this perspective. For example, Tang *et al*. carried out a prospective study of CSF NMDAR-antibody positivity of first episode psychosis with a relatively fast onset of <1 month and neurologic features and found 4/15 patients had NMDAR-Ab-E. They observed that these patients were more obviously unwell than those without the illness causing their psychosis, to the extent that the brief psychiatric rating scale was futile for two of the four, whereas all those without underwent a full assessment. Additionally Scott *et al.* prospectively screened for serum NR1-IgG in all patients with FEP admitted for inpatient management over 2 years in Queensland, Australia (176). In the resultant large representative cohort (n=113) they found 4 patients with positive serum NR1-IgG. They were investigated with CSF testing and 3 were found to have CSF NR1-IgG so can be considered definite cases. 2 of the 3 patients developed a diffuse encephalopathy with 1 of the 2 having seizures during the first week of admission subsequent to blood testing. All three patients were noted to have confusion and 2 of the 3 were not responsive to psychotropic medication. Both studies pre-enriched their screening cohorts for the severe end of their patient populations by selecting patients admitted for FEP management which is usually managed in the community in both study settings. The definite patients identified appear to be unified by being on the cusp of the transition from FEP to frank encephalopathy, a pattern seen in the Oxford mini-series studied here.

Taken together, this suggests that the evolving nature of the syndrome is probably key to detection. For FEP services accustomed to managing patients in the community, the need to admit a patient per se should raise the index of suspicion, as well as unsatisfactory responses to psychotropic medication. This appears to be a syndrome which shifts through traditional clinical filters such that while FEP would be the most sensible construct in the first few days or even weeks of the illness, the rapidly fluctuating and complex symptom constellation could also be incorporated as a further marker. Indeed, in many respects catatonia at a certain time point would have been a better descriptor than psychosis. The two are linked in the ICD-10 category ‘catatonic schizophrenia’, which is largely a historical artefact and newer classifications like DSM-V list catatonia as a separate category not requiring schizophrenia (189).

If a parsimonious catch-all description is needed to focus diagnostic suspicion then delirium supersedes all of these concepts. Delirium can incorporate time series features such as acute/sub-acute onset and fluctuation as well as qualitative features of confusion, memory impairment, polymorphic psychopathology and catatonia (190). Young adults developing a mental illness with loss of insight and disorganised behaviour is a powerful frame bias towards concepts that usually account for these presentations, but the distinct feature of NMDAR-Ab-E is to occupy this symptomatic space but then move on. Delirium is a term loaded with its own pre-conceptions of frail elderly co-morbid patients with intercurrent medical illness, but it should be remembered that delirium can occur at any age and is the clinical presentation of an encephalopathic brain state. NMDAR-Ab-E causes an encephalopathy, so perhaps the answer has been there all along and the problem lies with a disease that unlike

most brain syndromes evolves through diagnostic frames that are usually managed by specialties whose practice tends not to overlap.

This conclusion would suggest that unless every patient with FEP has a lumbar puncture then watchful suspicion would be needed to pick out this key differentiating factor. A future time-resolved survey from collaborators worldwide is now being planned which will help clarify how consistent the picture of NMDAR-Ab-E presented here is, as well as using electronic health record approaches to generate real world comparator groups to help determine the specificity of these features. The online survey tool, 'Qualtrics XM', will be used to enable easy remote data entry and compilation of responses. Each episode of illness should be coded as a separate survey and whether it was the first episode or a relapse. Basic demographic and clinical information is requested including: age, sex, neurological symptom profile and results of CSF/EEG/MRI brain. Then the patient journey is surveyed including order in which clinical specialties were seen, initial diagnoses, and factors which prompted suspicion of NMDAR-Ab-E. Finally, psychopathological items are listed with onset and offset in days from first symptom is requested for each. Importantly, given that the data source will still be a mixture of detailed interviews and review of case notes. For each item the respondent is asked whether the feature was *clearly* present or absent, or if not to note that it was unavailable/unclear. Unlike the literature study, this will permit weighting of the degree of certainty.

The items are organised within domains that are slightly more nuanced than the higher-level features used initially: mood-spectrum, sleep, disorganised, dissociative/catatonic, psychosis-spectrum, agitated/violent, child-like, suicidality,

obsessive-compulsive, eating, and language. There is free space to note anything that is missed by the survey. Within each category there are DSM-V cardinal features of the main primary disorders with which these patients were confused: schizophrenia, mania, and depression. There are also the most common and distinctive features identified from the NMDAR-Ab-E patients. For example, ‘multiple text messages’ is an item in the disorganised features question, blank facial expression in dissociative/catatonic features, while disproportionate strength, charging and defenestration are in agitated/violent features, and teddy bear and colouring are items in child-like features. There is also a screen for post-traumatic stress symptoms at follow-up; the anticipation being that relative to the trauma associated with the illness this will be minimal due to amnesia.

Finally, this study did not study patients with mental state disturbances in whom serum NR1-IgG positivity is detected without CSF NR1-IgG. However, unlike the picture elaborated here for the definite NMDAR-Ab-E cases with its clear qualitative parallels with NMDAR dysfunction models as well as large burdens of illness beyond the remit of usual psychosis scales, psychopathology inventories in serum only cases have not found any distinction with seronegative first episode psychosis (191).

Definite NMDAR-Ab-E is defined by NR1-IgG detectable in CSF, which due to the potential for receptors to sequester the antibodies implies high levels are present in the CNS, either from the periphery by mass action/blood-brain barrier disturbance and/or from intrathecal synthesis (77). The absence of CSF NR1-IgG and lack of similar syndrome does not necessarily exclude a role for circulating NR1-IgG in neural processes relevant to psychiatric disorders. However, it does suggest that if it

is directly relevant to brain functions relevant to psychiatric disorders, it would need to be different either in nature or degree. Neurophysiological studies using purified IgG from such patients are beginning to help answer this side of the puzzle (168). Having clarified the definite NMDAR-Ab-E phenotype, an approach whereby syndromes that are *a priori* not this disease can be considered and the nature of circulating NR1-IgG considered. This is explored further in the next chapter using non-encephalitic neuropsychiatric comparator cohorts.

4 The prevalence and clinical associations of NR1-IgG in non-encephalitic neuropsychiatric cohorts compared with NMDAR-Ab-E: bipolar disorder and traumatic brain injury

4.1 Introduction

As outlined in chapter 1, there is an inconsistent literature on the prevalence of NR1-IgG autoantibodies in primary psychiatric disorders. Most NR1-IgG screening efforts have been in serum cohorts of non-affective disorders because of the traditional role of NMDAR antagonists as schizophrenia models and the characterisation of the psychiatric phase of NMDAR-Ab-E as psychosis. To explore whether the previously reported rates of NR1-IgG seropositivity in first episode psychosis were syndrome-specific, here the live CBA was used in two cohorts of an alternative primary psychiatric disorder, bipolar affective disorder (BPAD), one from the depressive phase, one from the manic phase, and a traumatic brain injury (TBI) cohort. The phenotypic analysis in chapter 2 showed that definite NMDAR-Ab-E could frequently cause severe mood disturbances therefore there was in fact a similar rationale to screening psychosis. The TBI cohort was included both as a neurological disease control, but also to investigate whether a condition that possibly de-sequesters brain antigens into the periphery could enrichment for NR1-IgG seropositivity as per current models of post-HSVE NR1-autoimmunisation. These were complemented by a healthy volunteer cohort to estimate general population prevalence.

4.2 Cohort description

4.2.1 Healthy volunteers – Oxford cohort

This included 55 self-reported healthy volunteers who were recruited opportunistically as part of the immune factors in neurological disease study and donated a single serum sample.

4.2.2 Bipolar disorder cohorts

Both cohorts were from drugs trials: the comparative evaluation of quetiapine-lamotrigine combination versus quetiapine monotherapy in people with bipolar depression (CEQUEL) trial included participants with BPAD who were depressed and the melatonin in acute mania investigation United Kingdom (MIAMI-UK) trial included participants with BPAD who were acutely manic (table 4.1). Both trials collected longitudinal serum samples: CEQUEL collected samples at baseline and 12 weeks and MIAMI-UK collected samples at baseline, 1 week, and 3 weeks. Demographic information was available and mood scores (quick inventory of depressive symptomatology, self report version – QIDS-SR16 where ≤5 no depression; 6–10 mild; 11–15 moderate; 16–20 as severe; and ≥21 as very severe; Young mania rating scale – YMRS, where 20 is the cut-off most commonly used in research to include as a case of mania). In the CEQUEL study age frequencies were given as deciles rather than for individual participants.

4.2.4 Traumatic brain injury

Following an approach to Professor Sharp's traumatic brain injury team at Imperial College London discussing the above rationale this cohort was generously shared. It included 31 patients with paired serum and CSF samples and an additional 26 patients with a serum sample each making a total of 57 serum and

31 CSF samples (table 4.1). All patients had moderate to severe traumatic brain injury (Mayo clinic classification) and were all samples in the chronic phase (>3 months post-injury with median 1.5 years).

In total from the four comparator cohorts there were 500 serum samples and 31 CSF samples from 335 participants:

	Healthy volunteers	**CEQUEL**	**MIAMI-UK**	**Traumatic brain injury**
ISRCTN code	N/A	17054996	28988273	N/A
Baseline diagnosis	Nil reported	Bipolar disorder - Currently depressed	Bipolar disorder - Currently manic	Traumatic brain injury
Number of patients	56	183	39	57
Female	35/56 (62.5%)	76/143 (53%)*	22/39 (45%)	13/57 (23%)
Median age (years)	36	45**	43	39
Baseline QIDS-SR16 Mean, standard deviation	N/A	15.2, 5.3	7.6, 4.3	N/A
Baseline YMRS Mean, standard deviation	N/A	N/A	26.4, 5.4	N/A
Total number of samples	56 serum	286 serum	101 serum	57 serum, 31 CSF
1 time-point per patient	56	80	6	57 (31 CSF pairs)
2 time-points per patient	N/A	103	7	N/A
3 time-points per patient	N/A	N/A	27	N/A
Time-points				
Baseline	56	194	38	57 (31 CSF pairs)
1 week	N/A	N/A	33	N/A
3 weeks	N/A	N/A	30	N/A
12 weeks	N/A	99	N/A	N/A

Table 4.1 – **Summary of cohorts used for NR1-IgG serum studies.** *Demographic data available for sub-group of n=143. **Estimated from mid-point of deciles.
Abbreviations used: QIDS-SR = Quick inventory of depressive symptomatology, YMRS = Young mania rating scale

4.2.5 Definite NMDAR-Ab-E

Serum-CSF pairs from the main cohort described in chapter 2 with sufficient material to measure NR1-IgG in both were used. Generally, these were samples at which the diagnosis was established with which a median time from episode onset of 15.5 days was consistent (range 1-272). There were 39 pairs from 39 illness episodes from 38

patients (1 patient donated from 2 episodes). Demographic and OT associations were consistent with the definite NMDAR-Ab-E cohort as a whole: median age was 22, 31/38 patients were female (82%), and 16/38 were OT-associated cases (41%).

4.3 NR1-IgG in non-encephalitic cohorts: seroprevalence and clinical associations

4.3.1 Methods

Samples were tested at a starting dilution of 1:20 using a NR1 live CBA as described in chapter 2. Positive samples were repeated including serial dilution. Samples that were initially borderline positive then negative were deemed negative (n=3) and samples that were initially clearly positive then negative were run once more (n=1). Samples that were positive on both the initial and repeat run were deemed positive and end-point dilution was recorded. To confirm specificity, positive samples were run on untransfected HEK293T cells and HEK293T cells transfected with AQP4-EGFP. This showed no non-specific or cross-reactive binding, respectively.

4.3.2 Healthy volunteers

6 out of 55 healthy volunteers (11%) were positive for NR1-IgG (end-point dilution of 1:20 in three and 1:40 in three). There are two approaches to using this data to estimate a positivity cut-off based upon end-point dilution. The first is to use the mean plus three standard deviations, however the markedly skewed nature of the distribution makes this problematic. The alternative, which respects the distribution, is to add median absolute deviations to the median. The median absolute deviation is the median of a derivate data set in which each value is the initial value minus the median of the whole initial data set. Both approaches are tabulated below (table 4.2). A median-based approach found a cut-off of zero. Given that the initial dilution is

1:20, this would mean that any positive result at 1:20 would be considered positive. Using a mean-based approach a sample dilution of 33.3 would be considered positive. Given that samples are serially diluted with an equal volume, this was rounded up to 1:40. The median-based approach may be more statistically correct but in practice, the field has used both. Therefore, in subsequent analyses both were applied as well as a conservative cut-off of 1:100.

	End-point dilution
Mean	3.27
STDEV	10.01
Mean + 3 STDEV	33.30
Median	0
MAD	0
Median + 3 MAD	0

Table 4.2 – **Mean, median and derivatives of end-point dilutions of NR1-IgG in a healthy volunteer cohort.**
Abbreviations used: STDEV = standard deviation; MAD = median absolute deviation.

4.3.3 Bipolar disorder cohorts

NR1-IgG seropositive patients were found in both cohorts. 9/183 patients (4.9%) of the bipolar depression cohort were positive whereas 7/39 (17.9%) of the acute mania cohort were positive. These were stable over time; all positives at any single time-point were positive at further available time-points. All negative samples were negative throughout all available time-points. NR1-IgG seropositivity in the bipolar depression cohort was not more common than the healthy volunteer cohort at a threshold of 1:20 (OR=0.42, P=0.12; two-tailed Fisher's exact test) or 1:40 (OR=0.69, P=0.7; two-tailed Fisher's exact test). The acute mania cohort versus the healthy volunteer cohort had positive ORs at both 1:20 and 1:40 thresholds but neither was statistically significant (OR=1.79, P=0.37; OR=2.5, P=0.26; two-tailed Fisher's exact test). The MIAMI-UK cohort had a statistically significant higher

proportion of positive results compared to CEQUEL at both 1:20 and 1:40 thresholds (OR=4.3, P=0.01 and OR=3.7, P=0.04, respectively; Two-tailed Fisher's exact test). However, because the MIAMI-UK NR1-IgG levels positive samples were a lower level overall (median 1:60, vs. median 1:80) this difference was lost with the conservative 1:100 threshold as none of the samples were above this threshold (table 4.3).

		CEQUEL	MIAMI-UK
1:20 threshold	Total positive samples Total patients positive Patients positive 1 time-point only Patients positive 2 time-points only Patients positive 3 time-points	16/286 (6%) 9/183 (5%) 2* 7 N/A	18/101 (18%) 7/39 (18%) 1* 1# 5
1:40 threshold	Total positive samples Total patients positive Patients positive 1 time-point only Patients positive 2 time-points only Patients positive 3 time-points	13/286 (5%) 7/183 (4%) 1* 6 N/A	12/101 (12%) 5/39 (13%) 1* 1# 3
1:100 threshold	Total positive samples Total patients positive Patients positive 1 time-point only Patients positive 2 time-points only Patients positive 3 time-points	6/286 (2%) 4/183 (2%) 1*,1 2 N/A	0/101 (0%) 0/39 (0%) 0 0 0
End-point dilution (1:x) of positive samples	Median Inter-quartile range Mean Standard deviation	80 40-320 143.8 139.4	60 20-80 53.3 28.3

Table 4.3 – **NR1-IgG seropositivity rates in bipolar depression and acute mania cohorts.** Results are grouped according to positivity thresholds and summary statistics are given for all positive samples above the lowest threshold.
*One time point available #Two time points available

Seropositivity was not associated with any statistically significant differences in demographic (age, sex) or symptom severity (baseline mood score) in both bipolar depression and mania cohorts (table 4.4). However, data on other confounding variables was not available. Furthermore, the available data from CEQUEL for this analysis had several caveats: data was available on 143 patients and not on the

entire cohort tested, one of the seropositive samples identified transpired to be from a participant that withdrew so no clinical information was available making the denominator of the CEQUEL NR1-IgG column eight rather than nine, age data was in deciles so the mid-point of each decile was assumed, and baseline QIDS was available from seropositive individuals but not seronegative so the baseline whole cohort was used as a surrogate measure.

	Healthy volunteers			**CEQUEL**			**MIAMI-UK**		
	NR1-IgG +	**NR1-IgG -**	**Difference**	**NR1-IgG +**	**NR1-IgG -**	**Difference**	**NR1-IgG +**	**NR1-IgG -**	**Difference**
Median age Years	25.5	37.0	-11.5 P=0.05	35[#]	45	-10 P=0.294	43	42.5	+0.5 P=0.84
Female	5/6 (83%)	30/49 (61%)	+22% P=0.39	5/8 (63%)	71/135 (53%)	+10% P=0.72	4/7 (57%)	16/32 (50%)	+7% P>0.99
Baseline QIDS Mean, STDEV	N/A	N/A	N/A	13, 4.1	15.2, 5.3*	-2.2 P=0.25	7.7, 4.5	7.6, 4.3	+0.1 P=0.96
Baseline YMRS	N/A	N/A	N/A	Unavailable	Unavailable	N/A	28.4, 5.0	25.9, 5.4	+2.5 P=0.27

Table 4.4 – **Demographic and clinical associations with seropositive cases in CEQUEL and MIAMI-UK cohorts compared to healthy volunteers.** In CEQUEL the frequency distribution of age deciles was compared with Pearson Chi-square test. In the healthy and MIAMI-UK groups ages were compared with two-tailed Mann-Whitney test. The proportion of females in all cohorts was compared with two-tailed Fisher's exact test. Baseline QIDS means were compared with a two-tailed unpaired T test.

#estimated from mid-point of age decile frequencies
*overall cohort from trial report n=202

4.3.4 Traumatic brain injury

There was an overall positivity rate of 9% (5/57) in serum at both 1:20 and 1:40 cut-offs. However, none of the paired CSF samples were positive (table 4.5). The overall serum rate was not significantly different from healthy volunteers at a 1:20 cut-off or

1:40 cut-off (OR=0.79, P=0.7594 and OR=1.67, P=0.72, respectively; 2-tailed Fisher's exact test).

	Serum	CSF
1:20 threshold		
Paired serum:CSF patients positive	2/31 (6%)	0/31 (0%)
Unpaired and paired serum patients positive	5/57 (9%)	
1:40 threshold		
Paired serum:CSF patients positive	2/31 (6%)	0/31 (0%)
Unpaired and paired serum patients positive	5/57 (9%)	
1:100 threshold		
Paired serum:CSF patients positive	1/31 (3%)	0/31 (0%)
Unpaired and paired serum patients positive	2/57 (4%)	
End-point dilution (1:x) of positive samples		
Median	80	-
Inter-quartile range	120	-
Mean	96	-
Standard deviation	60.7	-

Table 4.5 – **NR1-IgG seropositivity rates in a traumatic brain injury cohort.** Results are grouped according to positivity thresholds and summary statistics are given for all positive samples above the lowest threshold.

4.3.5 Definite NMDAR-Ab-E: NR1-IgG in serum-CSF pairs

Paired serum-CSF samples from the main definite NMDAR-Ab-E cohort were compared with these non-encephalitic cohorts. The main finding was that all paired serum samples were positive when using a 1:20 cut-off (39/39, 100%), 34/39 (87%) at 1:40, and 24/39 (62%) at 1:100. Compared to the rate in healthy volunteers at the three cut-offs defined above (1:20, 1:40, and 1:100) these were all statistically significant (P<0.0001 at all dilutions, two-tailed Fisher's exact test; figure 4.1a). In all but one pair where serum NR1-IgG was 1:20 and CSF NR1-IgG was 1:32, all CSF NR1-IgG end-point dilutions were lower than serum. The two groups were significantly different (P<0.001, Two-tailed Wilcoxon matched-pairs signed rank test).

The median serum NR1-IgG end-point dilution was 1:160 (range 1:20-1:1280), the median CSF NR1-IgG end-point dilution was 1:32 (range 1:2-1:256), and the median difference between them was 1:140. Using Spearman's correlation co-efficient (non-normally distributed residuals) there was evidence of a moderate and significant positive correlation between serum and CSF NR1-IgG end-point dilution (R^2=0.52, P=0.0008). As shown in figure 4.1b, there was considerable variation in CSF at any given serum end-point dilution.

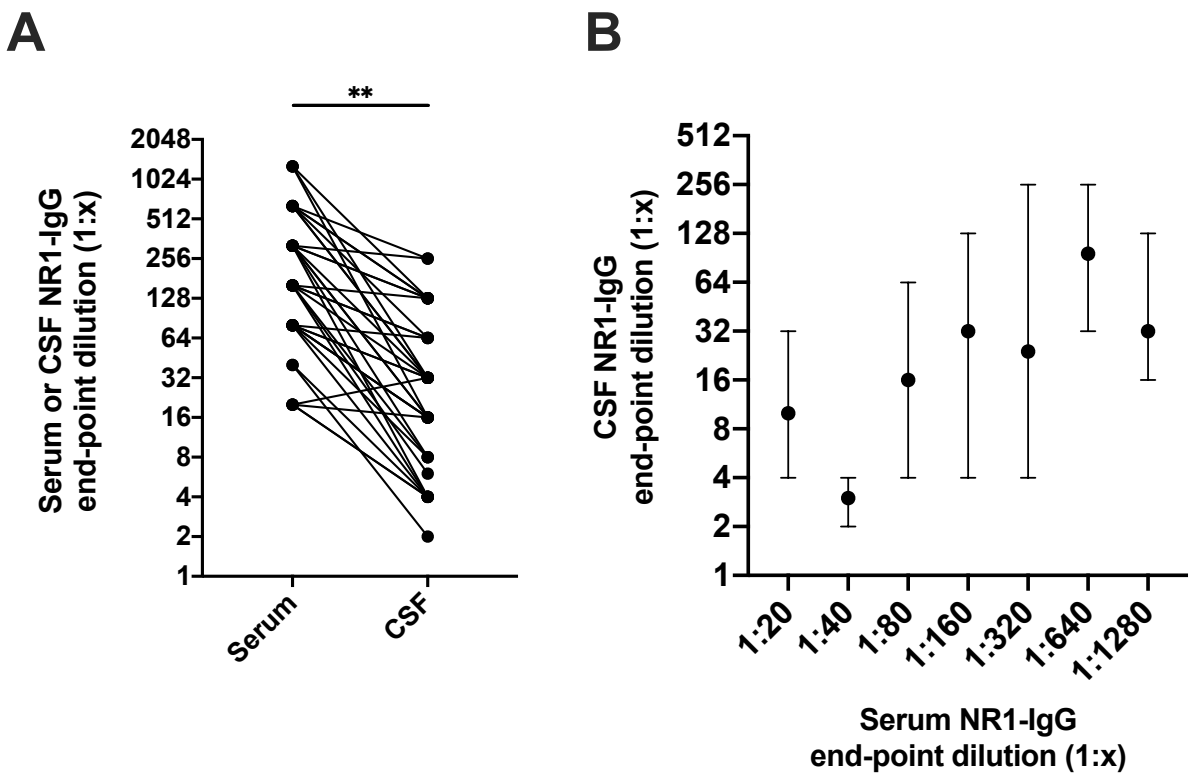


Figure 4.1 – **Relationship between serum and CSF NR1-IgG end-point dilutions.**

A – Pairwise comparison shows significant differences (P<0.001, Two-tailed Wilcoxon matched-pairs signed rank test).

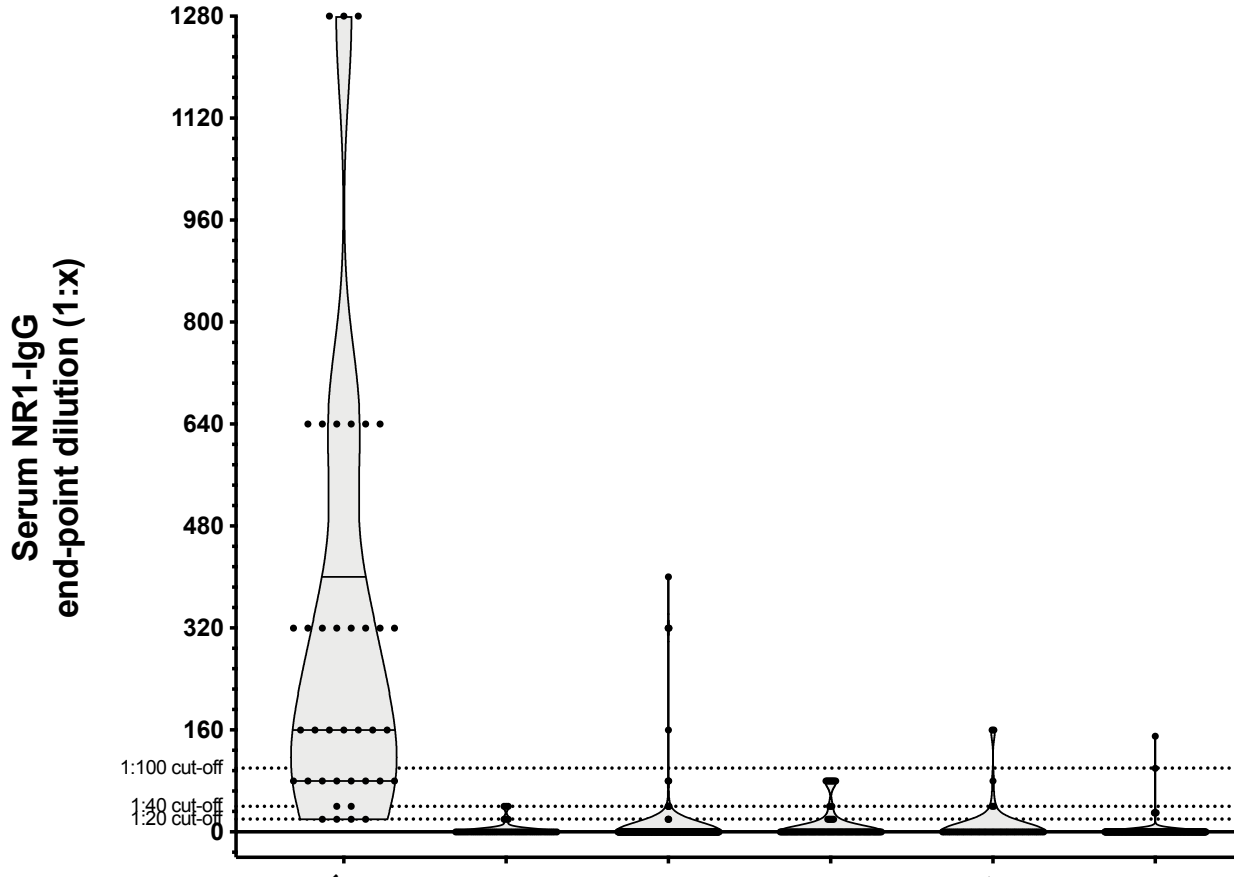
B – Median and range of CSF NR1-IgG end-point dilutions per doubling of serum NR1-IgG end-point dilution.

Both plots use Y-axis log2 scale consistent with serial dilution method of end-point dilution determination. The X-axis in B also uses a log2 scale.

4.3.6 Comparison between definite NMDAR-Ab-E, healthy volunteers and non-encephalitic neuropsychiatric comparators

Seropositivity in the definite NMDAR-Ab-E cohort was both proportionately more common than in healthy volunteers (1:20 cut-off; P<0.0001, two-tailed Fisher's exact test) and of a higher end-point dilution (P<0.001, two-tailed Mann-Whitney test) (figure 4.2). Trends from the non-encephalitic neuropsychiatric comparator groups versus healthy volunteers were that while all groups contained a seropositive sub-group, none were more proportionately more common. For purposes of comparison, published data from the prevalence of pathogenic antibodies in psychosis study (PPiP1), a community-based study which reported NR1-IgG in first episode psychosis, was included (191). They were also detected using a live CBA so are more comparable than published data using fixed CBAs.

Only the MIAMI-UK cohort had a positive odds ratio (1.79) but this was not significant (P=0.37) and the PPiP group was significantly less common (OR=0.26, P=0.02) (Two-tailed Fisher's exact test). When all patients were included, no group had a significantly higher end-point dilution than healthy volunteers, indeed the PPiP group was significantly lower (P=0.02; two-tailed Mann-Whitney test). However, given that *a priori* widespread seroprevalence was not expected in the comparator groups, comparison of the seropositive sub-groups could be considered more relevant. This found significantly higher end-point dilution in the CEQUEL and traumatic brain injury seropositive sub-groups versus the healthy volunteer seropositive sub-group (P=0.03 and P=0.04, respectively; two-tailed Mann-Whitney test).



	Cut-off	Definite NMDAR-Ab-E	Healthy volunteers	BPAD depression (CEQUEL)	BPAD acute mania (MIAMI-UK)	Traumatic brain injury	First episode psychosis (PPiP1)
Per-patient positivity rate	1:20	39/39 (100%)	6/55 (11%)	9/183 (5%)	7/39 (18%)	5/57 (9%)	7/228 (3%)
	1:40	34/39 (87%)	3/55 (5%)	7/183 (4%)	5/39 (13%)	5/57 (9%)	2/228 (1%)
	1:100	24/39 (62%)	0/55 (0%)	4/183 (2%)	0/39 (0%)	2/57 (4%)	2/228 (1%)
Proportion positive vs. healthy volunteers	1:20	*** OR=infinity P<0.0001	N/A	ns OR=0.42 P=0.12	ns OR=1.79 P=0.37	ns OR=0.79 P=0.76	ns OR=0.26 P=0.02
End-point dilution (1:x)							
Mean		320	3.3	7.8	9.4	8.4	1.8
STDEV		350.1	10	45.5	23.5	31.8	12.7
Median		160	0	0	0	0	0
Range		20-1280	0-40	0-400	0-80	0-160	0-150
End-point dilution vs. healthy *ALL samples*		** **P<0.001**	N/A	ns P=0.22	ns P=0.19	ns P=0.92	* P=0.02
End-point dilution vs. healthy *POSITIVE sub-group only*		** **P<0.001**	N/A	* **P=0.03**	ns P=0.18	* **P=0.04**	ns P=0.43

Figure 4.2 – **Distribution of NR1-IgG serum assays in definite NMDAR-Ab-E compared to healthy volunteers and non-encephalitic neuropsychiatric cohorts.**

The NMDAR-Ab-E samples are all from pairs with a NR1-IgG positive CSF sample. Individual samples are presented (black circles within a violin plot summary of the distribution (middle horizontal line is the median and upper and lower horizontal lines are bound of the interquartile range). Positivity cut-offs are indicated by dotted horizontal lines. Proportions compared with two-tailed Fisher's exact test and distributions compared using two-tailed Mann-Whitney test.

*P<0.05, **P<0.005, ***P<0.0005 Abbreviations used: NMDAR-Ab-E=NMDAR-Ab-E, ns=not significant, STDEV=standard deviation

4.4 Binding properties in NR1-IgG positive samples from non-encephalitic cohorts compared to NMDAR-Ab-E

4.4.1 NR1 co-localisation

To further validate whether the NR1-IgG antibodies were binding NR1, a commercial NR1 antibody was used to co-localise with bound patient IgG. NR1-transfected HEK293T cells were incubated with NR1-IgG positive samples from the NMDAR-Ab-E cohort, healthy control NR1-IgG seropositive group and NR1-IgG seropositive samples from the non-encephalitic neuropsychiatric cohorts. The samples were co-incubated with a commercial polyclonal rabbit anti-human NR1 antibody against N-terminal extracellular residues 385-399 which are nearby the putative epitope region of residue 368 from the (Alomone labs AGC-001). Serum and commercial antibody were diluted in the same well to a dilution of 1:40 and 1:1000 respectively. Following incubation with diluted serum the cells were washed and fixed as described in chapter 2 and then incubated sequentially with goat anti-human or IgG-Fc-γ AF594 and goat anti-rabbit IgG AF488 with wash steps in between.

All positive samples co-localised with the commercial antibody. The protocol was also run with the commercial antibody incubated separately following fixation and incubation with anti-human antibody. Both approaches yielded the same appearance (figure 4.3).

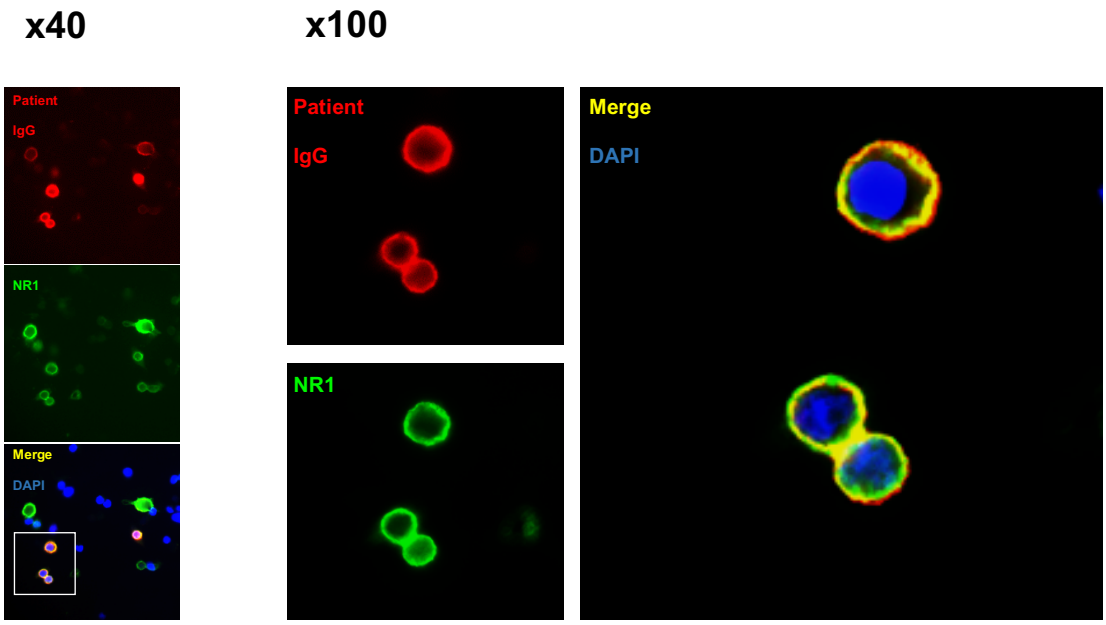


Figure 4.3 – **Patient IgG from non-encephalitic neuropsychiatric comparator groups co-localises with cell-surface expressed NR1.** A commercial antibody against NR1 (green) co-localises with human IgG on the surface of HEK293T cells NR1-transfected to express NR1. Patient IgG does not bind non-specifically to cells as demonstrated by absence of patient IgG on non-NR1-transfected cells (DAPI positive – blue). Representative images shown at 40x and 100x with oil immersion.

4.4.2 NR1 mutant N368Q live CBAs

As discussed in 1.4.5.1, mutation of NR1 residue 368, from asparagine to glutamine (N368Q), removed a site of N-linked glycosylation and abrogated binding of polyclonal NR1-IgG from both patient samples (120) and patient-derived recombinant monoclonal NR1-IgG from CSF B cells (75). Therefore, with the assistance of Ms. Selina Thomsen, the wild-type NR1 (*GRIN1*) plasmid used in all live NR1-transfected CBAs was modified by site-directed mutagenesis to create this mutation, confirmed by DNA sequencing.

HEK293T cells transfected with the N368Q *GRIN1* plasmid continued to express NR1 on the surface (figure 4.4a) detectable with the commercial antibody used previously in figure 4.3. However, consistent with published data, NR1-IgG positive sera from the definite NMDAR-Ab-E cohort no longer bound (figure 4.4b).

NR1-IgG positive sera from the healthy volunteers and non-encephalitic neuropsychiatric comparator groups were then tested on this version of the live CBA. Bindings in all samples was either completely abrogated or the end-point dilution markedly reduced (figure 4.4b and 4.4c). From the healthy volunteer cohort 1/6 samples remained positive at 1:20, 1/9 from CEQUEL remained positive at 1:40 and 1/5 from the traumatic brain injury group remained positive at 1:20. This was consistent with the majority of binding being against a similar epitope to NR1-IgG in definite NMDAR-Ab-E. Given that the commercial antibody was raised against peptide antigen this was consistent with the comparator group NR1-IgG also largely binding a conformational epitope.

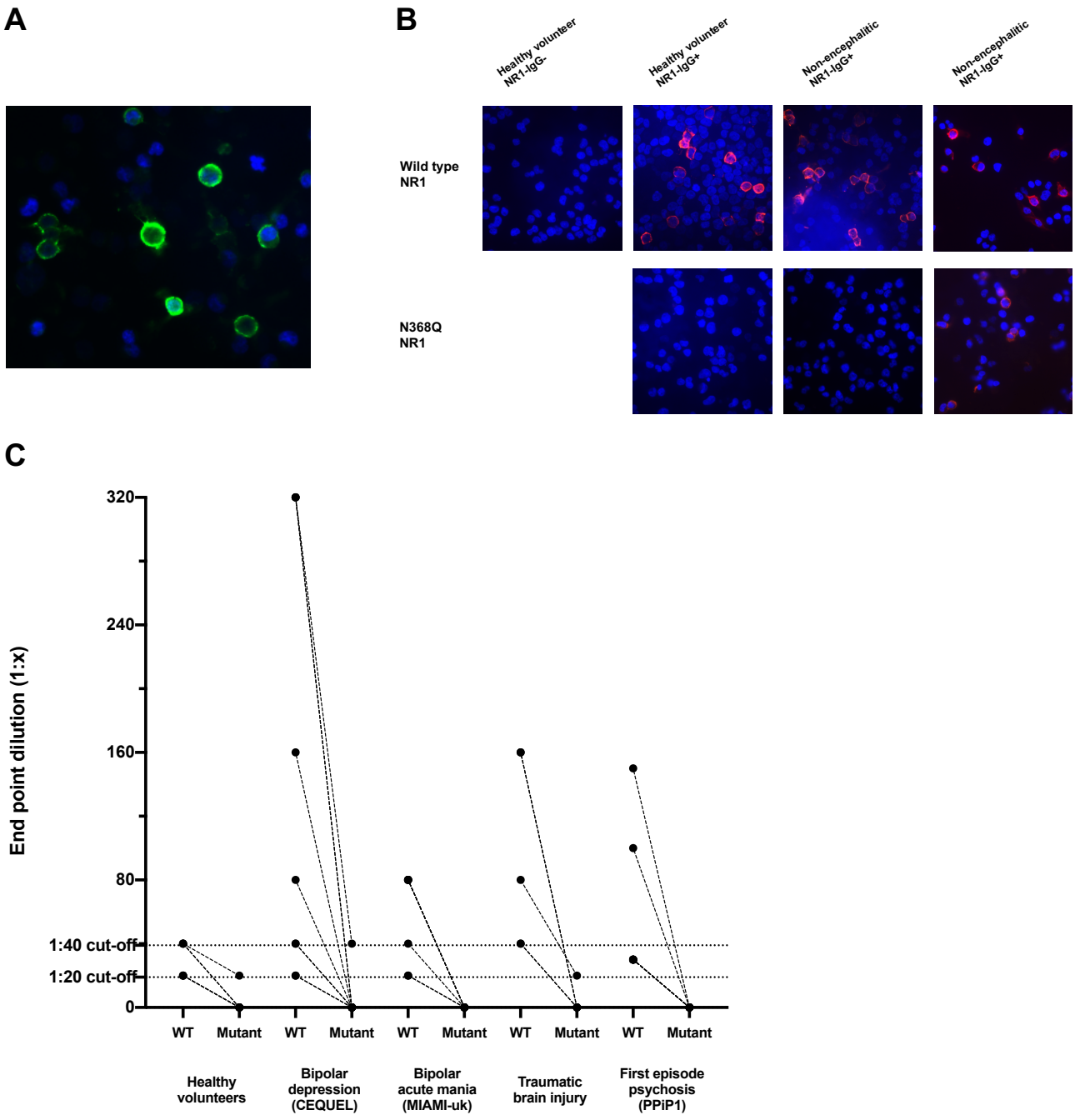


Figure 4.4 – **Binding properties of NR1-IgG on N368Q mutant NR1.**

A – Commercial antibody (green) against NR1 extracellular residues 385-399 binds cells expressing N368Q mutant.

B – Example live CBA appearances on wild type NR1 with a healthy volunteer negative sample, and positive samples from healthy and comparator cohorts. Examples of negative and positive appearances on the N368Q NR1 assay are shown beneath.

C – Summary of change in end-point dilution in NR1-IgG seropositive subgroups (WT=wild type).

4.4.3 Live neuron based assays (NBA)

Taken together, the mutant NR1 CBA data provided evidence against the non-encephalitic seropositive samples being false positives. As discussed in 1.6, many groups have used an alternative native antigen-based assay to assess the relevance of CBA positives, particularly in non-encephalitic discovery group. One of these is the live neuron based assay (NBA). The live NBA is similar to the live CBA in that NR1 can be expected to be expressed in its native conformation on the cell surface, but different in that the expression level is at physiological levels and spatially restricted rather than the high levels expressed across the cell surface in artificially transfected cells under a CMV promoter. Most probably, the high level of surface NR1 expression on the live CBA presents a high avidity surface such that lower affinity antibodies can bind.

Despite its potential relevance to explaining NR1 seropositivity findings across health and disease, the relationship between the NR1 live CBA and live NBA has received relatively little systematic attention. Therefore, the two were compared to explore the relationship between CBA end-point dilution and positivity on NBA with cohort status being the co-variate of interest, i.e. do the samples correlate simply or does definite NMDAR-Ab-E increase the likelihood of binding? A cohort was selected containing seropositive samples from the non-encephalitic neuropsychiatric comparators (≥1:40), seronegative healthy volunteer samples and the main definite NMDAR-Ab-E cohort, selected for a wide range of end-point dilutions (table 4.6). The distribution of end-point dilutions in OT and non-OT sub-groups was similar; the non-OT samples were non-significantly higher (Median 1:160 vs 1:320; range 1:20-1:500 vs 1:80-1:1000; P=0.06, two-tailed Mann-Whitney test).

	Definite NMDAR-Ab-E CBA positive	Healthy volunteers CBA negative	BPAD depression (CEQUEL) CBA positive	BPAD acute mania (MIAMI-UK) CBA positive	Traumatic brain injury CBA positive
Number of samples	30 OT=13 Non-OT=17	10	6	4	4
End-point dilution Median Range	 1:260 1:20-1000	 0 0	 1:200 1:40-320	 1:80 1:40-80	 1:120 1:40-160

Table 4.6 – **Cohort of samples used for the live CBA versus live NBA study.**

The live NBA was performed as described in 2.2.3. The live NBA was scored from 0-4 by myself and an experienced second rater (Dr Antonio Berretta). Scores were reviewed and a consensus recorded. Scores ≥ 2 were positive such that a characteristic punctate pattern binding could clearly be distinguished from background. Scores <2 were negative; non-zero scores suggested sub-threshold binding. Scores between 2-4 expressed level of positive staining (figure 4.5).

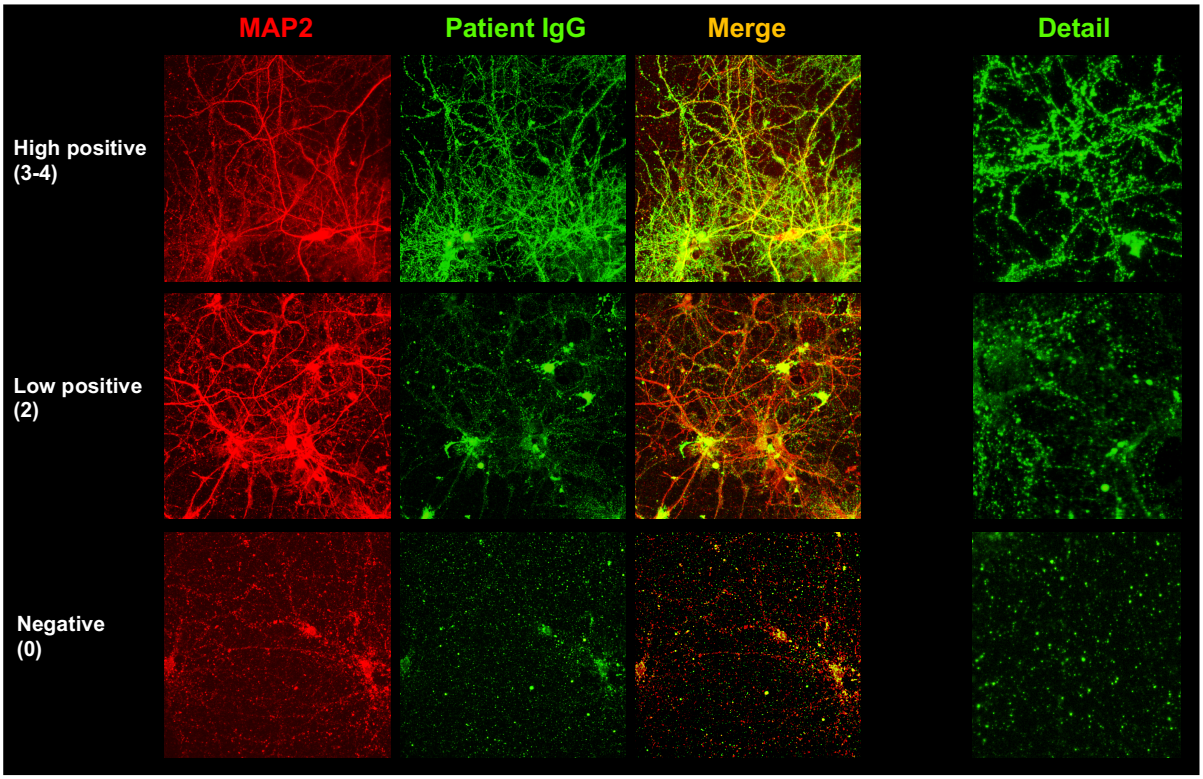


Figure 4.5 – **Live NBA positive and negative binding patterns.** A positive live NBA for NR1 is defined by patient IgG (green) binding neurons (MAP2, red) in a characteristic punctate pattern (score 2-4) which is distinct from background (score <2). Images recorded at 20x zoom with detailed excerpt alongside.
Abbreviations used: MAP2=Microtubule-associate protein 2

The first assay variation introduced was to compare the signal detection properties of a secondary goat anti-human IgG-Fc-γ with a rabbit anti-goat tertiary antibody AF-488 only with or without an additional goat anti-rabbit quaternary antibody AF-488. The tertiary + quaternary system tended to make the neuronal binding pattern clearer without causing spurious binding in seronegative samples (12/54 scores increased, of which 3/12 went from sub-threshold to positive, and 2/54 scores decreased without changing positive/negative status). End-point dilution (dilution of sample at which a positive neuronal pattern remained) followed a similar pattern with 10/54 increased and 1/54 decreased (figure 4.6). Representative images are shown in figure 4.7.

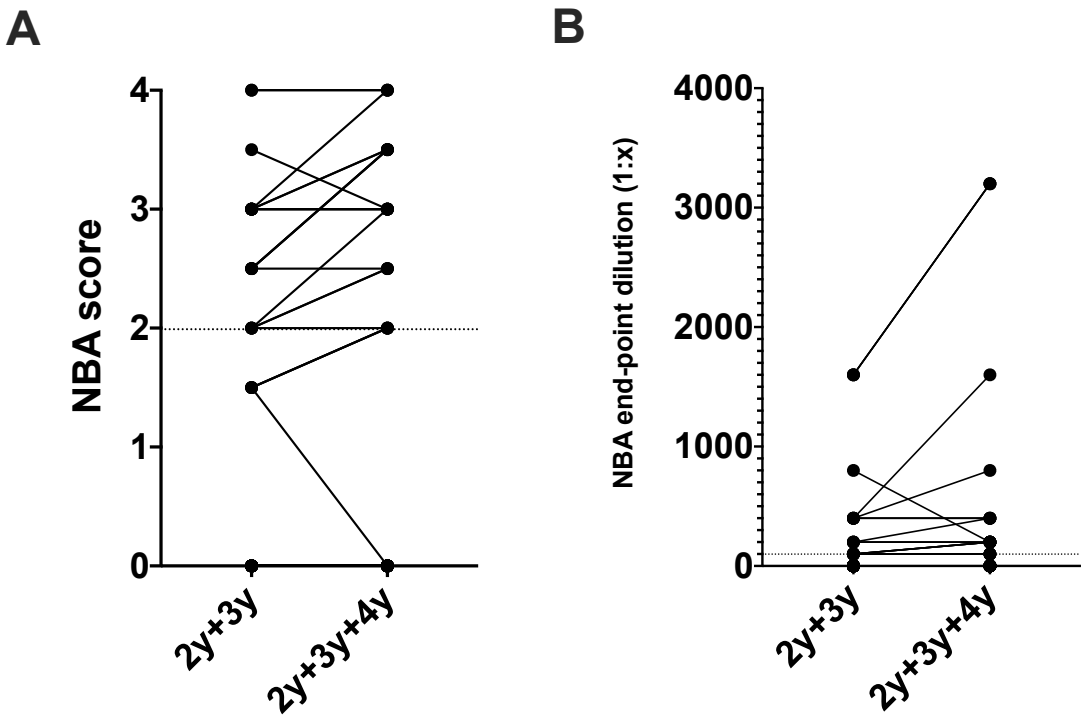


Figure 4.6 – **The effect of adding an additional reporter antibody on signal detection from live neuron based assay (NBA) – paired values**.

A – Paired NBA scores with or without a quaternary antibody.

B – Paired NBA end-point dilutions with or without a quaternary antibody.

Abbreviations used: 2y=secondary, 3y=tertiary, 4y=quaternary

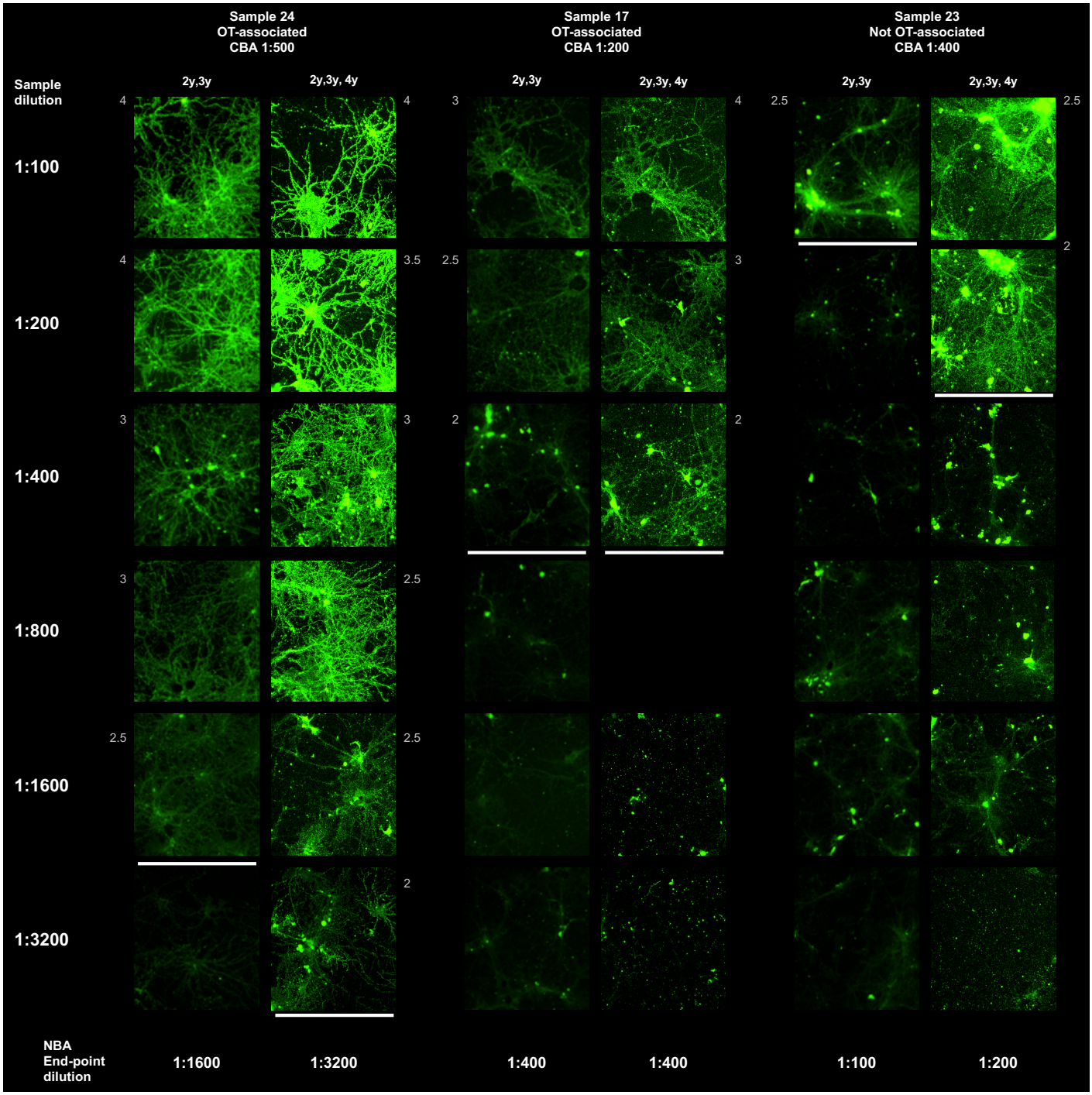


Figure 4.7 – **The effect of adding an additional reporter antibody on signal detection from live neuron based assay (NBA) – images.**

Three samples from patients with definite NMDAR-Ab-E were tested on the live NBA with high, medium and low positive patterns. The images are arranged vertically from low to high dilution, with the equivalent result with or without quaternary antibody. The NBA score for each image is adjacent and the end-point is indicated by a horizontal white line. Images were recorded at the same time at 20x on the same camera using the same software settings to allow comparison.

Next, to assess whether NBA end-point dilution may be a useful marker with or instead of NBA score, positive samples were serially diluted and the final dilution at which the score was 2 or more was recorded as the NBA end-point dilution. This found a moderate positive correlation (figure 4.8; R^2=0.52, P=0.0002, Pearson's linear correlation) suggesting that both measures could be usefully correlated with the sample CBA end-point dilution.

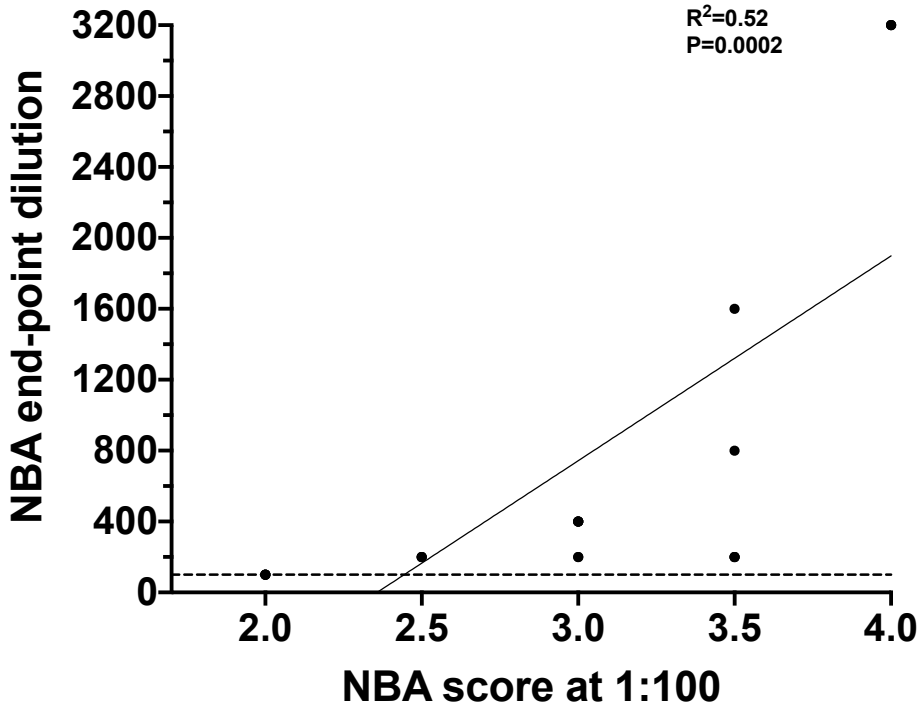


Figure 4.8 – **Relationship between NBA score at sample dilution of 1:100 and NBA end-point dilution of these samples.** Line of best fit derived by linear regression with Pearson's correlation co-efficient stated.

Overall, none of the CBA negative healthy volunteers were positive on the NBA, unambiguously all scoring zero. Similarly, none of the non-encephalitic neuropsychiatric comparator CBA positive samples met the threshold for positivity on the NBA, although one sample in each group was rated 0.5 (figure 4.9). Within the NMDAR-Ab-E group while 21/30 (70%) were positive, 9/30 (30%) were below threshold with 5/9 scoring 0, two scoring 0.5, and two scoring 1. Therefore, in this

selection of CBA positive sera deliberately selected to span a range of end-point dilutions, if the NBA were used as a confirmatory test then 30% of AE cases would be declared false positives (sensitivity 70%), but in this sample the AE syndrome specificity is 100%.

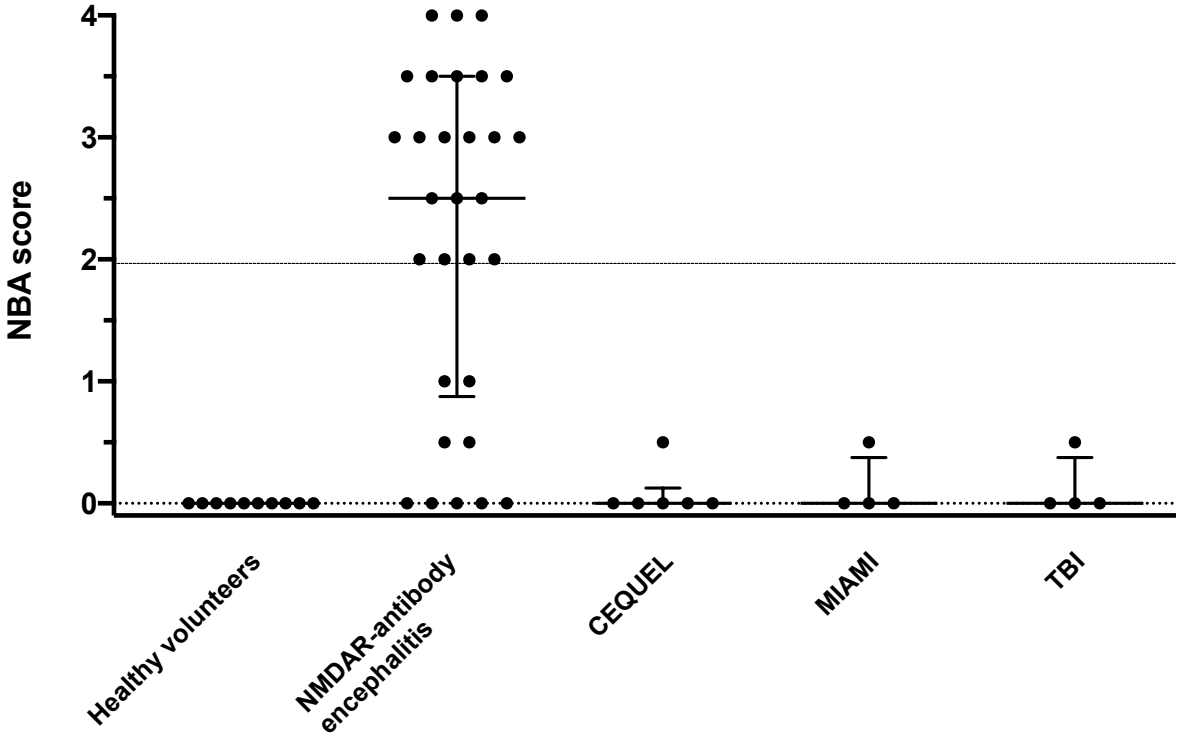


Figure 4.9 – **Distribution of live NBA scores from NR1-IgG live CBA negative healthy volunteers and positive autoimmune encephalitis and non-encephalitic neuropsychiatric comparator groups.**

All samples were screened at a dilution of 1:100. The dotted line indicates the NBA positivity cut-off of a score of 2. Error bars indicate the median and interquartile range.

To investigate the imperfect sensitivity of the live NBA for live CBA NR1-IgG positive samples from clinically and CSF NR1-IgG-proven cases of definite NMDAR-Ab-E, the CBA end-point dilutions were plotted against NBA end-point dilutions. This showed a weak and borderline non-significant correlation (Pearson R^2=0.13, P=0.05; figure 4.10a). The cause of this appeared to be different clusters such that some samples had low CBA end-point dilution and high NBA end-point dilution, some

samples had very high NBA end-point dilutions for moderate CBA end-point dilutions and some very high CBA end-point dilutions had modest NBA end-point dilutions.

OT status was the main clinical factor of interest that could explain this discrepancy. Grouping NBA positive and negative samples within OT and non-OT sub-groups found no difference in CBA end-point dilution in the OT group but in the non-OT group the NBA positive samples as a group had a significantly higher CBA end-point dilution (Median 1:400 vs 1:160, P=0.01, two-tailed Mann-Whitney test; figure 4.10b). Consistent with this, the CBA threshold for NBA positivity in the OT samples was lower than OT (1:20 vs. 1:320) and the non-OT NBA positive group CBA end-point dilution was significantly higher (median=1:180 vs. 1:400, P=0.04, two-tailed Mann-Whitney test; figure 4.10b).

This suggested that having an OT-associated illness lead to NR1-IgG that could bind to neuronally-expressed NR1 at a lower level. Indeed, when comparing NBA end-point dilutions with CBA end-point dilutions between the OT and non-OT groups, the OT group had a greater tendency for higher NBA end-point dilutions for any given CBA end-point dilution (median NBA-CBA difference 80 vs. -120, P=0.003, two-tailed Mann-Whitney test; figure 4.10c). This more consistent downward relationship from CBA to NBA was shown by pairwise statistically significant differences in the non-OT group which was absent in the OT group (P=0.1 vs. P=0.009; Wilcoxon matched-pairs signed rank test).

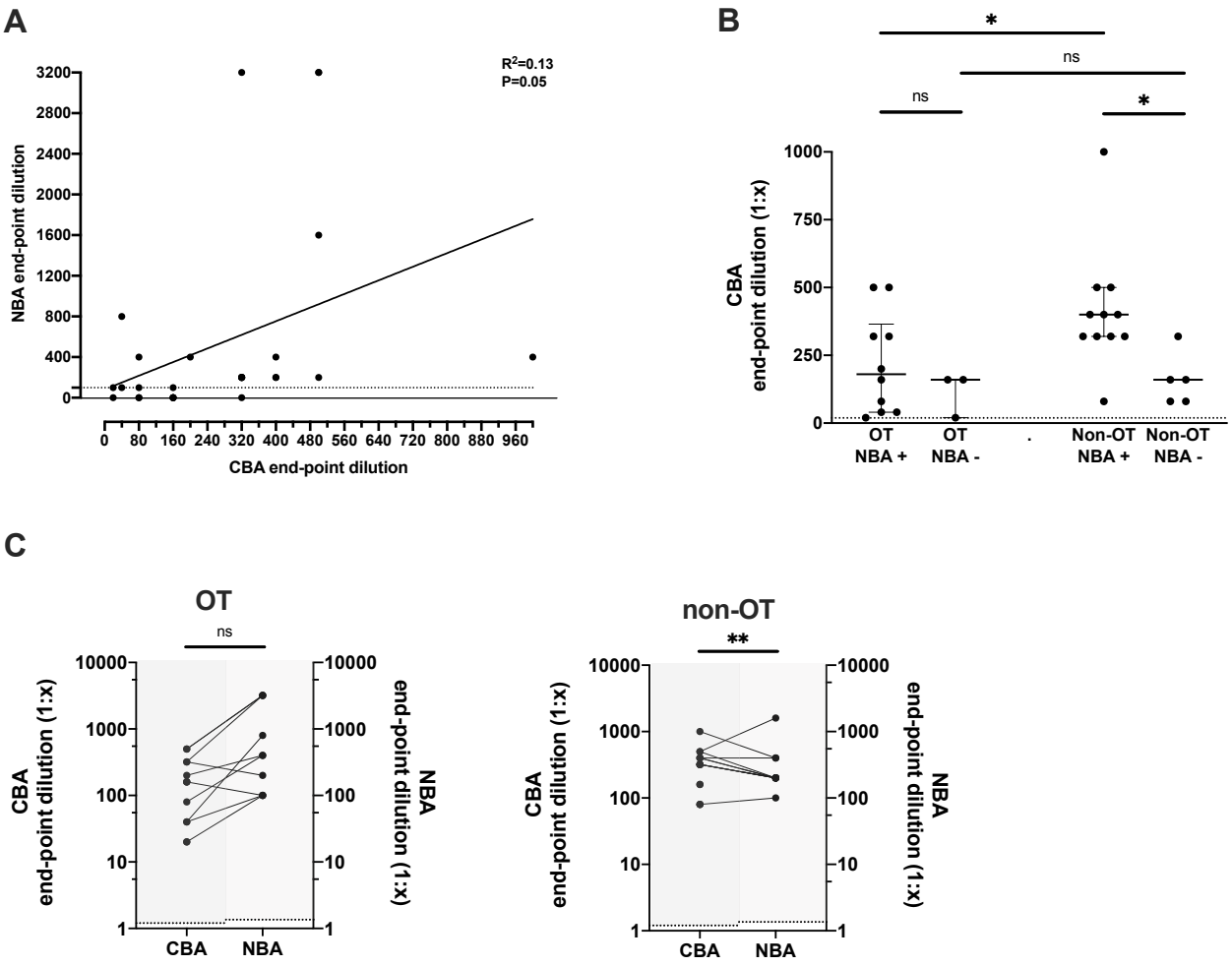


Figure 4.10 – **Correlation between CBA and NBA end-point dilutions analysed by OT status.**

A – Plot of CBA versus NBA end-point dilutions reveals a modest, borderline significant correlation with divergent relationships suggestive of sub-groups. Linear regression line of best fit plotted (Pearson's R^2=0.13, P=0.05).

B – CBA end-point dilution in NBA positive and negative NMDAR-Ab-E samples grouped by OT status. There was no statistically significant difference in the OT group but in the non-OT group NBA positive was higher than NBA negative (P=0.01, two-tailed Mann-Whitney test). Error bars show median and interquartile range. Comparing OT to non-OT, the non-OT group was higher than the OT group (P=0.04, two-tailed Mann-Whitney test).

C – Paired CBA-NBA end-point dilutions were significantly different in the non-OT group but not in the OT group (P=0.1 vs. P=0.009; Wilcoxon matched-pairs signed rank test).

*P<0.05 **P<0.005

4.5 Discussion and limitations

This chapter has studied NR1-IgG using two commonly used assay platforms (live CBA and live NBA) in healthy and patient cohort including the associated autoimmune encephalitis and non-encephalitic comparator groups. Using live CBA, NR1-IgG can be detected in all of these groups and the clinical association in individual samples cannot be distinguished using end-point dilution or for most by epitope modification. The groups did clearly differ in prevalence: at the most permissive threshold of 1:20 all sera from the paired CSF positive NMDAR-Ab-E cohort were positive but the majority of samples in the other groups were negative. Paired CSF samples in the traumatic brain injury comparator group, were all negative despite occasionally positive serum samples. Furthermore, live NBA completely discriminated between encephalitis and non-encephalitis CBA positive groups, however it had incomplete sensitivity with 30% of encephalitis samples negative. Within the encephalitis group, NBA-binding in the non-OT sub-group was more closely associated with CBA end-point dilution than the OT sub-group. Indeed, the OT sub-group was notable for containing samples of marginal CBA positivity that were far higher end-point dilutions on the NBA.

There are several limitations to consider for the generalisability of these findings. Firstly, the healthy control cohort was recruited opportunistically and not perfectly matched to the other cohorts and it was also relatively small. This is an important consideration for prevalence-based discussions, for example the comparator healthy volunteer cohort was larger (n=55 vs n=105) and had no positive NR1-IgG samples, making the modest 3% rate in the FEP cohort statistically significant (191). However, further expansion in healthy volunteer cohorts is needed because given the positivity

found here, the absence of positives in the published study is unlikely to be the most representative result possible.

Secondly, limited information was available regarding sources of non-disease-associated confounding variables such as substance use, smoking, alcohol, diet, and weight. This would have been more relevant had large differences in prevalence been found between the groups, but the main finding was a largely consistent low rate of positivity across groups. Alongside this, the bipolar disorder cohorts coming from trials rather than naturalistic studies may have introduced selection bias.

Thirdly, a lack of CSF samples in the bipolar disorder groups means that technically it cannot be completely certain that some of the patients were not in fact autoimmune encephalitis. Although improbable, evidence for this possibility comes from the potential for NMDAR-Ab-E to take a relapsing-remitting course with relapses more likely to present without clear neurologic features, and possibly with a mood-dominant syndrome (65). Hence, it could have been that some of these patients were misdiagnosed as bipolar disorder particularly because the disease was far less well known during the late 2000s recruitment phase of the CEQUEL and MIAMI-UK trials. However, on the other hand, to be included in these trials the patients received an extensive diagnostic interview using operationalised criteria such that the likelihood that such atypicality would be missed or deemed suitable for a trial is low.

Mindful of these caveats, the data presented here nonetheless do point towards a testable unifying model. Firstly, the trans-diagnostic background seroprevalence is consistent with a proportion of the general population with a mature naïve B cell repertoire capable of reacting against conformational NR1 epitopes. Upon exposure to NR1 autoantigen or similar epitopes in non-NR1 foreign antigen with co-stimulatory danger signals a NR1-directed B cell population could expand and affinity mature. This is consistent with the almost complete seroprevalence in the definite NMDAR-Ab-E cohort. The consistently higher end-point dilutions in serum than CSF suggest that this requires a peripheral onset; the differential levels are such that it is inconceivable that this could occur entirely intrathecally and diffuse passively into the periphery. The variable NBA binding properties also fit into this model if OT and non-OT cases are immunising with different efficiencies. This model predicts NR1-specific germinal centre reactions in NMDAR-Ab-E which could include NR1-IgM production and the production of NR1-antibodies from lymphoid sites with consistent cell populations such as TfH cells.

The lack of NBA binding in the non-encephalitic and healthy cohorts is consistent with these NR1-IgGs being lower affinity and therefore probably not affinity matured. However, the differential properties of the encephalitis cohort with 30% not binding, and OT-associated cases binding readily at low levels as judged by CBA end-point dilution suggests that affinity maturation and/or polyclonality is differentially enhanced in these cases. This is broadly consistent with rates in other studies that screen using a non-CBA-based approach then use a fixed CBA (107). It is also consistent with the fall in seropositivity rate in definite encephalitis when stricter cut-

offs are used, broadly consistent with the affinity filter perspective on multiple assay approaches.

This leads naturally on to the broader discussion of whether CBA NR1-IgGs in clinical contexts outside of encephalitis that do not bind complementary tests should be considered ‘false positives’. As with any test, this is determined by the question that it is being asked. This data implies they are false positives for autoimmune encephalitis but the commercial antibody co-localisation and N368Q mutant studies suggest that they share similar binding properties and are not analytic false positives. Indeed, although the non-encephalitic CBA positives and healthy volunteer CBA negatives were both negative on the live CBA, some non-encephalitic CBA positive samples were sub-threshold but not zero potentially suggesting that at a molecular rather histological resolution binding may be visualisable as per the single receptor tracking studies of the Groc laboratory (167). The fairest conclusion would be to suggest great caution when clinically testing serum without paired CSF without a suggestive clinical history of encephalitis and for research studies to be clear about the caveats introduced by single or combined assay approaches.

An immunological model of NR1-IgG genesis does not directly provide evidence against the hypothesis that these autoantibodies are modifying brain activity of seropositive patients with non-encephalitic mental disorders. However, if this is a non-syndrome-specific finding, then it does mean that other indices are necessary to support this hypothesis. One would be demographic or phenotypic features co-segregating alongside seropositivity. Lack of clinical and demographic differences between seropositive and seronegative groups within the bipolar disorder groups is

consistent with findings from first episode psychosis. Moreover, the bipolar disorder patients had chronic illness compared with relatively acute cases of first episode psychosis, suggesting that acuity is not relevant.

While the psychopathology of the non-encephalitic neuropsychiatric comparator groups was not studied directly, the severity and qualitative mix of features is not consistent with the signature presented in chapter 3, which was consistent with drug and genetic models. Therefore, if the NR1-IgGs are contributing to phenotype in these cases it is unlikely to be via widespread NMDAR dysfunction. But inconsistency with such a model does not exclude a role of NR1-IgG in modulating neural function in a psychopathology-relevant way. As discussed in chapter 1 there is considerable face validity to NMDAR dysfunction contributing to dysfunction across several serious mental illnesses without the gross dysfunction found in drug and genetic models. The psychopathology indices accessible here were not subtle, and it may be that other indices perhaps neuropsychological or electrophysiological such as EEG, MEG or functional imaging-based are needed. In individuals with other changes relevant to psychiatric illness such as polygenic risk, neurodevelopmental differences and/or stress-related brain states these antibodies may modulate brain function in a phenotype relevant way, assuming sufficient synaptic concentration.

Overall, the next logical step was to investigate immunising mechanisms in the clinical syndrome where the pathogenic role of NR1-IgG was strongest, definite NMDAR-Ab-E. Capitalising on the strengths of the host laboratory this was approached from the perspective of NR1-IgM and IgA isotypes in chapters 5 and direct investigation of NR1-secreting cells in lymphoid tissue in chapters 6 and 7.

5 The prevalence and clinical associations of IgM and IgA NR1-antibody isotypes in encephalitic and non-encephalitic cohorts

5.1 Development of a live CBA for IgM antibodies against NR1

5.1.1 Introduction

While it is IgG isotype antibodies against NR1 that have been shown to have pathogenic potential and are regarded as sufficient to account for NMDAR-Ab-E (75), non-IgG isotype NR1-antibodies could help resolve key immunopathogenic events. Additionally, comparison of these findings with comparator non-encephalitic neuropsychiatric cohorts would help to further understand the nature of NR1-seroreactivity in these groups.

Finding persistent and/or cycling levels of circulating NR1-IgM could be suggestive of recurrent germinal centre reactions against the NR1 antigen. Whereas absence of NR1-IgM in the context of persistent NR1-IgG could be considered more consistent with the prior establishment of a niched long-lived plasma cell population. Therefore, here the NR1 live CBA was modified for the detection of antigen-specific IgM isotype antibodies. Whereas other groups had previously reported NR1-IgMs with fixed NR1 CBAs (140,160,192), no studies had reported NR1-IgMs using a live CBA. The study was therefore of technical, clinical, and pathophysiological interest.

5.1.2 Methods

5.1.2.1 Patient cohort

Serum samples from 10 patients with definite NMDAR-Ab-E from the Oxford autoimmune neurology cohort (as described in chapter 2) were selected. Two patients had an ovarian teratoma associated with their illness. All patients were

female, the median age was 22.5 years, and age range was 16-71 years. A control cohort contained serum samples from 24 patients with neuropsychiatric systemic lupus erythematosus (NPSLE) and 20 healthy volunteers.

5.1.2.2 NR1-IgM Live CBA

The NR1 CBA was carried out as described in chapter 2 but with the use of a polyclonal goat anti-human Fc-μ-heavy chain cross-adsorbed secondary antibody labelled with AF594 (Invitrogen A21216). To determine optimum dilution of the secondary antibody varied dilutions were used on samples from cases and controls as outlined below.

5.1.2 Depletion of antibody isotypes

The following beads conjugated with antibody isotype-specific molecules were used: anti-IgA-conjugated agarose beads (Sigma A2691), anti-IgM-conjugated agarose beads (Sigma A9935), and protein G-conjugated sepharose beads (Sigma GE17-0618-01). The beads were handled using cut pipette tips to reduce risk of damage. Prior to adding the bead mix the tube was centrifuged at 2000G for 30 seconds and the supernatant ethanol layer was removed. Following resuspension in their carrier buffer a volume of bead mix twice the volume of serum sample used was added to a serum sample diluted in PBS in a 1mL Eppendorf tube. For example, if a serum sample was diluted 1:20 in a total volume of 500μL then 50μL of bead mix was added. Following addition of the diluted serum sample with bead mix the tube was placed on an upright circular rotator at 4°C overnight to ensure thorough mixing. The tube was retrieved, brought to room temperature, and centrifuged at 2000G for 30 seconds to pellet the beads. The supernatant was removed leaving residual volume

over the beads to minimise risk of bead contamination of the supernatant. 50µL aliquots of the supernatant were removed for parallel analysis with Ig isotype ELISAs for total isotype levels. Alongside the isotype depletions, diluted serum samples without bead mix were used as undepleted control samples.

5.1.3 Initial screen for serum NR1-IgM and optimisation of concentration of secondary antibody

An initial screen using the NR1-IgM live CBA on first available samples from the time course of the NMDAR-Ab-E patient sub-group revealed positive binding patterns in some patients and none in a small number of healthy controls used routinely in the NR1-IgG live CBA (Figure 5.1).

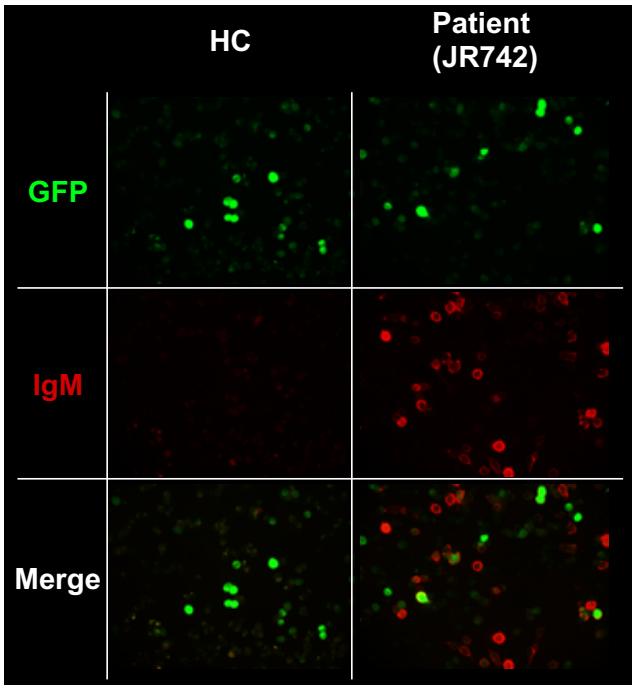


Figure 5.1 **Representative images from initial NR1-IgM live CBA.**

Cells were co-transfected with EGFP as a marker of transfection per se not NR1-specific transfection. The key aspect of staining is the absence of cell surface staining in the healthy control (left, HC) and the clear surface pattern of staining from the patient (right, patient). Image taken at 40x zoom.

Abbreviations used: HC=healthy control

Positive results (CBA score ≥1) were repeated with the sample serially diluted to find the dilution at which the sample remained positive. These results are tabulated in table 5.1 alongside age at onset, association with ovarian teratoma, and timing of the sample from onset (Table 5.1). The associations are discussed in more detail in 5.1.6 and extended further in 5.3. However, first this the NR1-IgM assay was further validated.

Patient	Age at onset, years	Ovarian teratoma?	Timing of first available sample (days from onset)	NR1-IgM (end-point dilution)
JR007	16	Yes	25	0
JR035	16	No	72	0
JR742	16	No	45	1:640
JR026	17	No	313	1:20
JR732	22	No	605	0
JR032	23	No	26	1:320
JR748	23	Yes	22	0
JR028	26	No	19	1:320
JR020	56	No	700	0
JR741	71	No	37	0

Table 5.1 – **Initial samples screened for NR1-IgM from a discovery cohort of ten patients with NMDAR-Ab-E.**

To explore whether more positive results could be detected using a higher concentration of secondary antibody, a high (JR032, 1:320) and a low positive (JR026, 1:20) sample were repeated at serial dilutions from 1:100 to 1:1600 (figure 5.2). This showed that the high positive sample retained at least the same end-point dilution from 1:100 – 1:800 dilution of secondary antibody but reduced to 1:80 using 1:1600. Extrapolating from the data, dilutions of secondary antibody from 1:100 – 1:400 would most likely have boosted the end-point dilution slightly.

In the low positive sample, all except 1:1600 achieved the same end-point dilution but 1:100 and 1:200 were more clearly positive at a primary dilution of 1:20 (CBA scores 2 and 3, respectively). The most concentrated secondary dilution of 1:100 increased the end-point dilution marginally to 1:40.

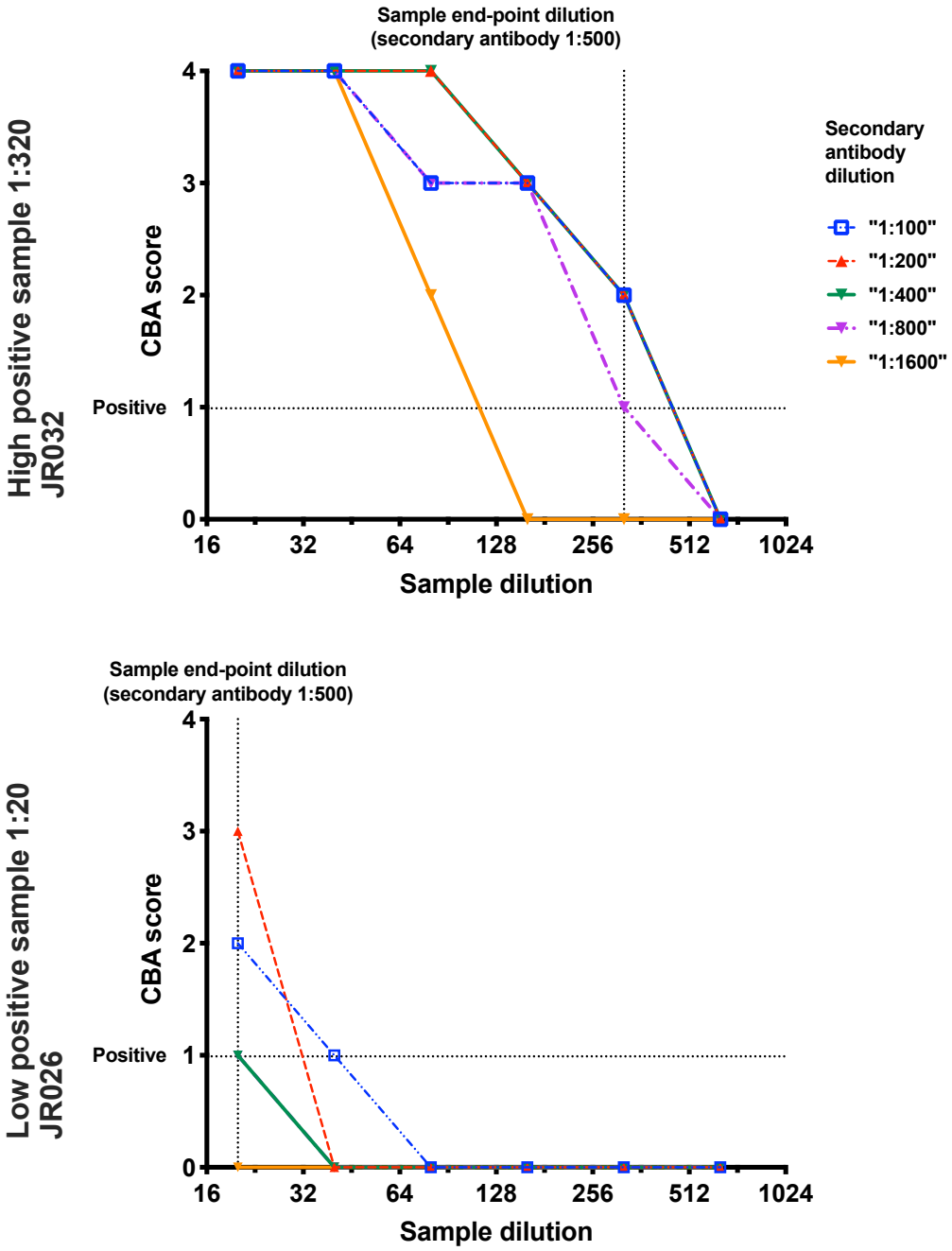


Figure 5.2 – **CBA scores in serially diluted high and low positive NR1-IgM positive samples using a serially diluted range of IgM secondary antibody.**

The top graph is the high positive sample (initial end-point dilution 1:320) and the bottom graph the low positive sample (initial end-point dilution 1:20). The sample range of dilution was 1:20–1:640 (x axis, log 2 scale) and the secondary antibody from 1:100–1:1600 (coloured lines, see legend). This found higher concentrations of secondary antibody lead to sensitivity gains which were marginal beyond 1:400.

Therefore, it appeared that marginal gains in sensitivity were possible with increasing the concentration of secondary antibody. However, this would also increase reagent costs and potentially compromise specificity due to higher likelihood of non-specific binding and/or higher background staining rendering genuine cell surface binding harder to discern. To further investigate this the control cohort was run at a serum dilution of 1:20 with moderate (1:500) and high (1:100) levels of secondary antibody. This found all samples were sub-threshold for positivity using the moderate level secondary antibody but 2/24 NPSLE samples became low positive (CBA score 1) using the high level secondary antibody.

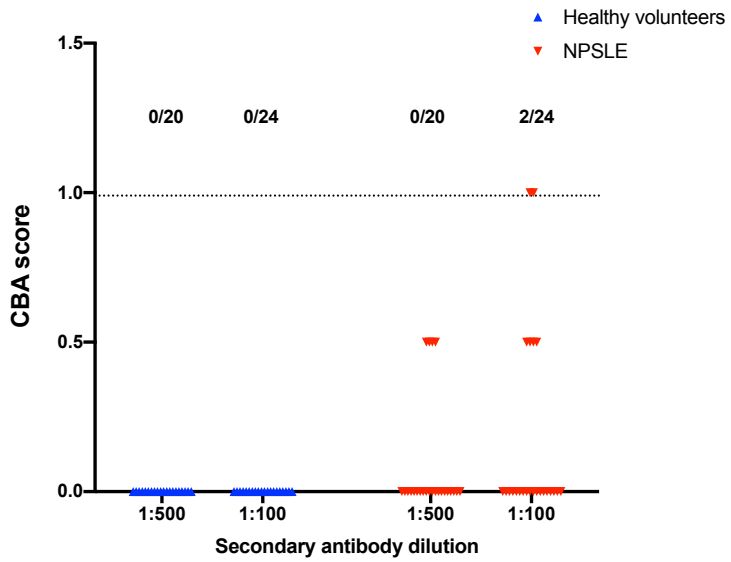


Figure 5.3 – **CBA scores in a control cohort of 20 healthy volunteers and 24 cases of neuropsychiatric systemic lupus erythematosus (NPSLE).**

IgM secondary antibody dilutions of 1:100 and 1:500 were used. Scores were all below the positivity threshold except in two NPSLE samples at the high concentration of secondary antibody which suggested that any gain in sensitivity from this concentration also risked loss of syndrome specificity.

Therefore, on balance whilst a high concentration anti-IgM secondary antibody could offer a mild degree of increased sensitivity, given the markedly increased amount of reagent required and the potential loss of specificity, the moderate level of 1:500 was chosen for future assays.

5.1.4 Demonstration of NR1-target specificity

To further evaluate the target specificity of these putative NR1-directed IgMs, the assay was repeated on the above cohorts using untransfected cells and cells transfected with EGFP only. This would help exclude non-specific HEK cell binding and non-specific binding artefactual to transfection. No binding was seen with either condition.

Next, to directly show NR1-specificity, a similar approach to chapter 4.3.1 was used. NR1-transfected cells were incubated with putative NR1-IgM positive serum and the commercial polyclonal rabbit anti-human NR1 antibody (Alomone labs AGC-001). Serum and commercial antibody were diluted in the same well to a dilution of 1:40 and 1:1000 respectively. Alongside this, the same set up was used with the anti-human IgG Fc-γ fluorescent antibody used in chapter 4 instead of the anti-human IgM Fc-μ antibody. Following incubation with diluted serum the cells were washed and fixed as described in chapter 2 and then incubated sequentially with goat anti-human Fc-μ (or Fc-γ) and goat anti-rabbit IgG AF488 with wash steps in between (Figure 5.4). As previously, the protocol was also run with the commercial antibody incubated separately following fixation and incubation with anti-human antibody. Both approaches yielded the same appearance.

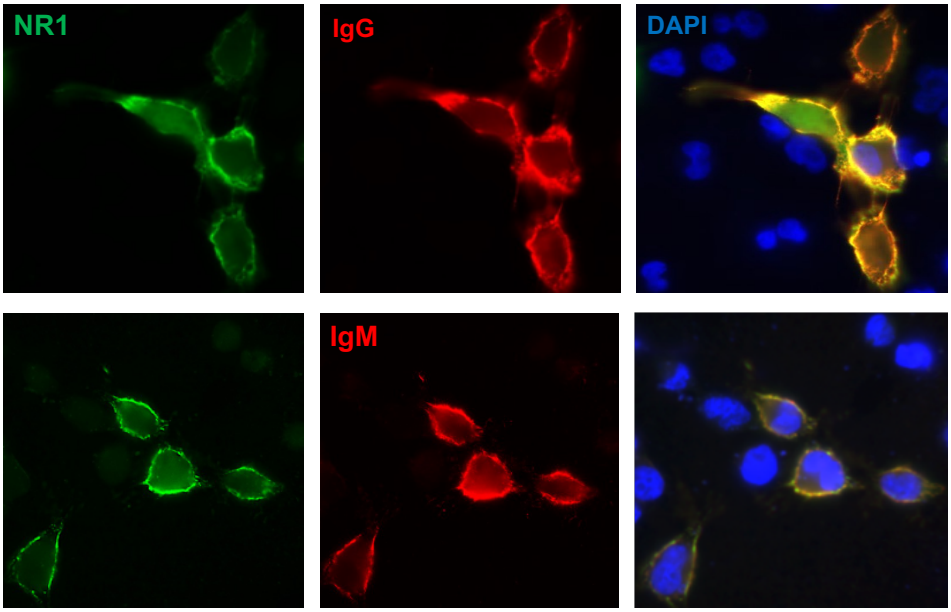


Figure 5.4 – **Co-localisation of patient IgM antibodies with NR1 expressed on transfected HEK293T cells using a commercial antibody against NR1.**

Images acquired at 100x zoom with oil immersion. In the left column green binding shows where the anti-rabbit antibody has bound rabbit anti-NR1 antibody, the middle column shows anti-human antibody bound to human IgG or IgM and the right column shows these two views merged and the co-localisation of the signals. DAPI staining is included to show cells without binding demonstrating that the binding is only to the cells expressing NR1 rather than every cell.

5.1.5 Demonstration of isotype specificity

The approach taken to demonstrate that the secondary antibody was binding IgM rather than IgG was to selectively deplete samples of each isotype and run the assay using the anti-IgG or anti-IgM secondary antibodies and assess binding. Six NR1-IgM positive samples were depleted as described in chapter 2. The isotype-depleted diluted serum sample was then run on NR1-IgG or NR1-IgM live CBAs. Aliquots of the diluted serum samples taken pre- and post-isotype depletion were tested on IgG and IgM ELISAs as described in chapter 2. It was found that depletion successfully removed total Ig of the targeted isotype (≥99% depletion) and the alternative secondary antibody did not bind to samples depleted of its isotypic target (Figure 5.5).

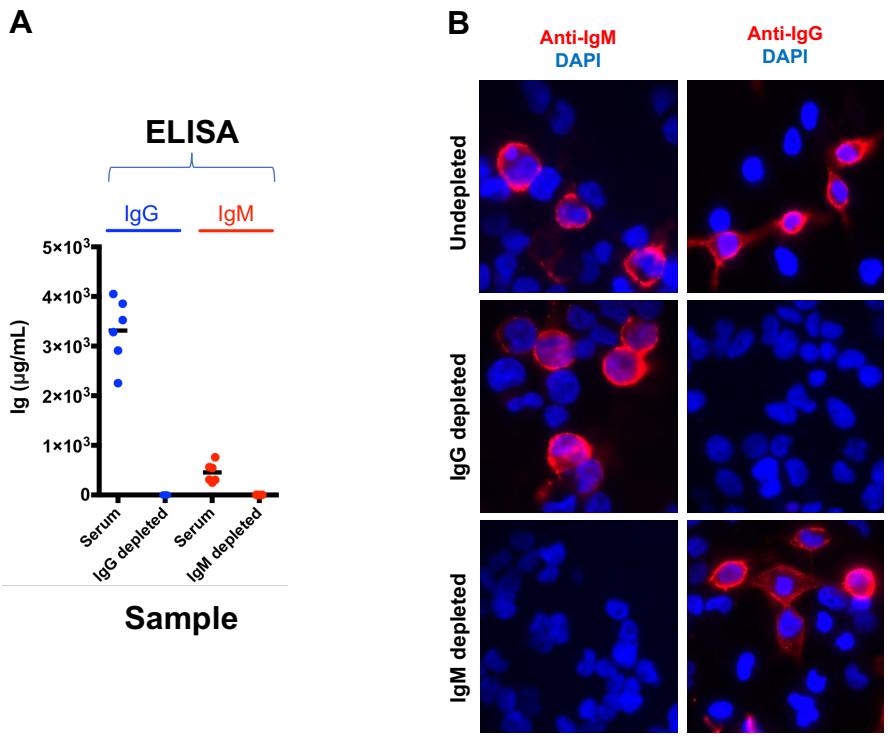


Figure 5.5 – **Depletion of serum samples of IgG and IgM and NR1-IgG and -IgM CBA on depleted samples.**

A - Plot of total IgG and IgM levels using ELISA. Blue dots are IgG measurements and red dots are IgM measurements. On the left of each pair of measurements is pre-depletion and on the right is post-depletion. This shows that the depletion method was effective.

B - At baseline NR1-IgG and IgM are present (undepleted), then using IgG depleted serum NR1-IgG is negative and NR1-IgM persists, and vice versa with IgM depleted serum. 100x zoom oil immersion lens.

5.1.6 Initial analysis of clinical associations

The initial screen of the first available sample from patients with NMDAR-Ab-E with and without OT suggested several hypotheses meriting further investigation. Firstly, 4/10 patients were NR1-IgM seropositive suggesting that it may not be a rare finding. Secondly, positivity from samples early in the illness suggested that it could be a relevant marker of mechanisms involved in disease induction and propagation (e.g. JR028, 032 and 742 had high titres at 19, 26, and 45 days respectively). Thirdly, absence in the two ovarian teratoma-associated cases suggested that these patients may immunise differently to non-teratoma-associated cases.

Therefore, following the above optimisation of the assay, available longitudinal samples from these patients were tested for NR1-IgM and end-point dilutions established in positive samples. This was also done for NR1-IgG for comparison with this class-switched isotype. To interpret the longitudinal trends, end-point dilutions of NR1-IgG and IgM from NR1-IgM positive patients were averaged using 4 nearest neighbours and a 0^{th} order polynomial smoothing function (Prism v8, Graphpad). In terms of NR1-IgG, this analysis was consistent with previous observations of seropositivity beyond clinical remission. The novel finding was that NR1-IgMs could also persist to some extent, at half of their peak for up to 6 months, considerably longer than the three day half-life of IgM. This suggested persisting active synthesis in this sub-group of patients (Figure 5.6).

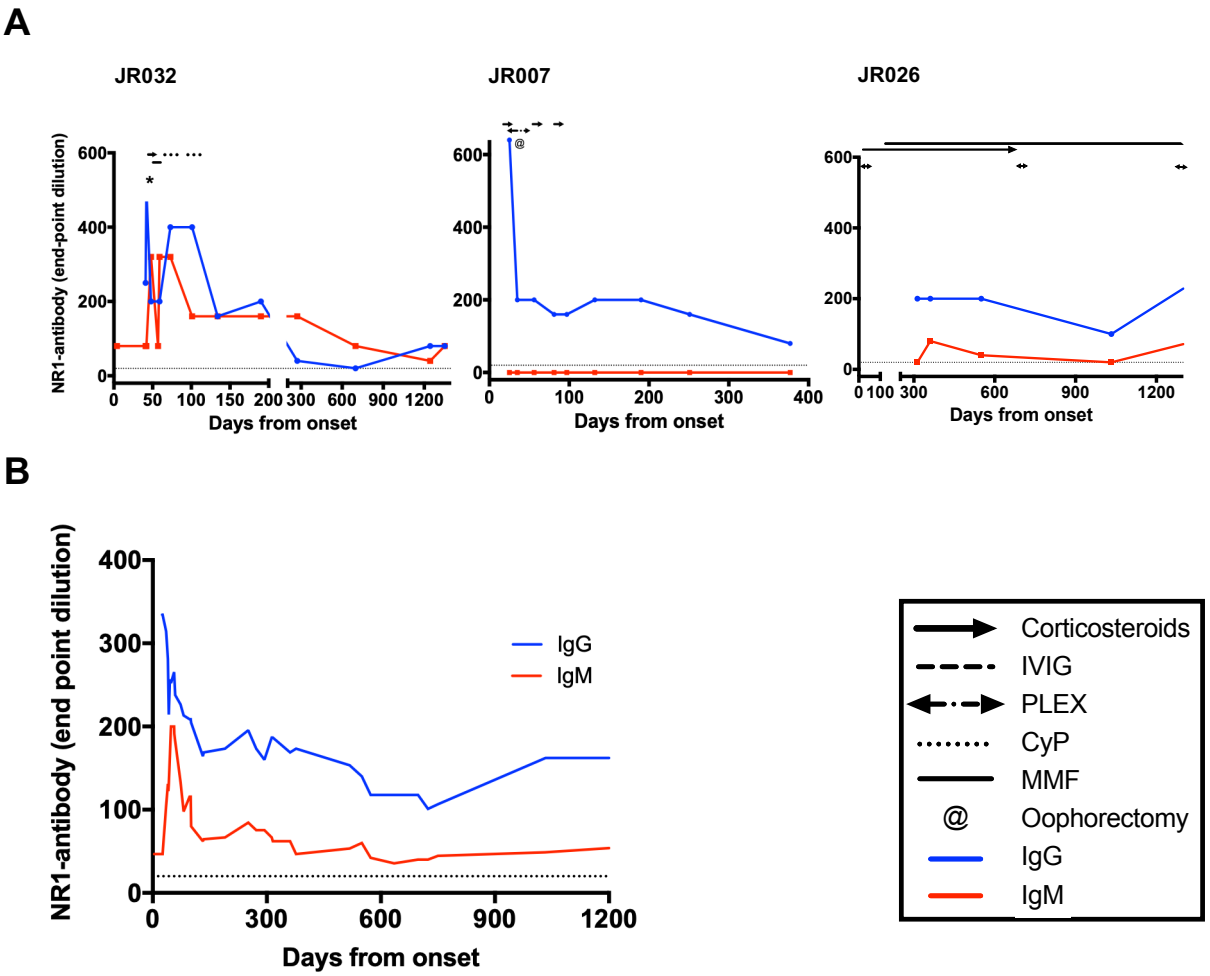


Figure 5.6 – **Individual and summated time-courses of serum NR1-IgG and -IgM.**

A - Serum NR1-IgG and -IgM levels in three of the NR1-IgM positive patients. Here the NR1-IgM serum level either tracked NR1-IgG (JR032), was absent despite significant NR1-IgG levels (JR007) or rose modestly at episode onset (JR026).

B – NR1-IgM positive patients were normalised over time by sample time from original symptom onset. The data was then smoothed for each isotype using a 0^{th} order polynomial function with 4 nearest neighbours. Alongside the predictable persistence of NR1-IgG seropositivity, NR1-IgM also remained positive. Treatments are listed with symbols in box.

Abbreviations used: IVIG = intravenous immunoglobulin, PLEX = plasma exchange, CyP = cyclophosphamide, MMF = mycophenolate mofetil

The working model most in need of further investigation was that there was active ongoing production of these antigen-specific antibodies, implicating lymphoid tissue and specifically, germinal centre reactions, as an anatomical focus for immunisation. Moreover, if the negative association with ovarian teratoma was borne out this could suggest that here germinal centre reactions had either commenced prior to disease

onset and antibody production was from fully isotype-switched antibody-secreting cells, or there were ongoing germinal centre reactions but with a strong bias away from IgM, or a combination of these mechanisms. The small patient series potentially introduced biases therefore the cohort size was increased via further recruitment and collaboration. This is presented in section 5.3.

5.2 Development of a live CBA for IgA antibodies against NR1

5.2.1 Introduction

Having shown that a live CBA could robustly detect NR1-IgMs, it was decided to similarly investigate NR1-specific IgA isotype antibodies in patients with NMDAR-Ab-E and controls. Like IgG, IgA is produced by class-switch recombination (CSR), a process in B cells whereby the current constant gene segment is looped out, bringing the downstream alpha form of the immunoglobulin constant region gene segment into conjunction with variable gene. Therefore NR1-IgA antibodies could be considered to be a marker of CSR, alongside NR1-IgGs.

Prior to this work, NR1-IgA antibodies had been reported in controls (160), following HSV encephalitis (140), and most robustly in CSF of patients with ovarian teratoma-associated NMDAR-Ab-E where it was concluded that they may represent a potential biomarker for this association (193). Given the initial negative NR1-IgM association with ovarian teratoma-associated NMDAR-Ab-E alongside the findings of Desestret *et al.* it was logical to assess the extent of a positive NR1-IgA association with ovarian teratoma status.

Similar to the NR1-IgM literature, groups had used fixed CBAs which not only potentially have sub-optimal specificity if not read conservatively (see chapter 1) but

also known to have reduced sensitivity for the detection of serum NR1-IgG (chapter 4 and (107)). Therefore, investigation of the prevalence and longitudinal progression of NR1-IgA in serum also was of technical interest given that Desestret *et al.* could not detect NR1-IgA in serum.

5.2.2 Methods

5.2.2.1 Patient cohort

Serum samples from four patients with OT-associated definite NMDAR-Ab-E from the Oxford autoimmune neurology cohort were selected. OT-associated cases were the initial focus due to the prior likelihood of NR1-IgA association. The demographic features were consistent with the cohort overall: all patients were female, the median age was 19.5 years, and age range was 16-31 years. Two samples per patient were used. 20 healthy volunteer serum samples were used as controls.

5.2.2.2 NR1-IgA Live CBA

The live CBA was modified in a manner as discussed in 5.1.2.2. Here the anti-IgG antibody was substituted for a polyclonal goat anti-human immunoglobulin A (IgA) α chain specific AF594-conjugated antibody (Jackson Labs 109-585-011). This was diluted 1:2 in glycerol to permit extended storage at -20°C.

5.2.2.3 Depletion of antibody isotypes

Isotype-specific depletion experiments were performed as described in 5.1.2.3.

5.2.3 Initial screen for serum NR1-IgA and optimisation of concentration of secondary antibody

The cohort was screened using a NR1-IgA live CBA with a serum dilution of 1:20. Initially the secondary antibody was diluted to 1:500 which did not find any positives. Therefore, it was repeated at 1:250 and 1:100 which did find positive binding. The results are tabulated below in table 5.2. In summary, 3 of the 4 patients were positive at both concentrations of secondary antibody at least one time point. One low positive result (CBA score 1) at 1:100 secondary dilution was negative at 1:250 but all the other samples that were positive at 1:100 were also positive at 1:250.

Patient code, sample time from onset (days)	**Age at onset, years**	**CBA score, Secondary 1:100**	**CBA score, Secondary 1:250**	**CBA score difference (1:100 – 1:250)**	
JR007 56 81	16	 1.5 1.0	 2.0 0	 -0.5 1.0	
JR748 51 134	23	 0.0 0.0	 0.0 0.0	 0.0 0.0	
JR817 5 13	31	 4.0 4.0	 3.0 1.5	 1.0 2.5	
JR819 11 16	16	 3.0 2.0	 1.0 1.0	 2.0 1.0	
				Mean difference	0.875

Table 5.2 – **CBA score for NR1-IgA in initial samples from four cases of OT-associated NMDAR-Ab-E.** Two concentrations of IgA secondary antibody were used and differences in score between high and low concentrations were used to approximate the effect.

All healthy control samples tested were negative at both concentrations of secondary antibody except one sample which was low positive (CBA score 1) at the higher concentration of 1:100. Therefore, given the absence of detection at 1:500, the

relatively large amount of secondary antibody required for 1:250, and risk of specificity loss at 1:100, an anti-IgA secondary antibody dilution of 1:250 was used in subsequent experiments.

5.2.4 Demonstration of NR1-target specificity

The same approach was used to demonstrate NR1-target specificity as was used in 5.1.4. Again, there was clear co-localisation between a commercial antibody against NR1 and IgA patient antibody as revealed by respective secondary antibodies (Figure 5.7).

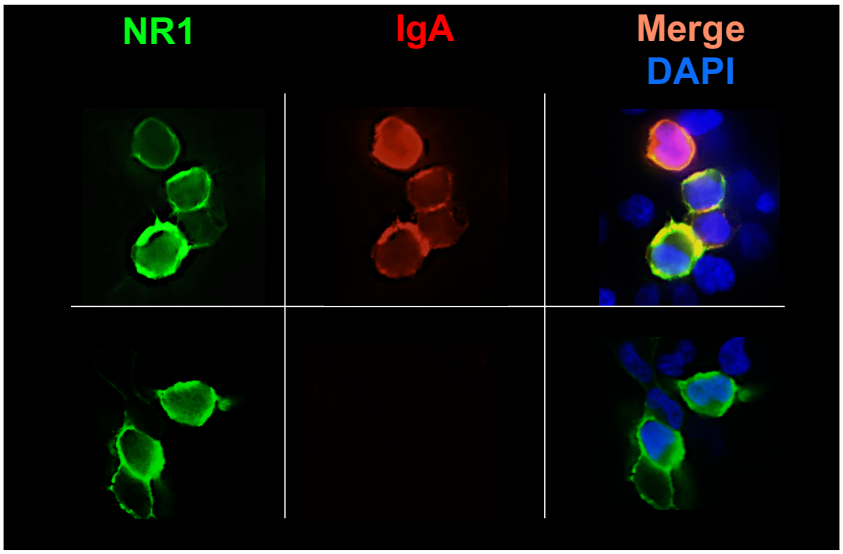


Figure 5.7 – **Co-localisation of patient IgA antibodies with NR1 expressed on transfected HEK293T cells**.

Top row – NR1-IgA positive sample. Bottom row – NR1-IgA negative sample. Left column – NR1 surface expression is demonstrated using a commercial rabbit anti-human antibody against NR1 and goat anti-rabbit AF488 labelled secondary antibody (green). Middle column– Patient IgA is bound to cell surface of the NR1-transfected cells. This is shown with a goat anti-human Fc-α antibody AF594 (red). Binding is absent in the negative sample. Right – Merge of two previous views shows co-localisation of two stains consistent with patient IgA binding to NR1 but not untransfected cells (DAPI-stained nuclei - blue). Only the commercial antibody staining is visible in the negative sample. Images acquired at 100x zoom with oil immersion.

5.2.5 Demonstration of isotype specificity

As in 5.1.5 a similar rationale was applied to demonstrate that the anti-IgA secondary was selectively detecting human IgA bound to transfected cells rather than an alternative isotype. However, given the demonstration of NR1-IgMs in 5.2, this was accounted for by expanding the depletion matrix to doubly deplete pairs of IgG/IgA/IgM. This would also further validate the isotype specificity of the anti-IgM secondary antibody. The day 16 sample from patient JR819 was triple positive for NR1-IgG, NR1-IgA, and NR1-IgM and therefore ideal for this experiment. As shown in figure 5.8 the secondary antibodies used in this project against IgG, IgA and IgM bound their target human antibody isotype but did not bind other isotypes. As before, aliquots of undepleted and double depleted diluted serum samples were kept and tested on Ig isotype ELISAs. This confirmed target isotype-specific depletion.

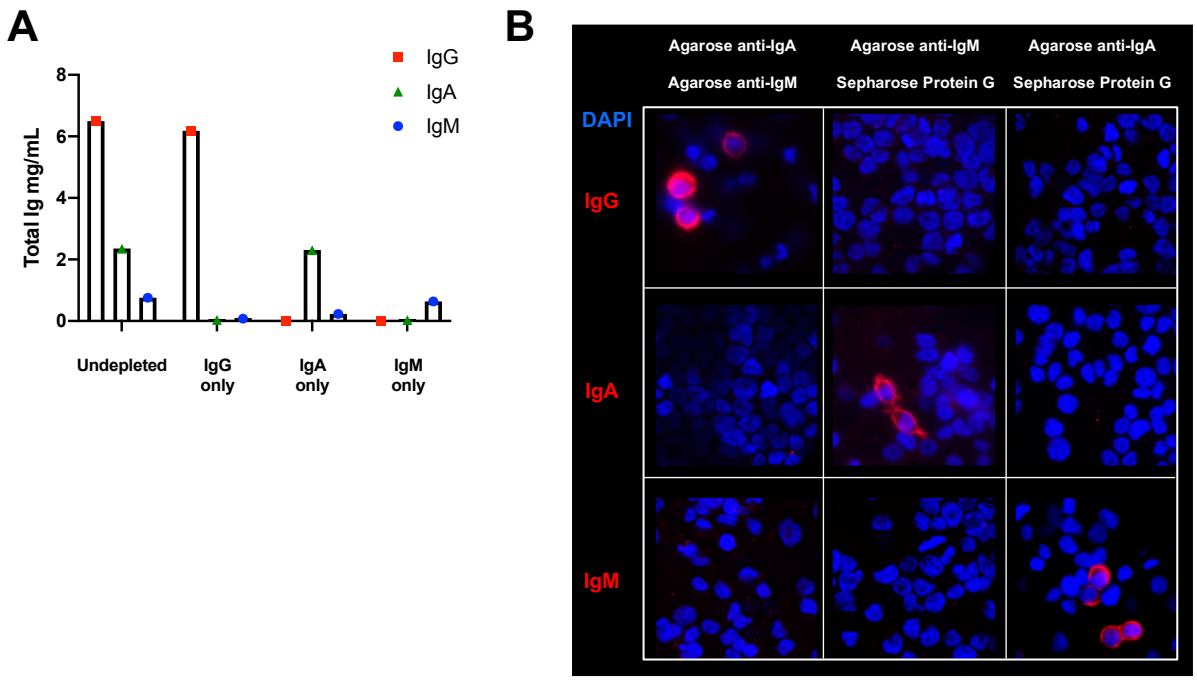


Figure 5.8 – **Depletion of antibody isotypes in a serum sample triple positive for NR1-IgG/IgA/IgM antibodies.**

A – ELISA for each antibody isotype in the depleted and doubly depleted samples (adjusted for serum dilution) shows near complete and specific depletion leaving behind the antibody isotype of interest.

B – NR1-specific live CBAs on each depletion combination shows no cross-reactivity between the secondary antibodies. Images acquired at 100x zoom with oil immersion lens.

5.3 The prevalence and longitudinal evolution of NR1-IgA and NR1-IgM antibodies in serum and CSF NMDAR-Ab-E patients with and without ovarian teratoma

5.3.1 Introduction

Experiments in 5.1 and 5.2 suggested that the NR1 live CBA could be used to detect IgM and IgA antibody isotypes against this target. Moreover, despite small cohort sizes there were intriguing clinical associations. NR1-IgM appeared to persist, potentially suggestive of recurrent germinal centre reactions in some patients. In patients with OT-associated disease, NR1-IgM was not detected in 2 patients despite high levels of circulating NR1-IgG, and NR1-IgA was detected in 3 of 4 patients with ovarian teratoma.

To develop this model further, the cohort was expanded to include all available samples of patients with definite NMDAR-Ab-E in the Oxford autoimmune neurology cohort supplemented by samples donated from collaborating centres. Furthermore, the assays were repeated on a healthy control cohort (n=55) recruited to the overarching immune factors in neurological diseases study.

5.3.2 Methods

NR1 live CBAs for IgG, IgA and IgM isotype antibodies were performed as described in chapters 2, 5.1.2, and 5.2.2. Cohorts were used as described in chapter 2.

5.3.3 Prevalence in serum and clinical associations

5.3.3.1 Prevalence of NR1-IgM and NR1-IgA in healthy volunteer serum cohort and derivation of positivity cut-offs

2 out of 55 healthy volunteers (3.6%) were positive for NR1-IgM (end-point dilution of 1:20 and 1:40) and no healthy volunteers (0%) were positive for NR1-IgA. For NR1-IgM, using a median-based approach any positive result would be considered positive and using a mean-based approach a sample dilution of 18.8 would be considered positive, while for NR1-IgA both approaches result in a cut-off of 0. Since the minimum starting dilution on live CBAs is 1:20 this meant that for both isotypes any positive sample would be above the cut-off. Therefore, samples positive at 1:20 were considered positive for both isotypes on this study (Table 5.3).

	End-point dilution	
	NR1-IgM	**NR1-IgA**
Mean	1.1	0
STDEV	5.9	0
Mean + 3 STDEV	18.8	0
Median	0	0
MAD	0	0
Median + 3 MAD	0	0

Table 5.3 – **Mean, median and derivatives of end-point dilutions of NR1-IgM and NR1-IgA sera in a healthy volunteer cohort.**

Abbreviations used: STDEV = standard deviation; MAD = median absolute deviation.

5.3.3.2 Prevalence of NR1-IgM and NR1-IgA in serum of NMDAR-Ab-E patients and OT association

In total, 285 serum samples from 105 patients with the definite NMDAR-Ab-E cohort were tested for NR1-IgM and NR1-IgA. Using the above cut-offs, 121 samples (42%) were positive for NR1-IgM and 76 (27%) were positive for NR1-IgA (Table 5.4).

Antibody	Samples tested, n	Samples positive, n (%)
NR1-IgA	285	76 (27)
NR1-IgM	285	121 (42)

Table 5.4 – **Rate of positivity for NR1-IgM and NR1-IgA in 284 serum samples from patients with definite NMDAR-Ab-E.**

Next, the prevalence of the two isotypes in OT (n=26 patients, 79 samples) and non-OT (n=79 patients, 206 samples) sub-groups was determined. As shown in table 5.5 there was a positive association between NR1-IgA and OT (35/79, 44% vs. 42/206, 20%; OR=3.1, P<0.0001, two-tailed Fisher's exact test) whereas there was a negative association between NR1-IgM and OT (24/79, 30% vs. 98/206, 48%; OR=0.64, P<0.01, two-tailed Fisher's exact test.

NR1-isotype	OT			non-OT			
	Samples tested, n	Samples positive, n (%)	End-point dilution of positives, median (range)	Samples tested, n	Samples positive, n (%)	End-point dilution of positives, median (range)	Odds ratio, P
NR1-IgA	79	35 (44)	1:40 (1:20-1:640)	206	42 (20)	1:40 (1:20-1:320)	3.1, P<0.0001
NR1-IgM	79	24 (30)	1:80 (1:20-1:640)	206	98 (48)	1:40 (1:20-1:1280)	0.64, P<0.01

Table 5.5 – **Prevalence of NR1-IgM and NR1-IgA positivity in serum samples from OT and non-OT sub-groups.** End-point dilution of the positive samples is given for each sub-group. The final column gives a contingency table analysis showing odds ratio for OT for each isotype given in final column with two-tailed Fisher's exact test.

5.3.3.3 Time course and interaction with teratoma status

This suggested that having an OT influenced NR1-autoantibody class-switching away from IgM towards IgA. To explore this further, the sample was further divided by time from illness onset. A time window approach was taken, collecting the samples into discrete durations that progressively escalated to broader windows to account for fewer later samples. Additionally, OT samples were divided by whether they were from a time point pre- or post-OT resection (time known in 22/26 OT patients included, median 46 days and range 10-840 days post-episode onset). A ratio of NR1-IgA to NR1-IgM was calculated that accounted for negative results by

substituting zero values were for 0.1 such that ratios of 1 were equal end-point dilutions, IgA>IgM was positive, and IgA<IgM was negative (Figure 5.9).

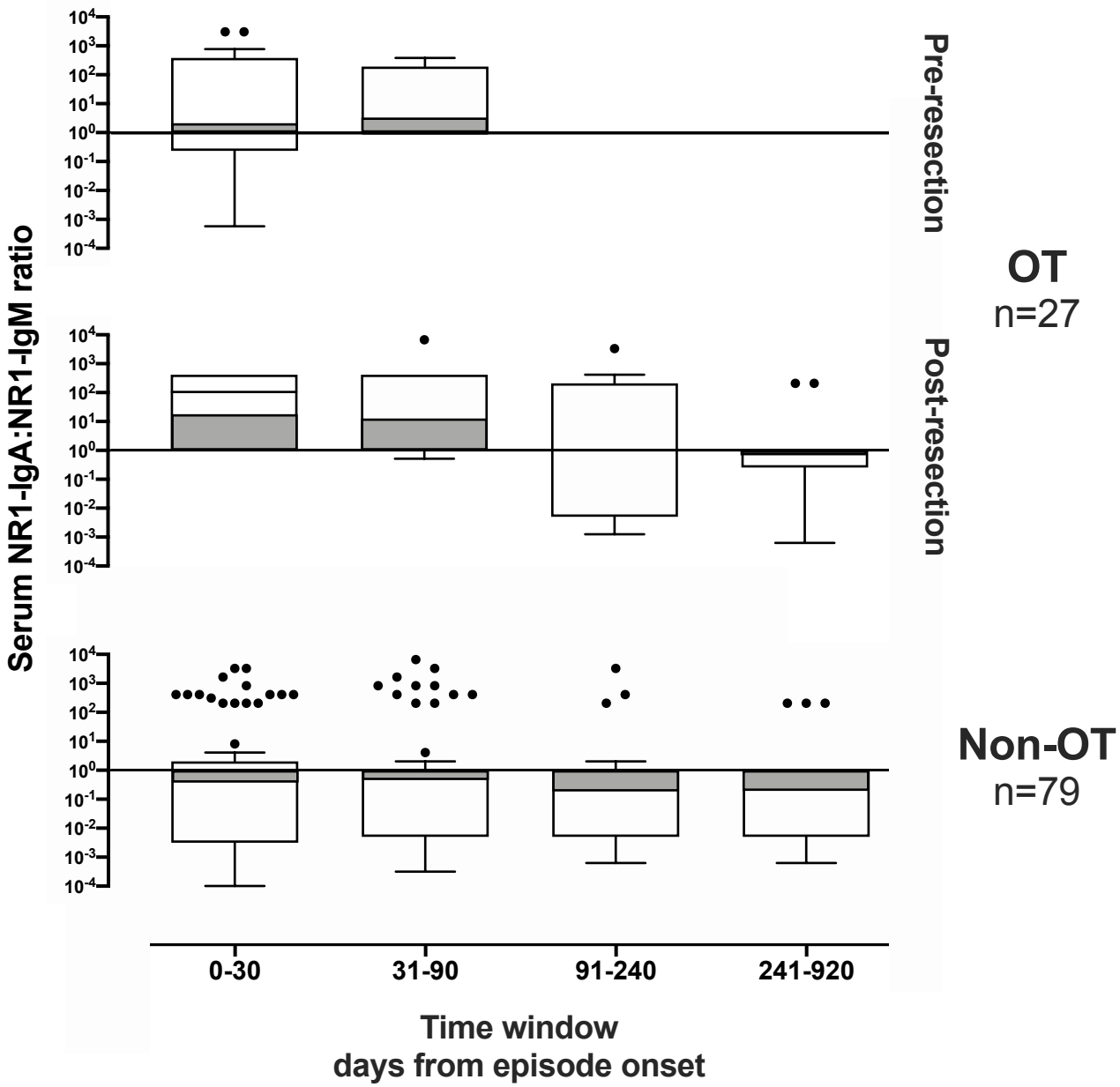


Figure 5.9 – **Evolution of serum NR1-IgA:NR1-IgM end-point dilution ratios in patients with and without OT.**

NR1-IgM and NR1-IgA end-point dilutions at time points following episode onset are summarised as ratios and grouped into time windows reflecting the data density. The values are summarized with Tukey box and whisker plots which include outliers as individual data points. Geometric means are indicated by grey shading. The number of patients in each sub-group are noted.

The non-OT subgroup was persistently <1 favouring NR1-IgM unlike the OT sub-group where pre-resection and early post-resection these were more variable where several bins were >1 favouring NR1-IgA. By the late time window (241-920 days) this was lost and NR1-IgA was favoured.

The time course of NR1-IgA:NR1-IgM ratios were plotted from three individual OT cases where the most longitudinal serum samples were available (figure 5.10). This showed two patients (JR007 and JR817 where there was initially a positive NR1-IgA:NR1-IgM ratio that normalised after oophorectomy. Patient JR819 alternatively presented with a ratio <1 favouring NR1-IgM which partially flattened after an ovary-preserving cystectomy to remove the OT. A few months later it swung towards NR1-IgA at which point a new OT was identified in the region which returned to neutral after complete oophorectomy of the affected ovary. Overall, these observations were supportive of a model whereby intra-tumour autoimmunisation was causally related to the polarisation which was absent from the non-OT cases.

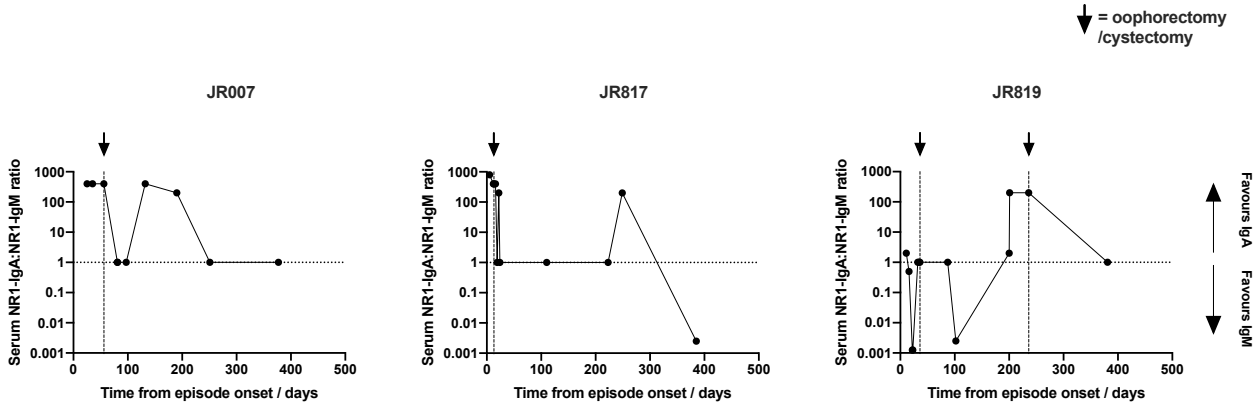


Figure 5.10 – **Time course of NR1-IgA:NR1-IgM serum ratios in individuals with OT and relationship with oophorectomy.**

Available serum samples from the first 500 days after initial illness onset are shown from three patients (JR007, JR817 and JR819). Downward arrows and vertical dotted lines indicate the time at which OT was operated with either oophorectomy or cystectomy.

Finally, given that time had now been demonstrated to be an important variable for NR1-IgA and NR1-IgM positivity according to OT-status, these associations were re-calculated by contingency table analysis for each isotype on a per patient basis including only the earliest available sample per episode and restricting to 40 days or less from episode onset. This resulted in 57 patient episodes of which 47 were female, median age 20 and 17 were OT-associated. This analysis showed a larger association between serum NR1-IgA positivity (OR=6.32, P=0.005) and OT-associated disease but no association between NR1-IgM and OT status (OR=0.83, P=0.78) which is consistent with a greater tendency for NR1-IgA production in OT but quite similar NR1-IgM production (table 5.6).

NR1-isotype	All			OT		non-OT			
	Patients tested, n	Patients positive, n (%)		Patients tested, n	Patients positive, n (%)	Patients tested, n	Patients positive, n (%)		Odds ratio, P
NR1-IgA	57	20 (35)		17	11 (65)	40	9 (23)		6.32, P=0.005
NR1-IgM	57	32 (56)		17	9 (53)	40	23 (40)		0.83, P=0.78

Table 5.6 – **Per-patient prevalence of NR1-IgM and NR1-IgA positivity in time-restricted serum samples from OT and non-OT sub-groups.** The earliest available sample was included from patients with samples from ≤40 days from onset. Odds ratio for OT for each isotype given in final column with two-tailed Fisher's exact test used for significance testing.

5.3.4 Prevalence of NR1-IgA and NR1-IgM single and double positives in CSF and OT association

Although serum was the principal focus of the investigation due to it providing a window into secreted circulating antibodies and hence initiation of autoimmunisation in the periphery, the comparison with CSF may also be relevant. CSF NR1-autoantibodies have usually been looked at from the perspective of mechanisms of brain pathology. There exists a body of literature examining whether NR1-IgA and NR1-IgM antibodies can mediate brain pathology in addition or instead of IgG (166), however this was not of relevance here. Instead, NR1-IgA and NR1-IgM was studied

in CSF to compare with the associations seen in serum. Indeed, using a fixed CBA Desestret *et al.* previously found a positive association between NR1-IgA and OT-associated disease in CSF but not serum (193). In contrast, using a live CBA this association was clearly demonstrable in serum.

A sub-group of the definite NMDAR-Ab-E cohort was studied that had sufficient CSF samples to perform NR1-IgA and NR1-IgM CBAs in addition to NR1-IgG studied in chapter 4. CSF is less available than serum because the procedure is rarely done more than once during an illness episode and less is obtained than blood. This is compounded by CBA testing starting with neat CSF because of the lower total Ig level. The lower total Ig level also makes the risk of non-specific binding far lower such that a typical binding pattern with neat CSF is accepted as a positive sample. Therefore, this CSF cohort was smaller than the serum cohort. It consisted of 74 CSF samples from 60 patients of which 10 patients had more than 1 CSF time point. 18 patients had an OT-associated illness and none of these had longitudinal CSF samples. Of this, 55 samples from 51 patients had a matched serum sample sufficient to test for NR1-IgA and NR1-IgM.

Both antibody classes were detectable: NR1-IgA (32/60, 53% patients positive at least once), NR1-IgM (31/60, 52% patients positive at least once) and double positivity at least once was found in 19/60 of patients (32%). These rates were notably lower than NR1-IgG which was by present in all the samples (table 5.7).

	NR1-IgA	NR1-IgM	NR1-IgA+NR1-IgM+
All CSF samples	33/74 (45%)	33/74 (45%)	21/74 (28%)
All patients positive at least once	32/60 (53%)	31/60 (52%)	19/60 (32%)
OT patients positive at least once	13/18 (72%)	14/18 (78%)	11/18 (61%)
Non-OT patients positive at least once	19/42 (45%)	17/42 (40%)	8/42 (19%)

Table 5.7 – **Positivity rate of NR1-IgA, NR1-IgM and both in CSF samples tested for both.**

OT associations were studied for each of these single or double positive combinations. The published data from Desestret *et al* was included as a comparison. For patients with multiple samples the earliest available was used as this was least likely to have been affected by treatments (table 5.8).

Like Desestret *et al.* there is a positive association between OT and CSF NR1-IgA but unlike that study it is marginally non-significant (Paired cohort: OR=3.01, P=0.09). The rates within the OT sub-group are similar such that the difference comes from the higher rate in the non-OT sub-group studied here. A larger sample size in the non-OT sub-group may have given a lower prevalence or it may be that live CBA is more sensitive. This would be consistent with findings with IgG isotypes but a larger sample size would be needed to exclude statistical power as the cause.

NR1-IgA+	Desestret *et al.* 2015	Current study
All	38/93 (41%)	32/60 (53%)
OT	17/20 (85%)	13/18 (72%)
Non-OT	21/73 (29%)	17/42 (46%)
Odds ratio, P	14.03, P<0.0001	3.01, P=0.09

Table 5.8 – **Association between OT and CSF NR1-IgA in the published study of Desestret *et al.* compared to the current study.** Significance calculated with two-tailed Fisher's exact test.

For NR1-IgM, in contrast to serum, there was a positive association with OT status. Unlike the CSF NR1-IgA trend, the odds ratio for CSF NR1-IgM positivity and OT-associated illness (OR=6.30) was statistically significant (P=0.004) (table 5.9).

NR1-IgM+	Current study
All	29/60 (52%)
OT	14/18 (78%)
Non-OT	15/42 (36%)
Odds ratio, P	6.30, 0.004

Table 5.9 – **Association between OT and CSF NR1-IgM.** Significance calculated with two-tailed Fisher's exact test.

Analysis of CSF NR1-IgA NR1-IgM double positives revealed the highest odds ratios in this data set for OT status. Comparing to patients who on their earliest CSF sample were not double positive, i.e. including single positive CSF NR1-IgA or NR1-IgM gave a statistically significant OR=6.88 (P=0.002), and comparing against only true double negatives, i.e. excluding single positives, gave a higher OR=12.38 (P=0.002) (table 5.10).

NR1-IgA+ NR1-IgM+	Versus not double positive	Versus double negative
All	19/60 (32%)	19/39 (49%)
OT	11/18 (61%)	11/13 (85%)
Non-OT	8/42 (19%)	8/26 (31%)
Odds ratio, P	6.68, 0.002	12.38, 0.002

Table 5.10 – **Contingency table analysis of OT status and CSF NR1-IgA NR1-IgM double positives.** Comparison is with either patients who were not double positive i.e. including single positives, or with fully double negatives patients i.e. excluding single positives. Significance calculated with two-tailed Fisher's exact test.

Review of the end-point dilutions for NR1-IgA and NR1-IgM in OT and non-OT sub-groups found that NR1-IgA positives in the OT sub-group were higher than non-OT but not for NR1-IgM (figure 5.11a: median=1:8 vs 1:2; P=0.003, two-tailed Mann-Whitney test). Then looking at NR1-IgA:NR1-IgM ratios using the same strategy as serum there was no overall difference between OT and non-OT sub-groups (figure 5.11b).

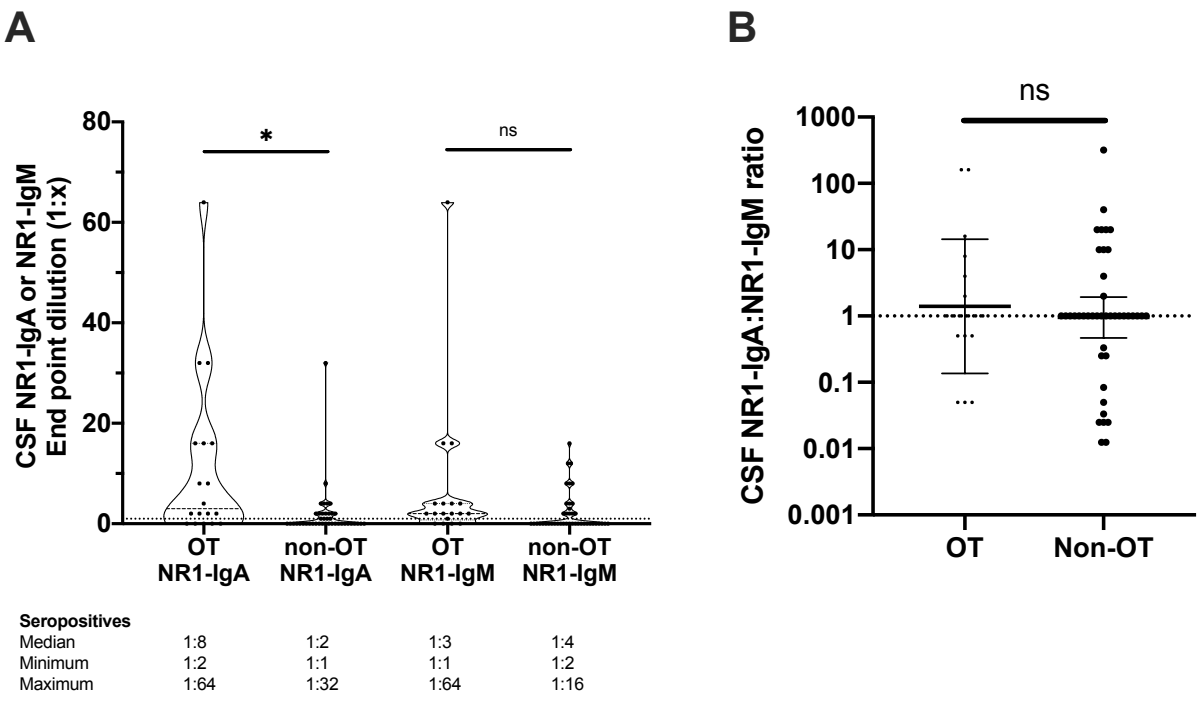


Figure 5.11 – **Distribution of CSF NR1-IgA and NR1-IgM end-point dilutions and ratio between them in OT and non-OT sub-groups.** A – Violin plot of distribution of end-point dilutions in sub-groups. Comparisons are between positive results (two-tailed Mann-Whitney test). B – Distribution of NR1-IgA:NR1-IgM ratios (comparison with two-tailed Mann-Whitney test).

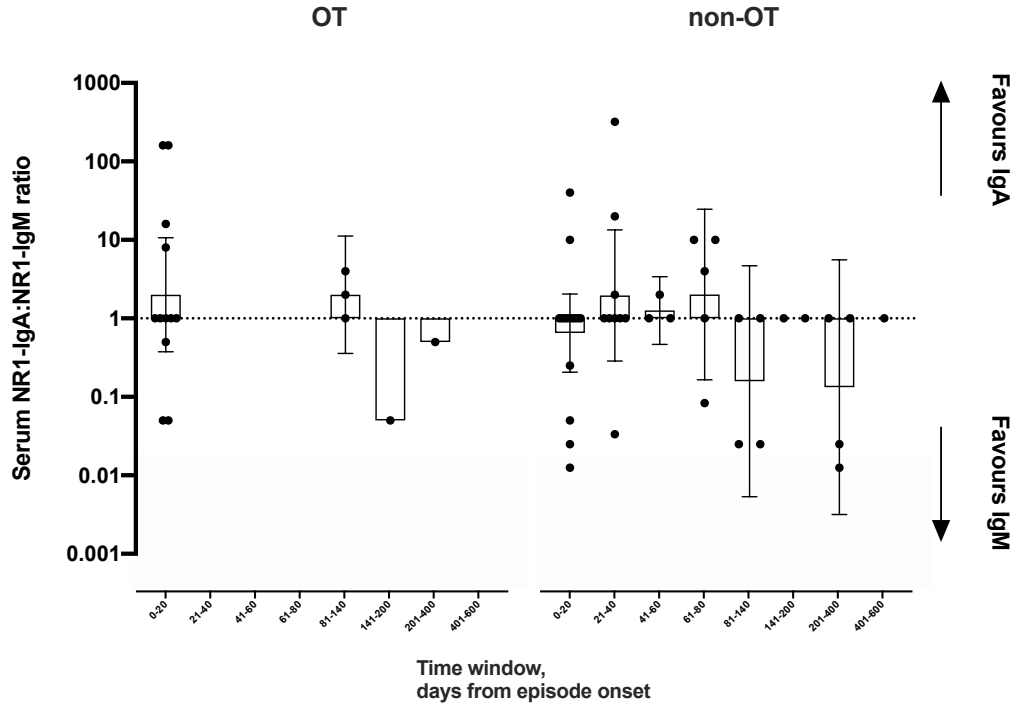


Figure 5.12 – **Evolution of CSF NR1-IgA:NR1-IgM end-point dilution ratios and patients with and without OT.** Amongst paired data with known timepoints ratios were plotted in discrete time windows, which scale with time to reflect density of data. Negative values (end-point dilution=0) were converted to 0.1 to permit calculation of ratios. Hence values >1 NR1-IgM is higher and vice versa for <1. Scatter plot of Individual values summarised by geometric mean (boxes) and 95% confidence intervals (error bars).

A smaller number of time points made longitudinal comparison less possible than with serum. However, generally it appeared that NR1-IgA diminished over time in both sub-groups (figure 5.12). Most of the samples were single time points, however, there were 10 patients non-OT patients with longitudinal samples, either within the same episode or sampled across relapses. The general themes seen were: CSF NR1-IgA and NR1-IgM can vary over time with either class appearing or disappearing from detection threshold, they tend to disappear outside of the acute phase but can persist well beyond the acute phase.

At their earliest sample, 4/10 were double negative, 3/10 were single positive, and 3/10 were double positive. 3/4 remained double negative at subsequent samples and 1/4 developed NR1-IgA positivity during the acute phase. Of the 3 single positives all changed at subsequent samples: one from NR1-IgA to double positive acutely to NR1-IgM at resolution, one from NR1-IgA to NR1-IgM then double negative at resolution, and one from NR1-IgM to double negative acutely. 5/10 patients had a sample during clinical resolution (median time from onset=345 days; range=145-579 days) which were all double negative except one which was NR1-IgM positive. Representative trends are shown in figure 5.13.

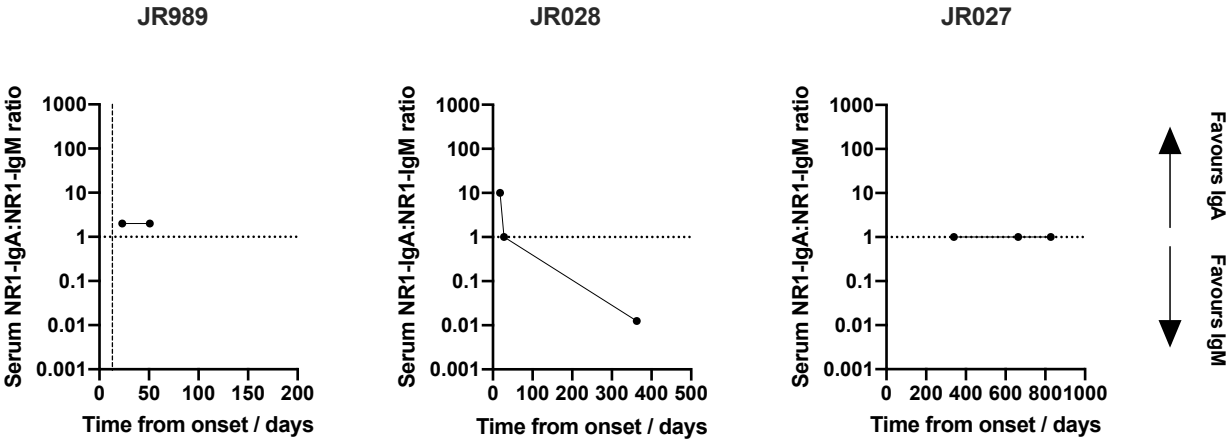


Figure 5.13 – **Longitudinal CSF NR1-IgA:NR1-IgM in individual patients**.

JR989 was double positive with a slight bias to NR1-IgA which was constant in the acute phase. JR028 began with NR1-IgA single positive then evenly double positive acutely and NR1-IgM single positive during remission. JR027 had three episodes during which each acute sample was double negative.

The OT associations were re-analysed using time-restriction to the first 40 days post-episode onset to remove the effect of change over time (table 5.11). All analyses gave positive associations with OT, but compared to unrestricted analyses, this gave a more robust association with CSF NR1-IgA (OR=7, P=0.03 vs. OR=3.01, P=0.09) and a less robust NR1-IgM association (OR=5.57, P=0.07 vs. OR=6.30, P=0.004). Both double positive analyses remained significant with comparison against double negatives greater but compared to the time-unrestricted analyses were also less robust. These comparisons were all consistent with time-dependence of NR1-IgA associations.

	NR1-IgA+	**NR1-IgM+**	**NR1-IgA+ NR1-IgM+ Vs. not double positive**	**NR1-IgA+ NR1-IgM+ Vs. double negative**
OT	9/12 (75%)	9/12 (75%)	7/12 (58%)	7/8 (88%)
Non-OT	6/20 (30%)	7/13 (54%)	3/20 (15%)	3/13 (23%)
Odds ratio, P	7, 0.03	5.57, 0.07	7.93, 0.02	23.33, 0.008

Table 5.11 – **Time-restricted prevalence and OT associations of CSF NR1-IgA, NR1-IgM, and double positive patients.** Double positives were compared to patients that were not double positive i.e. including single positives and double negatives only i.e. excluding single positives. Two-tailed Fisher's exact test.

5.3.5 Linkage in serum-CSF pairs and clinical associations

Finally, NR1-IgA and NR1-IgM were compared in paired serum-CSF samples. This cohort was also time-restricted to ≤ 40days from episode onset. As noted in table 5.12, the demographic and OT properties are consistent with the overall cohort.

	Total number	Number female	Median age	OT	Non-OT
All	51	33	22	17	34
Time-restricted	26	22	22	22	14

Table 5.12 – **Clinical and demographic properties of serum-CSF pairs.**

Initially, each sample was classified according to isotype positivity in each compartment and sub-classified on teratoma status with and without time restriction to 40 days from episode onset. As previously, for patients with more than one sample the cohort was restricted to the first available sample (table 5.13). For the whole group, there were almost equal positivity rates in at least one compartment for each isotype (31/51 NR1-IgA and 30/51 NR1-IgM). Of the positives, positivity in both serum and CSF was more common for both isotypes than dissociation, however, this was marginal for NR1-IgA (16/31 NR1-IgA and 20/30 NR1-IgM). Of the dissociated samples, NR1-IgA was more frequently negative in serum and positive in CSF (11/15) whereas for NR1-IgM this was more evenly split (6/10).

The time-restricted sub-group showed similar properties with at least one compartment positive in 14/26 for NR1-IgA and 15/26 for NR1-IgM. There was a similar trend of NR1-IgA being more commonly dissociated between compartments with 7/14 serum-CSF double positive versus 12/15 for NR1-IgM. Again, the NR1-IgA dissociation was towards CSF single positivity with 6/7 dissociated samples in this group.

Regarding OT association, there were equal rates of isotype positivity in at least one compartment within the OT group and within the non-OT group (OT NR1-IgA 13/17 and NR1-IgM 13/17 non-OT NR1-IgA 18/34 and NR1-IgM 17/34 both P>0.999 on two-tailed Fisher's exact test). However, both isotype-specific positivity rates were higher in the OT group than the non-OT group. In the time-restricted sub-group these relationships were similar but the absolute proportions in the OT group were higher and in the non-OT group lower leading to a greater although non-significant differences within OT and non-OT groups (OT NR1-IgA 10/12 and NR1-IgM 9/12; non-OT NR1-IgA 4/14 and NR1-IgM 6/14; P>0.999 and P=0.69, respectively on two-tailed Fisher's exact test).

Within the positive results, for both isotypes serum-CSF double positive results were more common in the OT group than non-OT but this was more pronounced for NR1-IgM+ (NR1-IgA: OT 8/13, non-OT 8/18 vs. NR1-IgM: OT 11/13, non-OT 9/17). CSF single positivity was the more common direction of dissociation in all sub-groups except for non-OT NR1-IgM where serum or CSF single positivity were equal. In the time-restricted sub-group there were similar relationships but the differences in serum-CSF double positive rates between OT and non-OT became more pronounced for NR1-IgA compared to time-unrestricted and less pronounced for NR1-IgM compared to time unrestricted (NR1-IgA: OT 6/10, non-OT 1/4 vs. NR1-IgM: OT 8/9, non-OT 4/6).

	NR1-IgA				NR1-IgM			
	Positive			Negative	Positive			Negative
	Serum + CSF +	Serum + CSF -	Serum - CSF +	Serum - CSF -	Serum + CSF +	Serum + CSF -	Serum - CSF +	Serum - CSF -
All patients	16/51	4/51	11/51	20/51	20/51	4/51	6/51	21/51
(Time-restricted)	7/26	1/26	6/26	12/26	12/26	2/26	1/26	11/26
OT	8/17	1/17	4/17	4/17	11/17	0/17	2/17	4/17
(Time-restricted)	6/12	1/12	3/12	2/12	8/12	0/12	1/12	3/12
Non-OT	8/34	3/34	7/34	16/34	9/34	4/34	4/34	17/34
(Time-restricted)	1/14	0/14	3/14	10/14	4/14	2/14	0/14	8/14

Table 5.13 – **Prevalence and OT associations of CSF NR1-IgA, NR1-IgM, in paired serum-CSF samples with and without time-restriction.**

These relationships were then further explored by looking at these relationships within individuals. As with NR1-IgG, in serum-CSF pairs where both were positive, serum end-point dilutions were always higher than CSF, by approximately 10-fold. The differences were greater and more statistically significant for NR1-IgM than NR1-IgA (P=0.001 for both OT and non-OT vs. 0.02 and 0.03 for NR1-IgA; Wilcoxon matched-pairs signed rank test, figure 5.14).

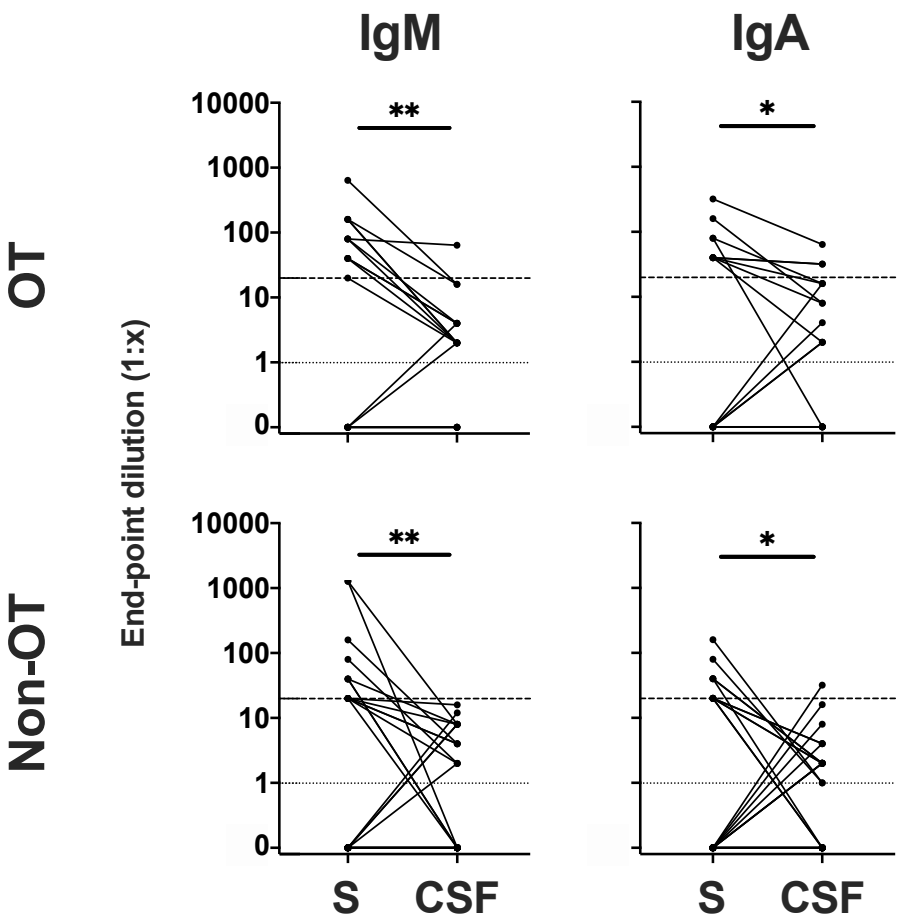


Figure 5.14 – **Relationships between NR1-IgA and NR1-IgM in serum and CSF in patients with and without an OT.**

Scatter plots of NR1-IgA and NR1-IgM levels in paired serum (S) and CSF samples. Individuals are connected by lines. CSF positivity cut-off marked by narrow dotted line (y=1) and serum by broad dashed line (y=20). Positive serum-CSF NR1-autoantibody isotypes pairs are compared with Wilcoxon matched-pairs signed rank test.

5.4 NR1-IgM and NR1-IgA in non-encephalitic neuropsychiatric comparator and healthy volunteer cohorts

Given the patterns in definite NMDAR-Ab-E, it was instructive to screen the comparator cohorts screened for NR1-IgG in chapter 4. The same cohorts as described were used and NR1-IgM and NR1-IgA live CBAs were used as described above. Any positive results were repeated and end-point dilution found.

	Healthy volunteers	Bipolar depression (CEQUEL)	Bipolar acute mania (MIAMI-UK)	Traumatic brain injury
NR1-IgM	2/55 (4%)	4/183 (2%) P=0.62	0/39 (0%) P=0.51	3/57 (5%) P=0.99
End-point dilution (median, range)	1:30, 1:20-1:40	1:160, 1:40-1:160	-	1:40, 1:20-1:40
NR1-IgA	0/55 (0%)	6/183 (3%) P=0.34	1/39 (3%) P=0.42	1/57 (2%) P=0.99
End-point dilution (median, range)	-	1:100, 1:20-1:320	1:80, -	1:20, -

Table 5.14 – **Prevalence and level of NR1-IgA and NR1-IgM in healthy volunteers and non-encephalitic neuropsychiatric comparator cohorts.** Rates are shown on a per patient basis with at least one sample positive. Proportion positive versus healthy volunteers is compared with two-tailed Fisher's exact test.

None of the positive samples were seen longitudinally within the same patient except the single NR1-IgA positive sample MIAMI-UK which was seen at 2 of 3 time points. None of the samples were double positive for NR1-IgM and NR1-IgM and none were also positive for NR1-IgG. Overall, none of the cohorts were significantly more frequent than controls for either NR1-IgM or NR1-IgA (table 5.14).

5.5 Discussion and limitations

A live CBA was developed that could detect autoantibodies of IgA and IgM isotypes against NR1. This was shown by co-localisation of patient binding antibody with commercial antibody and isotype-specific depletion. Complementary assays were not used, but findings in chapter 4 with NR1-IgG suggested these act as affinity/polyclonality filters and reduce overall detection sensitivity. The aim here was to study mechanisms of autoimmunisation rather than pathogenicity against neurons so additional assays were not relevant. NR1-IgA and NR1-IgM were rare in serum from healthy volunteers and non-encephalitic neuropsychiatric comparator cohorts, but greatly enriched in both serum and CSF of definite NMDAR-Ab-E. This observation fits with the model suggested in chapter 4 that seropositivity in these

groups is unlikely to be causally distinct from healthy volunteers and is more probably a general population phenomenon.

The rates in these comparator cohorts were slightly lower than some published studies. For example, Dahm and colleagues found NR1-IgM in 74/1703 (4%) and NR1-IgA in 76/1703 (4%) healthy volunteers and NR1-IgM in 69/1378 (5%) and NR1-IgA in 73/1378 (5%) patients with schizophrenia (160). This study used a fixed CBA without a complimentary test. When using the non-commercial fixed CBA with a complementary test the rates are far lower, e.g. Hara et al. found NR1-IgM or NR1-IgA in sera from 22/300 (7%) of patients with non-encephalitic neurological and psychiatric disorders which reduced to 10/300 (3%) with a TBA and 7/300 (2%) with a live NBA (194). The latter rates are closer to the findings with the live CBA used here.

In the large multi-centre longitudinal cohort of serum and CSF from patients with definite NMDAR-Ab-E there were clear patterns in serum and CSF that differed between patients with and without OT, and over time. Both OT and non-OT had a marked tendency to make NR1-IgM compared to controls. However, early in their illness, OT patients had a marked NR1-IgA-dominant serum and NR1-IgA and NR-IgM double positivity in CSF. During illness resolution, particularly following the removal of OT, the serum in these patients tended to shift away from NR1-IgA polarisation whereas even during clinical resolution NR1-IgM polarisation persisted in the non-OT patients up to ~3 years after illness onset. This was consistent with a recurrent germinal centre reaction model but with increased class-switching to NR1-

IgA in the OT patients driven by the OT itself. This suggested direct investigation of lymphoid tissue including the OT itself was relevant to test this model.

From a technical perspective, finding associations in serum as well as CSF in contrast to a previous report was probably explained by the live CBA being a generally more sensitive approach with serum than fixed as discussed with NR1-IgG. However, direct comparison with a fixed CBA would be needed to prove this.

Unlike serum, CSF in the OT patients was positively associated with NR1-IgM suggesting local B cell populations enter the CNS early in the illness secreting antibody locally. Uncoupling of both isotypes was also found in non-OT patients consistent with compartment dissociation. Paired serum-CSF positive time points were always of a higher level in serum which is consistent with peripheral generation of serum antibody rather than CSF to serum diffusion, but the difference is too low to suggest passive diffusion, further supporting intrathecal cell migration to account for CNS antibody. The few long-term follow-up samples available suggested CSF isotype patterns were less enduring than serum also suggesting a dissociated mechanism for their synthesis. This fits with evidence from recombinant monoclonal NR1-specific IgA and IgM made from ASC and B memory cell populations cloned from CSF (75).

6 NR1-specific germinal centre reactions in ovarian teratoma associated with NMDAR-Ab-E: a tertiary lymphoid organ?

6.1 Introduction

Several lines of evidence from chapters 4 and 5 suggested that patients with an ovarian teratoma associated with their illness had a distinct immunological profile. Firstly, in chapter 4 the CBA versus NBA comparison suggested that ovarian teratoma-associated NR1-IgG may tend to have different binding properties, potentially higher affinity. If this were the case, then affinity maturation involving somatic hypermutation and clonal selection in germinal centres would be expected. Secondly, in chapter 5 the NR1-autoantibody isotype profile of ovarian teratoma-associated samples showed a greater tendency to class-switch to IgA, which decreased following oophorectomy, also implying that the teratoma could be the physical substrate for this process. In this chapter, ovarian teratoma samples were investigated using cell culture, flow cytometry, and immunohistochemistry to explore the hypothesis that the ovarian teratoma acts as a tertiary lymphoid organ (TLO). As outlined in 1.2.4 the key features of a TLO include B, T, and antigen-presenting cells (particularly follicular dendritic cells) organising as germinal centres at a non-lymphoid site associated with new development of supporting vessels such as lymphatics and high endothelial venules (HEV) (28,29).

6.2 Patient cohort

A group of participants from the Oxford cohort participated by donating tissue to the experiments conducted in the next two chapters. Six OT patients and two non-OT patients were included. Of the OT patients, material from four was used in cell culture, flow cytometry and/or histology experiments. Tissue from the other two

participants could not be obtained because they were recruited from clinics outside Oxford. All but one of the Oxford cohort also participated in the lymph node study in chapter 7 (table 6.1).

Tissue from international collaborators contributed to histology experiments. To compare with secondary lymphoid tissue in this illness, contact was made with Professor David Nauen (Department of Pathology, Johns Hopkins University, USA) who had published a case report that included post-mortem lymph node tissue from a case of fatal treatment-resistant NMDAR-Ab-E(149). Sections were kindly donated and this was labelled ‘Baltimore’. Professor Keiko Tanaka (Brain Research Institute, Niigata University Graduate School of Medicine, Japan) donated sections from a surgically resected colorectal carcinoma from a patient with coincident NMDAR-Ab-E. In both cases local consent protocols were followed.

Participant details						Experiment details				
Participant	**Antigen**	**OT?**	**OT type**	**Sex**	**Age at onset**	**OT culture**	**OT histology**	**OT flow cytometry**	**LN flow cytometry**	**LN cell culture**
JR-NC1	None (Migraine)	N/A	-	M	31	N/A	N/A	N/A	Yes - pilot	N/A
JR-NC2	None (Migraine)	N/A	-	F	31	N/A	N/A	N/A	Yes	N/A
JR-NC3	None (Migraine)	N/A	-	M	74	N/A	N/A	N/A	Yes	N/A
JR-NC4	Glycine Receptor	No	N/A	F	57	N/A	N/A	N/A	Yes	Yes -unfractionated
JR819	NMDAR	Yes	First lesion (a): Unilateral Mature Recurrence (b): Unilateral Mature	F	19	Yes Yes	Yes No	Yes Yes	Yes	Yes -unfractionated
JR817	NMDAR	Yes	Unilateral Mature	F	31	Yes	Yes	Yes	Yes	Yes -unfractionated
JR748	NMDAR	Yes	Unilateral Immature	F	23	Yes	Yes	No	Yes	Yes
JR007	NMDAR	Yes	Unilateral Mature	F	16	No	Yes	No	No	No
JR717	NMDAR	Yes	Unilateral Mature	F	28	No	No	No	Yes	Yes -unfractionated -bulk sort
JR747	NMDAR	Yes	Bilateral Right – immature Left – mature	F	19	No	No	No	Yes	Yes -unfractionated
JR770	NMDAR	No	N/A	F	31	N/A	No	N/A	Yes	Yes -unfractionated x2 -bulk sort
JR1082	NMDAR	No	N/A	F	19	N/A	No	N/A	Yes	Yes -unfractionated
Baltimore	NMDAR	No	N/A	F	18	N/A	Yes	N/A	No	No
Japan	NMDAR	No	N/A	F	55	No	Yes [colorectal Ca]	No	No	No

Table 6.1 – **Participants participating in chapter 6 and 7 studies.** OT type as per clinical histopathology report.
Abbreviations used: F=Female, FNA=fine needle aspiration, M=Male, N/A=not applicable, LN=lymph node, OT=ovarian teratoma

6.3 Cell culture and measurement of NR1-specific and total antibody in resulting supernatant

6.3.1 Materials and methods

The following data are based around surgically resected ovarian teratoma material from patients JR748, JR817 and JR819a and b. Consultee consent was given as the patients were acutely unwell and lacked capacity at the time of surgery. Once mental capacity was regained all participants gave consent and agreed with the consultee decision.

In theatre, once the lesion had been removed adequately, the surgeon cut a portion of the lesion for research purposes whilst ensuring sufficient material was available for diagnostic pathology (figure 6.1a). If the tumour was cystic, the cyst fluid was aspirated where possible. Material was put into B cell media on ice and returned to the lab.

Solid aspects of the tumour were cut into smaller explants approximately 5mm in diameter. These were transferred into 10mL of B cell media and centrifuged at 200G for 5 minutes twice with media aspirated and replaced each time in order to wash any contaminating serum. The explants were then rested in B cell media. The remainder of the material was cut into progressively smaller material within B cell media in a petri dish. This material was washed twice as above. Following this, the supernatant material was resuspended in B cell media and filtered through a 35μm mesh cell strainer. A cell count was performed using Tuerk's solution to identify nucleated cells. Sufficient material was retained to culture $2x10^5$ cells/well. The remaining material was then resuspended in equal volumes of freezing media,

cooled initially overnight with a cool cell device to -80°C, then moved to -180°C liquid nitrogen storage.

Culture plates were set up immediately following preparation of material from patients JR748, JR817, and the recurrent lesion of JR819 (figure 6.1b). Explants and dissociated cells were exposed to either 'maintenance' (IL-6 only) or 'activation' conditions (soluble CD40 ligand, IL-2, IL-21, IL-6, IL-1β, TNFα and R848) as described in chapter 2. Cultures were incubated for 13 days then supernatants harvested and tested for NR1-IgG at a starting dilution of 1:2 on the NR1 live CBA.

6.3.2 Results

Both material preparations gave rise to a proportion of culture supernatants that were positive for NR1-IgG. However, the dissociated cells only produced NR1-IgG under activation conditions, whereas explants produced equally frequently in maintenance and activation conditions (55% vs. 50% of wells respectively). Moreover, the rate of production from explants was higher than dissociated cells (20% of wells; figure 6.1c). There was insufficient material to test for other NR1-antibody isotypes or against non-NR1-antigens. However, the binding pattern was characteristic of strong positive NR1-IgG.

For JR817, total IgG was also measured using IgG ELISA as described in chapter 2. This showed that in both cytokine conditions explants made more IgG than dissociated cells (two-tailed Mann-Whitney test $P<0.001$; figure 6.1d). For explants, there was no significant difference in total IgG between activation and maintenance cytokine conditions ($P=0.18$, two-tailed Mann-Whitney test), but consistent with

observations from Makuch *et al.* (146), the activation condition produced greater levels of total IgG than maintenance (two-tailed Mann-Whitney test P=0.03) (figure 6.1d). NR1-specific IgG secretion from explants correlated with total IgG under both activation and maintenance conditions (Pearson's R^2=0.54 P=0.02 and R^2=0.69 P=0.003, respectively) but not with dissociated cells under activation conditions (Pearson's R^2=0.033 P=0.59).

These findings indicated that the ovarian teratoma itself was capable of producing NR1-IgG. The ability of explants to secrete large amount of IgG containing NR1-antigen specificity irrespective of activating cytokines suggested that autonomous NR1-antibody-secreting cells had been formed and were contained within the tissue. It may have been that niched plasma cells were disrupted on dissociation such that IgG secretion was account for by differentiation of B cells *in vitro*. The differential total IgG secretion seen between activation and maintenance conditions is consistent with differentiation of NR1-ASCs from patient PBMCs (146). The main caveat was that absolute numbers of lymphocytes in the explants were unknown and so the lower rate in the dissociated cells may have been due to a lower chance of the sample containing NR1-specific cells. Nonetheless, the principal observation of total and NR1-specific IgG secretion from unstimulated explant tissues strongly suggested that NR1-ASCs were being generated within the OT.

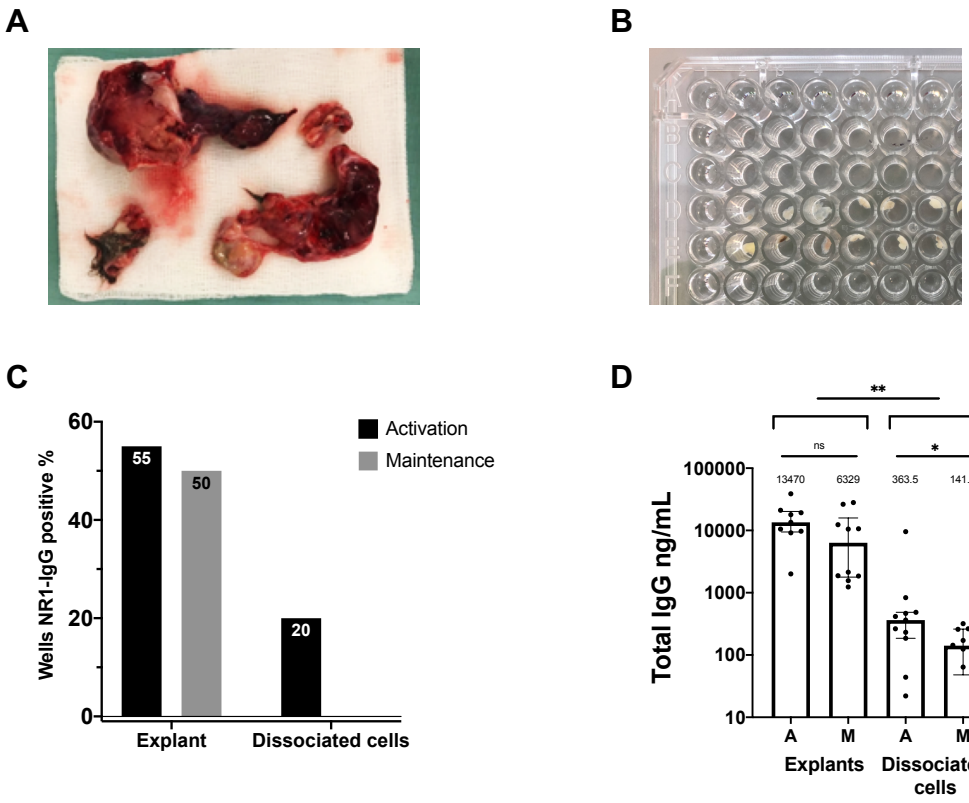


Figure 6.1 – **Culture of ovarian teratoma material under activation and maintenance cytokine conditions.**

A – Photograph of JR817 ovarian teratoma following resection via laparoscopic technique. B – Detail from photograph of culture plate following 13 day incubation showing explants in rows D and E. C – Proportion of NR1-IgG positive wells from three experiments (JR817, JR819a, and JR819b) comparing between activation (black) and maintenance (grey) conditions and explant and dissociated cell preparations. D – Total IgG from JR817 culture supernatants. Bars are median and error bars inter-quartile range. Median value is stated above each bar. E – Total IgG from JR817 culture supernatants plotted against NR1-IgG end-point dilution for activation (top) and maintenance (bottom). Explants are red and dissociated cells are blue.
Abbreviations used: A=activation, M=maintenance. *P<0.05 **P<0.005

6.3.3 Measurement of NR1-antibodies in tumour-associated fluids

JR748 was a genuinely cystic tumour (JR748) whereas the other three OTs were either removed in pieces or not sufficiently cystic to aspirate frank fluid. For these lesions, the initial supernatant wash fluid from material preparation was used. For JR819b (recurrent lesion) there was free fluid in the peritoneal cavity which was also retrieved by the surgeon. NR1-specific IgG, IgA and IgM antibodies were measured in the wash/cystic fluid, peritoneal fluid, and paired serum (figure 6.2).

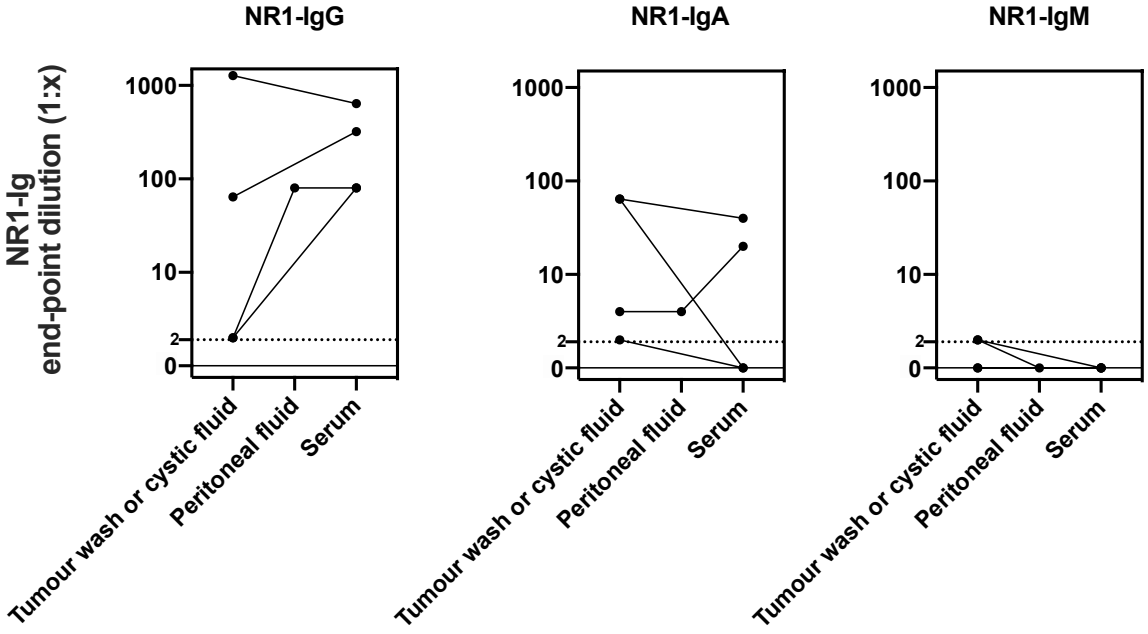


Figure 6.2 – **NR1-autoantibody isotype levels in four OT lesions and paired serum.** Continuous line marks negative samples and dotted line at 1:2 marks the initial dilution.

NR1-IgG was always present in both tumour and serum, NR1-IgA was always present in the tumour but not always in serum (2/4), and NR1-IgM was absent from both except the two JR819 instances where it was just detectable in the tumour but not in the serum. JR748 is the lesion where quantitation is likely to most accurately reflect *in vivo* status. Here, NR1-IgG was notably higher in the cystic fluid than serum (1:1280 vs 1:640) and NR1-IgA was present in the cystic fluid at a high level (1:64) but absent in serum. Overall there were no isotypes that were present in serum but

not in the tumour but there were tumour isotypes that were absent in serum. This suggests that the tumour is a site of active production rather than antibodies diffusing in from the circulation. These inferences fit with the inferences from the culture experiments and suggested a need to further characterise the cellular phenotype of the samples.

6.4 Flow cytometric characterisation of B cell infiltrates

The first approach used to further characterise the material was flow cytometry. As described in chapter 2, samples were retrieved from liquid nitrogen storage, thawed, stained and run on a flow cytometer.

6.4.1 B cell panel

The following B cell-focused panel was used to analyse dissociated cells from JR817 and JR819 first lesion (table 6.2).

Target	Dye	Clone	Manufacturer	Dilution
CD3 CD14 Dead cells	PB PB DAPI	UCHT1 HCD14	Biolegend Biolegend	1:100 1:100
CD19	BV510	SJ25C1	BD	1:50
CD27	BV605	O323	Biolegend	1:20
IgD	FITC	IA6-2	BD	1:50
CD138	PE	44F9	Miltenyi	1:50
CD20	APC	2H7	BD	1:50
CD38	APC-H7	HB7	BD	1:40

Table 6.2 – **B cell-focused staining panel used to study OT samples.**

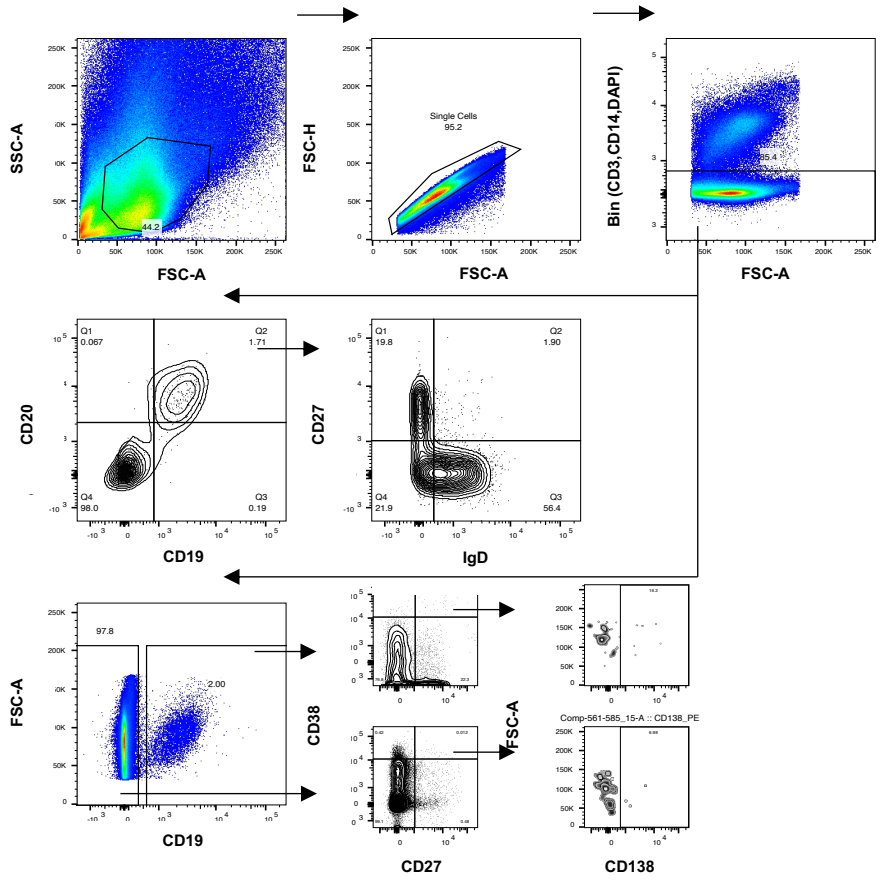
In this experiment paired PBMCs were analysed concurrently with the tumour samples. There was clear evidence of B cell (CD19+CD20+) lineages within the lesion including B naïve (CD19+CD20+IgD+CD27-), (switched) B memory (CD19+CD20+IgD-/+CD27+) and ASC lineages (CD19+CD27+CD38+ ±CD138) (figure 6.3a-b). Compared to PBMCs, B cells were a markedly smaller proportion of

the live single cell CD3-CD14- gate in both patients (PBMC:OT ratio JR817=50, JR819a=447). This is most likely due to the material; whereas PBMCs are an enriched white cell fraction of blood, the dissociated teratoma tissue contained multiple non-leucocytic tumour components.

Within B cell populations there were greater differences in naïve than memory cells between PBMC and teratoma and this was the opposite direction between the two patients (PBMC:OT ratio JR817=1.35, JR819a=0.51). Notably, the naïve compartment was markedly smaller in JR819a than excepted (19.9% of B cells), which probably caused the difference in direction. This may be idiosyncratic, related to disease or treatment, or spurious.

ASCs were rare as a proportion of live CD19+ cells in both patients in both PBMCs and teratoma. However, for both participants they were more common in the teratoma material (PBMC:OT ratio JR817=0.25, JR819a=0.52) supportive of the OTs as centres of ASC differentiation. CD138+ ASCs were equal between PBMC and OT in JR817 but could not be detected in JR817a. ASCs with and without CD138 were far less common in the CD19 negative gate which is likely due to contaminating events entering this gate in the tumour material.

A



B

Patient	B cells			ASCs			
				CD19+		CD19-	
	B cells CD19+CD20+	**B naïve CD19+CD20+ IgD+CD27-**	**B memory CD19+CD20+ IgD-CD27+**	**CD27+ CD38+**	**CD27+ CD38+ CD138+**	**CD27+ CD38+**	**CD27+ CD38+ CD138+**
	%Live single cell CD3-CD14-	%CD19+CD20+	%CD19+CD20+	%CD19+	%CD27+ CD38+	%CD27+ CD38+	%CD27+ CD38+
JR817							
PBMC	85.6	75.9	13.9	0.13	16.5	0.68	11.1
OT	1.71	56.4	19.8	0.52	16.2	0.012	6.98
Ratio	*50*	*1.35*	*0.70*	*0.25*	*1.02*	56	1.59
JR819a							
PBMC	80.4	19.9	35.2	0.38	7.89	0.33	2.4
OT	0.18	39.1	32.2	0.73	0	0.01	1.19
Ratio	*447*	*0.51*	*1.09*	*0.52*	*0*	*33*	*2.02*

Figure 6.3 – **Flow cytometric analysis of dissociated material from ovarian teratoma and paired PBMCs from two patients.**

A – Gating strategy (JR817 tumour sample shown): Following inclusion of lymphocyte size/granularity events, doublets were excluded, and CD3,CD14 and DAPI staining events excluded. Next CD19+CD20+ defined B cells were categorised as naïve or memory based on reciprocal IgD/CD27 status. Separately, CD27+CD38+ populations were gated from CD19+ and CD19- populations, and from these CD138+ cells were gated.

B – Table of proportions from these samples using this gating strategy. PBMC:OT ratios are presented for each population from each patient's sample.

6.4.2 B memory cell antibody isotype panel

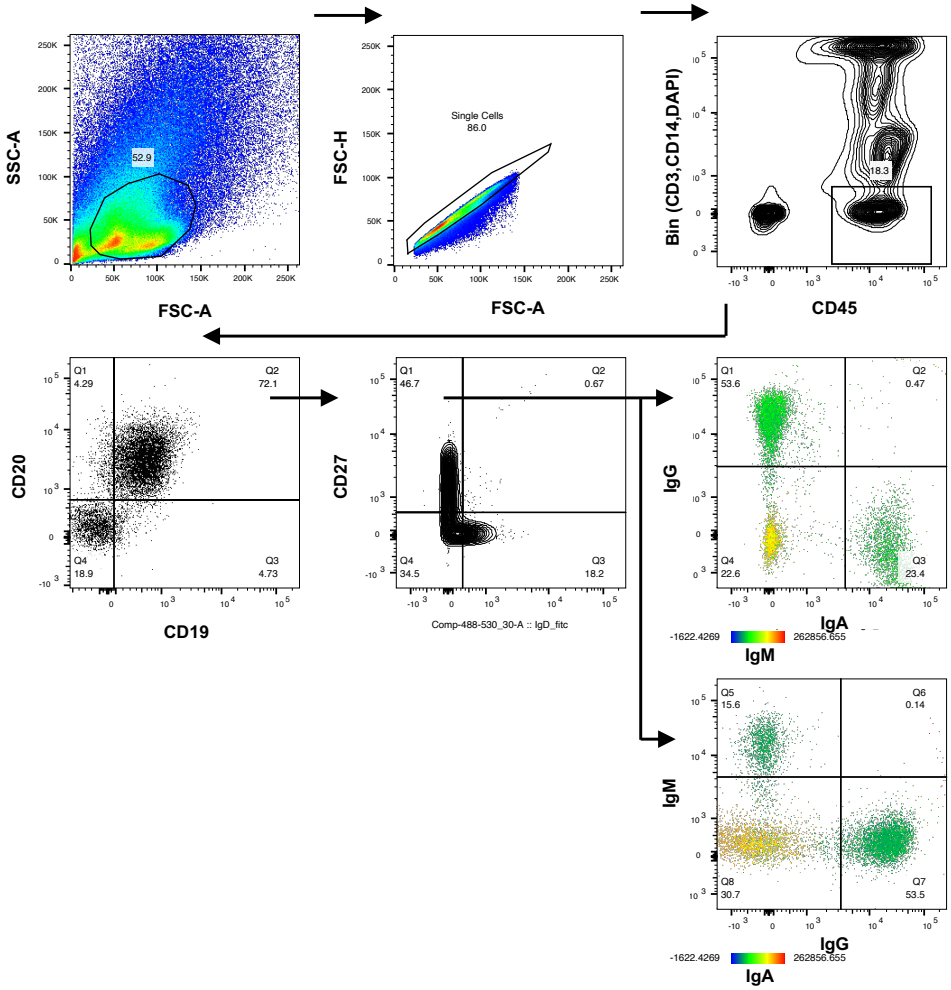
IgG, IgA and IgM antibody markers were included in a panel to further investigate the surface immunoglobulin isotype of the B memory cells differentiating in the OT (table 6.3). A sample of dissociated material from JR819b was available for this analysis. CD45 was included to enrich for leucocytes in anticipation of the contamination found in the initial experiment.

Target	Dye	Clone	Manufacturer	Dilution
CD3 CD14 Dead cells	PB PB DAPI	UCHT1 HCD14	Biolegend Biolegend	1:100 1:100
CD27	BV605	O323	Biolegend	1:20
CD20	BV711	2H7	Biolegend	1:40
IgD	FITC	IA6-2	Biolegend	1:50
IgA	PE	IS11-8E10	Miltenyi	1:25
IgG	PE-CF594	G18-145	BD	1:100
IgM	AF-647	MHM-88	Biolegend	1:50
CD45	AF-700	2D1	Biolegend	1:40
CD19	APC-Cy7	SJ25C1	BD	1:40

Table 6.3 – **B cell flow cytometry staining panel to investigate surface immunoglobulin expression.**

As shown in figure 6.4 this material was also infiltrated with B cells. CD45 was a useful marker, showing that the bin negative gait contained non-leucocytic events (figure 6.4a). Consequently, the CD45+Bin- gate was 49.9% CD19+CD20+ B cells compared to <2% seen in 6.3.3.1. Within the B memory gate there was evidence of all subtypes singly positive for each isotype (IgG (54.1%) > IgA (23.8%) > IgM (15.0%); figure 6.4a-b). This supported the suggestion that there was B cell class-switching to IgG and IgA isotypes within the teratoma. The presence of IgM+ B memory cells was of interest given the NR1-IgM detected in this material.

A



B

	B cells CD19+CD20+ %Live single cell CD45+CD3-CD14-	**B naïve CD19+CD20+ IgD+CD27-** %CD19+CD20+	**B memory CD19+CD20+ IgD-CD27+** %CD19+CD20+	**B memory isotype subsets** %CD19+CD20+ IgD-CD27+
JR819b OT	72.1	18.2	46.7	$IgG^-IgA^-IgM^+$ 15.6 $IgM^-IgA^-IgG^+$ 53.5 $IgM^-IgG^-IgA^+$ 23.4

Figure 6.4 – **Flow cytometric analysis of dissociated material from OT JR819b.**

A – Gating strategy: Following inclusion of lymphocyte size/granularity events, doublets were excluded, and CD45-CD3+CD14+DAPI staining events excluded. Next CD19+CD20+ defined B cells of which IgD-CD27+ (B memory cells) were included. Of this gate cells were classified into IgA vs. IgG and IgG vs. IgM with the third isotype as a colour heatmap where red end of spectrum is higher MFI. In this way the B memory isotype subset is positively identified with others excluded from the count.

B – Table of proportions from this sample categorised using this gating strategy.

6.5 Immunohistochemistry

6.5.1 Chromogenic staining

The above experiments and findings from NBA in chapter 4 were suggestive of a B-cell infiltrate capable of differentiating into class-switched ASCs. Such findings would usually associate with germinal centre organisation of B and T cells.

As discussed in chapter 1, germinal centres are transient immune structures optimised for B cell affinity maturation towards a retained antigenic target. They usually develop in secondary lymphoid organs like lymph nodes but can also occur ectopically in other organs in settings such as chronic inflammation, autoimmunity, or neoplasia, called ‘tertiary lymphoid organs’ (TLO). Encephalitis-associated OTs were also a good TLO candidate given the combination of neoplasia, antigen-specific autoimmunity, and the therapeutic efficacy of lesion resection (121).

To identify germinal centres, histological panels were developed (table 6.4). I planned the panels and performed subsequent analyses. Sections were made from paraffin embedded tissue based upon recommendations by Dr Darren Fowler (Consultant Pathologist) of regions where there were hypercellular aggregates. These had a high prior likelihood of being lymphocytic infiltrates. Histology antibodies were optimised, tissues stained, and digitally scanned with a Hamamatsu slide scanner by Ms. Tasneem Hassan-Ali from the Oxford centre for histopathology research (OCHRe).

Panel	Target	Clone	Manufacturer
Panel 1	CD3	LN10	Leica
	CD20	L26	Dako
	CD27	ab70103 polyclonal	Abcam
	CD38	ab140799 polyclonal	Abcam
	CD138	MI15	Leica
	NR1	1H13L3	Thermo Fisher
	MAP2	AMAB91375 polyclonal	Merck
Panel 2	CD3	LN10	Leica
	CD4	PA0427	Leica
	CXCR5	HPA042432 polyclonal	Merck
	PD1	73-10	Leica
	CD20	L26	Dako
	CD27	ab70103 polyclonal	Abcam
	CD38	ab140799 polyclonal	Abcam
	CD138	MI15	Leica
	CXCR4	44716	R&D Systems
	CD21	13135	Santa Cruz biotechnology
	NR1	1H13L3	Thermo Fisher
	MAP2	AMAB91375 polyclonal	Merck
	GFAP	GA5	Leica

Table 6.4 – **Immunohistochemistry panels for chromogenic OT staining**. Panel 1 was developed first. It was used to explore potential lymphocytic infiltration and antigen association. Subsequently, panel 2 was developed to provide more detailed information on B and T cell populations, follicular dendritic cells, and neuroglial tissue.

Panel 1 demonstrated lymphocytic infiltrations in both JR007 and JR748. In the latter there was a region of densely packed with B cells (CD20+) and T cells (CD3+) on the periphery of the lesion (figure 6.4a-d). Some of the B cells also expressed CD27 suggesting B memory cells. Amongst the CD27+ cells some expressed CD38 suggesting the differentiation of ASCs. There was also CD27 staining in the CD3 region implying T cell activation. These findings complemented flow cytometry data but also demonstrated germinal centre-like structural organisation, as predicted in the previous findings. Within this region there was dense NR1 staining which appeared to overlap with the CD27 staining. Moreover, MAP2+ cells of neuronal morphology were adjacent to the NR1 staining but not co-localised. This suggesting that the NR1 could have been lymphocyte-expressed rather than the target antigen.

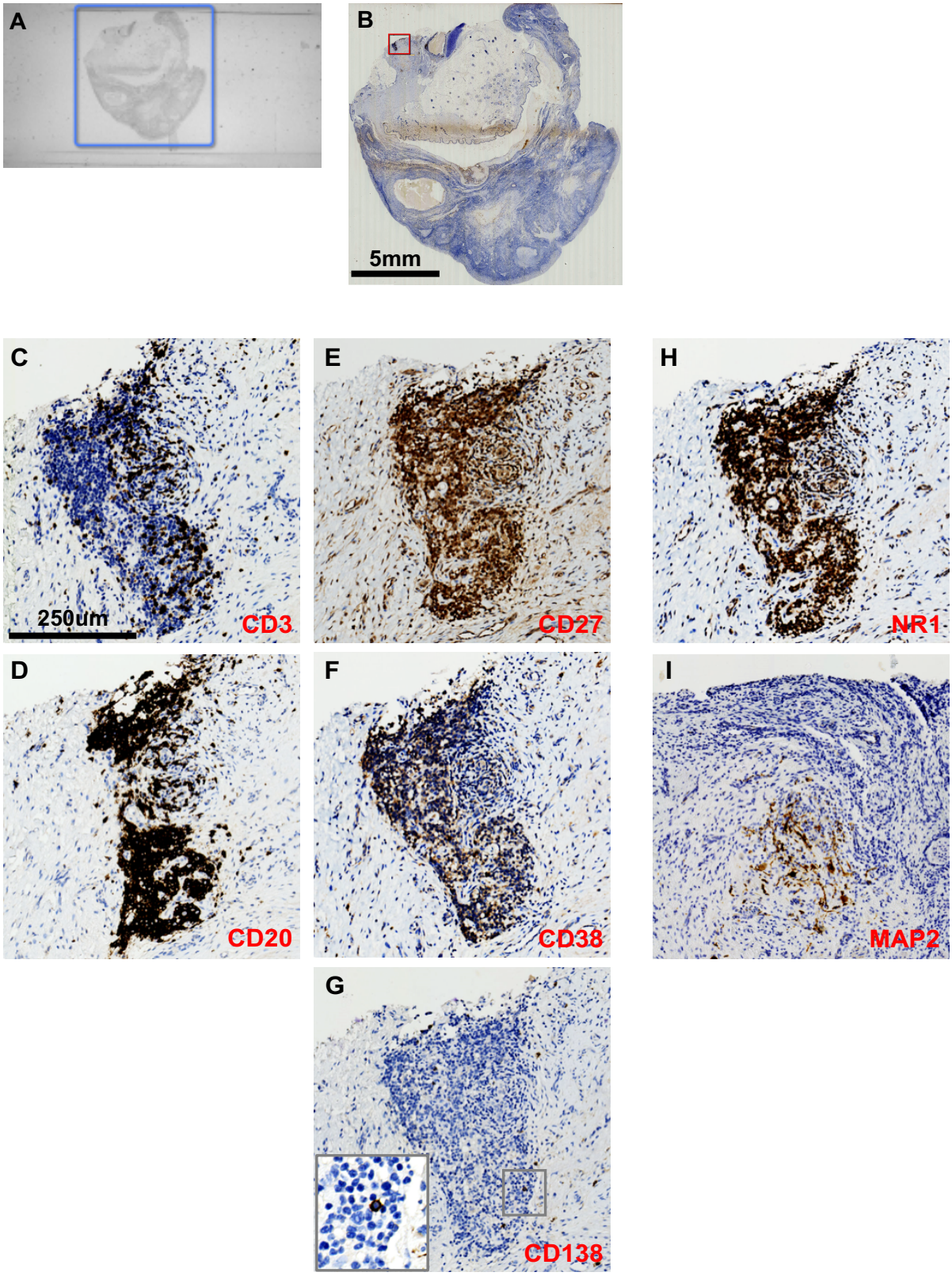


Figure 6.5 – **Panel 1 immunohistochemistry on serial sections from OT JR748.**

A – unstained section on slide showing gross morphology.
B – CD3 staining showing region of interest (C-I) in red box.
C-I – 10x zoom on region of interest in serial sections. Markers are noted in bottom right corner of each image.
G – grey box demarcates inset showing rare individual CD138-stained cells. Images contributed to Makuch *et al.* (146).

Having demonstrated germinal centre-like organisation of lymphocytic infiltrates with panel 1, panel 2 was designed to explore this further via markers for T follicular helper cells (TfH: CD3+CD4+CXCR5+PD1+), germinal centre B cells (GCBC: CD19+CXCR4+), follicular dendritic cells (CD21+), and astrocytic tissue (GFAP+) in addition to markers from panel 1.

Lymphocytic infiltration was present in all samples assessed (JR007, JR817, JR819). The clearest example was JR817 (figure 6.6). There were scattered CD3+ and CD20+ cells throughout the section, but, as in panel 1, there were dense focal hypercellular regions; B and T cell regions overlapped but the T cell region appeared more extensive (figure 6.6c and e). CD27 staining overlapped with both populations, as seen in JR748 with panel 1. Within the CD20+CD27+ regions there were rarer CD38+ and CD138+ cells on the periphery suggestive of ASC and plasma cell differentiation (figure 6.6c inset). There was CXCR4 expression within the CD20+ regions, possibly suggestive of B cells entering a germinal centre phenotype.

T helper cell infiltrates (CD3+CD4+) were co-located amongst the B cell infiltrate implying cell-cell interaction and the potential for co-stimulation. Within the T helper population there were more rarely cells that were CXCR5+ and slightly less commonly cells that were also PD1+. This CXCR5+PD1+ double positive population would be regarded as T follicular helper cells in secondary lymphoid tissue and are suggestive of a germinal centre-type reaction.

Further evidence of a germinal centre-like organisation of these infiltrates were CD21+ cells forming a sustentacular meshwork within a hypercellular region (figure

6.5e). This was also typical of an emerging germinal centre follicle where follicular dendritic cells support the structure, as would usually occur in secondary lymphoid tissue.

Extending the observation of NR1 staining seen with panel 1, there was again NR1 staining evident. It was most prominent within the hypercellular lymphocytic region and had a similar staining pattern to other lymphocytes makers (figure 6.5f). There was also NR1 staining within regions positive for MAP2 and GFAP with associated neuro-glial morphology. These regions were adjacent to the lymphocytic regions but not directly within them. Overall, this was consistent with there being neuroglial elements present within the lesion and located nearby the germinal centre-like structures but that the prominent NR1 staining may be lymphocytic in origin rather than retained antigen. There is a reported role for NMDA receptors in T cell activation (195).

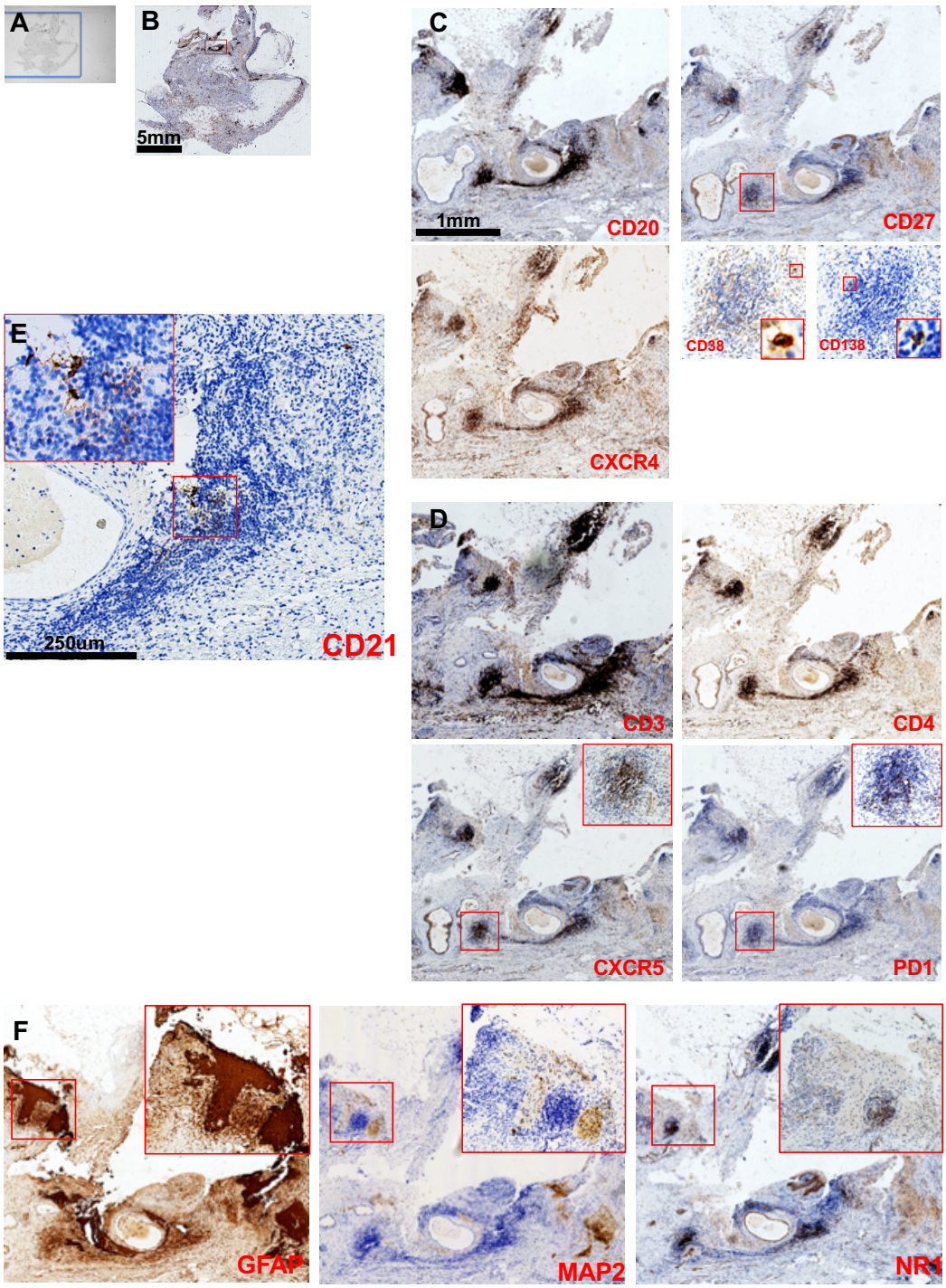


Figure 6.6 – **Panel 2 immunohistochemistry on serial sections from JR817 ovarian teratoma**.

A – Unstained section. B – CD3 staining showing region of interest (red box). C – B cell markers: the red box in CD27 shows a region of interest in which CD38 and CD138 staining is highlighted beneath, each with a further inset containing an example of a positive cell (2.5x zoom). D – T cell markers: CD4+ T cells positive for CXCR5 and/or PD1 (2.5x zoom). E – CD21 stained cells forming a sustentacular meshwork were consistent with follicular dendritic cells (10x zoom). F – Neuroglial markers (GFAP, MAP2 and NR1): The red boxed region shows an area of interest with co-localised staining of all three markers with an adjacent lymphocytic region containing stronger cellular NR1 staining consistent with NR1 being expressed in both neuroglial tissue and in lymphocytes.

6.5.2 Multiplex immunofluorescence histology

These findings were strongly suggestive of lymphocytic infiltration organised in germinal centre-like structures in OTs associated with NMDAR-Ab-E. To demonstrate this in further detail a multiplex approach was applied. Conventional single staining limits spatial co-localisation due to the need for multiple sections, whereas this approach permitted six markers on a single section. B cell, T cell/FDC panels, and vascular/neural panels were developed.

Paraffin-embedded sections were used. Ms. Tasneem Hassan-Ali and Ms Leticia Campo from the translational oncology group optimised the antibodies on tonsil and once expected binding was confirmed both singly and in multiplex, the cases were stained. These were digitally scanned and spectrally unmixed with the Vectra Polaris automated quantitative pathology imaging system (Akoya biosciences) then remixed using HALO image analysis software (Indica labs), from which images were acquired.

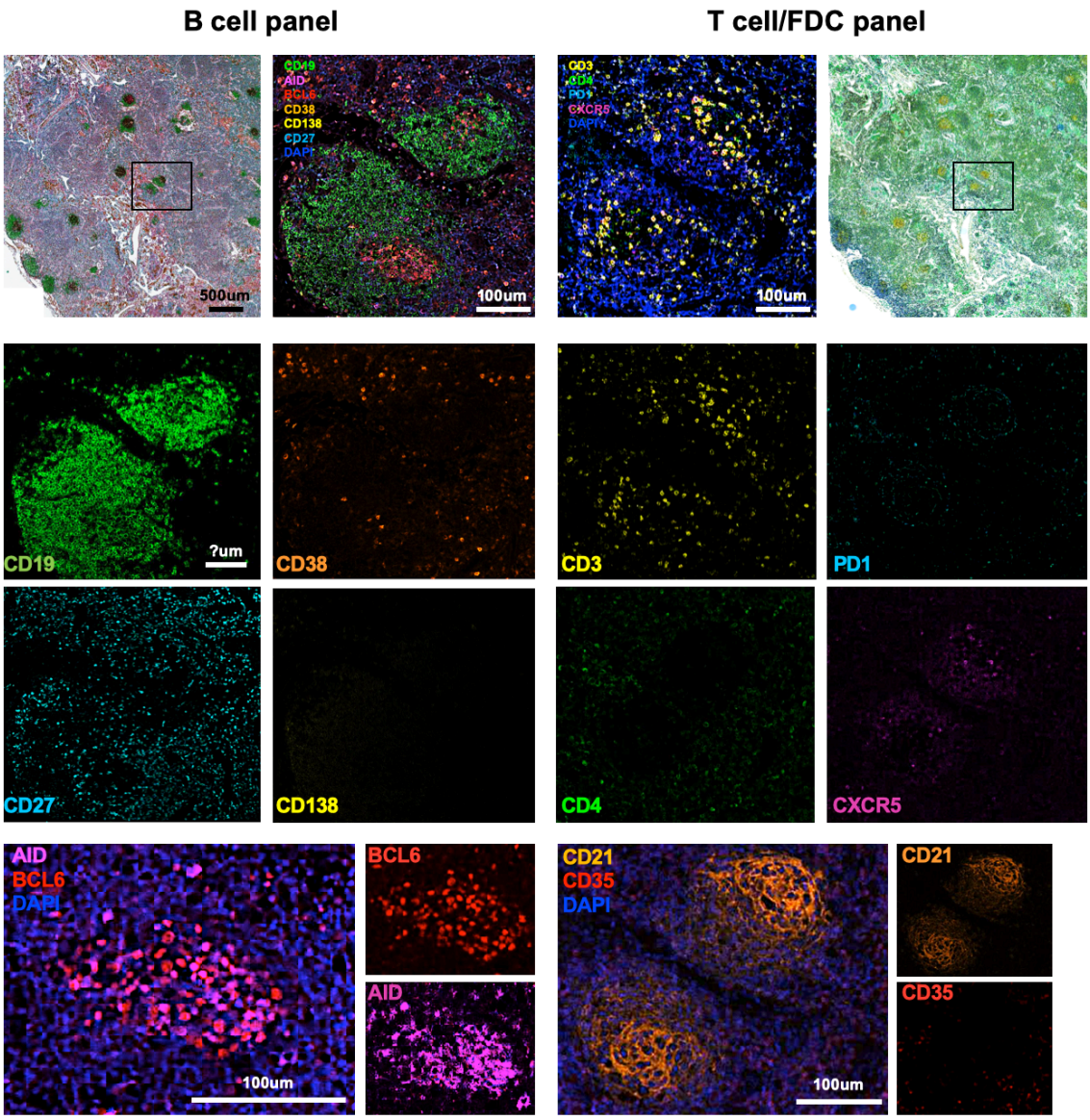
Alongside four targets associated with B cell maturation into antibody-secreting cells (CD19, CD27, CD38, CD138), two markers of germinal centre B cell biology were used: B-cell lymphoma 6 protein (BCL6) and activation-induced cytidine deaminase (AID) (table 6.5). As outlined in chapter 1, BCL6 is a transcription factor which is expressed for a B cell to enter a germinal centre phenotype and AID is an enzyme involved in both somatic hypermutation and class-switch recombination. Both would be expected present within a B cells population in a putative germinal centre-like region.

The T/FDC panel contained markers for T helper cells (CD3 and CD4) and markers found on T follicular helper cells (CXCR5 and PD1) in germinal centres in secondary lymphoid organs. Follicular dendritic cells express complement receptors CD21 and CD35, so these were the markers of choice to attempt to identify these cells (table 6.5). The vascular/neural panel included GFAP and MAP2 to identify neuro-glial tissue, LAMP3 to identify dendritic cells, PNAd for high endothelial venules, and Podoplanin for lymphatic vessels.

Target	Antibody code	Manufacturer	Fluorochrome	Assigned colour
B cell panel				
CD19	BT51E	Leica	Opal 520	Green
CD138	MI15	Thermo Fisher	Opal 540	Yellow
CD38	Polyclonal	Abcam	Opal 570	Orange
BCL6	LN22	Leica	Opal 620	Red
AID	ZA001	Thermo Fisher	Opal 650	Magenta
CD27	EPR8569	Abcam	Opal 690	Cyan
T cell/FDC panel				
CD4	LN10	Leica	Opal 520	Green
CD3	4B12	Leica	Opal 540	Yellow
CD21	2G9	Leica	Opal 570	Orange
CD35	EP197	Cell marque	Opal 620	Red
CXCR5	HPA042432	Atlas	Opal 650	Magenta
PD1	NAT105	Cell marque	Opal 690	Cyan
Vascular/neural panel				
GFAP	PA0026	Leica	Opal 520	Green
LAMP3	HPA051467	Atlas	Opal 540	Yellow
PNAd (MECA-79)	sc-19602	Santa Cruz	Opal 570	Orange
MAP2	AMAb91375	Sigma	Opal 620	Red
Podoplanin	GTX31231	GeneTex	Opal 650	Magenta

Table 6.5 – **Multiplex immunofluorescence histology B and T/FDC cell staining panels.** Antibodies are listed in fluorochrome spectral order. Assigned colour post-processing is listed.

Three tissues each associated with active NMDAR-Ab-E were compared: post-mortem cervical lymph node, colorectal carcinoma, and ovarian teratoma (listed in table 6.1 as ‘Baltimore’, ‘Japan’, and JR007, respectively). The lymph node was previously found to have dense collections of CD138+ plasma cells and was associated with highly treatment-resistant NMDAR-Ab-E in which the patient died (149) whereas the ovarian teratoma was from a case of NMDAR-Ab-E where resection was associated with clinical recovery. Given that lymph node tissue per se is likely to contain *bona fide* germinal centres and that this patient was thought to have high level of immune activity, this tissue was considered a good candidate with which to compare with the OT for germinal centre markers and organisation.



Vascular/neural panel

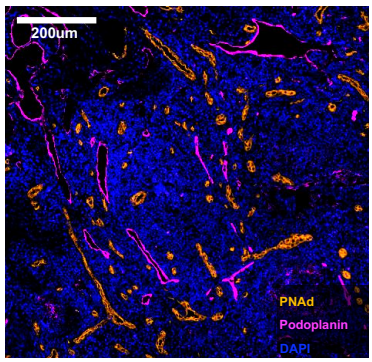


Figure 6.7 – **Multiplex immunofluorescence staining with B, T and FDC panels of post-mortem lymph node from a patient with NMDAR-Ab-E.**

Each panel is initially shown inverted at 2x zoom. The black box demarcates the region of interest viewed at 10x zoom then at 20x zoom on the bottom row. This was two germinal centre structure adjacent to each other. There were CD19+ cells throughout the structure and CD3+ cells scattered around the margins and deeper within, some of which expressed CXCR5. Some but not all of the T cells were CD4 positive. CD27 positivity co-localised with the majority of B cells and some of these also expressed CD38 and of these some expressed CD138. B cells expressing CXCR5 had less CD27 positivity and were found within the core AID+BCL6+ region. The B cells in this region were within a CD21+ cell mesh. From the vascular panel, representative PNAd+ and Podoplanin+ high endothelial venule and lymphatic vessels are shown.

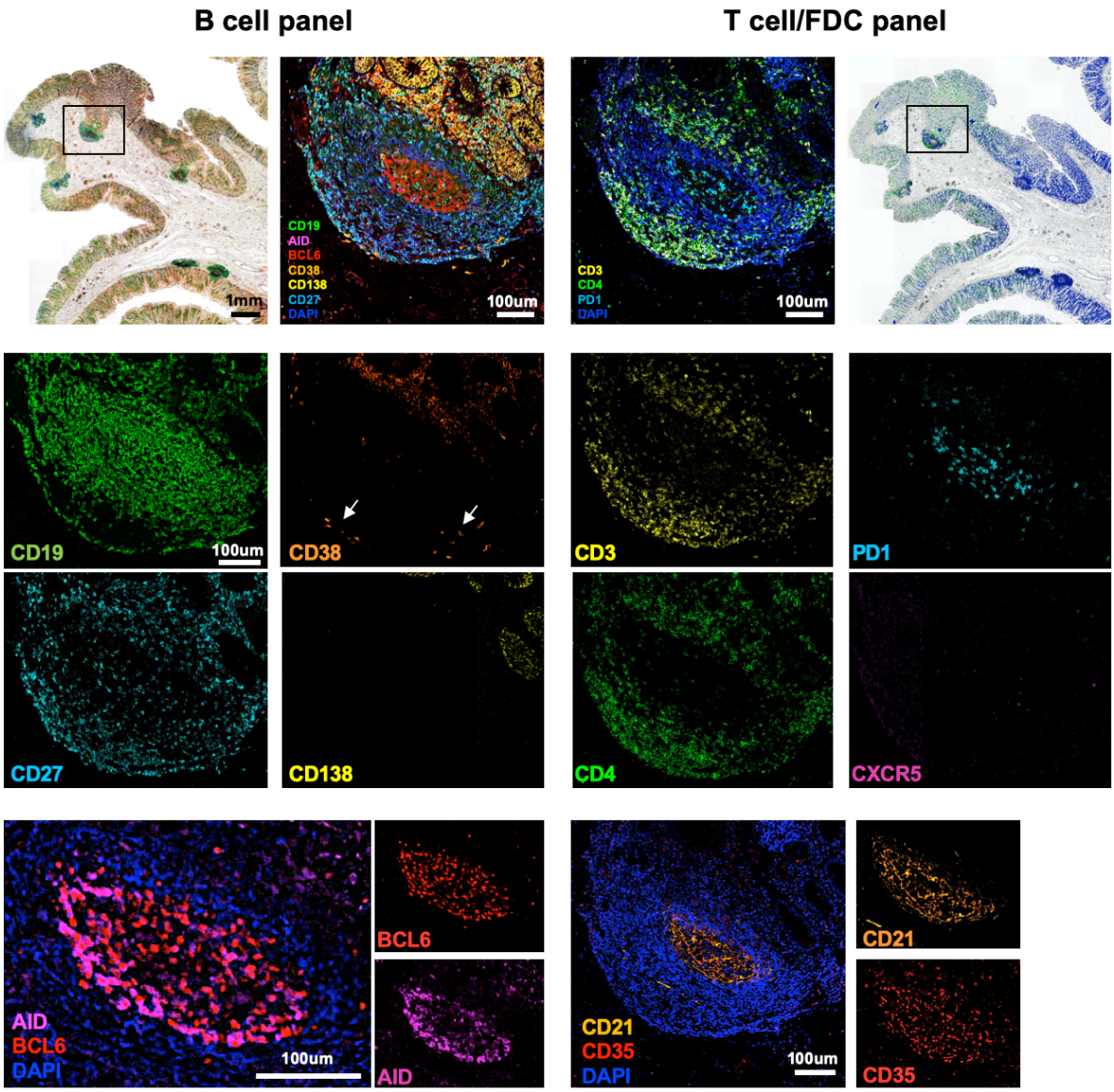


Figure 6.8 – **Multiplex immunofluorescence staining with B, T and FDC panels of colorectal carcinoma from patient with NMDAR-Ab-E.**

Colorectal carcinoma (Japan). Each panel is initially shown without fluorescence at 2x zoom. The black box demarcates the region of interest viewed at 10x zoom then at 20x zoom on the bottom row. CD19+ cells are throughout the structure with CD3+ cells largely around the margins, where there are fewer B cells. There is CD27+ staining in B and T cell zones. There are CD38+ B cells on the edge of the structure and upwards into the neighbouring epithelium (white arrows). These were not positive for CD138. The majority of the CD3+ cells were CD4+ but the majority of PD1 expression was not on CD3 and there CXCR5 was not detectable. The B cells in the centre were positive for BCL6 and most also expressing AID. They were embedded in a mesh like structure made by CD21+CD35+ follicular dendritic cells.

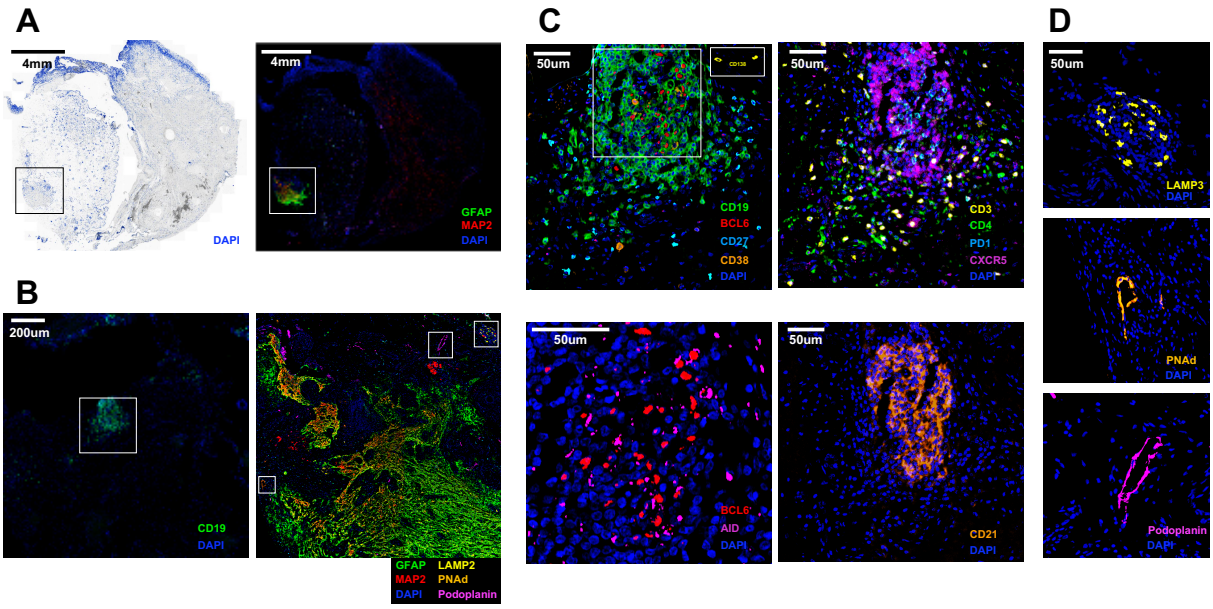


Figure 6.9 – **Multiplex immunofluorescence staining with B, T and FDC panels of OT from patient with NMDAR-Ab-E.**

A – Ovarian teratoma (JR007) at low power showing DAPI staining (left) with region of interest (black box) then showing GFAP and MAP2 staining (white box).

B – The region of interest from (A) at higher power zoom showing CD19 from the B cell panel (left) and the same region using the vascular/neural panel showing GFAP, MAP2, LAMP2, PNAd and Podoplanin. The B cell dense region outlined in the white box in the left image is then presented in (C).

C – Lymphocyte dense region showing B cell panel (top left) with occasional CD27+ or CD38+ cells outside a hypercellular core with BCL6+. There was also AID+ cells (bottom left, detail from white box). The T cell panel stains (top right) show occasional CD3+ and/or CD4+ cells around the B cell region. PD1 and CXCR5 staining is largely in the B rather than T cell region. A CD21+ meshwork co-localise with the B cell rich core probably suggesting follicular dendritic cells(bottom right).

D – Single stains with DAPI from vascular/neural multiplex presented in (B): LAMP3 positive cells (dendritic cells), PNAd+ vessel (high endothelial venule), and podoplanin+ vessel (lymphatic).

The multiplex approach provided further evidence of germinal centre structures within an encephalitis-associated OT that showed much overlap with typical germinal centres from the patient lymph node, albeit with slightly less organisation (figures 6.7 and 6.9). Both OT and LN germinal centre structures showed densely packed CD19+ B Cells. Differentiation into ASCs was seen with CD38 expression in both samples. CD138+ cells were not seen in the lymph node region presented above but could be seen elsewhere in the lymph node. In the OT, CD138 expression on multiple non-lymphocytic cell types made this harder to discern but a few cells nearby the GC-like regions could be seen.

Both tissues had clear evidence of BCL6+ B cells, many of which expressed AID, organised as a core within a CD21+ cellular meshwork of likely follicular dendritic cells. Both regions had T cells which were largely peripheral relative to B cells and in both cases CXCR5 staining was predominantly B cell rather than T cell. In the OT, contrary to a typical TfH phenotype, PD1 expression was largely absent from T cells and mainly present in the B cell region.

The colorectal carcinoma sample also had multiple sub-epithelial GC-like structures with the B and T cell features described above. These GCs were closer in organisation to the lymph node than the OT.

6.6 Discussion and limitations

This set of experiments provides evidence that in NMDAR-Ab-E associated with ovarian teratoma, the teratoma itself is a centre for NR1 autoimmunisation and consequent NR1-ASC differentiation and NR1-autoantibody production. Firstly, *ex vivo* material from these tumours secreted NR1-IgG *in vitro* using IL-6 alone showing that NR1-ASCs are present. Secondly, explants were more effective than dissociated cells at making NR1-IgG irrespective of stimulating condition. This suggested that there were probably both *bona fide* NR1-plasma cells occupying a survival niche but also NR1-specific B memory cells that could differentiate into NR1-ASCs. Thirdly, there were NR1-antibody isotypes present in tumour material that were not present in serum. In the OT that contained genuinely cystic fluid that could be tested directly from the source, NR1-IgG end-point dilution was higher in the cyst than serum. These observations supported local synthesis of NR1-antibodies that were often class-switched to IgA, as well as IgG. Fourthly, flow cytometry and histology showed clear B cell populations ranging from naïve to germinal centre to memory to antibody-secreting phenotypes suggestive of an active germinal centre reaction. Moreover, histology showed phenotypes such as CXCR5+PD1+ T cells, BCL6+AID+ B cells within CD21+ follicular dendritic cell meshworks and CD38+ ASCs. These were highly consistent with organising follicles and would be highly unlikely to be present unless a germinal centre reaction was occurring. Finally, the presence of a sustentacular meshwork emanating from CD21+ cells with FDC-type morphology is highly consistent with an organising follicle. These observations are clear and striking, but qualitative; future work using the multiplex staining will take an unbiased machine-learning approach to quantify these relationships more precisely.

Together with data from chapter 5 which suggested that NR1-IgG associated with ovarian teratoma-associated NMDAR-Ab-E cases preferentially bound live neurons compared to NR1-IgG from non-teratoma associated encephalitis and non-encephalitis-associated NR1-IgG seropositivity, the observations here suggest that the ovarian teratoma is a site for NR1-antibody affinity maturation. Whilst the ultimate proof of SHM would come from sequence analysis of NR1-specific teratoma-derived monoclonal antibodies, the evidence here appears sufficient to consider these teratomas tertiary lymphoid structures and is consistent with findings in other germ cell tumours (35).

The serological studies in chapters 4-5 were consistent with ovarian teratoma not only predisposing to more affinity matured (and therefore likely more somatically hyper-mutated) NR1-IgG but also a propensity to class-switching to NR1-IgA in addition to the pathogenic IgG antibodies. In this chapter, flow cytometry revealed IgA-switched B memory cells in OT material suggesting a potential cellular substrate. If it is assumed that SHM and CSR are relatively coupled within a germinal centre reaction, one explanation would be that these are protracted reactions due to persistent antigen provided by tumour tissue and therefore class-switched antibodies including IgA are probable. However, it has recently been recognised that SHM and CSR are not necessarily coupled within a GC reaction, indeed it was shown in a vaccine model that CSR is largely completed prior to SHM (27), and may occur in extrafollicular reactions. If this is the case in autoimmunity too, then evidence of antigen-specific CSR could not necessarily be explained by evidence of GC reactions.

An alternative hypothesis is that local tumour-related factors bias CSR towards IgA. For example, mucosal immunity can lead to IgA production and the teratoma expresses multiple mucosal tissue phenotypes which could directly or by secreted factors influence the lymphocytic infiltrate. It may also be that the lymphocytic infiltrates themselves, secrete signalling molecules such as IL-21 within the relatively encapsulated microenvironment of leading to large local concentrations. In the future, analysis of cytokine and chemokine profiles in teratoma fluid compared to serum could test this hypothesis.

While this work advances knowledge of disease-associated OTs as sites of GC reactions, it has not addressed why this happens in a small minority of OTs. Two studies were published during the latter stages of this thesis which converge on similar findings shown here and present data helpful to this question. Nolan *et al.* reported an OT series with 11 associated with NMDAR-Ab-E and 61 not associated (134). They found that the AE-associated OTs were significantly more likely to contain a high percentage of neuroglial tissue suggesting that greater amounts of antigen may be needed to induce the antigen-specific response. They also found that while both OT sub-groups had lymphocytic aggregates the encephalitis-associated OT aggregates were more likely to have GCs and these were usually associated with neuroglial tissue within Rokitansky nodules (solid component of OT). Chefdeville *et al.* also found a similar highly significant bias towards neuroglial tissue in AE-associated OTs including an association with tertiary lymphoid structures. Nolan *et al.* found that neurons in NMDAR-Ab-E-associated OTs were less commonly mature, and Chefdeville *et al.* found that NR1 expression in such OTs were more commonly glial than neuronal and a proportion had features of glioma.

Hence it may not only be the amount of NR1 expressed in neuroglial tissue, but also its context (i.e. with glia) or its nature (i.e. glioma-like tissue may express mutated NR1 antigen). Neoantigens can provoking robust tumour immunity therefore retrieval and sequencing of NR1 DNA from these samples would be a relevant future direction which may require cellular micro-dissection given expression in both neuroglial as well as lymphocytic populations. Furthermore, while the multiple strands of evidence presented here suggest NR1-directed GC reactions are occurring in NMDAR-Ab-E-associated OTs, a critical proof would be to pull out single NR1-specific B cells from the material either by antigen-bait cell sorting and single cell culture.

These findings are informative when considering the more common form of the disease without OT. Whereas the OTs appear to have a combination of large amounts/abnormal of antigen coupled with the potential for a lymphocyte-favourable microenvironment, the scope for such a focal immunoreaction is markedly less without such a lesion.

This correlates with the efficacy of OT removal compared to first line immunotherapies (steroid/plasma exchange/IVIG) alone in recovery and propensity to relapse (56,58,121). Indeed, without an OT, patients are more likely to require 2nd line immunotherapies (rituximab/cyclophosphamide). These studies suggest a time dependency to resection response, compatible with the lymphocytes seeding to distant sites including longer to seed in the CNS, rendering the disease more like the non-OT form with a non-focal distribution of NR1-reactive lymphocytes.

In the non-OT patients, the immune response proceeds at least initially in the periphery. This is supported by near complete seropositivity, higher serum NR1-IgG end-point dilutions than CSF, and the ability of *ex vivo* patient PBMCs to secrete NR1-antibodies much like the OT material (146). Assuming there is a peripheral initiation then secondary lymphoid tissue i.e. lymph nodes would be the main candidate location given its role in adaptive immune responses. Therefore, the final stage of this investigation aimed to obtain lymphocytes from lymph nodes of patients with NMDAR-Ab-E with and without an associated ovarian teratoma.

7 Ultrasound-guided fine needle aspiration to investigate cervical lymph nodes as a source of NR1-specific B cells

7.1 Inception of project

7.1.1 Rationale and approvals

Access to secondary lymphoid tissue would provide cellular material for phenotypic analysis and cultured to for evidence of NR1-specific B cells compared to peripheral blood. Moreover, validation of such an approach in human participants would also form a platform for future investigations in this field and for other more common neurological and psychiatric conditions where direct assessment of lymph node cells is of value.

Prior to this set of experiments there was empirical evidence of the relevance of lymphoid tissue to NR1 autoimmunisation in NMDAR-Ab-E. Firstly, as discussed in chapter 6, Nauen reported a case that was refractory to multiple treatments leading to death and at post-mortem there were no ASCs in the CNS but extensive ASCs in cervical lymphoid tissue (149). Secondly, Iwamoto *et al.* reported a case of NMDAR-Ab-E where FDG-PET imaging showed accumulation of signal in an enlarged right obturator lymph node which upon resection was associated in marked improvement of symptoms (196). The authors reported the node as histopathologically normal but speculated that it may have been a site for NR1 autoantibody production.

Although these studies suggested relevance of secondary lymphoid organs to pathogenesis, the two methods used, post-mortem examination and surgical resection, were exceptional single case reports and could not form the basis of a study in human participants. In contrast, ultrasound-guided fine needle aspiration

(FNA) is used routinely in clinical practice for the investigation of head and neck masses including lymph nodes. The technique became established because it is both very low risk but also that the cells obtained correlate well with findings from invasive biopsy and final histopathologic diagnosis (197). In a research setting, FNA has been used successfully in primates to map the response to HIV vaccines (198). This study found that lymph node FNA usually provided >100,000 immune cells, including germinal centre B cells and T follicular helper cells, and that the frequencies were highly consistent with excisional biopsy of whole lymph node.

Advice from expert radiologist colleagues was that the safest and most accessible region for human participants was the cervical nodes. Fortuitously, this region is also the most relevant to CNS immunity. Firstly, there is now extensive data to suggest that the CNS has a meningeal lymphatic system which drains into cervical lymph nodes (CLNs), providing a conduit for efflux of CNS waste including potentially antigenic molecules into secondary lymphoid tissue (147,199,200). Secondly, there have been a few studies on the relationship between CNS B cells and draining cervical lymph nodes in neuroinflammatory disease such as post-mortem multiple sclerosis samples (201), and experimental autoimmune encephalomyelitis animal models (202), (203).

Despite this, FNA of CLNs has rarely been used in the investigation of CNS autoimmune disease in human participants. On review of the literature, only one study was found that harnessed this technique to study a brain-orientated question. Fabriek *et al.* identified brain antigens in macrophages from CLNs in MS patients

obtained by FNA (204). However, neither flow cytometry nor cell culture were used to interrogate the material further.

Following discussion with the University of Oxford clinical trials and research governance team, a major amendment to the immune factors in neurological diseases study (REC16/YH/0013) was submitted including FNA of CLNs which included a description in the participant information leaflet. This was approved by the NHS research ethics committee overseeing the study (appendix). The project was subsequently approved the Oxford University Hospitals NHS foundation trust research and development committee.

7.1.2 Study logistics

A protocol was agreed with the department of radiology whereby participants would attend the ultrasound department of the JR hospital at 0800AM. This not only meant that equipment and senior radiologists (Dr Edward Green, Dr Nicholas McGlashan and supervising Consultant Radiologist Dr Fintan Sheerin) were available, but also that there was a full day to work on the samples fresh. The procedure was discussed with participants prior to informed consent being obtained and recorded on the study consent form. On the day of the procedure it was explained again by the radiologist and a further procedure-specific consent form was completed. Blood was taken for paired PBMCs and serum after the FNA procedure.

7.2 Technical development

7.2.1 Flow cytometry antibody staining panels

Panels were designed to provide a flow cytometric phenotype of populations likely to be encountered in a lymph node that were relevant to the main study question of assessing germinal centre reactions. Broadly these were B cells, T cells and an accessory panel looking at additional B cell markers such as the germinal centre B cell markers CD83 and CXCR4 and dopamine receptor D1, a newly reported marker of activated B cells (205). It was anticipated that B and T cells be present in peripheral blood and lymph node, but subsets such as T follicular helper cells and germinal centre B cells would be enriched in lymph nodes. A sort panel was later developed which utilised these markers to obtain salient B and T populations.

Many flow cytometry antibodies were previously used in the laboratory and optimal dilutions known, but those which the group had not used before were serially diluted and run on PBMCs as single stains to identify the optimal dilution. Then fluorescence minus one (FMO) panels were run to check populations were staining as expected and define the cut-offs/gates for those populations.

The panels and anticipated identifiable populations are summarised in tables 7.1 and 7.2, respectively. After these initial studies, the pan-leucocyte marker CD45 was introduced to improve the separation of leucocytes from contaminating material. This is described in further detail in 6.4.5.

Panel	Target	Dye	Clone	Manufacturer	Dilution
B cell panel	Live-Dead	DAPI	-		
	CD3	PB	UCHT1	Biolegend	1:100
	CD14	PB	HCD14	Biolegend	1:100
	CD24	BV510	ML5	Biolegend	1:40
	CD27	BV605	O323	Biolegend	1:20
	IgG	BV711	G18-145	BD	1:100
	CD20	FITC	2H7	BD	1:40
	IgD	PE-CF594	IA6-2	BD	1:100
	CD19	PE-Cy7	SJ25C1	BD	1:40
	IgM	APC	G20-127	BD	1:10
	CD45	AF700	2D1	Biolegend	1:40
	CD38	APC-Cy7	HB7	BD	1:40
B cell accessory panel	Live-Dead	DAPI	-		
	CD3	PB	UCHT1	Biolegend	1:100
	CD14	PB	HCD14	Biolegend	1:100
	IgD	BV510	IA6-2	Biolegend	1:50
	CD27	BV605	O323	Biolegend	1:20
	DRD1A	PE	L205G1	Biolegend	1:50
	CD83	PE-CF594	HB15e	Biolegend	1:50
	CD19	PE-Cy7	SJ25C1	BD	1:40
	CXCR4	APC	12G5	Biolegend	1:20
	CD45	AF700	2D1	Biolegend	1:40
	CD38	APC-Cy7	HB7	BD	1:40
T cell panel	Live-Dead	DAPI	-		
	CD3	BV510	UCHT1	BD	1:20
	CXCR5	BV711	J252D4	Biolegend	1:20
	CD40L	FITC	24-31	Biolegend	1:20
	ICOS	PerCP-CY5.5	C398.4A	Biolegend	1:20
	PD1	APC	J105	eBioscience	1:20
	CD45	AF700	2D1	Biolegend	1:40
	CD4	APC-Cy7	RPA-T4	Biolegend	1:40
	Live-Dead	DAPI	-		
Sort panel	Live-Dead	DAPI	-		
	CD3	PB	UCHT1	Biolegend	1:100
	CD27	BV605	O323	Biolegend	1:20
	CD20	BV711	2H7	Biolegend	1:40
	IgD	FITC	IA6-2	BD	1:50
	CD38	PE	HIT2	BD	1:40
	CD4	PE-CF594	RPA-T4	BD	1:50
	CXCR5	PE-Cy7	J252D4	Biolegend	1:40
	PD1	APC	J105	eBioscience	1:20
	CD45	AF700	2D1	Biolegend	1:40
	CD19	APC-Cy7	SJ25C1	BD	1:40

Table 7.1 – **Antibody staining panels used in fine needle aspiration experiments.**

B cell (DAPI-CD3-CD14-CD19+)			
Transitional	CD24+ CD38+		
B naïve	CD20+ IgD+ CD27-		
B memory	CD20+ CD27+		
B unswitched memory		IgD+	
B switched memory		IgD-	
IgG+ B switched memory			IgM- IgG+
Antibody secreting cell (ASC)	CD27+ CD38+		
B cell accessory (DAPI-)			
Germinal centre B cell phenotypes	CD3- CD19+	CD83 CXCR4	
Dopamine D1 receptor expressing B cells	CD3- CD19+	DRD1	CD27 CD38
T cell (DAPI-CD3+)			
T helper	CD4+		
Activation markers		CD40L ICOS	
T follicular helper		CXCR5+ PD1+	

Table 7.2 – **Anticipated populations using B cell, B cell accessory and T cell panels developed for fine needle aspiration study.** The markers are arranged hierarchically.

7.2.2 Radiological approach

Following consent, the participant was positioned into a horizontal position and an initial ultrasound scan of the neck including doppler was used to identify accessible cervical lymph nodes sufficiently distant from major vessels (Siemens Acuson S2000 system and 18L6 HD probe). Normal reactive lymph nodes were identified by the characteristic echogenic fatty hilum. This was either a level I or level V node and varied according to individual differences in anatomy (figure 7.1a and b).

Following identification of the target node sterile conditions were established: skin surface sterilised, sterile gloves, and ultrasound probe inserted into a sterile translucent plastic casing. The target node was then visualised and a sterile 23G needle was inserted through the skin into the node (figure 7.1c). The needle was agitated in a rotatory corkscrew motion within the node for approximately 30 seconds and then removed. The needle tip was placed into 0.5mL of sterile PBS in an Eppendorf container and this was aspirated into a 5mL syringe. The needle was removed and the suspended FNA material was ejected gently into a fresh Eppendorf container. This was done a total of 2-3 times depending on how much material was present. The node was accessed twice in total.

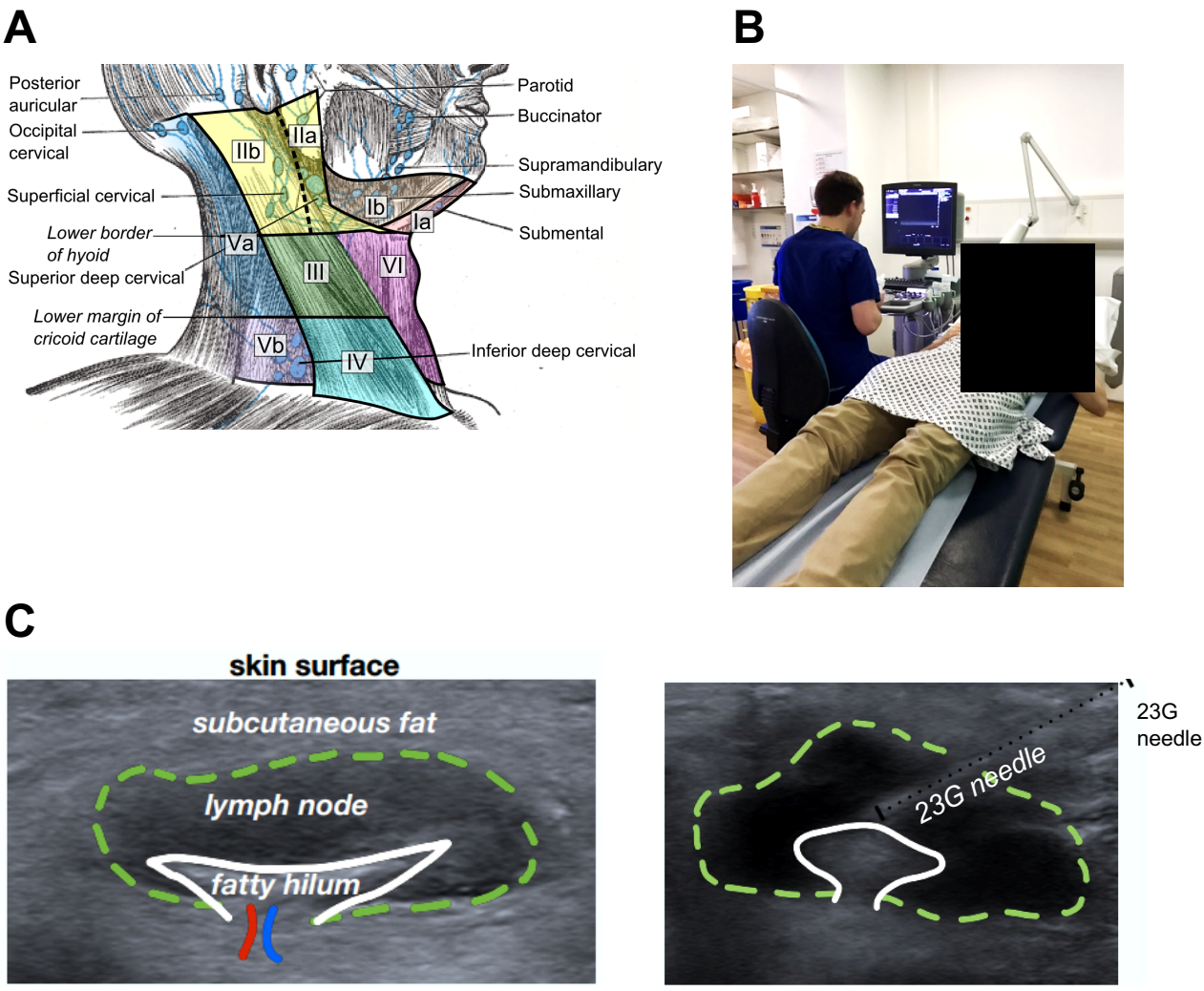


Figure 7.1 – **Ultrasonographic identification of cervical lymph node and fine needle aspiration.**

A – Cervical lymph node levels. Levels I, II, and V were accessed in this study.
(Image reproduced from Wikimedia commons (Häggström M) – open access CC1.0 license)

B – Participant and radiologist pre-procedure set-up in ultrasound room. JR-NC1 pictured with Dr Green.

C – Radiographic demarcation of the lymph node (hypoechoic parenchyma and fatty hyperechoic hilum within the subcutaneous fat) and then access with 23G needle.

7.2.3 Preparation of FNA sample

The FNA material suspended in PBS was combined and if necessary supplemented with further PBS to make a total volume of 5mL (figure 7.2a). A cell count was performed and the remaining material was centrifuged at 200G for 5 minutes (acceleration 7, deceleration 7). The supernatant aspirate wash was removed, stored

in labelled cryovials and frozen at -80°C for future experiments. Initially red cell lysis was used to attempt to remove red cells. However, the white cell yield was extremely poor. Nonetheless, there was a significant degree of red cell debris which made accurate white cell counts challenging and added noise to flow cytometry sampling.

Three steps were added to optimise this. Firstly, the initial count on unprocessed FNA material was conducted with Tuerk's solution. This excludes red cells by lysis but preserves white cells. Overall in the cohort who underwent FNA the median initial white cell count in the FNA samples was 1.36 x 10^6 mononuclear cells (range 0.6 – 22.8 x10^6).

Secondly, CD45 was included in flow cytometry staining panels. CD45, also known as leucocyte common antigen (LCA), allows for the positive identification of white cells such that non-leucocytes can be gated out prior to gating target lymphocyte populations. CD45 gating of single cells within the lymphocyte gate on the scatter plot enriched the subsequent gate for relevant populations (figure 7.2d). However, this was not an ideal solution on its own because the high number of irrelevant events were adding noise to the sample and potentially reducing the fidelity of the multi-colour panels.

Thirdly therefore, a physical method was used to pre-process the sample. The Ficoll density gradient solution approach used in the PBMC protocol was scaled down for use on the FNA material. The initial FNA pellet was resuspended in 200µL PBS-1% BSA and carefully pipetted onto 500µL of Ficoll density gradient solution in a cluster tube. The cluster tube was anchored in the centre of a tip box and then centrifuged

at 400G for 30 minutes (acceleration 3, deceleration 0). This yielded a pellet containing red cells with other debris and a buffy coat-type layer visible above the density gradient (figure 7.2b). The buffy coat was gently aspirated and resuspended in 2mL of PBS-1% BSA. This was centrifuged at 200G for 5 minutes (acceleration 7, deceleration 7) yielding a clearly visible cellular pellet (figure 7.2c). This material was then resuspended in PBS-1% BSA and divided into aliquot for use in cell culture or flow cytometric phenotyping. The material was divided such that there were at least 1×10^5 cells available for cell culture and at least 1×10^5 cells per flow cytometry staining panel. Paired peripheral blood was processed in parallel with the FNA preparation to obtain time-matched PBMCs. The method used was as described in chapter 2.2.5.1.

The density gradient centrifugation procedure enriched for leucocytes (CD45+:CD45- ratio 1:4 vs 4:1; figure 7.6d-e). Indeed, the centrifugation pellet was almost entirely CD45 negative (99.7%, figure 7.2f). This showed that the procedure was very effective at removing debris whilst retaining leucocytes. CD45 pre-gating further reduced the proportion of irrelevant material (Bin-CD19- 23.9% down to 2.85%) but the number of CD19+ events was similar (Bin-CD19+ 3061 without versus 3006 with) (both figure 7.2e – top right).

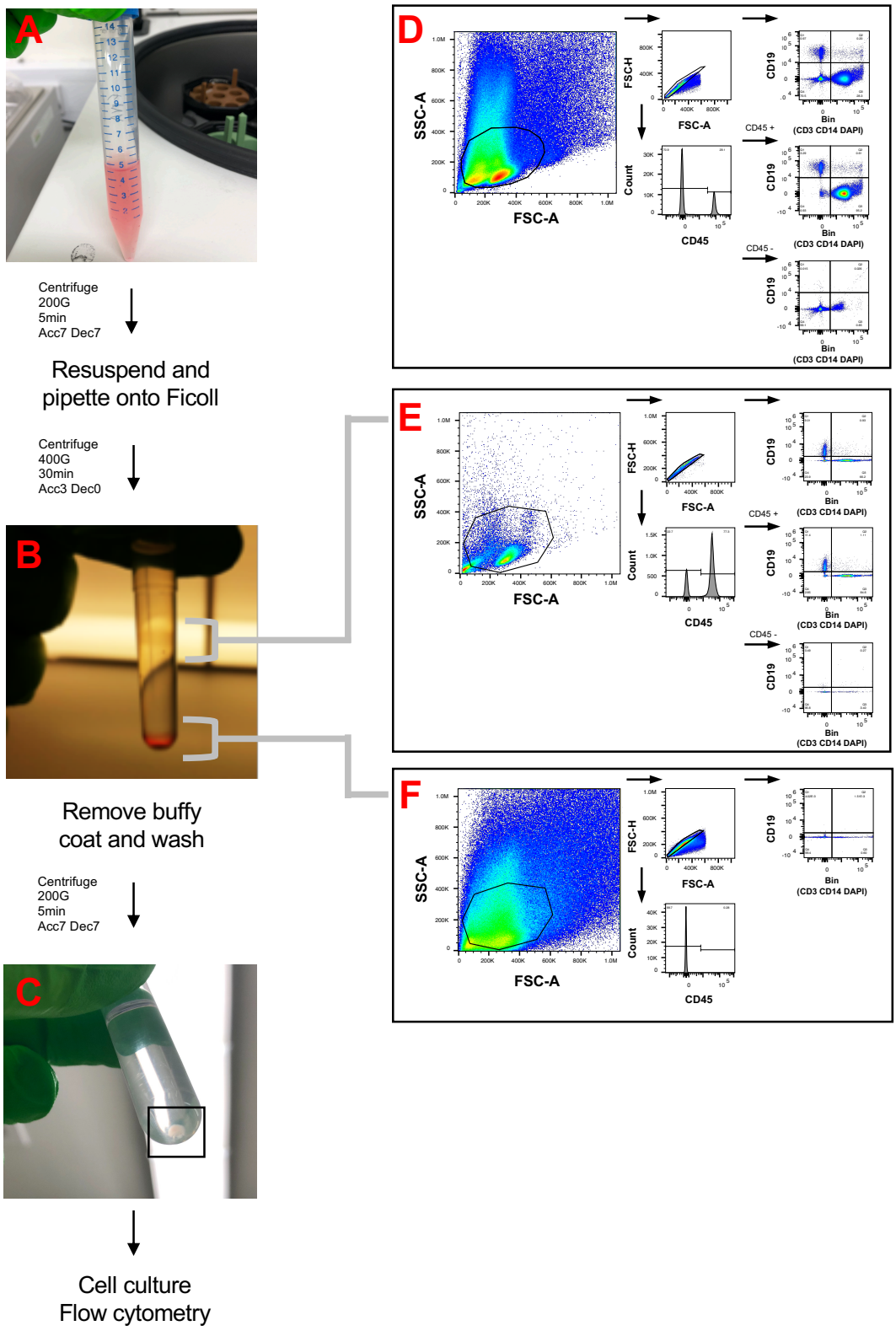


Figure 7.2 – **Fine needle aspiration sample preparation.**

Raw material (A) was centrifuged, resuspended and separated into buffy coat and red cells/debris with density gradient centrifugation (B). The buffy coat was removed and washed (C). D shows flow cytometry without further processing. Lymphocyte identification is possible but improved with CD45. E and F show the same but with Ficoll pre-processing. The buffy coat (E) is highly debris-depleted such that CD45 makes less of a difference. The pellet (F) was almost entirely free of CD45+ cells.

7.3 Flow cytometric characterisation of CLN versus PBMCs

FNA cells were washed with flow cytometry buffer (PBS-0.1% BSA) and divided into three for each of the staining panels in parallel with three PBMC aliquots, unstained PBMCs, and single stain beads for compensation controls, as described in 2.2.4.1. Material was stored at 4°C until analysis on the afternoon of the FNA procedure. There were clear differences between peripheral blood and lymph node cell populations. Events with the scatter properties of lymphocytes were present in both sample types, whereas events in a monocyte/granulocyte gate were effectively absent from the lymph node FNA sample (figure 7.3a). Both T and B cells were present in both samples in the lymphocyte scatter region (figure 7.3b – T cells shown).

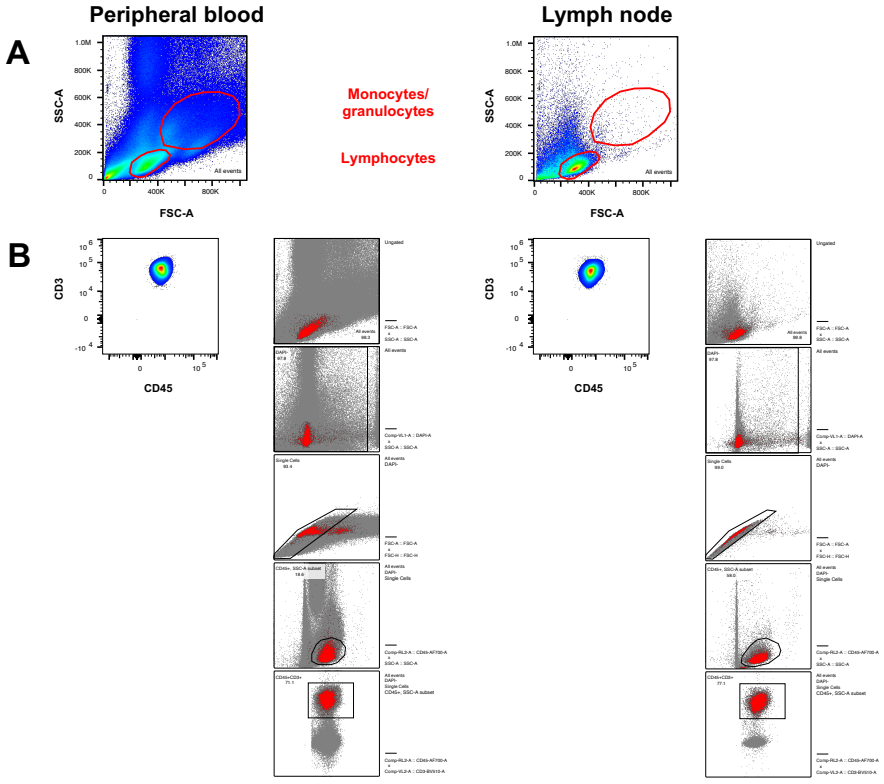


Figure 7.3 – **Comparison of peripheral blood and lymph node flow cytometry.**

A – Forward scatter versus side scatter for each sample. Red boundaries show expected granulocyte/monocyte (top large oval) versus lymphocyte (bottom small oval) populations. B – T cells identified as DAPI-CD45+CD3+ events are shown and back-gated in ancestor gates (red dots).

7.3.1 B cell panel

The following gating strategy was used (figure 7.4):

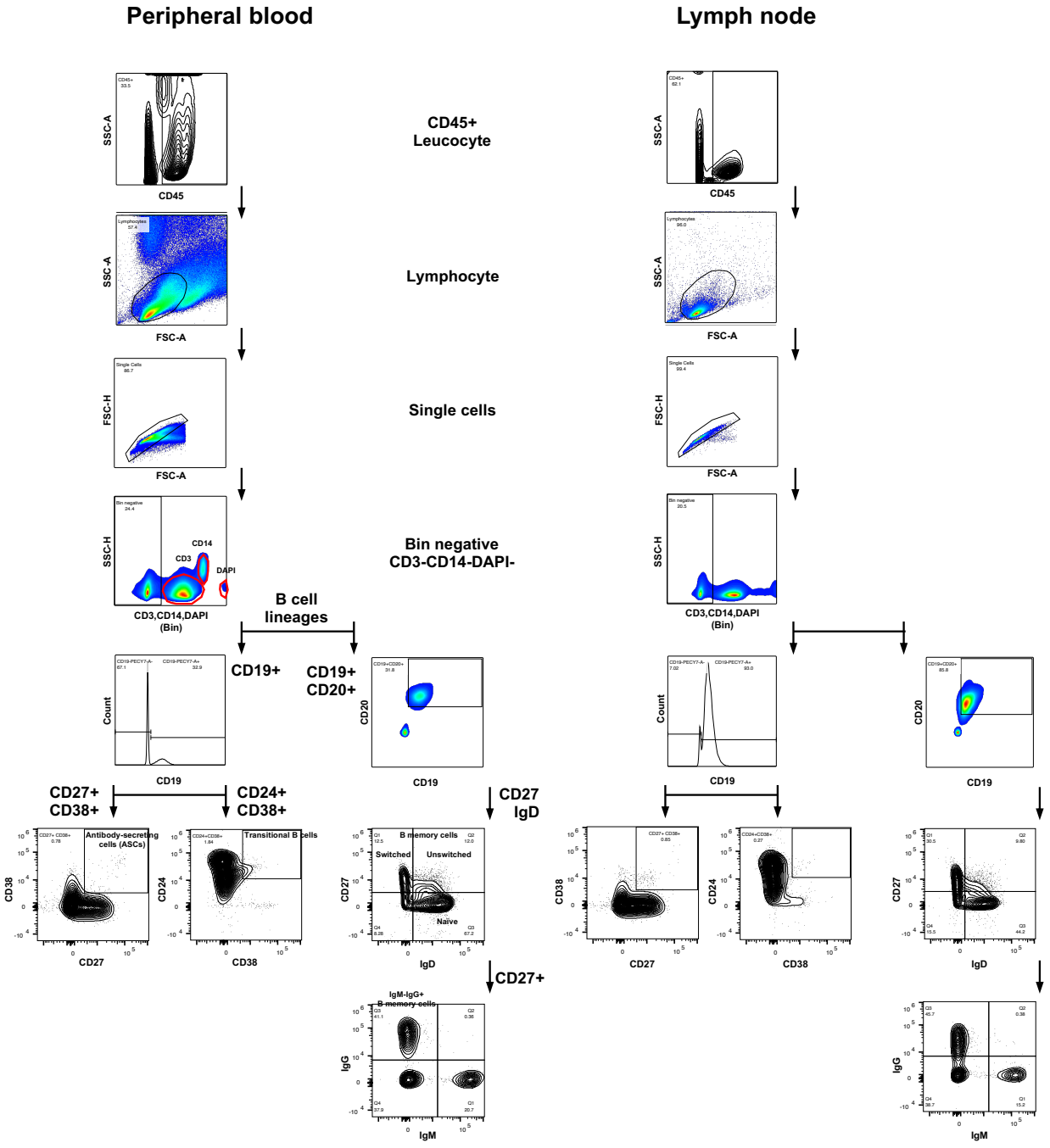


Figure 7.4 – **Gating strategy for B cell lineages in peripheral blood and lymph node material.**

CD45 was used to include leucocytes, lymphocytes where then included based on scatter, doublets were excluded and the negative portion of the bin gate was included (thereby excluding CD3, CD14 and DAPI stained cells). Note absent high SSC-A and CD14+ events in the lymph node material. CD19+ cells were then included. CD20 was also used as the parent gate for B naïve and memory cells.
Abbreviations used: FSC = forward scatter, SSC = side scatter, A = area, H = height.

There were significant differences in frequency between peripheral blood and lymph node for transitional B cells, naïve B cells, IgG+ memory B cells, and antibody-secreting cells (figure 7.5). The most prominent of these was transitional B cells (P=0.002). Overall the pattern gave further evidence that the lymph node samples were a genuinely distinct population from peripheral blood. Furthermore, the pattern was consistently with B cell physiology, for example transitional B cells are relatively new migrants from bone marrow to periphery therefore it would expected for them to be more common in blood than lymph node (206). Association of these frequencies with clinical factors is discussed alongside cell culture results later in this chapter (7.4).

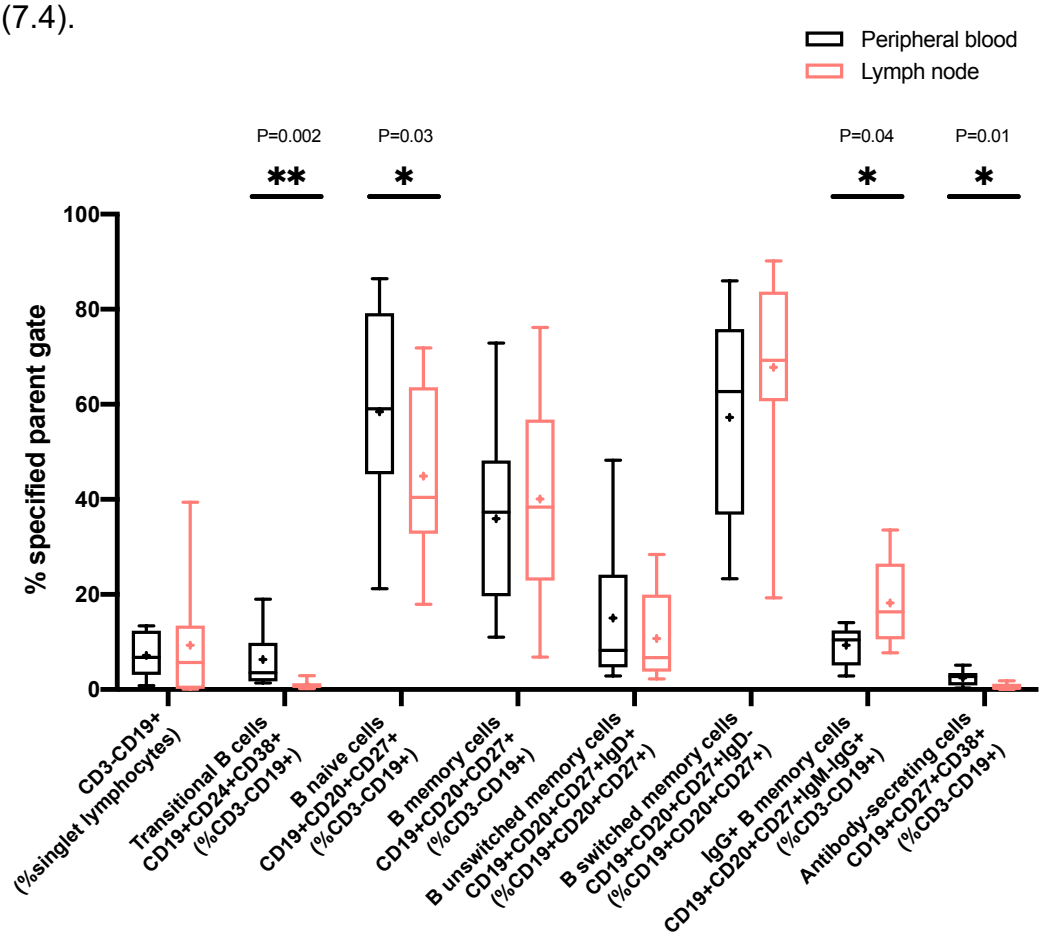


Figure 7.5 – **Frequency of B cell lineage sub-sets in paired peripheral blood and lymph node samples in 10 participants with NMDAR-Ab-E.** Box and whisker plot where horizontal line is the median and + sign is the mean. Parent gate denominators given in parentheses for each population. Paired statistical comparisons made with two-sided Wilcoxon matched-pairs signed rank test (*P<0.05, **P<0.005). Peripheral blood=black, Lymph node=pink.

7.3.2 B cell accessory panel

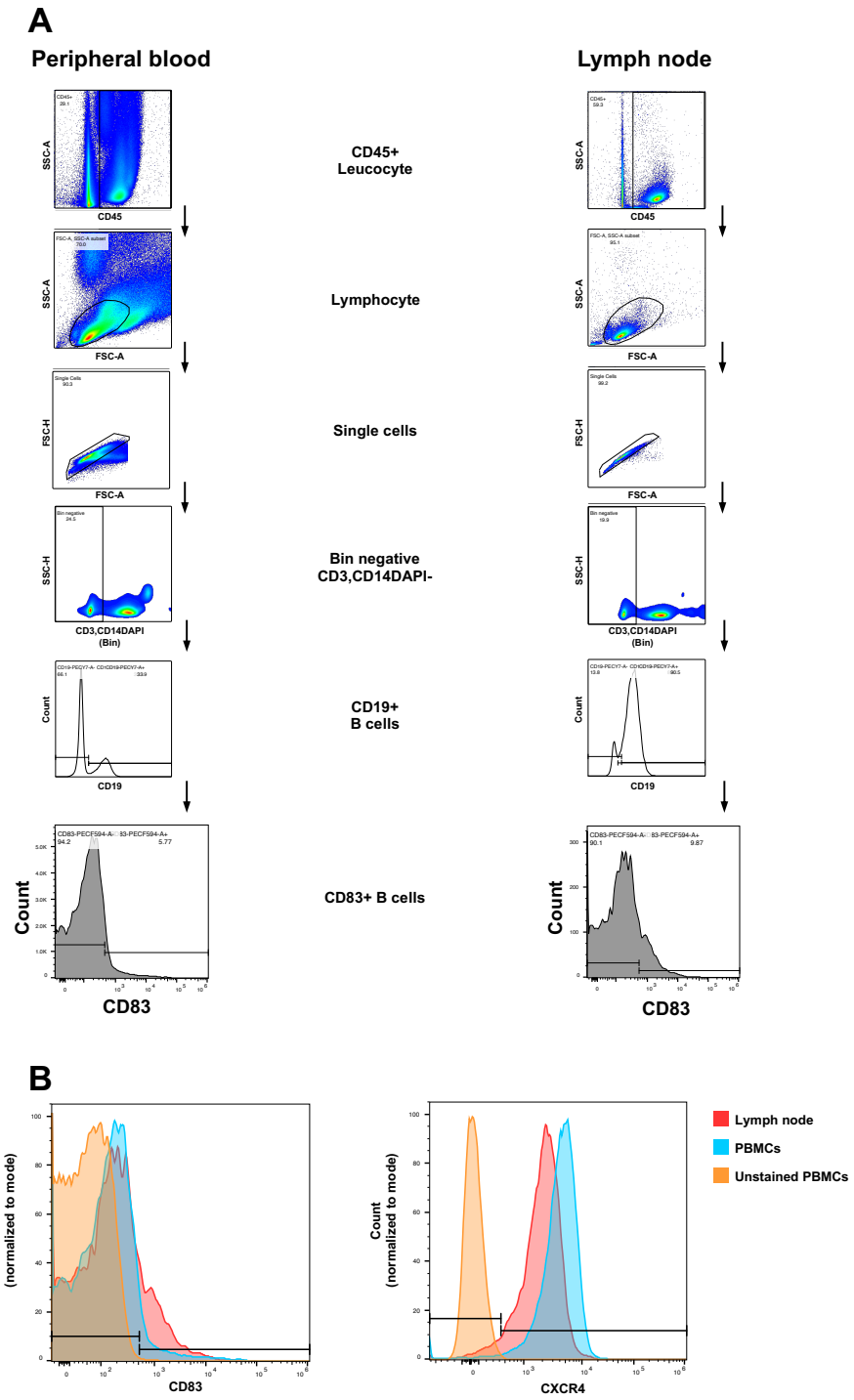


Figure 7.6 – **Gating strategy for B cell accessory panel in peripheral blood and lymph node material**.

A – The same initial sequence was used as for the main B cell panel. CD83 was gated within the CD19+ populations. B – Histograms of CD83 and CXCR4 staining within CD19+ cells on both material types compared to unstained PBMCs (orange). CD83 (left) consistently had more cells in the lymph node material (red) than PBMCs (blue) compared to CXCR4 (right).
Abbreviations used: FSC = forward scatter, SSC = side scatter, A = area, H = height.

There was no appreciable DRD1 staining over background in any of the samples. CD83 and CXCR4 positivity within the CD19+ population was present in both sample types. However, CXCR4 staining appeared to be present in both compartments and more commonly in peripheral blood which did not fit with the need for a lymphoid enriched B cell subtype marker. Conversely, CD83 was higher in the lymph node aspirates compared to PBMCs (figure 7.6a and b). Therefore, CD83 was used without CXCR4 as a germinal centre B cell phenotypic marker. As shown in figure 6.11, CD83+ staining was always more common in the lymph node aspirate than peripheral blood P=0.02, figure 7.7).

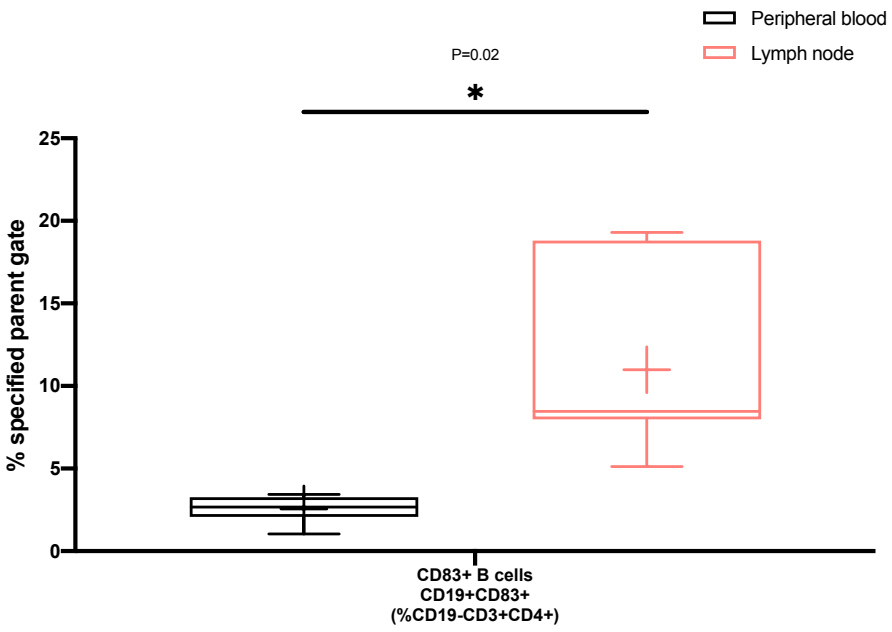


Figure 7.7 – **Frequency of CD83+ B cell sub-set in paired peripheral blood and lymph node aspirate.**

Box and whisker plot where horizontal line is the median and + sign is the mean. Parent gate denominator given in parentheses. Paired statistical comparisons made with two-sided Wilcoxon matched-pairs signed rank test (*P<0.05). Peripheral blood=black, Lymph node=pink.

7.3.3 T cell panel

The following gating strategy was used (figure 7.8):

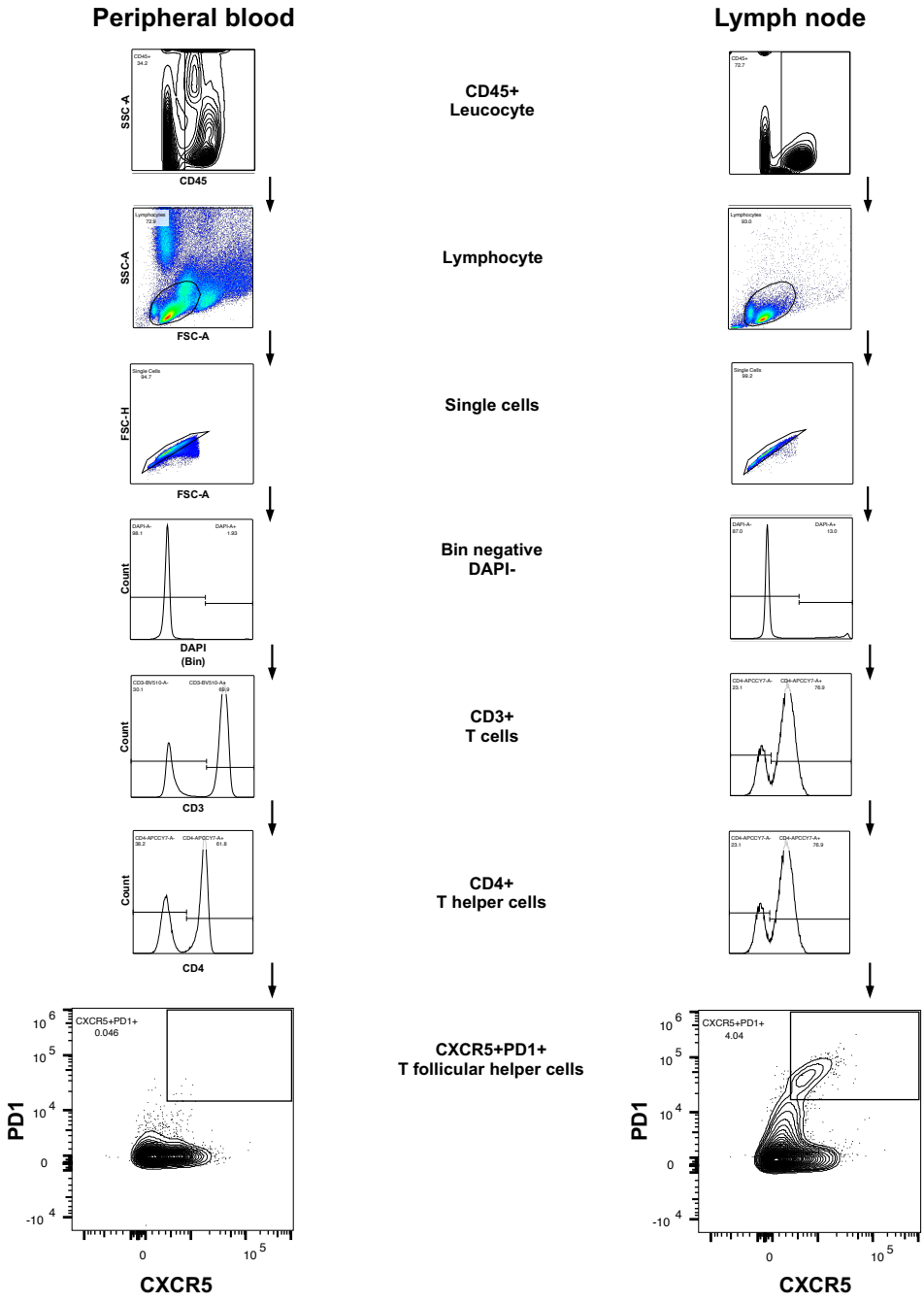


Figure 7.8 – **Gating strategy for T cell lineages in peripheral blood and lymph node material.**

The initial strategy was the same as the B cell panels except CD3 and CD14 were not included in the bin gate. CD3+ and CD4+ were then gated in turn to derive overall T cell then T helper cell subsets. CXCR5 and PD1 double positive populations were then gated from the CD3+CD4+ population. These were labelled T follicular helper (TfH) cells.
Abbreviations used: FSC = forward scatter, SSC = side scatter, A = area, H = height.

There were no statistically significant differences in frequency of T and T helper cells between the two compartments (figure 7.9a). However, the CXCR5+PD1+ T follicular helper sub-set of the T helper cell population was significantly enriched in the lymph node aspirate (P=0.008) (Figure 7.9b). This is similar in pattern, but inverse in direction, to differences in transitional B cell populations between the two compartments and is consistent with the role of TfH cells in orchestrating germinal centre reactions, a function of lymphoid tissue. ICOS and CD40L antibodies did not give signal above background so were not considered further.

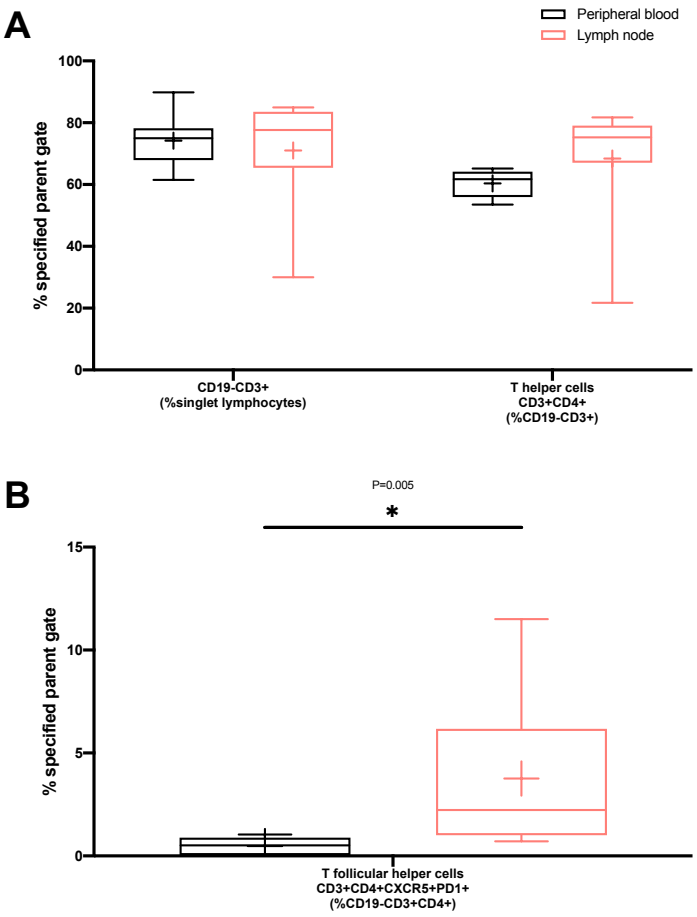


Figure 7.9 – **Frequency of T cell lineage sub-sets in paired peripheral blood and lymph node.**

A – T cell and T helper cell populations and B – T follicular helper cell populations. Box and whisker plot where horizontal line is the median and + sign is the mean. Parent gate denominators given in parentheses for each population. Paired statistical comparisons made with two-sided Wilcoxon matched-pairs signed rank test (*P<0.05, **P<0.005). Peripheral blood=black, Lymph node=pink.

7.3.4 T cell-B cell correlations in peripheral blood and lymph node samples

In germinal centre reactions TfH cells are induced to differentiate by germinal centre B cells which efficiently present processed cognate antigen. These TfH populations provide trophic support to B cells. To investigate this further and provide relationships with which subsequent *in vitro* culture experiments could be integrated, TfH populations in the lymph node aspirates and equivalent populations in peripheral blood were correlated with paired B cell subsets in lymph node aspirate and peripheral blood. This found a statistically significant linear correlation between lymph node TfH frequency and lymph node but not peripheral CD83+ B cells, consistent with the relationship described above (Pearson's R^2=0.82, P=0.0049; figure 7.10a,). Moreover, there was no correlation with peripheral TfH frequency and CD83+ B cell frequency in either sample type.

However, despite ASCs being the product of germinal centre reactions there was no correlation between lymph node TfH frequency and ASC frequency in either sample type nor was there between lymph node CD83+ B cells and ASCs (graph not shown), but there was between peripheral TfH frequency and peripheral ASC frequency (Pearson's R^2=0.66, P=0.014; figure 7.10b). The nature of circulating TfH-like cells is less well defined than canonical lymph node TfH cells. It may be the case that both populations are regulated by a common process, but a causal relationship is harder to infer than the spatially co-located lymph node populations.

There were no statistically significant correlations found in this sample between lymph node or peripheral TfH frequency and B naïve, memory and IgG+ memory cells (figure 7.10c-e).

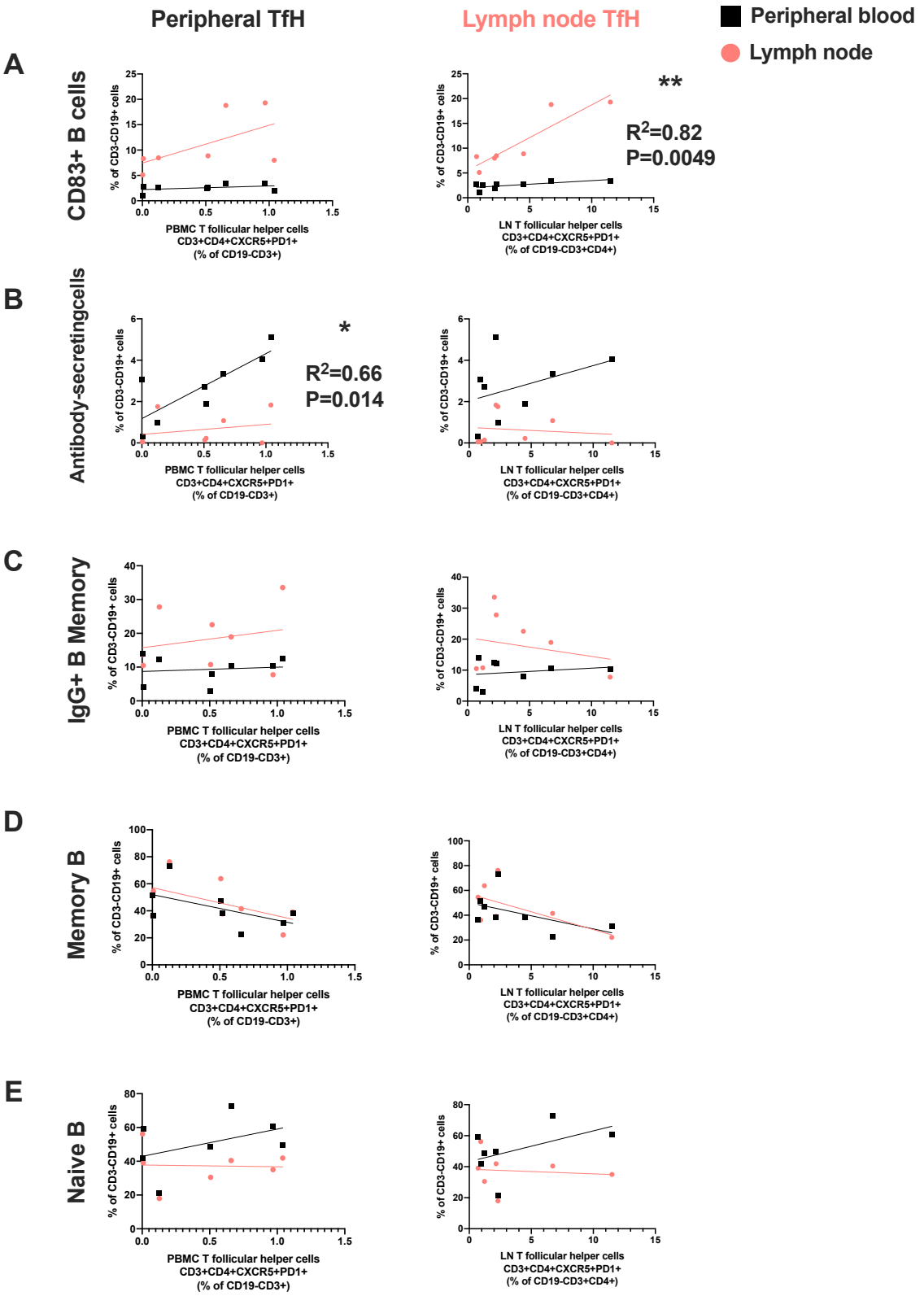


Figure 7.10 – **Correlation of T follicular helper cells (CD3+CD4+CXCR5+PD1+) as a percentage of T helper cells (CD3+CD4+ cells) from lymph node and peripheral blood versus B cell subsets.** A - CD83+ B cells, B - antibody secreting cells, C - IgG+ memory B cells, D - memory B cells, and E - naïve B cells. B-cell subsets are gated as previously and expressed as a percentage of total B cells (CD3-CD19+). Outcomes of statistically significant linear regression analyses are indicated with asterisks (*P<0.05, **P<0.005). Peripheral blood=black, Lymph node=pink.

In order to contextualise the populations with NR1 antigen-specific processes these populations were correlated with serum NR1-IgG levels. This showed a significant correlation between NR1-IgG level and peripheral ASC frequency but not lymph node ASC frequency (figure 7.11a). Furthermore, NR1-IgG level also correlated with both lymph node and peripheral blood TfH-phenotype CD4+ T cell subset frequency with the stronger correlation with lymph node compartment (figure 7.11b). This suggested that the process driving peripheral NR1-IgG production was linked with circulating antibody-secreting cells and TfH differentiation, consistent with a germinal centre-based model.

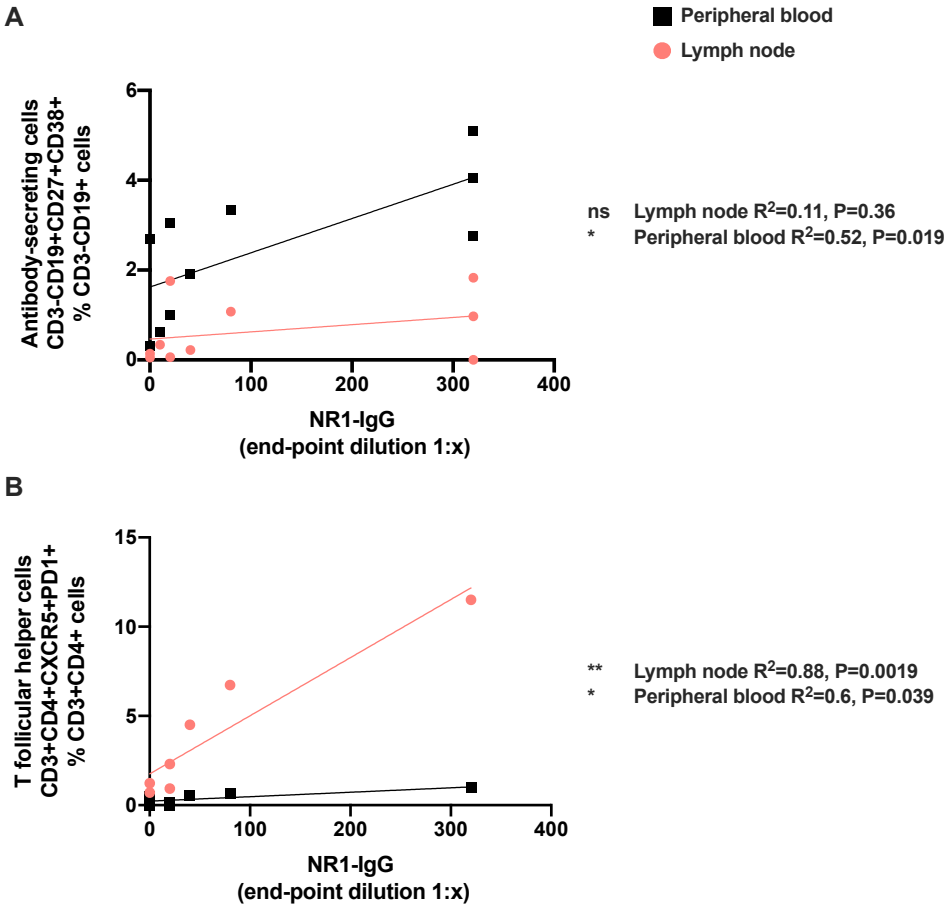


Figure 7.11 – **Correlation between NR1-IgG level and frequency of antibody-secreting cells and T follicular helper cells in peripheral blood and lymph node.** A – correlation with antibody-secreting cells. B – correlations with T follicular helper cells. Outcome of linear regression analysis is given adjacent to each plot (*P<0.05, **P<0.005). Peripheral blood=black, Lymph node=pink.

7.4 Lymphocyte cell culture

To investigate NR1 antigen-specific cells within the two sample types, cell culture and NR1-IgG live CBA of culture supernatants was used. During the evolution of the study unfractionated and bulk B cell sorted lymphocyte cell culture was used. The majority of results of disease relevance are from the unfractionated cultures. These are described below in turn.

7.4.1 Unsorted cell culture

Initial sample preparation proceeded as described in 6.4.4. After removal of sufficient material for flow phenotyping the remainder of the sample was used for cell culture. Following a further centrifugation step and removal of PBS-1% BSA supernatant, each pellet was resuspended in B cell media to a concentration of $1x10^6$ cells/mL. Cell suspensions were then kept on ice whilst the culture plate was prepared.

As described in 2.2.5.2, a flat bottom 96 well culture plate was prepared in a sterile hood. Firstly, the perimeter wells were each filled with 200µL of sterile D-PBS with penicillin-streptomycin. This was because these wells were most vulnerable to evaporation and infection. The remainder of the wells were available for use for cell culture. Next, stock cytokines that had been thawed immediately prior to sample preparation were retrieved from 4°C temporary storage. A B cell media-activation cytokine mixture was prepared for 100µL/well according to the concentrations described in chapter 2. This was added to each well to be used for cell culture followed by 100µL/well of cells. The cells were added and mixed gently by multi-channel pipette. 30 wells of PBMCs were prepared and as many wells as possible of lymph node aspirate cells were prepared in the row immediately beneath (figure

7.12). This varied according to the yield of the sample following removal of adequate sample for flow cytometry. The remaining unused wells were filled with 200µL/well of D-PBS-Penicillin Streptomycin. The plate was labelled with the experiment code, date, and sample location was indicated on the lid overlying the wells. The plate was immediately incubated for 13 days at 37°C with 5% CO_2 and 90% humidity. The remaining PBMCs were cryopreserved.

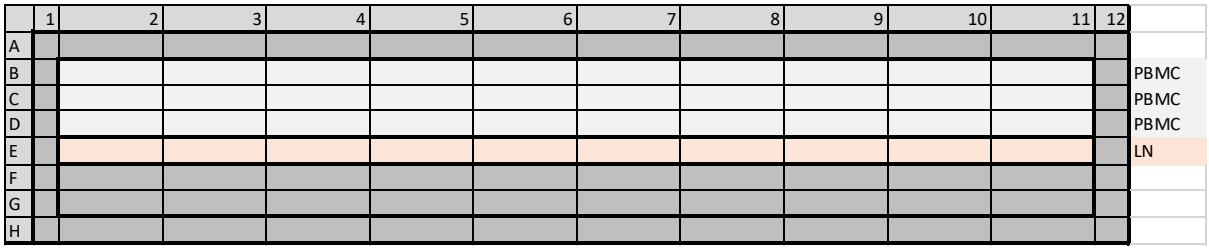


Figure 7.12 – **Cell culture plate set-up used in unfractionated culture experiments.**

The light grey region indicates well used for PBMCs and the pink region indicates wells used for lymph node aspirate cells. Every well not used for cell culture contained D-PBS with penicillin streptomycin antibiotic (dark grey).

In a pilot experiment from two non-NMDAR-Ab-E participants the IL-6 only maintenance condition was used as per the teratoma culture experiments. While previous experiments found that this condition did not lead to useful levels of Ig production (146) (36), given that lymph node aspirate material was from a different site potentially with plasma cells that would respond to it, this was piloted. This showed clear benefits of activation conditions in both compartments ($P<0.001$ for both compartments; figure 7.13). Given the limited number of lymph node aspirate cells compared to PBMCs, activation conditions were used for subsequent experiments. Later, it became clearer that ASCs were a rare population, vindicating this decision.

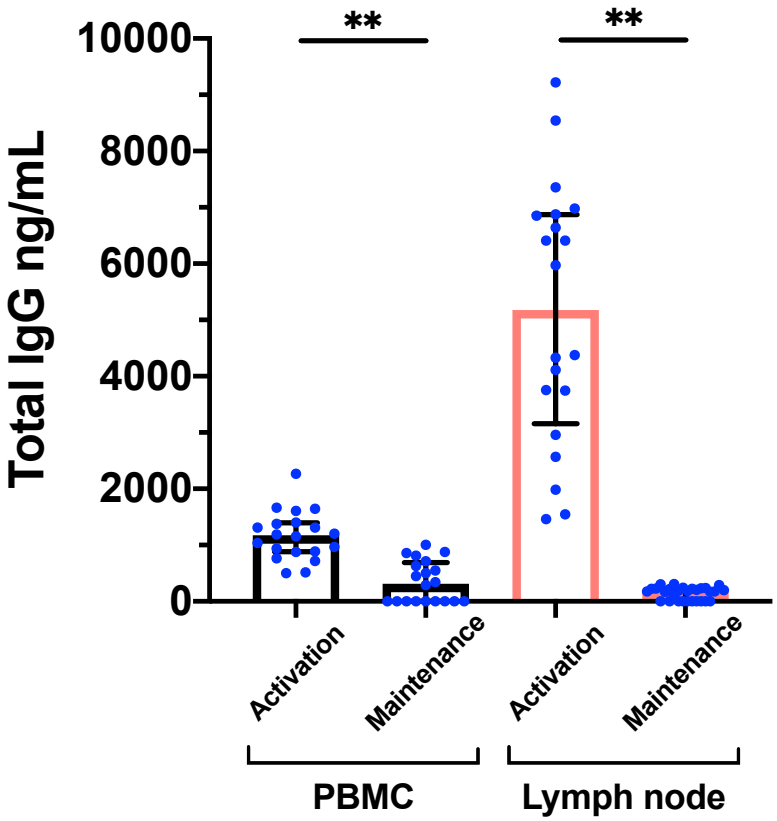


Figure 7.13 – **IgG production from peripheral blood and lymph node cultured under activation and maintenance conditions.**

Total IgG was measured using an IgG ELISA. Activation conditions were: soluble CD40 ligand, IL-2, IL-21, IL-6, IL-1β, TNFα and R848. Maintenance conditions included IL-6 without the other cytokines. Each blue circle represents a well. Bars indicate median and error bars are interquartile range. Between group comparison with two-tailed Mann-Whitney test (**P<0.005). Peripheral blood=black, Lymph node=pink.

Proceeding with patients with NMDAR-Ab-E, paired lymph node aspirate and PBMC samples from seven visits from six patients were cultured using the unfractionated method (table 7.3).

Participant	Age at visit	Visit	OT?	Acuity	Lymph node	Days from onset -episode -all	Serum NR1-IgG end-point dilution	Immunotherapy (IT)				
								Cumulative	Current	Time to surgery	Time to 1st line IT	Time to 2nd line IT
JR770	35	1/2	No	Acute	Ib	131 1743	1:320	IVMP/Pred, PLEX, IVIG, MMF, CyP	Pred, CyP	N/A	240	2419
JR770	36	2/2	No	Non-acute	Ia	777 2389	1:80	IVMP/Pred, PLEX, IVIG, MMF, CyP	None	N/A	240	2419
JR1082	37	1/1	No	Non-acute	Ib	5198 6658	1:20	IVMP/Pred, IVIG, Aza, MMF	Pred	N/A	3285*	None
JR819	19	1/1	Yes**	Acute	Va	102 102	1:320	IVMP/Pred, PLEX	Pred	41	16	None
JR817	32	1/1	Yes***	Non-acute	Ia	249 249	Marginally detectable	IVMP/Pred, PLEX, IVIG	None	15	7	None
JR747	21	1/1	Yes***	Non-acute	Ia	1037 1037	1:20	IVMP/Pred, PLEX	None	90	74	None
JR717	32	1/1	Yes***	Non-acute	Ia	1180 1180	0	IVMP/Pred, PLEX	None	88	27	None

Table 7.3 – **Participant demographic and clinical factors at fine needle aspiration visits in the unfractionated culture method series.** Acute defined as <3 months from episode onset.

Abbreviations: Aza = azathioprine, CyP = cyclophosphamide, IVMP = intravenous methylprednisolone, MMF = mycophenolate mofetil, OT = ovarian teratoma-associated, Pred = oral prednisolone, PLEX = plasma exchange.

*Onset of first episode of illness in prior to identification of NMDAR-antibodies as cause. First treatment was during subsequent relapse after the disease had been characterised.
**OT resected by cystectomy but recurrence 3 months after visit such that it was unclear whether the lesion was entirely removed after the first operation.
***OT resected prior to visit.

7.4.1.1 Total IgG

IgG ELISA was performed on culture supernatants. This found a clear difference between lymph node cells and PBMCs in favour of lymph node cells producing more total IgG (difference between medians=11648 ng/mL, P<0.001; figure 7.14a). This may be due to the composition of the cells. As demonstrated by flow cytometry, the lymph node sample white cells were predominantly lymphocytic (~98% of DAPI- single cell CD45+ gate) but less so in the PBMC samples (~80% of DAPI- single cell CD45+ gate). B cell proportions were ~6% in both sample types so if 100,000 white cells were cultured then there could be expected to be 58,000 in the lymph node material versus 48,000 in the PBMCs. This difference in 10,000 cells would probably not explain the difference in total IgG production. There also could have been a contribution from the activation status of the lymphocytes. Whereas the circulating lymphocytes may have been relatively quiescent, it may have been that the lymph node aspirate B cells could have been participating in a germinal centre reaction (as suggested by CD83 positivity) so already primed to produce antibody and/or they may have been helped by TfH cells.

To determine whether there were any clinical correlates associated with this difference, the samples were first sub-divided on OT association. Here, the difference between sample types was consistent and there were no significant differences between OT and non-OT PBMC and lymph node cultures, respectively (figure 7.14b). Next, within the acuity sub-groups, lymph node aspirate remained greater than PBMC, but there was a difference between the acute and non-acute PBMC groups (difference between medians=2020 ng/mL, P<0.001; figure 7.14c). However, this difference was markedly smaller than the persistent differences

between lymph node and PBMC groups. The PBMC difference could either be a genuine disease phase effect, in which case it could be due to disease biology or the effects of immunosuppressive medication given in the acute phase, or it could be artefactual reflecting the variance in the PBMC culture results per se and smaller sample size in the acute group.

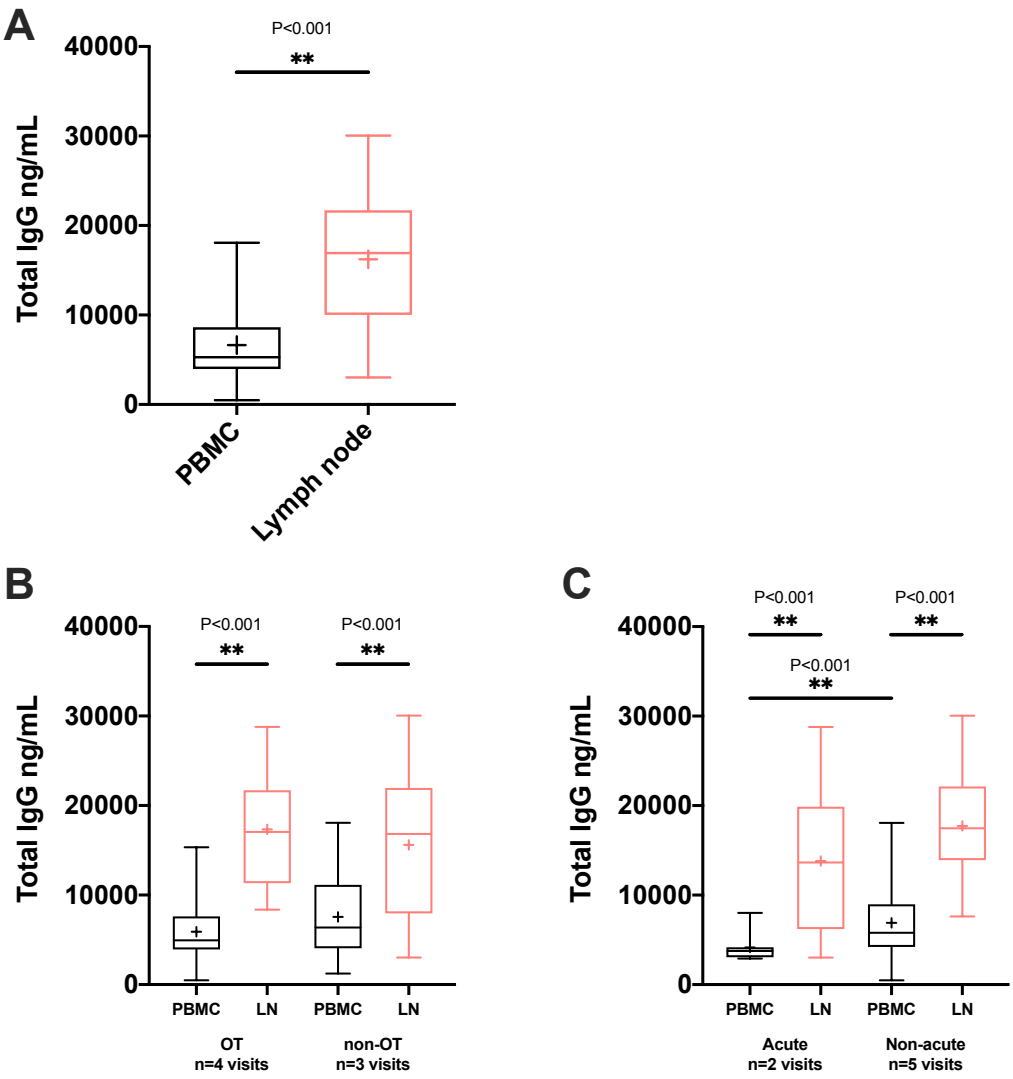


Figure 7.14 – **Total IgG in culture supernatants from unfractionated paired PBMC and lymph node aspirate cell cultures.**

Total IgG was measured using IgG ELISA and presented as differences between the two sample types in all visits (A) and divided on OT-associated illness status (B) and acuity of sampling where acute is <3 months from episode onset (C). Data is presented with box and whisker plots where whiskers show the range, box shows the inter-quartile range, horizontal line is median line, and + is the mean. Between group significance testing was performed with two-tailed Mann-Whitney tests.
*P<0.05, **P<0.005.

7.4.1.2 NR1-specific IgG

The culture supernatants were tested for NR1-specific IgG using a live CBA. 75µL supernatant fluid was diluted 1:3 in sample buffer. The CBA was run as described previously with a two-layer approach to boost sensitivity: unlabelled goat anti-human secondary Fc-γ antibody (1:750) was incubated for one hour followed by a wash step and one hour incubation with an AF-594 labelled rabbit anti-goat tertiary antibody (1:750). Positive results were repeated and confirmed by a second observer experienced in reading CBAs (Dr Patrick Waters).

Consistent with findings previously reported by Makuch *et al.* (146), NR1-IgG positive supernatants from some NMDAR-Ab-E patient-derived PBMCs were also found (figure 7.15a). The novel finding here was that there were also positive results from lymph node-aspirate derived culture supernatants. Therefore, similar to the teratoma experiments this demonstrated that there were NR1-specific B cells present in the cervical lymph nodes of some patients.

Participant, visit	**Culture supernatant NR1-IgG positivity Total number of wells positive / total number of wells (%)**	
	Peripheral blood	**Lymph node**
JR770, 1/2	**1/9 (11%)**	**2/10 (20%)**
JR770, 2/2	**5/30 (17%)**	**4/20 (20%)**
JR819, 1/1	0/6 (0%)	**1/6 (17%)**
JR817, 1/1	**2/20 (5%)**	0/10 (0%)
JR747, 1/1	0/30 (0%)	0/4 (0%)
JR717, 1/1	**1/30 (3%)**	0/3 (0%)
JR1082, 1/1	**2/30 (7%)**	0/10 (0%)

Table 7.4 – **Frequency of NR1-IgG positivity from paired PBMC-lymph node aspirate cell cultures.** Positive results are **highlighted and in bold**.

5/7 PBMC samples were positive from time points ranging up to 6658 days after onset of the illness (JR1082) consistent with the formation of NR1-specific B memory cell populations (table 7.4). 3/7 lymph node cell culture supernatants were positive for NR1-IgG. In terms of total IgG production, the wells positive for NR1-specific IgG were representative of the group as a whole (figure 7.15b). There were no statistically significant differences between NR1-specific positive and negative sub-groups for either sample type.

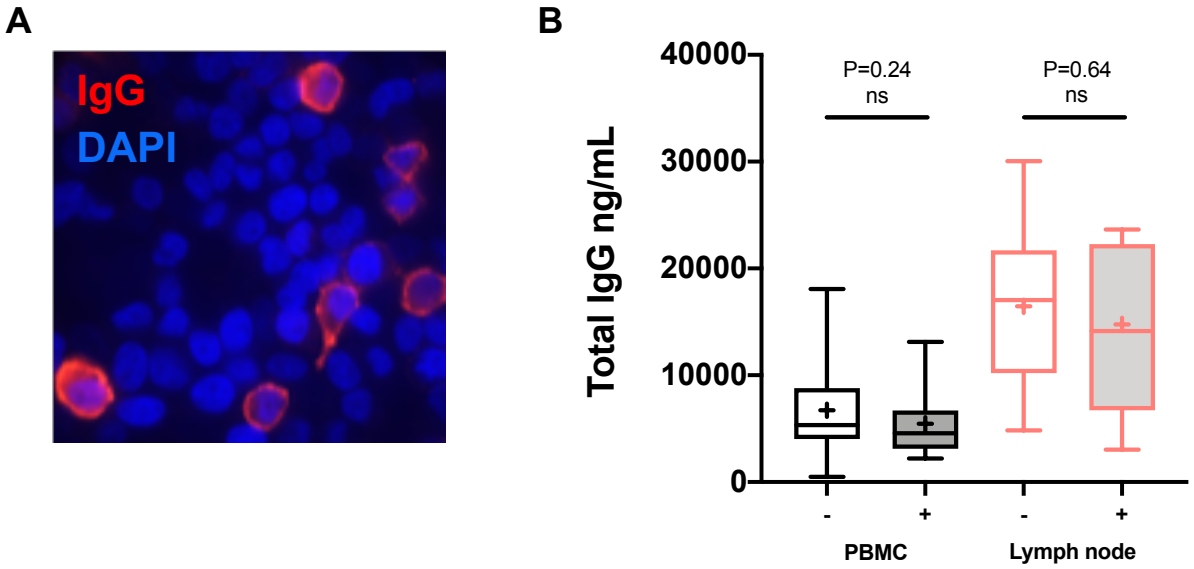


Figure 7.15 – **Relationship between NR1-IgG and total IgG production *in vitro* from peripheral blood and lymph node cell culture.**

A – Example of staining pattern on NR1 live CBA from lymph node cell culture supernatant tested at 1:3 dilution. Red surface binding indicates where NR1 antibody bound transfected cells. (100x zoom, oil immersion lens).

B – The distribution and average levels of total IgG in the two sample types are plotted. They are sub-divided on NR1-IgG positivity status. Box and whisker plot showing range, interquartile range where horizontal line is the median and '+' is the mean. PBMCs have a black border and lymph node a pink border. Grey shading is the NR1-IgG positive group.

The NR1-IgG positive lymph node cultures were from JR770 and JR819, of which JR770 provided two visits, one acutely and one non-acutely (figure 7.16). In each case the frequency of positivity was greater in the lymph node culture supernatants than from paired PBMCs, with PBMCs being negative in JR819. Alongside negative lymph node culture supernatants in the other PBMC positive samples, this went against the possibility that lymph node positivity was principally due to circulating NR1-specific cells entering the lymph node.

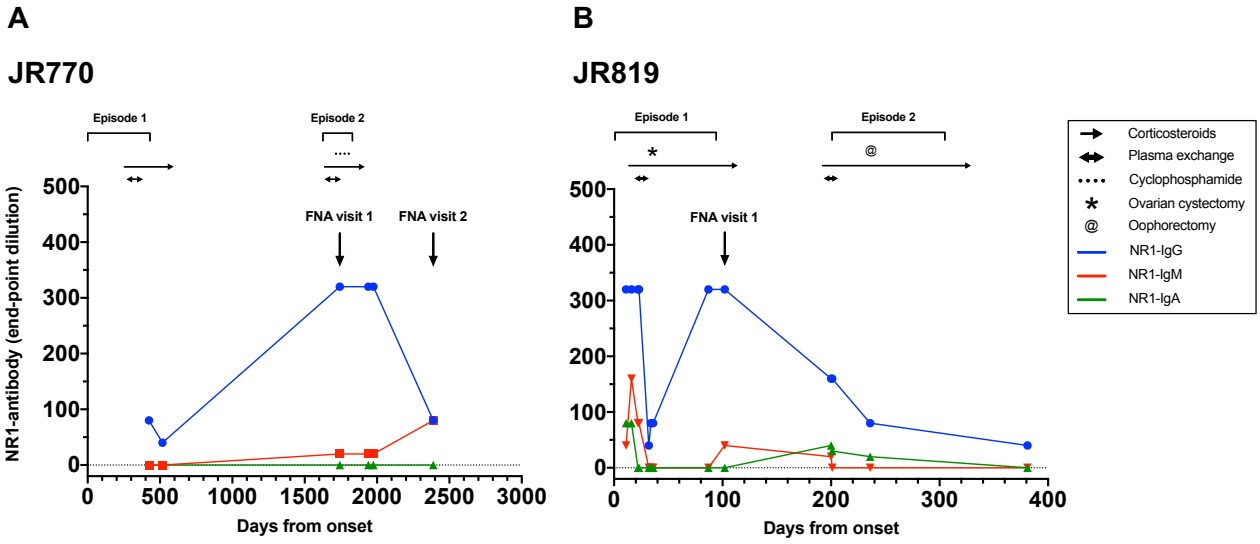


Figure 7.16 – **Time course of serum NR1 antibody levels relative to clinical phases, treatments and aspiration visits in lymph node cell culture NR1-IgG positive patients.**

JR770 is shown in A and JR819 in B. Legend for symbols and colour code is given in the box.

7.4.1.3 Correlation of NR1-IgG production and markers of germinal centre activity

Next, to elaborate whether there was evidence to support an association between local germinal centre activity, the culture positive and culture negative groups were correlated with relevant flow cytometry markers (TfH and CD83+ B cells), and CXCL13 level.

7.4.1.3.1 TfH and CD83+ B cell markers

Alongside the NMDAR-Ab-E NR1-IgG culture positive and culture negative sub-groups, three neurological control participants (JR-NC2-4) were included for comparison. Correlation with TfH and CD83+ B cell populations from flow cytometry data showed that there was a trend towards larger populations of both in the culture positive lymph node samples more than culture negative but none of these were statistically significant (figure 7.17a). This was likely due to JR819, which compared to JR770 did not stand out from the culture negative values. Similarly, when repeating the LN TfH-CD83+ B cell correlations as performed in 6.4.5.3, it emerged that the points from JR770 were at the higher end of the correlation while JR819 was at the lower end within the culture negative data points (figure 7.17b).

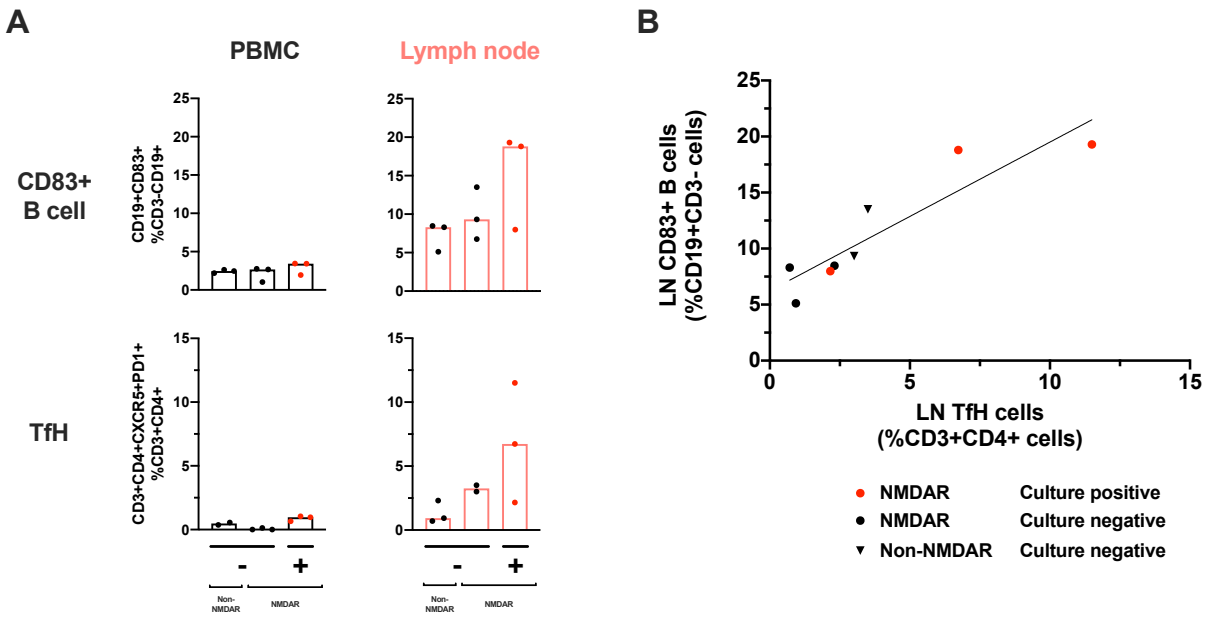


Figure 7.17 – **Relationship between germinal centre-related flow cytometry parameters and lymph node cell culture NR1-IgG positivity.** In addition to 6 NMDAR-Ab-E patients with bulk culture and paired PBMC-lymph node flow cytometry, three non-NMDAR-Ab-E neurological control participants were included for comparison. Flow cytometry data was unavailable for JR817.

A – Frequency of CD83+ B cells as a percentage of CD3-CD19+ cells (top row). T follicular helper cells as a percentage of CD3+CD4+ cells (bottom row). PBMC are shown in the left column (black bars) and lymph node samples in the right column (pink bars). Participants are sub-divided on NR1-IgG culture positivity (indicated by – or +). Bar heights indicate median.

B – Correlation of frequency of lymph node T follicular helper cells with lymph node CD83+ B cells with indication of NR1-IgG culture positivity status (positive=red, negative=black; NMDAR-Ab-E=circles, Non-NMDAR-Ab-E=triangles).

7.4.1.3.2 CXCL13

CXCL13 is a chemokine secreted by follicular dendritic and other stromal cells in lymphoid follicles. It acts via the receptor CXCR5 and also has been previously suggested as a circulating biomarker of germinal centre activity (207). It has received attention in NMDAR-Ab-E as a biomarker of disease activity in CSF but not serum (208).

Here a commercial ELISA system (R&D systems, DCX130) as used by Havenar-Daughton *et al.* was used to test the paired serum-lymph node aspirate acellular fluid samples. Additionally, a group of healthy volunteer serum samples and serum and CSF samples from the definite NMDAR-Ab-E cohort were also tested to contrast with other compartments. The kit was used as described in 2.2.6.2. To account for dilution of the acellular aspirate fluid, the concentration reported by the CXCL13 ELISA for this material was multiplied by a dilution factor. The dilution factor was derived by dividing the volume of acellular fluid by the original volume of aspirate material, i.e. the extent to which it had been diluted. The original volume of aspirate material per needle pass was estimated to as 20μL, so each diluted volume was divided by 40.

There were no statistically significant group differences in CXCL13 level between healthy control serum and encephalitis serum (figure 7.18a). Moreover, contrary to the findings of Leypoldt *et al.*, CSF CXCL13 was not higher than serum and instead was significantly lower than both cohorts in this sample (two-tailed Mann-Whitney test; $P<0.001$). However, range of levels in CSF was wide with many undetectable but some higher. To explore this further the encephalitis serum and CSF CXCL13 levels were correlated with paired NR1-IgG level which showed no correlation in serum but a significant positive correlation in CSF (Pearson's $R^2=0.02$, $P=0.21$ vs $R^2=0.52$, $P=0.008$; figure 7.18b and c). This was informative because in CSF, antibody level is a better correlate of disease activity than in serum, suggesting that the correlation with CXCL13 was more likely to have biological meaning. Given that serum NR1-IgG is not a good disease activity marker, time was correlated with serum CXCL13 as a surrogate marker of disease activity. However, there was not a

correlation with this parameter either (Pearson's R^2=0.002, P=0.65). This either suggested that germinal centre reactions were not occurring in these patients or that CXCL13 was not as useful a marker as had been thought. Given the weight of evidence for germinal centre reactions and the better performance in CSF, the latter was more likely.

The lymph node data had both the highest median but also the greatest variance, with a bimodal distribution ranging from undetectable to high levels, akin to CSF. This was consistent with sub-groups and suggested that the marker performed best in discrete anatomical compartments. To evaluate the extent to which the lymph node CXCL13 groups mapped onto cell culture outcomes, paired serum-lymph node values were plotted based on NR1-IgG production from lymph node cells in culture. CXCL13 was undetectable in all but one of the culture negative lymph node fluid (JR817), whereas the culture positive values were all positive. The two highest points were from the two JR770 visits, whereas the JR819 visit was less than the JR817 culture negative value. Therefore, the JR770 CXCL13 values were consistent with the high TfH and CD83+ B cell frequency providing evidence of local germinal centre activity whereas there was less to support this for JR819.

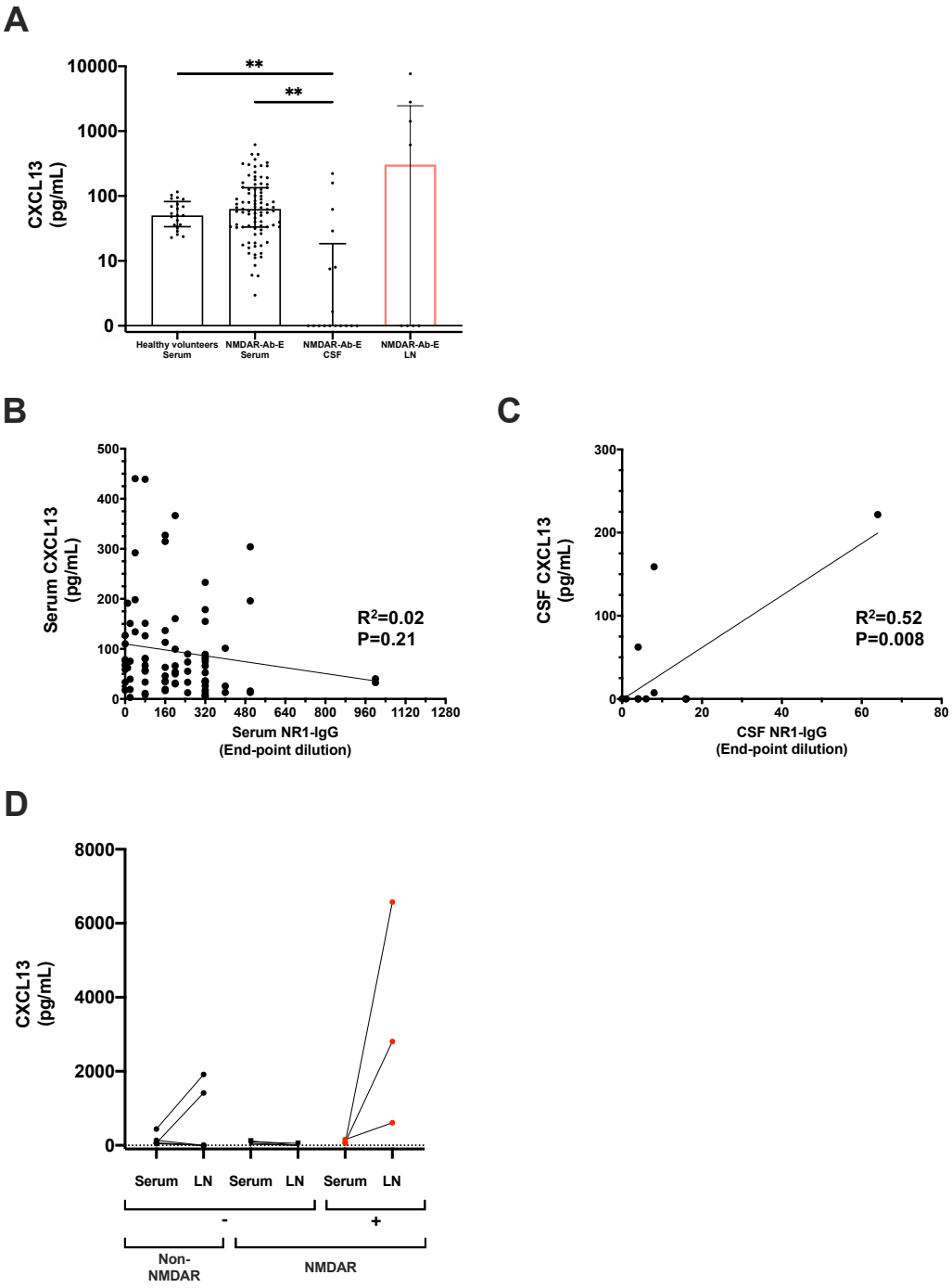


Figure 7.18 – **Comparison of CXCL13 levels in different compartments.**

A – Levels in serum of healthy volunteer and NMDAR-Ab-E patients, and CSF and lymph node fluid (pink) from NMDAR-Ab-E patients. Median indicated by bars, interquartile range by error bars. Comparisons with two-tailed Mann-Whitney test (**P<0.005).

B – Correlation between CSF NR1-IgG and CSF CXCL13 levels.

C - Correlation between serum NR1-IgG and serum CXCL13 levels. D – CXCL13 levels in serum and paired (black lines) lymph node aspirate samples subdivided on NR1-IgG culture positivity. For comparison four neurological control participants (JR-NC1-4) are included.

7.4.2 Bulk sorted B cell culture

The unfractionated cell culture system had previously been shown to cause differentiation into antibody-secreting cells (146). Also, work on neuromyeltis optica had shown that using the same system with bulk-sorted memory B cells, and in some cases naïve B cells, could generate antigen-specific antibody *in vitro* (36). If germinal centre reactions were underlying the cells that produced NR1-specific antibodies in the unfractionated system then B memory cells would be the relevant population to study. However, the results of Wilson *et al.*, monoclonal antibody data which had suggested pathogenic NR1-IgG were sometimes unmutated and to provide a comparator B cells population, B naïve cells were also relevant.

Therefore, the protocol was modified to enable cells from the paired PBMC-lymph node samples to be sorted into B memory and B naïve populations. CD4+ T cells were also sorted into CXCR5 positive and negative populations for cryopreservation for future experiments beyond the scope of this thesis.

The protocol differed from the unfractionated cultures in that instead of directly culturing cells, the portion dedicated to cell culture was labelled with the sort panel antibody staining mix as described in 7.2.1. To ensure accurate population discrimination on the flow cytometer, unstained and PBMCs stained with FMO panels were also prepared. Sort gates were used as described for phenotyping. Cell sorts were run with Mr. Craig Waugh, flow cytometry technician at the WIMM flow cytometry facility. Cells were sorted over 4 hours into 1mL of B cell media in labelled 5mL Falcon polystyrene tubes. FNA samples were prioritised over PBMC such that

the FNA sample was always sorted to sample exhaustion and PBMCs were sorted until the end of the allotted time on the cell sorter.

Following the sort, the total cell count per tube was noted and the tubes were returned to tissue culture. They were centrifuged at 200G for 5 minutes and resuspended in B cell media to make a concentration of 1 x 10^4 cells per 100µL for B memory cells and 2 x 10^4 cells per 100µL for B naïve cells. 100µL of B cell media-activation cytokine cocktail was added to each well used with 100µL of cell mix. As previously, PBS-penicillin streptomycin was added to perimeter wells, and unused wells.

NMDAR-Ab-E patients JR770 and JR717 kindly participated in an additional study visit. Both were clinically well with serum NR1-IgG level of 1:320 and undetectable, respectively. Additionally, two patients with other antibody-mediated CNS disorders also participated: JR061 was a 72 year old man with a stable epileptic disorder associated with Caspr2-autoantibodies and JR870 was a 71 year old woman with LGI1-antibody encephalitis. JR870 had had a single episode of the illness 6 months prior to the study visit that had appeared to have spontaneously remitted without medication. At the study visit she reported a return of similar seizure symptoms and soon after was treated for a relapse with prednisolone. Therefore, the study visit was inadvertently acute and an opportunity to study an unmedicated relapse of autoimmune encephalitis.

The culture system was able to produce antibody detectable by IgG and IgM ELISA of culture supernatants (figure 7.19). The distribution of IgG and IgM was consistent with the sorted cell types. B memory cells, which were not sorted based on surface Ig status, produced both isotypes, whereas B naïve cells almost exclusively produced IgM. This suggested that the B naïve cells were not class-switching *in vitro,* also reported in a similar system and cytokine cocktail (209). For B memory cells the lymph node wells tended to produce more IgG and IgM, but the variance in the lymph node wells was greater. For IgM the difference was significant (P=0.02), but outlying wells from FNA_011 B memory produced IgG to such an extent that the difference with lymph node B memory IgG was not significant.

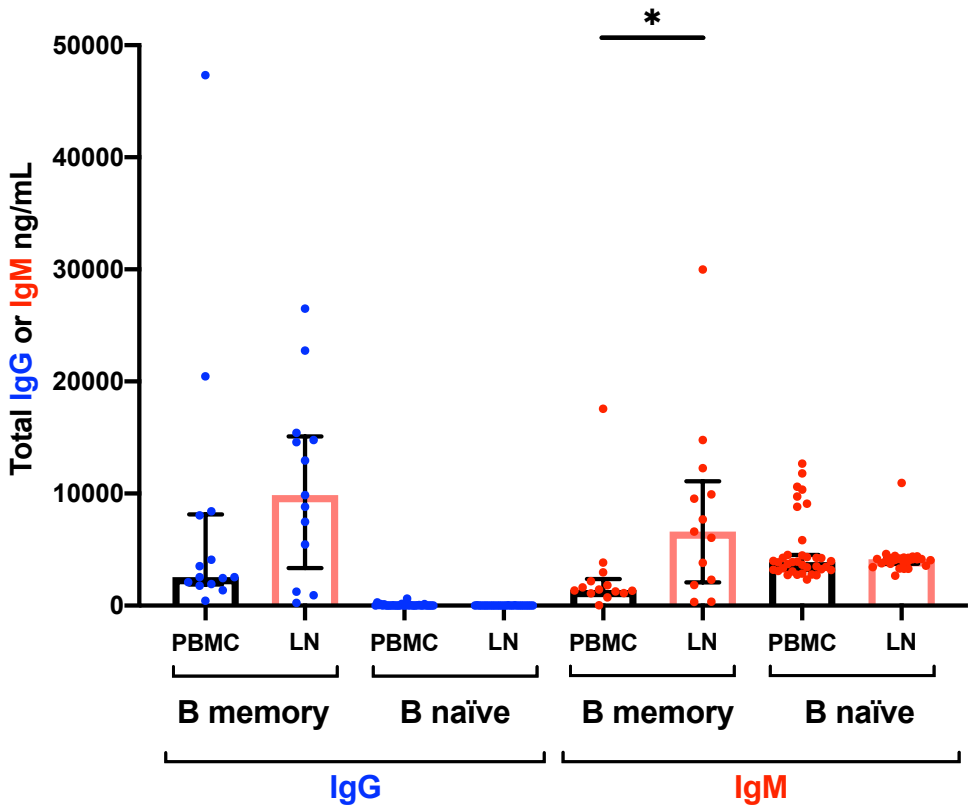


Figure 7.19 – **Total IgG and IgM produced from sorted PBMC and lymph node memory and naïve B cell cultures.**

Individual values are plotted as circles. Median indicated by bars and inter-quartile range with error bars. For each cell type and Ig isotype PBMC was compared to lymph node with a two-tailed Mann-Whitney test. Black=PBMC, Pink=lymph node, Blue=IgG and Red=IgM; *P<0.05

Culture supernatants were tested for antigen-specific IgG and IgM using live CBAs for the respective antigen using a 1:3 dilution as per the unfractionated culture system (table 7.5). No antigen-specific antibodies were detected from the B naïve cell wells from either PBMCs or lymph node. For the NMDAR-Ab-E participants, NR1-IgG positivity was detected in 1 of 2 PBMC B memory cell wells from JR717 but not JR770. For the Caspr2 epilepsy patient (JR061), 1 of 4 PBMC B memory cell wells were positive for Caspr2-IgG and in the LGI1-antibody encephalitis patient (JR870), 1 of 3 PBMC B memory cell wells were positive for LGI1-IgM. This participant was the only participant to have antigen-specific antibodies in sorted lymph node B cells: 1 of 12 lymph node B memory wells were LGI1-IgG positive and 2 of 12 were LGI1-IgM positive.

Participant	**Antigen**	**Culture supernatant antigen-specific IgG and IgM positivity Total number of wells positive / total number of wells (%)**			
		Peripheral blood		**Lymph node**	
		B memory	**B naïve**	**B memory**	**B naïve**
JR770	NMDAR	IgG 0/5 (0%) IgM 0/5 (0%)	IgG 0/8 (0%) IgM 0/8 (0%)	IgG 0/1 (0%) IgM 0/1 (0%)	IgG 0/1 (0%) IgM 0/1 (0%)
JR717	NMDAR	**IgG 1/2 (50%)** IgM 0/2 (0%)	IgG 0/6 (0%) IgM 0/6 (0%)	IgG 0/2 (0%) IgM 0/2 (0%)	IgG 0/1 (0%) IgM 0/1 (0%)
JR061	Caspr2	**IgG 1/4 (25%)** IgM 0/4 (0%)	IgG 0/24 (0%) IgM 0/24 (0%)	IgG 0/3 (0%) IgM 0/3 (0%)	IgG 0/6 (0%) IgM 0/6 (0%)
JR870	LGI1	IgG 0/3 (0%) **IgM 1/3 (33%)**	IgG 0/10 (0%) IgM 0/10 (0%)	**IgG 1/12 (8%)** **IgM 2/12 (17%)**	IgG 0/23 (0%) IgM 0/23 (0%)

Table 7.5 - **Frequency of antigen-specific IgG and IgM positivity from paired PBMC-lymph node aspirate bulk B cell-sorted cell cultures.** Positive results are **highlighted and in bold.**

With the exception of JR870 this approach did not find any positive wells from lymph node cells, in contrast to the unfractionated approach. It could be argued that this was related to patient factors, indeed JR870 transpired to be relapsing and, although not a case of NMDAR-Ab-E, does suggest the general relevance of lymphoid enrichment in the evolution of this category of disease. However, JR770 produced NR1-IgG at two timepoints both acute and non-acute with the unfractionated approach whereas the single well obtained here did not produce NR1-IgG. Although it could be patient-related, it is more likely due to the technique.

With the exception of JR870 when the aspirate provided a large cell number to generate multiple wells (possibly related to disease activity), in general few wells were possible. This could mean that not enough B cells were being isolated from a potentially rare antigen-specific population, they were excluded by the gates, or that being cultured without other cellular components such as cognate T cells, limited the level of antibody production. Given that a positive result was found with PBMC B memory cells in JR717, it may have been the combination of a rare population and a relatively small number of cells, of which a proportion may have died during preparation, sorting, and transport that restricted the rate of positivity. Overall, the total IgG and IgM produced were lower than from the unfractionated cultures, but nonetheless compatible with antigen-specific antibody production.

Due to these caveats and the limited cell number obtainable from lymph node aspiration compared to PBMC preparations, this method was not pursued further.

7.5 Discussion and limitations

The technique of ultrasound-guided fine needle aspiration was used to obtain cervical lymph node material from patients with NMDAR-Ab-E with and without OTs and neurological controls with and without antibody-mediated conditions. A clear conclusion is that FNA can be used safely and effectively in this group of participants. From a baseline of a well-established clinical tool but barely used in neuroimmunological research, this study achieved ethics, local NHS R&D approval and established a research pipeline. There were no complications of the procedure and participants found the visit comfortable. During the study the FNA material was explored including optimised preparation via Ficoll density gradient centrifugation and CD45 staining to improved lymphocyte identification and harvesting. Flow cytometry using stains for surface T and B cell markers established that the material was distinct from peripheral blood with absent granulocyte populations and enrichment for lymph node distinctive populations such as T follicular helper cells. In addition to classifying the cells by flow cytometry, the cells were successfully cultured and reliably secreted immunoglobulins *ex vivo*. This was then extended to studying memory and naïve B cell populations with bulk sorting.

The reliability of these technical aspects permitted further disease-relevant observations. The principal novel finding was that cells from three lymph node samples from two patients secreted NR1-specific IgG. This was independent of total IgG secretion and in one of the two patients correlated very well with TfH and CD83+ B cell proportions and CXCL13 level in the aspirate. This was the case both acutely and in clinical remission. This patient did not have an ovarian teratoma but was diagnosed late in her initial illness episode and at that stage did not receive 2nd line immunotherapy. The other patient had an ovarian teratoma which was thought to

have been removed prior to the sample being obtained, but it later transpired that it grew back rapidly so lymphocytic and antigen material was likely leftover. This patient's lymph node sample did not correlate with markers of germinal centre activity. This may have been an overflow of cells, decompartmentalised from the ovarian cystectomy rather than a local germinal centre reaction per se. The common factor between both patients was under-treatment. While all the OT cases underwent surgery relatively soon after onset (median 41 days, range 15-90), JR819 was the only patient to have cystectomy rather than complete oophorectomy. The lesion reappeared 4 months later in the same location, suggestive of residual cells which developed into the recurrent lesion. Both non-OT cases in this series had delayed treatment compared to the other contemporary Oxford cases from the overall study cohort (JR770=240 days and JR1082=3285 days vs. median=25 days, range=6-50) but unlike JR770, JR1082 was culture negative. It was possible that JR1082 had a more 'burnt out' disease due to almost 20 years since onset (JR770 visits were 1743 and 2389 days after initial onset versus 6658 in JR1082).

Case JR819 shows overlap between the OT- and non-OT associated cases. The lymph node study visit was conducted 64 days after the initial operation and two months prior to relapse at which point a clear lesion was found. Therefore, at the time of the FNA study visit there was probably already appreciable growth. Serologically, NR1-IgM persistently outweighed NR1-IgA, more consistent with non-OT cases. Given that the OT material did produce NR1-antibodies *in vitro* it is unlikely that the OT was irrelevant, more that it was potentially fast growing and/or not well encapsulated, which could account for the recurrence, the serological picture, and the lymph node aspirate positivity.

Taken together, this chapter provides direct evidence for the role of secondary lymphoid tissue and germinal centre reactions in the immunopathogenesis of NMDAR-Ab-E. It is the first study to do this in human participants, however there are several approaches that could improve the resolution of these findings in future work. The first is the nature of the cohort itself. Whilst it was an achievement to have recruited the cohort presented here, a far larger cohort sampled over time in a uniform manner from acute phase to remission would be preferable. A larger cohort would permit more robust statistical analyses with respect to controlling for treatment factors and making inferences compared to healthy and disease control populations rather than the within disease comparisons made here. However, whether this is feasible in a rare disease where there is almost always a prominent neuropsychiatric burden may not be realistic. It could be the case that cohorts like this are always sampled opportunistically and whilst biology can be deeply studied in a small number of samples, only modest population inferences can be made.

The next aspect to consider is deepening the cellular phenotype using intracellular markers with fixed-permeabilised cells. While the surface markers used here have good correlation with intracellular markers, to make an even stronger case for germinal centre B cells and T follicular helper cells, BCL6 would have been useful. This intracellular target was not exploited, as our central aim was to preserve cells for unfractionated cultures but could be feasible in future protocols.

Thirdly, while NR1-IgG was produced in unfractionated cell culture methods it was not from bulk sorted B cells, including JR770, a patient whose lymph node samples produced NR1-IgG at a high well frequency from two distant time points using

unfractionated methods. This may simply be due to numbers such that unfractionated methods do not loose cells which can not only be lost by the sort method but also the extra duration of processing outside from source to incubator. The solution in the longer term is likely to move towards single B cell sorted methods, particularly using antigenic bait to enrich for NR1-specific cells. Single cell methods would be informative for frequency of NR1-specific cells between compartments and also allow recombinant monoclonal antibodies to be made and their phylogeny analysed to test the model outlined here.

Fourth, while antibody production was the main outcome studied here with a linked focus on B cell biology, the method produced TfH populations which correlated well with NR1-production *in vitro*. Studying these cells in more detail including frequency of NR1-specific T cells and T cell receptor clones present in lymph node versus the periphery could help address the extent of T-cell dependency.

Finally, future studies using this material may focus on the non-lymphocytic aspects namely antigen drainage from the CNS into the CLNs both free but also in micro-vesicles (210,211). This would require additional validation to evaluate the degree of contamination from peripheral blood macromolecules and would almost certainly necessitate a modified clinical approach such as a single needle pass and potentially also alternative sample processing depending on the protein biochemical method applied.

8 Conclusion

This thesis has investigated the psychopathology and immunobiology of NMDAR-Ab-E including the prevalence of NR1-autoantibodies in non-encephalitic neuropsychiatric comparator groups.

The psychiatric onset presents a window of opportunity to suspect the diagnosis before critical illness develops. This is complicated by splits between mental and physical healthcare in language, location, and access to diagnostic investigations. A clinical focus is therefore central; this study looked at cases reported in the literature and directly studied participants. The study identified a more prominent mood component than usually discussed, especially depressive mood at onset. It also found regressed behaviour in the post-acute phase, previously largely overlooked in adults. At peak, as reported previously there is undoubtedly a psychosis present with characteristic features of NMDAR antagonism: highly disorganised, disinhibited, dissociative, and impulsive. While at its peak the syndrome overlaps prominently with classical accounts of catatonia, the presence of disorientation and impaired memory as well as oscillation fits more broadly with delirium.

In context of the real-world breadth of first episode psychosis, this approach is well placed to help exclude the diagnosis in oligo-symptomatic, insidious, slowly evolving syndromes, however the breadth of these clinical services also includes rapid onset, fast-evolving presentations. In such ‘organic’-looking presentations, the threshold to consider the diagnosis should be low and it may prove harder to achieve specificity on clinical grounds alone. Consequently, if we want to make this diagnosis without ‘hard’ neurological features then there will be an obligation to re-configure acute

psychiatric services to offer lumbar punctures. A safe and pragmatic approach could involve collaboration with ECT suite anaesthetists – a potential focus for future studies.

NR1-IgG was detected in sera from healthy volunteers and non-encephalitis neuropsychiatric comparator groups at a similar low frequency, whereas in definite NMDAR-Ab-E the majority of patients were seropositive. From an individual patient perspective, positive samples from the different cohorts could not be differentiated by level or NR1 N368Q mutation. However, using a complementary neuron based assay, all non-encephalitis sera were negative, but so were 30% from definite patients. Moreover, the samples from definite patients with an ovarian teratoma had a greater tendency for higher NBA level for any given CBA level than the non-teratoma cases. A unifying explanation is that there were varying degrees of affinity maturation, enriched in the definite patients, most prominently in the OT patients. For the non-encephalitis cohorts, rather than each having an autoimmune sub-group, the more probable explanation is a general population sub-group that may or may not have relevance either as a biomarker or modulator of neural function.

This was explored further by measuring NR1-autoantibody IgM and IgA isotypes in these cohorts. Again, these were uncommon in the non-encephalitic cohorts but common in definite NMDAR-Ab-E. Consistent with germinal centre reactions NR1-IgMs were common. OTs were polarised towards NR1-IgA which was lost after OT removal whereas polarisation toward NR1-IgM in non-OT cases persisted well beyond clinical remission. This was consistent with more prominent class-switching in the OT cases.

This was likely explained by intra-tumoural NR1-autoimmunisation in the OT cases. Consistent with this, NR1-IgG was always detectable in tumour fluid, as were NR1-IgAs which were occasionally unpaired with serum. Flow cytometry of OT material showed naïve B cells and memory B cells of IgM, IgG and IgA isotype specificities, and cultured *ex vivo* material secreted NR1-IgG. Histology revealed germinal centre organisation of lymphocytic infiltrates with BCL6+ germinal centre B cells interspersed with follicular dendritic cells; a characteristic germinal centre structure. NR1 staining could be seen both within and near these structures in neuroglial structures. Whether the NR1 within the germinal centres is lymphocytic rather than antigen will need further evaluation in future studies as will the antigen-specificity of the B cells.

Finally, fine needle aspiration of cervical lymph nodes investigated whether there was evidence of NR1-directed GC reactions in these secondary lymphoid organs. None of the material from patients with adequately treated OTs secreted NR1-IgG *in vitro*. This was consistent with the immunisation being limited to the ectopic GCs in the since removed OT, whereas in 2/6 patients with partially-treated disease, NR1-IgG was detected in culture supernatants.

The set of experiments presented here support a key role for germinal centre reactions in the immunobiology of NMDAR-Ab-E. The data consolidates the role of OTs as tertiary lymphoid organs, as well as the novel direct assessment of secondary lymphoid organs showing their contribution to NR1-autoimmunisation. This suggests that GC-targeted therapies such as B cell depletion should be a priority for translational research, particularly timing as a routine therapy rather than

as a reserve 2nd line treatment. Going full circle, the time-dependence of these mechanisms prioritises prompt clinical recognition.

9 Appendix

1. Excerpt from participant information sheet relating to fine needle aspiration

Ultrasound-guided Fine Needle Aspiration (FNA) (if relevant to you). FNA allows us to sample immune cells in lymph nodes under your chin (submental lymph nodes). This is a site outside of the brain where immune cells learn to make antibodies that target brain molecules, contributing to autoimmune brain diseases. FNA is a well-established, quick and safe method to obtain this sample. It is used routinely to assess other diseases of the head and neck, and has a very low complication rate, equivalent to blood taking. An experienced radiologist uses an ultrasound probe to locate the node and then passes a fine needle to draw up the cells. The main risks are local discomfort, infection, bleeding/bruising and damage to local structures. These are rare, and the radiologist minimises them by aseptic technique and precise ultrasound-guidance. The submental nodes are not near major blood vessels or nerves which further reduces the risk of unintended damage. The technique does not damage the node and will not affect your immune system.

2. Research ethics committee notice of favourable amendment

NHS
Health Research Authority
Yorkshire & The Humber - Leeds East Research Ethics Committee
Jarrow Business Centre
Rolling Mill Road
Jarrow
NE32 3DT

Tel: 0207 1048 088

Please note: This is the favourable opinion of the REC only and does not allow the amendment to be implemented at NHS sites in England until the outcome of the HRA assessment has been confirmed.

09 February 2017

Dr Sarosh Irani
Senior Clinical Fellow and Honorary Consultant Neurologist
University of Oxford, Level 6, West Wing
Nuffield Department of Clinical Neurosciences
John Radcliffe Hospital
Oxford
OX3 9DS

Dear Dr Irani

Study title: **Immune Factors in Neurological Diseases**
REC reference: **16/YH/0013**
Amendment number: **Substantial Amendment 1, 19/01/17**
Amendment date: **25 January 2017**
IRAS project ID: **195152**

The above amendment was reviewed at the meeting of the Sub-Committee held by correspondence.

Summary of amendment

This amendment was submitted in order to include the option for participants to donate cells from lymph nodes in the neck for research purposes, include the option for participants to have a blood sample taken at their GP Practice, and include additional investigators to the study.

Ethical opinion

Following the review of this amendment, the Sub-Committee requested that the 'additional' section of the amended consent form should be changed to 'optional' section to make it clear that participation for the 2 additional activities, FNA and Video, can be refused, whilst still participating in the original study.

A revised version of the consent form was provided as request by the Sub-Committee.

The Sub-Committee was satisfied with the response.

The members of the Committee taking part in the review gave a **favourable** ethical opinion of the amendment on the basis described in the notice of amendment form and supporting documentation.

Approved documents

The documents reviewed and approved at the meeting were:

Document	*Version*	*Date*
Notice of Substantial Amendment (non-CTIMP)	Substantial Amendment 1, 19/01/17	25 January 2017
Other [Schedule of Events]	1	23 January 2017
Other [Statement of Activities]	1	23 January 2017
Other [GP practice bloods - covering letter]	1	23 January 2017
Participant consent form	3.0 - clean	08 February 2017
Participant consent form	3.0 - tracked	08 February 2017
Participant information sheet (PIS)	3.0 - clean	19 January 2017
Participant information sheet (PIS)	3.0 - tracked	19 January 2017
Research protocol or project proposal	3.0 - clean	19 January 2017
Research protocol or project proposal	3.0 - tracked	19 January 2017

Membership of the Committee

The members of the Committee who took part in the review are listed on the attached sheet.

Working with NHS Care Organisations

Sponsors should ensure that they notify the R&D office for the relevant NHS care organisation of this amendment in line with the terms detailed in the categorisation email issued by the lead nation for the study.

Statement of compliance

The Committee is constituted in accordance with the Governance Arrangements for Research Ethics Committees and complies fully with the Standard Operating Procedures for Research Ethics Committees in the UK.

We are pleased to welcome researchers and R & D staff at our Research Ethics Committee members' training days – see details at http://www.hra.nhs.uk/hra-training/

16/YH/0013: **Please quote this number on all correspondence**

Yours sincerely
pp

Sarah Rothera

Dr Deborah Jane Fox
Vice-Chair

E-mail: nrescommittee.yorkandhumber-leedseast@nhs.net

A Research Ethics Committee established by the Health Research Authority

3. List of publications associated with this thesis in chronological order:

Al-Diwani A*, Pollak TA*, Langford AE, Lennox BR. Synaptic and Neuronal Autoantibody-Associated Psychiatric Syndromes: Controversies and Hypotheses. Front Psychiatry. 2017;8(2):13–11.

Al-Diwani A*, Pollak TA*, Irani SR, Lennox BR. Psychosis: an autoimmune disease? Immunology. 2017 Aug 3;152(3):388–401.

Makuch M*, Wilson R*, Al-Diwani A*, Varley J, Kienzler A-K, Taylor J, et al. N-methyl-D-aspartate receptor antibody production from germinal center reactions: therapeutic implications. Ann Neurol. 2018 Feb 6;83(3):553–561.

Al-Diwani A, Lennox BR. Neuroimmunology 2017: making progress over 20 years. Lancet Psychiatry. 2017 Dec 19;5(1):9–10.

Al-Diwani A, Handel A, Townsend L, Pollak T, Leite MI, Harrison PJ, Lennox BR, et al. The psychopathology of NMDAR-antibody encephalitis in adults: a systematic review and phenotypic analysis of individual patient data. Lancet Psychiatry. 2019 Mar;6(3):235-246

Al-Diwani A, Linighan R, Perkins C, Critchlow G, Lennox BR, Leite MI, et al. On being autoimmune in psychiatric places: 10 characteristic mental state features in patients with definite NMDAR-antibody encephalitis. JNNP 2019 May;90(Suppl 2):A1–A2

Ramanathan D*, Al-Diwani A*, Waters P, Irani S. The autoantibody-mediated encephalitides: from clinical observations to molecular pathogenesis. J Neurol. 2019 Oct 26. doi: 10.1007/s00415-019-09590-9. Epub ahead of print.

* contributed equally

References

1. Netea MG, Schlitzer A, Placek K, Joosten LAB, Schultze JL. Innate and Adaptive Immune Memory: an Evolutionary Continuum in the Host's Response to Pathogens. Cell Host and Microbe. 2019 Jan 9;25(1):13–26.

2. Murphy K, Weaver C. Janeway's Immunobiology. Ninth Edition. New York: Garland Science (Taylor & Francis Group).

3. Liu X, Wu J. History, applications, and challenges of immune repertoire research. Cell Biology and Toxicology; 2018 Oct 27;:1–17.

4. Pieper K, Grimbacher B, Eibel H. B-cell biology and development. J Allergy Clin Immunol. 2013 Apr;131(4):959-71.

5. Cowan JE, Takahama Y, Bhandoola A, Ohigashi I. Postnatal Involution and Counter-Involution of the Thymus. Front Immunol. 2020 May 12;11:239–11.

6. Rock KL, Reits E, Neefjes J. Present Yourself! By MHC Class I and MHC Class II Molecules. Trends in Immunology. 2016 Nov;37(11):724–37.

7. Nutt SL, Hodgkin PD, Tarlinton DM, Corcoran LM. The generation of antibody-secreting plasma cells. Nat Rev Immunol. 2015 Feb 20;15(3):160–71.

8. Pupovac A, Good-Jacobson KL. An antigen to remember: regulation of B cell memory in health and disease. Current Opinion in Immunology. 2017 Apr 1;45:89–96.

9. Akkaya M, Kwak K, Pierce SK. B cell memory: building two walls of protection against pathogens. Nat Rev Immunol. 2019 Dec 12;:1–10.

10. Suan D, Sundling C, Brink R. Plasma cell and memory B cell differentiation from the germinal center. Current Opinion in Immunology. 2017 Apr 1;45:97–102.

11. Bannard O, Cyster JG. Germinal centers: programmed for affinity maturation and antibody diversification. Current Opinion in Immunology. 2017 Apr 1;45:21–30.

12. Wang W, Singh S, Zeng DL, King K, Nema S. Antibody Structure, Instability, and Formulation. Journal of Pharmaceutical Sciences. 2007 Jan;96(1):1–26.

13. Forsström B, Bisławska Axnäs B, Rockberg J, Danielsson H, Bohlin A, Uhlen M. Dissecting Antibodies with Regards to Linear and Conformational Epitopes. Mantis NJ, editor. PLoS ONE. 2015 Mar 27;10(3):e0121673–11.

14. Stavnezer J, Schrader CE. IgH Chain Class Switch Recombination: Mechanism and Regulation. The Journal of Immunology. 2014 Nov 19;193(11):5370–8.

15. Chi X, Li Y, Qiu X. V(D)J recombination, somatic hypermutation and class switch recombination of immunoglobulins: mechanism and regulation. Immunology. 2020 Feb 27;160(3):233–47.

16. Collins AM, Jackson KJL. On being the right size: antibody repertoire formation in the mouse and human. Immunogenetics; 2018 Feb 15;:1–16.

17. Nemazee D. Mechanisms of central tolerance for B cells. Nat Rev Immunol. 2017 Apr 3;17(5):281–94.

18. Goodnow CC, Crosbie J, Adelstein S, Lavoie TB, Smith-Gill SJ, Brink RA, et al. Altered immunoglobulin expression and functional silencing of self-reactive B lymphocytes in transgenic mice. Nature. 1988 Aug 25;334(6184):676–82.

19. Burnett DL, Langley DB, Schofield P, Hermes JR, Chan TD, Jackson J, et al. Germinal center antibody mutation trajectories are determined by rapid self/foreign discrimination. Science. 2018 Apr 13;360(6385):223–6.

20. De Silva NS, Klein U. Dynamics of B cells in germinal centres. Nat Rev Immunol. 2015 Feb 6;:1–12.

21. Heesters BA, van der Poel CE, Das A, Carroll MC. Antigen Presentation to B Cells. Trends in Immunology. 2016 Dec 1;37(12):844–54.

22. Crotty S. T Follicular Helper Cell Biology: A Decade of Discovery and Diseases. Immunity. 2019 May 21;50(5):1132–48.

23. Manz RA, Thiel A, Radbruch A. Lifetime of plasma cells in the bone marrow. Nature. 1997 Jul 10;388(6638):133–4.

24. Halliley JL, Tipton CM, Liesveld J, Rosenberg AF, Darce J, Gregoretti IV, et al. Long-Lived Plasma Cells Are Contained within the CD19-CD38hiCD138+ Subset in Human Bone Marrow. Immunity. 2015 Jul 21;43(1):132–45.

25. Dominguez-Villar M, Hafler DA. Regulatory T cells in autoimmune disease. Nature Publishing Group. 2018 Jun 19;:1–9.

26. Brink R, Phan TG. Self-Reactive B Cells in the Germinal Center Reaction. Annu Rev Immunol. 2018 Apr 26;36(1):339–57.

27. Roco JA, Mesin L, Binder SC, Nefzger C, Gonzalez-Figueroa P, Canete PF, et al. Class-Switch Recombination Occurs Infrequently in Germinal Centers. Immunity. 2019 Jul 26;:1–22.

28. Jones GW, Jones SA. Ectopic lymphoid follicles: inducible centres for generating antigen-specific immune responses within tissues. Immunology. 2015 Dec 10;147(2):141–51.

29. Corsiero E, Nerviani A, Bombardieri M, Pitzalis C. Ectopic Lymphoid Structures: Powerhouse of Autoimmunity. Front Immunol. 2016 Oct 17;7(10):447–6.

30. Humby F, Bombardieri M, Manzo A, Kelly S, Blades MC, Kirkham B, et al. Ectopic Lymphoid Structures Support Ongoing Production of Class-Switched Autoantibodies in Rheumatoid Synovium. PLoS Med. 2009 Jan 13;6(1):e1–17.

31. Lehmann-Horn K, Wang S-Z, Sagan SA, Zamvil SS, Büdingen von HC. B cell repertoire expansion occurs in meningeal ectopic lymphoid tissue. JCI Insight. 2016 Dec 8;1(20):1–18.

32. Lin L, Hu X, Zhang H, Hu H. Tertiary Lymphoid Organs in Cancer Immunology: Mechanisms and the New Strategy for Immunotherapy. Front Immunol. 2019 Jun 20;10:646–10.

33. Helmink BA, Reddy SM, Gao J, Zhang S, Basar R, Thakur R, et al. B cells and tertiary lymphoid structures promote immunotherapy response. Nature. 2020 Jan 11;:1–28.

34. Cabrita R, Lauss M, Sanna A, Donia M, Larsen MS, Mitra S, et al. Tertiary lymphoid structures improve immunotherapy and survival in melanoma. Nature. 2020 Jan 8;:1–20.

35. Willis SN, Mallozzi SS, Rodig SJ, Cronk KM, McArdel SL, Caron T, et al. The Microenvironment of Germ Cell Tumors Harbors a Prominent Antigen-Driven Humoral Response. The Journal of Immunology. 2009 Mar 1;182(5):3310–7.

36. Wilson R, Makuch M, Kienzler A-K, Varley J, Taylor J, Woodhall M, et al. Condition-dependent generation of aquaporin-4 antibodies from circulating B cells in neuromyelitis optica. Brain. 2018 Feb 13;74:1474–12.

37. Elkon K, Casali P. Nature and functions of autoantibodies. Nat Rev Rheumatol. 2008 Sep;4(9):491–8.

38. Bashford-Rogers RJM, Bergamaschi L, McKinney EF, Pombal DC, Mescia F, Lee JC, et al. Analysis of the B cell receptor repertoire in six immune-mediated diseases. Nature. 2019 Sep 25;574(7776):122–6.

39. Avrameas S, Selmi C. Natural autoantibodies in the physiology and pathophysiology of the immune system. Journal of Autoimmunity. 2013 Mar 1;41(C):46–9.

40. Maria PA, Kypros N. Maternal autoimmune disorders and fetal defects. The Journal of Maternal-Fetal & Neonatal Medicine. 2017 Jun 23;0(0):1–9.

41. Witebsky E, Rose NR, Terplan K, Paine JR, Egan RW. Chronic thyroiditis and autoimmunization. J Am Med Assoc. American Medical Association; 1957 Jul 27;164(13):1439–47.

42. Rose NR, Bona C. Defining criteria for autoimmune diseases (Witebsky's postulates revisited). Immunology Today. 1993 Sep;14(9):426–30.

43. Vincent A, Huda S, Cao M, Cetin H, Koneczny I, Rodriguez-Cruz P, et al. Serological and experimental studies in different forms of myasthenia gravis. Ann NY Acad Sci. 2018 Jan 29;1413(1):143–53.

44. Nataf S. Evolution, immunity and the emergence of brain superautoantigens. F1000Res. 2017 Feb 21;6:171–17.

45. Brierley JB, Corsellis J, Hierons R, Nevin S. Subacute encephalitis of later adult life mainly affecting the limbic areas. Brain. 1960;83(3):357–68.

46. Corsellis J, Goldberg GJ, Norton AR. “Limbic encephalitis” and its association with carcinoma. Brain. 1968;91(3):481–96.

47. Gultekin SH, Rosenfeld MR, Voltz R, Eichen J, Posner JB, Dalmau J. Paraneoplastic limbic encephalitis: neurological symptoms, immunological findings and tumour association in 50 patients. Brain. 2000 Jul;123(7):1481–94.

48. Sinha S, Newsom-Davis J, Mills K, Byrne N, Lang B, Vincent A. Autoimmune aetiology for acquired neuromyotonia (Isaacs' syndrome). The Lancet. 1991 Jul 13;338(8759):75–7.

49. Liguori R, Vincent A, Clover L, Avoni P, Plazzi G, Cortelli P, et al. Morvan's syndrome: peripheral and central nervous system and cardiac involvement with antibodies to voltage-gated potassium channels. Brain. 2001 Dec;124(12):2417–26.

50. Buckley C, Oger J, Clover L, Tüzün E, Carpenter K, Jackson M, et al. Potassium channel antibodies in two patients with reversible limbic encephalitis. Ann Neurol. 2001 Jul;50(1):73–8.

51. Vincent A, Buckley C, Schott JM, Baker I, Dewar BK, Detert N, et al. Potassium channel antibody-associated encephalopathy: a potentially immunotherapy-responsive form of limbic encephalitis. Brain. 2004 Mar;127(3):701–12.

52. Irani SR, Alexander S, Waters P, Kleopa KA, Pettingill P, Zuliani L, et al. Antibodies to Kv1 potassium channel-complex proteins leucine-rich, glioma inactivated 1 protein and contactin-associated protein-2 in limbic encephalitis, Morvan's syndrome and acquired neuromyotonia. Brain. 2010 Sep;133(9):2734–48.

53. Lai M, Huijbers MG, Lancaster E, Graus F, Bataller L, Balice-Gordon R, et al. Investigation of LGI1 as the antigen in limbic encephalitis previously attributed to potassium channels: a case series. The Lancet Neurology. 2010 Aug;9(8):776–85.

54. Vitaliani R, Mason W, Ances B, Zwerdling T, Jiang Z, Dalmau J. Paraneoplastic encephalitis, psychiatric symptoms, and hypoventilation in ovarian teratoma. Ann Neurol. 2005 Oct;58(4):594–604.

55. Dalmau J, Tüzün E, Wu HY, Masjuan J, Rossi JE, Voloschin A, et al. Paraneoplastic anti-N-methyl-D-aspartate receptor encephalitis associated with ovarian teratoma. Ann Neurol. 2007 Jan;61(1):25–36.

56. N-methyl-D-aspartate antibody encephalitis: temporal progression of clinical and paraclinical observations in a predominantly non-paraneoplastic disorder of both sexes. 2010 Jun;133(6):1655–67.

57. Dalmau J, Gleichman AJ, Hughes EG, Rossi JE, Peng X, Lai M, et al. Anti-NMDA-receptor encephalitis: case series and analysis of the effects of antibodies. The Lancet Neurology. 2008 Dec;7(12):1091–8.

58. Dalmau J, Lancaster E, Martinez-Hernandez E, Rosenfeld MR, Balice-Gordon R. Clinical experience and laboratory investigations in patients with anti-NMDAR encephalitis. The Lancet Neurology. 2011 Jan;10(1):63–74.

59. Granerod J, Ambrose HE, Davies NW, Clewley JP, Walsh AL, Morgan D, et al. Causes of encephalitis and differences in their clinical presentations in England: a multicentre, population-based prospective study. Lancet Infectious Diseases. 2010 Dec 10;10(12):835–44.

60. Dubey D, Pittock SJ, Kelly CR, McKeon A, Lopez-Chiriboga AS, Lennon V, et al. Autoimmune Encephalitis Epidemiology and a comparison to Infectious Encephalitis. Ann Neurol. 2018 Jan 2;:1–34.

61. Höftberger R, Titulaer MJ, Sabater L, Dome B, Rózsás A, Hegedus B, et al. Encephalitis and GABAB receptor antibodies: novel findings in a new case series of 20 patients. Neurology. Wolters Kluwer Health, Inc. on behalf of the American Academy of Neurology; 2013 Oct 22;81(17):1500–6.

62. Van Coevorden-Hameete MH, de Bruijn MA, de Graaff E, Bastiaansen DA, Schreurs MWJ, Demmers JA, et al. The expanded clinical spectrum of anti-GABABR encephalitis and added value of KCTD16 autoantibodies. Brain. 2019 Jun 1;142(6):1631–43.

63. Irani SR, Stagg CJ, Schott JM, Rosenthal CR, Schneider SA, Pettingill P, et al. Faciobrachial dystonic seizures: the influence of immunotherapy on seizure control and prevention of cognitive impairment in a broadening phenotype. Brain. 2013 Oct;136(Pt 10):3151–62.

64. Thompson J, Bi M, Murchison AG, Makuch M, Bien CG, Chu K, et al. The importance of early immunotherapy in patients with faciobrachial dystonic seizures. Brain. 2017 Dec 18;141(2):348–56.

65. Kayser MS, Titulaer MJ, Gresa-Arribas N, Dalmau J. Frequency and characteristics of isolated psychiatric episodes in anti–N-methyl-d-aspartate receptor encephalitis. JAMA Neurol. 2013 Sep 1;70(9):1133–9.

66. Pettingill P, Kramer HB, Coebergh JA, Pettingill R, Maxwell S, Nibber A, et al. Antibodies to GABAA receptor α1 and γ2 subunits: clinical and serologic characterization. Neurology. 2015 Mar 24;84(12):1233–41.

67. Bien CG, Vincent A, Barnett MH, Becker AJ, Blümcke I, Graus F, et al. Immunopathology of autoantibody-associated encephalitides: clues for pathogenesis. Brain. 2012 May;135(Pt 5):1622–38.

68. Martinez-Hernandez E, Horvath J, Shiloh-Malawsky Y, Sangha N, Martinez-Lage M, Dalmau J. Analysis of complement and plasma cells in the brain of patients with anti-NMDAR encephalitis. Neurology. 2011 Aug 9;77(6):589–93.

69. Platt MP, Agalliu D, Cutforth T. Hello from the Other Side: How Autoantibodies Circumvent the Blood–Brain Barrier in Autoimmune Encephalitis. Front Immunol. 2017 Apr 21;8:299–44.

70. Ehrenreich H. Autoantibodies against N-methyl-d-aspartate receptor 1 in health and disease. Current Opinion in Neurology. 2018 Feb;:1–7.

71. Planagumà J, Leypoldt F, Mannara F, Gutiérrez-Cuesta J, Martín-García E, Aguilar E, et al. Human N-methyl D-aspartate receptor antibodies alter memory and behaviour in mice. Brain. 2014 Nov 11;138(1):94–109.

72. Petit-Pedrol M, Sell J, Planagumà J, Mannara F, Radosevic M, Haselmann H, et al. LGI1 antibodies alter Kv1.1 and AMPA receptors changing synaptic excitability, plasticity and memory. Brain. 2018 Nov 1;141(11):3144–59.

73. Ladépêche L, Planagumà J, Thakur S, Suárez I, Hara M, Borbely JS, et al. NMDA Receptor Autoantibodies in Autoimmune Encephalitis Cause a Subunit-Specific Nanoscale Redistribution of NMDA Receptors. Cell Reports. 2018 Jun 26;23(13):3759–68.

74. Binks S, Varley J, Lee W, Makuch M, Elliott K, Gelfand JM, et al. Distinct HLA associations of LGI1 and CASPR2-antibody diseases. Brain. 2018 May 18;141(8):2263–71.

75. Kreye J, Wenke NK, Chayka M, Leubner J, Murugan R, Maier N, et al. Human cerebrospinal fluid monoclonal N-methyl-D-aspartate receptor autoantibodies are sufficient for encephalitis pathogenesis. Brain. 2016 Oct;139(Pt 10):2641–52.

76. Van Sonderen A, Schreurs MW, de Bruijn MA, Boukhrissi S, Nagtzaam MM, Hulsenboom ES, et al. The relevance of VGKC positivity in the absence of LGI1 and Caspr2 antibodies. Neurology. 2016 May 2;86(18):1692–9.

77. Castillo-Gomez E, Kästner A, Steiner J, Schneider A, Hettling B, Poggi G, et al. The brain as immunoprecipitator of serum autoantibodies against N-Methyl-D-aspartate receptor subunit NR1. Ann Neurol. 2016 Jan;79(1):144–51.

78. Pettingill P, Chang T, Irani SR, Water PJ. Controversies in the detection of neural autoantibodies. Advances in Clinical Neuroscience and Rehabilitation. 2016 Sep 20:16(2):5–7.

79. Waters P, Reindl M, Saiz A, Schanda K, Tuller F, Kral V, et al. Multicentre comparison of a diagnostic assay: aquaporin-4 antibodies in neuromyelitis optica. Journal of Neurology, Neurosurgery & Psychiatry. 2016 Aug 12;87(9):1005–15.

80. Waters PJ, Komorowski L, Woodhall M, Lederer S, Majed M, Fryer J, et al. A multicenter comparison of MOG-IgG cell-based assays. Neurology. 2019 Mar 12: 92(11):e1250-e1255.

81. Hansen KB, Traynelis SF. Structure, function, and allosteric modulation of NMDA receptors. Journal of General Physiology. 2018 Jul 30;150(8):1–25.

82. Ramirez A, Arbuckle MR. The N-Methyl-D-Aspartate Receptor_ Memory, Madness, and More. Biological Psychiatry. 2017 Jul 1;82(1):e1–e3.

83. Petersen RC, Stillman RC. Phencyclidine (PCP) Abuse: An Appraisal. National Institute on Drug Abuse NIDA Monograph. 1978 Aug 1.

84. Isaacs SO, Martin P, Washington JA Jr., SO I, P M, JA W Jr. Phencyclidine (PCP) abuse. Oral Surg Oral Med Oral Pathol. 1986 Feb;61(2):126–9.

85. Yesavage JA, Freeman AM, Bourgeois ML. Time distortion in acute phencyclidine (PCP) psychosis. A correlation between 30 seconds estimation and urine drugs levels. Encephale. 1978;4(3):281–5.

86. Milhorn HT. Diagnosis and management of phencyclidine intoxication. Am Fam Physician. 1991 Apr 1;43(4):1293–302.

87. Rosse RB, Collins JP, Fay-McCarthy M, Alim TN, Wyatt RJ, Deutsch SI. Phenomenologic comparison of the idiopathic psychosis of schizophrenia and drug-induced cocaine and phencyclidine psychoses: a retrospective study. Clin Neuropharmacol [Internet]. 1994 Aug;17(4):359–69.

88. Bey T, Patel A. Phencyclidine intoxication and adverse effects: a clinical and pharmacological review of an illicit drug. Cal J Emerg Med. 2007 Feb;8(1):9–14.

89. Pomarol-Clotet E, Honey GD, Murray GK, Corlett PR, Absalom AR, Lee M, et al. Psychological effects of ketamine in healthy volunteers. The British Journal of Psychiatry. 2018 Jan 2;189(2):173–9.

90. Martial C, Cassol H, Charland-Verville V, Pallavicini C, Sanz C, Zamberlan F, et al. Neurochemical models of near-death experiences: A large-scale study based on the semantic similarity of written reports. Consciousness and Cognition. 2019 Jan 31;69:52–69.

91. Martinak B, Bolis RA, Black JR, Fargason RE, Birur B. Dextromethorphan in Cough Syrup: The Poor Man's Psychosis. Psychopharmacol Bull. 2017 Sep 15;47(4):59–63.

92. Stanciu CN, Penders TM. Mania After Misuse of Dextromethorphan. Journal of Addiction Medicine. 2015;9(2):159–60.

93. Lemke JR, Geider K, Helbig KL, Heyne HO, Schütz H, Hentschel J, et al. Delineating the GRIN1 phenotypic spectrum: A distinct genetic NMDA receptor encephalopathy. Neurology. 2016 Jun 7;86(23):2171–8.

94. Okamura H, Oomori N, Uchitomi Y. An acutely confused 15-year-old girl. The Lancet. 1997 Aug;350(9076):488–1.

95. Nokura K, Yamamoto H, Okawara Y, Koga H, Osawa H, Sakai K. Reversible limbic encephalitis caused by ovarian teratoma. Acta Neurol Scand. 1997 Jun;95(6):367–73.

96. Kamei S, Kuzuhara S, Ishihara M, Morita A, Taira N, Togo M, et al. Nationwide survey of acute juvenile female non-herpetic encephalitis in Japan: relationship to anti-N-methyl-D-aspartate receptor encephalitis. Intern Med. 2009;48(9):673–9.

97. Dale RC, Irani SR, Brilot F, Pillai S, Webster R, Gill D, et al. N-methyl-D-aspartate receptor antibodies in pediatric dyskinetic encephalitis lethargica. Ann Neurol. 2009 Nov;66(5):704–9.

98. SHILL HA. Malignant catatonia secondary to sporadic encephalitis lethargica. Journal of Neurology, Neurosurgery & Psychiatry. 2000 Sep 1;69(3):402–3.

99. Punja M, Pomerleau AC, Devlin JJ, Morgan BW, Schier JG, Schwartz MD. Anti-N-methyl-D-aspartate receptor (anti-NMDAR) encephalitis: an etiology worth considering in the differential diagnosis of delirium. Clinical Toxicology. 2013 Aug 22;51(8):794–7.

100. Caroff SN, Campbell EC. Risk of neuroleptic malignant syndrome in patients with NMDAR encephalitis. Neurol Sci. 2014 Dec 6;36(3):479–80.

101. Huang C, Kang Y, Zhang B, Li B, Qiu C, Liu S et al. Anti-N-methyl-d-aspartate receptor encephalitis in a patient with a 7-year history of being diagnosed as schizophrenia: complexities in diagnosis and treatment. Neuropsychiatr Dis Treat. 2015 Jun;11:1437–1442.

102. Simabukuro MM, Freitas CH de A, Castro LHM. A patient with a long history of relapsing psychosis and mania presenting with anti-NMDA receptor encephalitis ten years after first episode. Dement neuropsychol. 2015 Sep;9(3):311–4.

103. The Exorcism of Doctor Escudero. 2015 Sep 1. Available from: https://granta.com/the-exorcism-of-doctor-escudero/

104. Graus F, Titulaer MJ, Balu R, Benseler S, Bien CG, Cellucci T, A clinical approach to diagnosis of autoimmune encephalitis. Lancet Neurol. 2016 Apr;15(4):391–404.

105. Armangue T, Santamaria J, Dalmau J. When a serum test overrides the clinical assessment. Neurology. 2015 Mar 31;84(13):1379–1381

106. Kaneko A, Kaneko J, Tominaga N, Kanazawa N, Hattori K, Ugawa Y, et al. Pitfalls in clinical diagnosis of anti-NMDA receptor encephalitis. Journal of Neurology. 2018 Jan 20;265(3):586–96.

107. Gresa-Arribas N, Titulaer MJ, Torrents A, Aguilar E, McCracken L, Leypoldt F, et al. Antibody titres at diagnosis and during follow-up of anti-NMDA receptor encephalitis: a retrospective study. The Lancet Neurology. 2014 Feb;13(2):167–77.

108. Zandi MS, Irani SR, Lang B, Waters P, Jones PB, McKenna P, et al. Disease-relevant autoantibodies in first episode schizophrenia. J Neurol. 2011;258(4):686–688.

109. Rossi M, Mead S, Collinge J, Rudge P, Vincent A. Neuronal antibodies in patients with suspected or confirmed sporadic Creutzfeldt-Jakob disease. Journal of Neurology, Neurosurgery & Psychiatry. 2015 Jun;86(6):692–4.

110. Zandi MS, Paterson RW, Ellul MA, Jacobson L, Al-Diwani A, Jones JL, et al. Clinical relevance of serum antibodies to extracellular N-methyl-D-aspartate receptor epitopes. Journal of Neurology, Neurosurgery & Psychiatry. 2015 Jul;86(7):708–13.

111. Bergink V, Armangue T, Titulaer MJ, Markx S, Dalmau J, Kushner SA. Autoimmune Encephalitis in Postpartum Psychosis. Am J Psych. 2015 Sep 1;172(9):901–8.

112. Caroff SN, Hurford I, Lybrand J, Campbell EC. Movement disorders induced by antipsychotic drugs: implications of the CATIE schizophrenia trial. Neurologic Clinics. 2011 Feb;29(1):127–48–viii.

113. Moscato EH, Peng X, Jain A, Parsons TD, Dalmau J, Balice-Gordon RJ. Acute mechanisms underlying antibody effects in anti-N-methyl-D-aspartate receptor encephalitis. Ann Neurol. 2014 Jun 27;76(1):108–19.

114. Hughes EG, Peng X, Gleichman AJ, Lai M, Zhou L, Tsou R, et al. Cellular and synaptic mechanisms of anti-NMDA receptor encephalitis. J Neurosci. 2010 Apr 28;30(17):5866–75.

115. Mikasova L, De Rossi P, Bouchet D, Georges F, Rogemond V, Didelot A, et al. Disrupted surface cross-talk between NMDA and Ephrin-B2 receptors in anti-NMDA encephalitis. Brain. 2012 May;135(5):1606–21.

116. Planagumà J, Haselmann H, Mannara F, Petit-Pedrol M, Grünewald B, Aguilar E, et al. Ephrin-B2 prevents N-methyl-D-aspartate receptor antibody effects on memory and neuroplasticity. Ann Neurol. 2016 Aug 2;80(3):388–400.

117. Symmonds M, Moran CH, Leite MI, Buckley C, Irani SR, Stephan KE, et al. Ion channels in EEG: isolating channel dysfunction in NMDA receptor antibody encephalitis. Brain. 2018;141(6):1691-1702.

118. Finke C, Kopp UA, Scheel M, Pech L-M, Soemmer C, Schlichting J, et al. Functional and structural brain changes in anti-N-methyl-D-aspartate receptor encephalitis. Ann Neurol. 2013;74(2):284-296.

119. Peer M, Prüss H, Ben-Dayan I, Paul F, Arzy S, Finke C. Functional connectivity of large-scale brain networks in patients with anti-NMDA receptor encephalitis: an observational study. Lancet Psychiatry. 2017;4(10):768-774.

120. Gleichman AJ, Spruce LA, Dalmau J, Seeholzer SH, Lynch DR. Anti-NMDA receptor encephalitis antibody binding is dependent on amino acid identity of a small region within the GluN1 amino terminal domain. J Neurosci. 2012 Aug 8;32(32):11082–94.

121. Titulaer MJ, McCracken L, Gabilondo I, Armangue T, Glaser C, Iizuka T, et al. Treatment and prognostic factors for long-term outcome in patients with anti-NMDA receptor encephalitis: an observational cohort study. Lancet Neurology. 2013 Feb;12(2):157–65.

122. Yan B, Wang Y, Zhang Y, Lou W. Teratoma-associated anti-N-methyl-D-aspartate receptor encephalitis. Medicine. 2019 May;98(21):e15765–5.

123. Mangler M, Trebesch de Perez I, Teegen B, Stöcker W, Prüss H, Meisel A, et al. Seroprevalence of anti-N-methyl-d-aspartate receptor antibodies in women with ovarian teratoma. Journal of Neurology. 2013 Aug 24;260(11):2831–5.

124. Trillsch F, Eichhorn P, Oliveira-Ferrer L, Kuempfel T, Burges A, Mahner S, et al. No need for NMDA receptor antibody screening in neurologically asymptomatic patients with ovarian teratomas. Journal of Neurology. 2017 Dec 21;265(2):431–2.

125. Gong S, Zhou M, Shi G, Guo J, Chen N, Yang R, et al. Absence of NMDA receptor antibodies in patients with ovarian teratoma without encephalitis. Neurol Neuroimmunol Neuroinflamm. 2017 Apr 11;4(3):e344–2.

126. Dabner M, McCluggage WG, Bundell C, Carr A, Leung Y, Sharma R, et al. Ovarian Teratoma Associated With Anti-N-Methyl D-Aspartate Receptor Encephalitis. International Journal of Gynecological Pathology. 2012 Sep;31(5):429–37.

127. Jandu AS, Odor PM, Vidgeon SD. Status epilepticus and anti-NMDA receptor encephalitis after resection of an ovarian teratoma. Journal of the Intensive Care Society. 2016 Oct 25;17(4):346–52.

128. West-Watson WN, Young CJ. Failed splenectomy in acholuric jaundice, and the relation of toxaemia to the haemolytic crises. BMJ. 1938 Jun 18;1:1305–9.

129. Raimundo PO, Coelho S, Cabeleira A, Dias L, Gonçalves M, Almeida J. Warm antibody autoimmune haemolytic anaemia associated with ovarian teratoma. BMJ Case Rep. 2010 May 19; bcr.06.2009.1971

130. Groeneveld M, Vergeldt TFM, Novotny VMJ, Coppus SFPJ. Complete Remission of Immune Thrombocytopenic Purpura After Dermoid Cystectomy. Journal of Gynecologic Surgery. 2019 Feb;35(1):48–50.

131. Sun B. A tumultuous case of episodic apnoea. Journal of Neurology, Neurosurgery & Psychiatry. 2020 Jan 9;90(12):e1–e65.

132. Herrmann ML, Bruchner N, Martin P, Wildgruber D. Psychosis associated to CASPR2 autoantibodies and ovarian teratoma_ A case report. Psychiatry Research. 2019 Dec 13;:112725.

133. Fang B, McKeon A, Hinson SR, Kryzer TJ, Pittock SJ, Aksamit AJ, et al. Autoimmune Glial Fibrillary Acidic Protein Astrocytopathy. JAMA Neurol. 2016 Nov 1;73(11):1297–11.

134. Nolan A, Buza N, Margeta M, Rabban JT. Ovarian Teratomas in Women With Anti-N-methyl-D-Aspartate Receptor Encephalitis: Topography and Composition of Immune Cell and Neuroglial Populations Is Compatible With an Autoimmune Mechanism of Disease. Am J Surg Pathol. 2019 Jul;43(7):949–64.

135. Day GS, Laiq S, Tang-Wai DF, Munoz DG. Abnormal neurons in teratomas in NMDAR encephalitis. JAMA Neurol. 2014 Jun;71(6):717–24.

136. Chefdeville A, Treilleux I, Mayeur M-E, Couillault C, Picard G, Bost C, et al. Immunopathological characterization of ovarian teratomas associated with anti-N- methyl-D-aspartate receptor encephalitis. Acta Neuropathologica Communications; 2019 Mar 8;:1–11.

137. Mueller SH, Färber A, Prüss H, Melzer N, Golombeck KS, Kümpfel T, et al. Genetic predisposition in anti-LGI1 and anti-NMDA receptor encephalitis. Ann Neurol. 2018 Apr 23;83(4):863–9.

138. Eker A, Saka E, Dalmau J, Kurne A, Bilen C, Ozen H, et al. Testicular teratoma and anti-N-methyl-D-aspartate receptor-associated encephalitis. Journal of Neurology, Neurosurgery & Psychiatry. 2008 Sep;79(9):1082–3.

139. Souyris M, Cenac C, Azar P, Daviaud D, Canivet A, Grunenwald S, et al. TLR7 escapes X chromosome inactivation in immune cells. Science Immunology; 2018 Jan 26;3(19):1–11.

140. Prüss H, Finke C, Höltje M, Hofmann J, Klingbeil C, Probst C, et al. N-methyl- D-aspartate receptor antibodies in herpes simplex encephalitis. Ann Neurol. 2012 Dec 31;72(6):902–11.

141. Hacohen Y, Deiva K, Pettingill P, Waters P, Siddiqui A, Chretien P, et al. N-methyl- D-aspartate receptor antibodies in post-herpes simplex virus encephalitis neurological relapse. Mov Disord. 2013 Sep 6;29(1):90–6.

142. Armangue T, Leypoldt F, Málaga I, Raspall-Chaure M, Marti I, Nichter C, et al. Herpes simplex virus encephalitis is a trigger of brain autoimmunity. Ann Neurol. 2014 Feb 25;75(2):317–23.

143. Armangue T, Spatola M, Vlagea A, Mattozzi S, Cárceles-Cordon M,Martinez-Heras E, et al. Frequency, symptoms, risk factors, and outcomes of autoimmune encephalitis after herpes simplex encephalitis: a prospective observational study and retrospective analysis. Lancet Neurology. 2018 Jul 20;17(9):760–772.

144. Jones BE, Tovar KR, Goehring A, Okada NJ, Gouaux E, Westbrook GL. Anti-NMDA receptor encephalitis in mice induced by active immunization with conformationally-stabilized holoreceptors. Sci Transl Med. 2019;11(500):eaaw0044.

145. During MJ, Symes CW, Lawlor PA, Lin J, Dunning J, Fitzsimons HL, et al. An oral vaccine against NMDAR1 with efficacy in experimental stroke and epilepsy. Science. 2000 Feb 25;287(5457):1453–60.

146. Makuch M, Wilson R, Al-Diwani A, Varley J, Kienzler A-K, Taylor J, et al. N-methyl-D-aspartate receptor antibody production from germinal center reactions: therapeutic implications. Ann Neurol. 2018 Feb 6;83(3):553–561.

147. Louveau A, Smirnov I, Keyes TJ, Eccles JD, Rouhani SJ, Peske JD, et al. Structural and functional features of central nervous system lymphatic vessels. Nature. 2015 Jun 1;523(7560):337–41.

148. Da Mesquita S, Louveau A, Vaccari A, Smirnov I, Cornelison RC, Kingsmore KM, et al. Functional aspects of meningeal lymphatics in ageing and Alzheimer's disease. Nature. 2018 Jul 25;560(7717):185–91.

149. Nauen DW. Extra-central nervous system target for assessment and treatment in refractory anti-N-methyl-d-aspartate receptor encephalitis. Journal of Critical Care. 2017 Feb 1;37:234–6.

150. Dalmau J. NMDA receptor encephalitis and other antibody-mediated disorders of the synapse. Neurology. 2016 Dec 5;87(23):2471–82.

151. Al-Diwani A, Pollak TA, Langford AE, Lennox BR. Synaptic and Neuronal Autoantibody-Associated Psychiatric Syndromes: Controversies and Hypotheses. Front Psychiatry. 2017;8(2):13–11.

152. Baumeister A. The Search for an Endogenous Schizogen : The Strange Case of Taraxein. J of the Hist of the Neurosciences. 2011 Apr;20(2):106–22.

153. Bechter K. Encephalitis, Mild Encephalitis, Neuroprogression, or Encephalopathy—Not Merely a Question of Terminology. Front Psychiatry. 2019 Feb 6;9:aad8670–8.

154. Knight JG. Dopamine-receptor-stimulating autoantibodies: a possible cause of schizophrenia. The Lancet. 1982 Nov 13;2(8307):1073–6.

155. Al-Diwani A, Pollak TA, Irani SR, Lennox BR. Psychosis: an autoimmune disease? Immunology. 2017 Aug 3;152(3):388–401.

156. Steiner J, Walter M, Glanz W, Sarnyai Z, Bernstein H-G, Vielhaber S, et al. Increased Prevalence of Diverse N -Methyl-D-Aspartate Glutamate Receptor Antibodies in Patients With an Initial Diagnosis of Schizophrenia. JAMA Psychiatry. 2013 Mar 1;70(3):271–8.

157. Steiner J, Teegen B, Schiltz K, Bernstein H-G, Stoecker W, Bogerts B. Prevalence of N-Methyl-D-Aspartate Receptor Autoantibodies in the Peripheral Blood. JAMA Psychiatry. 2014 Jul 1;71(7):838–2.

158. Gaughran F, Lally J, Beck K, McCormack R, Gardner-Sood P, Coutinho E, et al. Brain-relevant antibodies in first-episode psychosis: a matched case–control study. Psychol Med. 2017 Sep 18;48(8):1257–63.

159. Beck K, Lally J, Shergill SS, Bloomfield MAP, MacCabe JH, Gaughran F, et al. Prevalence of serum N-methyl-D-aspartate receptor autoantibodies in refractory psychosis. Br J Psychiatry. 2015 Feb;206(2):164–5.

160. Dahm L, Ott C, Steiner J, Stepniak B, Teegen B, Saschenbrecker S, et al. Seroprevalence of autoantibodies against brain antigens in health and disease. Ann Neurol. 2014 Jul;76(1):82–94.

161. Masdeu JC, GonzáLez-Pinto A, Matute C, Ruiz De Azúa S, Palomino A, De Leon J, et al. Serum IgG antibodies against the NR1 subunit of the NMDA receptor not detected in schizophrenia. Am J Psychiatry. 2012 Oct;169(10):1120–1.

162. Snijders G, Titulaer MJ, Bergink V, Bastiaansen AE, Schreurs MWJ, Ophoff RA, et al. No neuronal autoantibodies detected in plasma of patients with a bipolar I disorder. Psychiatry Research. 2017 Nov 11;259:460–2.

163. Oviedo-Salcedo T, de Witte L, Kümpfel T, Kahn RS, Falkai P, Eichhorn P, et al. Absence of cerebrospinal fluid antineuronal antibodies in schizophrenia spectrum disorders. British Journal of Psychiatry. 2018 Mar 28;:1–3.

164. Hoffmann C, Zong S, Mané-Damas M, Molenaar PC, Losen M, Titulaer MJ, et al. Absence of Autoantibodies Against Neuronal Surface Antigens in Sera of Patients With Psychotic Disorders. JAMA Psychiatry. 2019 Nov 20;:1–4.

165. Hammer C, Stepniak B, Schneider A, Papiol S, Tantra M, Begemann M, et al. Neuropsychiatric disease relevance of circulating anti-NMDA receptor autoantibodies depends on blood-brain barrier integrity. Molecular Psychiatry. 2014 Oct;19(10):1143–9.

166. Castilo-Gómez E, Oliveira B, Tapken D, Bertrand S, Klein-Schmidt C, Pan H, et al. All naturally occurring autoantibodies against the NMDA receptor subunit NR1 have pathogenic potential irrespective of epitope and immunoglobulin class. Mol. Psychiatry. 2016 Aug 9;22(12):1776–1784.

167. Jézéquel J, Rogemond V, Pollak T, Lepleux M, Jacobson L, Gréa H, et al. Cell- and single molecule-based methods to detect anti-NMDA receptor autoantibodies in first episode psychosis patients from the OPTiMiSE project. Biological Psychiatry. 2017 Jul 5;82(10):766–772.

168. Jézéquel J, Johansson EM, Dupuis JP, Rogemond V, Gréa H, Kellermayer B, et al. Dynamic disorganization of synaptic NMDA receptors triggered by autoantibodies from psychotic patients. Nature Communications. 2017 Nov 16;8(1791):1–15.

169. Ehrenreich H. Autoantibodies against the N-Methyl-d-Aspartate Receptor Subunit NR1: Untangling Apparent Inconsistencies for Clinical Practice. Front Immunol. 2017 Mar 1;8:302–7.

170. Al-Diwani A, Lennox BR. Neuroimmunology 2017: making progress over 20 years. The Lancet Psychiatry. 2017 Dec 19;5(1):9–10.

171. Cahalan S. Anti-N-Methyl-D-Aspartate Encephalitis: A Patient's Perspective. Biological Psychiatry. 2016 May 1;79(9):708–9.

172. Pollak TA, Lennox BR, Vincent A, Nicholson TR. Antibody-mediated encephalitis and psychosis. Xenitidis K, Campbell C, editors. British Journal of Psychiatry. 2012 Apr;200(4):344–345.

173. Herken J, Prüss H. Red Flags: Clinical Signs for Identifying Autoimmune Encephalitis in Psychiatric Patients. Front Psychiatry. 2017 Feb 16;8(5):90–21.

174. Moran N, Munro N, Lawson K, David AS. Safe management of psychiatrically disturbed patients on non-psychiatric wards in the UK. BMJ. 2014 Feb 19;348(feb19 2):g1466–6.

175. Lejuste F, Thomas L, Picard G, Desestret V, Ducray F, Rogemond V, et al. Neuroleptic intolerance in patients with anti-NMDAR encephalitis. Neurol Neuroimmunol Neuroinflamm. 2016 Aug 29;3(5):e280–7.

176. Scott JG, Gillis D, Ryan AE, Hargovan H, Gundarpi N, McKeon G, et al. The prevalence and treatment outcomes of antineuronal antibody-positive patients admitted with first episode of psychosis. BJPsych open. 2018 Mar 16;4(02):69–74.

177. Pollak TA, Lennox BR. Time for a change of practice: the real-world value of testing for neuronal autoantibodies in acute first-episode psychosis. BJPsych open. 2018 Jul;4(4):262–4.

178. Bygrave AM, Kilonzo K, Kullmann DM, Bannerman DM, Kätzel D. Can N-Methyl-D-Aspartate Receptor Hypofunction in Schizophrenia Be Localized to an Individual Cell Type? Front Psychiatry. 2019 Nov 21;10:86–23.

179. Hughes GC, Choubey D. Modulation of autoimmune rheumatic diseases by oestrogen and progesterone. Nature Reviews Rheumatology; 2014 Aug 26;10(12):740–51.

180. Dalmau J, Graus F. Antibody-Mediated Encephalitis. N Engl J Med. 2018 Mar;378(9):840–51.

181. Bergink V, Rasgon N, Wisner KL. Postpartum Psychosis: Madness, Mania, and Melancholia in Motherhood. American Journal of Psychiatry. 2016 Dec;173(12):1179–88.

182. Borsboom D, Cramer AOJ. Network Analysis: An Integrative Approach to the Structure of Psychopathology. Annual Rev Clin Psychol. 2013 Mar 28;9(1):91–121.

183. McNally RJ. Can network analysis transform psychopathology? Behaviour Research and Therapy. 2016 Nov 1;86:95–104.

184. Bastian M, Heymann S, Jacomy M. Gephi: an open source software for exploring and manipulating networks. International AAAI Conference on Weblogs and Social Media. Proc Int AAAI Conf Weblogs Soc Media. 2009:361–62.

185. Varley JA, Webb AJS, Balint B, Fung VSC, Sethi KD, Tijssen MAJ, et al. The movement disorder associated with NMDAR antibody-encephalitis is complex and characteristic: an expert video-rating study. Journal of Neurology, Neurosurgery & Psychiatry. 2019 Jun;90(6):724-726

186. Heron J, McGuinness M, Blackmore ER, Craddock N, Jones I. Early postpartum symptoms in puerperal psychosis. BJOG: An International Journal of Obstetrics & Gynaecology. 2008 Jan 5;115(3):1–6.

187. “Her brain is on fire”: Neurological condition affecting young women discovered that makes them hysterical, then catatonic. 2013 Feb 10. Available from: https://www.dailymail.co.uk/news/article-2276370/Her-brain-Neurological-condition-affecting-young-women-discovered-makes-hysterical-catatonic.html

188. Van Os J. “Schizophrenia” does not exist. BMJ. 2016 Feb 2;352:i375–3.

189. Wilcox J, Reid Duffy P. The Syndrome of Catatonia. Behavioral Sciences. 2015 Dec;5(4):576–88.

190. Restrepo-Martínez M, Chacón-González J, Bayliss L, Ramírez-Bermúdez J, Lewis FG, Espinola-Nadurille M. Delirious mania as a neuropsychiatric presentation in patients with anti-NMDAr encephalitis. Psychosomatics. 2019 Mar 14;61(1):64–69.

191. Lennox BR, Palmer-Cooper EC, Pollak T, Hainsworth J, Marks J, Jacobson L, et al. Prevalence and clinical characteristics of serum neuronal cell surface antibodies in first-episode psychosis: a case-control study. Lancet Psychiatry. 2017 Jan;4(1):42–8.

192. Choe C-U, Karamatskos E, Schattling B, Leypoldt F, Liuzzi G, Gerloff C, et al. A clinical and neurobiological case of IgM NMDA receptor antibody associated encephalitis mimicking bipolar disorder. Psychiatry Research. Elsevier; 2013 Jul 30;208(2):194–6.

193. Desestret V, Chefdeville A, Viaccoz A, Bost C, Ducray F, Picard G, et al. CSF IgA NMDAR antibodies are potential biomarkers for teratomas in anti-NMDAR encephalitis. Neurol Neuroimmunol Neuroinflamm. 2015 Nov 24;2(6):e166–10.

194. Hara M, Martinez-Hernandez E, Ariño H, Armangue T, Spatola M, Petit-Pedrol M, et al. Clinical and pathogenic significance of IgG, IgA, and IgM antibodies against the NMDA receptor. Neurology. 2018 Apr 16;90(16):e1386–94.

195. Miglio G, Varsaldi F, Lombardi G. Human T lymphocytes express N-methyl-d-aspartate receptors functionally active in controlling T cell activation. Biochemical and Biophysical Research Communications. 2005 Dec;338(4):1875–83.

196. Iwamoto T, Shiokawa Y, Nakao S. Improvement of NMDA encephalitis by active lymph node removal. Journal of Anesthesia. 2013 Dec 20;28(4):646–6.

197. Scott GD, Lau HD, Kurzer JH, Kong CS, Gratzinger DA. Flow immunophenotyping of benign lymph nodes sampled by FNA: Representative with diagnostic pitfalls. Cancer Cytopathology. 2018 Sep 7;126(9):797–808.

198. Havenar-Daughton C, Carnathan DG, la Peña de AT, Pauthner M, Briney B, Reiss SM, et al. Direct Probing of Germinal Center Responses Reveals Immunological Features and Bottlenecks for Neutralizing Antibody Responses to HIV Env Trimer. Cell Reports. 2016 Nov 22;17(9):2195–209.

199. Absinta M, Ha SK, Nair G, Sati P, Luciano NJ, Palisoc M, et al. Human and nonhuman primate meninges harbor lymphatic vessels that can be visualized noninvasively by MRI. Elife 2017 Oct 3; 6:e29738.

200. Eide PK, Vatnehol SAS, Emblem KE, Ringstad G. Magnetic resonance imaging provides evidence of glymphatic drainage from human brain to cervical lymph nodes. Scientific Reports. 2018 May 8;8(1):7194.

201. Stern JNH, Yaari G, Vander Heiden JA, Church G, Donahue WF, Hintzen RQ, et al. B cells populating the multiple sclerosis brain mature in the draining cervical lymph nodes. Science Translational Medicine. 2014 Aug 6;6(248):248ra107–7.

202. van Zwam M, Huizinga R, Heijmans N, van Meurs M, Wierenga-Wolf AF, Melief M-J, et al. Surgical excision of CNS-draining lymph nodes reduces relapse severity in chronic-relapsing experimental autoimmune encephalomyelitis. J Pathol. 2009 Mar;217(4):543–51.

203. Podkowa A, Miller RJ, Motl RW, Fish R, Oelze ML. Focused Ultrasound Treatment of Cervical Lymph Nodes in Rats with EAE: A Pilot Study. Ultrasound in Medicine & Biology. 2016 Sep 13;:1–8.

204. Fabriek BO, Zwemmer JNP, Teunissen CE, Dijkstra CD, Polman CH, Laman JD, et al. In vivo detection of myelin proteins in cervical lymph nodes of MS

patients using ultrasound-guided fine-needle aspiration cytology. Journal of Neuroimmunology. 2005 Apr;161(1-2):190–4.

205. Papa I, Saliba D, Ponzoni M, Bustamante S, Canete PF, Gonzalez-Figueroa P, et al. TFH-derived dopamine accelerates productive synapses in germinal centres. Nature. 2017 Jul 20;547(7663):318–323.

206. Bemark M. Translating transitions - how to decipher peripheral human B cell development. J Biomed Res. 2015 Jul;29(4):264–84.

207. Havenar-Daughton C, Lindqvist M, Heit A, Wu JE, Reiss SM, Kendric K, et al. CXCL13 is a plasma biomarker of germinal center activity. Proc Natl Acad Sci USA. 2016 Mar 8;113(10):2702–7.

208. Leypoldt F, Höftberger R, Titulaer MJ, Armangue T, Gresa-Arribas N, Jahn H, et al. Investigations on CXCL13 in Anti– N-Methyl- D-Aspartate Receptor Encephalitis. JAMA Neurol. 2015 Feb 1;72(2):180–7.

209. Muir L, McKay PF, Petrova VN, Klymenko OV, Kratochvil S, Pinder CL, et al. Optimisation of ex vivo memory B cell expansion/differentiation for interrogation of rare peripheral memory B cell subset responses. Wellcome Open Res. 2017 Oct 5;2:97–25.

210. Lindenbergh MFS, Stoorvogel W. Antigen Presentation by Extracellular Vesicles from Professional Antigen-Presenting Cells. Annu Rev Immunol. 2018 Apr 26;36(1):435–59.

211. García-Silva S, Benito-Martín A, Sánchez-Redondo S, Hernández-Barranco A, Ximénez-Embún P, Nogués L, et al. Use of extracellular vesicles from lymphatic drainage as surrogate markers of melanoma progression and BRAFV600Emutation. J Exp Med. 2019 May 6;216(5):1061–70.